SYNTHESIS AND CHARACTERIZATION OF MELAMINE-BASED DENDRIMERS WITH POTENTIAL BIOLOGICAL APPLICATIONS

A Dissertation

by

HANNAH LOUISE CRAMPTON

Submitted to the Office of Graduate Studies of
Texas A&M University
in partial fulfillment of the requirements for the degree of

DOCTOR OF PHILOSOPHY

May 2008

Major Subject: Chemistry

SYNTHESIS AND CHARACTERIZATION OF MELAMINE-BASED DENDRIMERS WITH POTENTIAL BIOLOGICAL APPLICATIONS

A Dissertation

by

HANNAH LOUISE CRAMPTON

Submitted to the Office of Graduate Studies of
Texas A&M University
in partial fulfillment of the requirements for the degree of

DOCTOR OF PHILOSOPHY

Approved by:

Chair of Committee,	Eric E. Simanek
Committee Members,	David E. Bergbreiter
	Gerard L. Coté
	François P. Gabbaï
Head of Department,	David H. Russell

May 2008

Major Subject: Chemistry

ABSTRACT

Synthesis and Characterization of Melamine-Based Dendrimers with Potential Biological Applications. (May 2008)

Hannah Loiuse Crampton, B.S., Trinity University

Chair of Advisory Committee: Dr. Eric E. Simanek

The convergent strategy towards dendrimer synthesis is well-suited to generate macromolecules with a diverse periphery, at the expense of time and effort, while the divergent strategy has historically been effective at yielding higher generation dendrimers, although they are often plagued by impurities. Both the convergent and divergent routes were applied to the synthesis of melamine-based dendrimers, offering a comparison of the routes within a system.

Generation-1 dendrons heterogeneously functionalized with Boc-protected amines and hydrazones were synthesized convergently and coupled to a generation-1 *tris*(piperazine) core to yield a generation-2 dendrimer bearing 18 Boc-amines and three hydrazones. Although the yield for the final coupling step was rather low (56%), the yields for all intermediate steps were quite high. Attempts toward obtaining a generation-3 dendrimer through this route were unsuccessful due presumably to steric hindrance. The materials obtained showed no impurities in their ^{1}H and ^{13}C NMR and mass spectra, although several chromatographic purifications were necessary throughout the synthesis.

A divergent strategy based on addition of a dichlorotriazine monomer to polyamine cores was used to synthesize dendrimers of generations 1-5. All intermediates and dendrimers were either purified by precipitation, or did not need purification. ^{1}H NMR spectroscopy indicated that reactions were complete up to **G4-NH$_2$** by integration, and mass spectroscopy confirmed that assignment. HPLC and GPC of **G*n*-Cl** dendrimers showed sharp peaks for G1-G3, but **G4-Cl** appeared to have a small amount of impurities that are similar in size and polarity to the fully-substituted dendrimer. The G1-G3 dendrimers were confidently assigned as pure by conventional organic chemistry standards, but the assignment of purity to higher generations remained tentative.

A **G1-Cl** dendrimer was functionalized with imidazole, and then deprotected and PEGylated with PEG_{5000} to yield a water soluble dendrimer. The imidazole-capped, Boc-protected dendrimer and the deprotected dendrimer were characterized by ^{1}H and ^{13}C NMR spectroscopy and mass spectrometry. The degree of PEGylation on the PEGylated material could not be definitively ascertained; however, the material is capable of solubilizing very hydrophobic Zn-phthalocyanines in water.

ACKNOWLEDGMENTS

I would like to thank Dr. Eric Simanek for being a kind and understanding mentor, and for always letting me do things my own way. Thanks also to all of my friends and colleagues along the way who helped make this a fun experience. I would like to acknowledge the National Science Foundation for generous support through a Graduate Research Fellowship and a GK-12 Fellowship. Finally, I would like to thank my wonderful husband and all of my family. Without your love, support, and countless hours of babysitting, cooking, and cleaning, I never would have made it with my sanity intact.

TABLE OF CONTENTS

TABLE OF CONTENTS, cont'd.

TABLE OF CONTENTS, cont'd.

LIST OF FIGURES

LIST OF FIGURES, cont'd.

LIST OF FIGURES, cont'd.

LIST OF TABLES

CHAPTER I

INTRODUCTION: SYNTHETIC STRATEGIES TOWARDS DENDRIMER SYNTHESIS AND AN OVERVIEW OF PHOTODYNAMIC THERAPY AND PHTHALOCYANINES

Dendrimer Synthesis

Dendrimers, macromolecules with highly and regularly branched architectures, were first introduced by Vögtle in 1978.[1] Unlike traditional linear polymers, dendrimers are generated through iterative organic syntheses leading to the possibility, in theory, of obtaining single chemical entities. The controlled nature of their synthesis also allows for precise control over the size, shape, and surface functionality of these molecules. Dendrimers may be synthesized through a divergent approach, from the core outwards; a convergent approach, from the periphery inward to the core; or through the hypercore method, a merging of the two previous approaches. Each method has advantages and disadvantages that must be examined along with the chemical nature of the monomers to be used when choosing a route for a particular dendrimer synthesis.

The divergent strategy (Figure 1.1) was pioneered by Newkome[2] and Tomalia[3] in 1985, the latter of whose poly(amido amine) (PAMAM) dendrimers are now commercially available and quite ubiquitous. In this strategy a multifunctional core (generation-0) is reacted with a multifunctional monomer that may be protected. The protecting groups are removed, and a new reactive generation-1 dendrimer is revealed. This sequence is carried out through several iterations to build higher generations.

This dissertation follows the style of *Journal of the American Chemical Society*.

Generation-building reactions occur on the surface of the molecule, lowering steric hindrance and making larger dendrimers more accessible. However, the number of reactions required at each generations increases exponentially (96 reactions must occur to build a generation-5 PAMAM dendrimer), and a statistical mixture of products resulting from incomplete substitution is obtained, especially at higher generations. These impurities become increasingly more difficult to identify through spectroscopic techniques at higher generations due to self-similarity, and are often impossible to isolate, although they can be minimized through the use of extreme reaction conditions such as large excesses of reagents or high heat. Although one can imagine using different monomers during the synthesis of each generation to incorporate variety, in reality most divergently synthesized dendrimers lack structural diversity, particularly in the end groups.

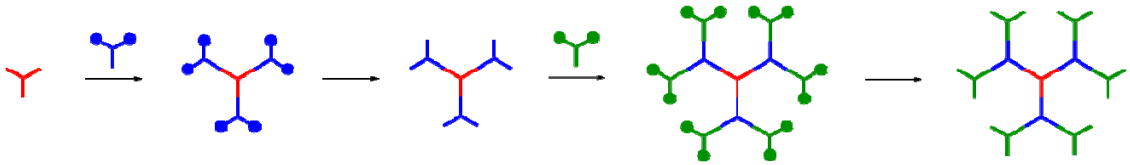

Figure 1.1. Divergent dendrimer synthesis.

The convergent route (Figure 1.2) was introduced by Hawker and Fréchet in 1990[4] and addresses these issues, but has limitations of its own. Using this strategy, a dendron with a protected focal point and surface groups is elaborated inward. The focal point is deprotected and reacted with a branching unit that has a new protected focal point or with a multifunctional core. The surface protecting groups are removed post-

synthetically. Only a few reactions occur per molecule in each step, so side products are minimal and easily separated due to the large difference in size. Although excess dendrons are frequently used to obtain complete substitution, they are often easy to separate from the product. This route is amenable to the addition of diversity at each step, and unsymmetrical dendrimers may be generated.[5,6] However, since generation-building reactions occur in the interior of the molecule, steric constraints often prohibit the synthesis of higher generations.

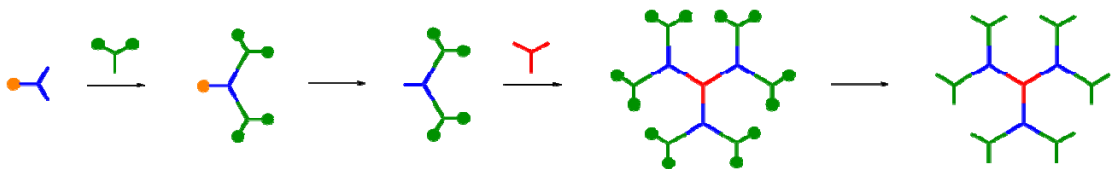

Figure 1.2. Convergent dendrimer synthesis.

The hypercore approach[7] combines the divergent and convergent strategies. A dendritic wedge of multiple generations is formed convergently, and then coupled to a first- or second-generation core synthesized divergently. This can produce dendrimers of purity comparable to those formed from convergent synthesis, but of higher generation since the core is larger and less sterically hindered.

Although each of these methods has its disadvantages, they all produce macromolecules of exceptional purity in comparison to traditional polymeric materials. This makes them ideally suited for use as biological agents, as the FDA prefers drugs that are monodisperse and unambiguously identified. The use of polymeric materials as

pharmaceuticals and drug delivery agents is well documented[8], as well as specifically the use of dendrimers. [9-11]

The EPR Effect

The last twenty years has seen the advent of the use of polymeric materials in pharmaceuticals, and particularly for antitumor drug delivery because their high molecular weight, and therefore large size, may impart selective accumulation of the material in tumor tissue through the *enhanced permeability and retention* effect (EPR effect).[12] Maeda attributes the EPR effect to two factors: the discontinuous endothelium of tumor vasculature (their so-called 'leaky' vasculature), which allows large molecules circulating in the blood stream to pass through, and the lack of effective lymphatic drainage in tumors (Figure 1.3). These effects together cause the passive accumulation of macromolecules in solid tumor tissue, which may increase the tumor concentration of antitumor drugs up to 70-fold when drug-delivery systems are injected intravenously.[13,14] The majority of tumors have transvascular pore sizes in the 380-780 nm range, but some may have pores as large as 1.2-2 μm.[15]

The EPR effect can be augmented by the application of various endogenous factors as well.[16] Tumors lack smooth muscle around the blood vessel, so angiotensin-II induced hypertension causes a selective increase in blood flow to tumors. As the normal blood vessels contract, tightening cellular junctions and increasing blood flow rate, tumoral blood vessels do not constrict, and passive dilation of any intravenous molecules into the tumor occurs. Vasodilators can also augment the EPR effect by widening the endothelial gaps of tumor vessels. NO-releasing agents, PGI_2 (prostaglandin) agonists,

and angiotensin-converting enzyme (ACE) inhibitors, which increase the concentration of bradykinins, all cause vasodilation which increases the blood flow to all cells, but also has a pro-EPR effect.

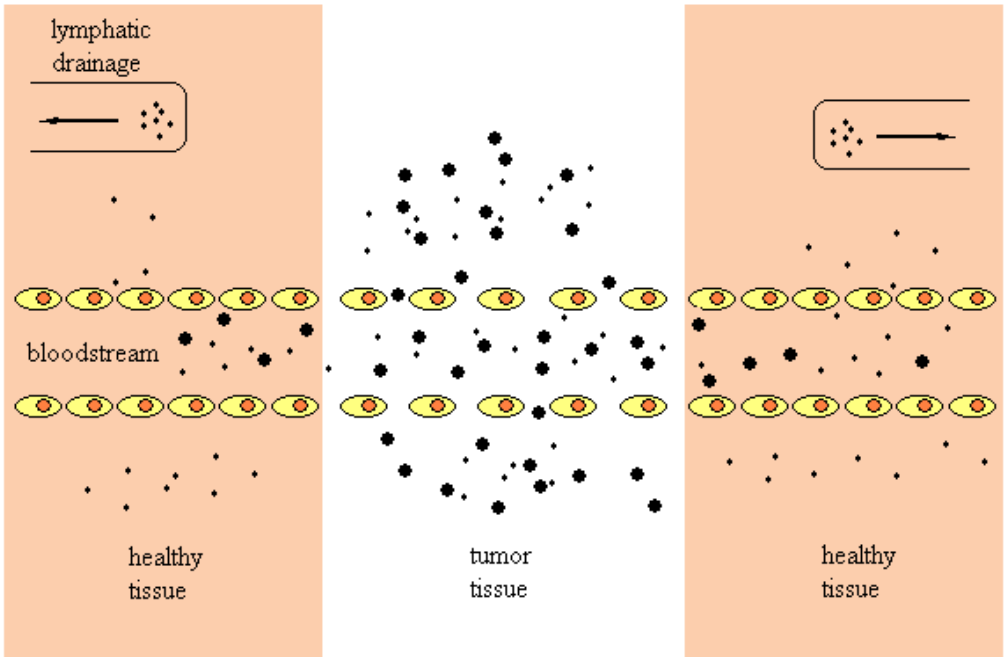

Figure 1.3. Schematic of the EPR Effect.

An ideal polymeric drug delivery vehicle should have a molecular weight above the renal threshold of ~40 kDa, while the degradation products of the polymer should be below 40 kDa or be biodegradable. [12,17] Also, the plasma concentration of the conjugate must remain high for more than 6 hours (in mice and rats) as measured by the area under the time-concentration curve (AUC).[16]

Dendrimers *in vivo*

In the realm of macromolecules, dendrimers are particularly well-suited for drug delivery because of their defined and organized structure, their monodispersity, and their potential for diverse functionalization within a molecule. Drugs may be non-covalently encapsulated within a dendrimer or covalently bound to reactive surface sites. One could imagine attaching solubilizing groups or cell-targeting agents such as antibodies or proteins to the periphery as well (Figure 1.4).

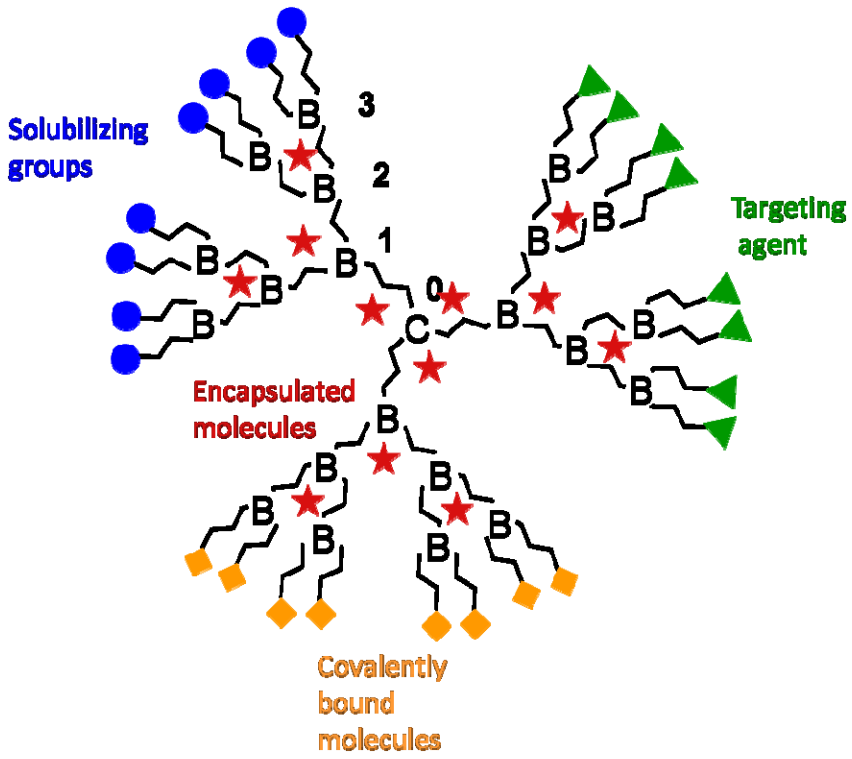

Figure 1.4. Generalized schematic of a dendrimer.

Several issues must be taken into consideration for the *in vivo* use of any molecule; namely solubility, cytotoxicity, hemocompatibility, immunogenicity, and

organ accumulation. These factors have been studied for several classes of dendrimer. The cytotoxicity of dendrimers has been found to generally increase with increasing generation and concentration.[18] In a computational study of PAMAM dendrimers by Pricl, the radius of gyration, molecular shape, and dimensions of the dendrimers were related to cytotoxicity, where non-cytotoxic dendrimers were characterized by a dense, globular shape and a smooth surface pattern.[19] Surface functionality is most predictive of cytotoxicity. Cationic PAMAM[20] and melamine-based dendrimers[21] were much more cytotoxic than their anionic or poly(ethylene glycol)-functionalized (PEGylated) counterparts. Generation-7 cationic PAMAM dendrimers interact with dimyristoylphosphatidylcholine lipid bilayers, causing the formation of 15-40 nm wide holes in the bilayers.[22] The formation of holes in cell membranes *in vivo* disturbs the electrolyte flux and causes cell death.[23]

Similarly, cationic PAMAM dendrimers showed generation-dependent hemolysis at generations larger than 1 and concentrations above 1mg/mL.[20] Cationic diaminobutane (DAB) and diaminoethane (DAE) dendrimers were hemolytic above 1 mg/mL, without a generation dependency, and anionic PAMAM and DAB were not hemolytic. Cationic melamine dendrimers are more hemolytic than anionic or PEGylated dendrimers.[21]

The biodistribution of dendrimers has been reported using parenterally administered dendritic-based imaging agents.[20,24,25] As expected, lower generation, smaller dendrimers showed rapid renal elimination, and larger dendrimers, as well as

charged and hydrophobic dendrimers, are eliminated by the liver.[26] Dendrimers with hydrophilic or PEGylated surfaces have much longer circulation times.

It has been proposed that the interaction of charged dendrimers, particularly cationic ones, with serum albumin is the main cause of the dendrimers' immunogenic activity. Albumin, a biomolecule with a formal charge of -15, is the most abundant protein in mammals, and is key to the transport and deposition of many substances in the blood.[27] PEGylation reduces many of the adverse effects, including cyto- and hemotoxicity, caused by dendrimers due to a reduction or shielding of the charged surfaces of the dendrimer by the PEG chains.[28]

Dendrimers as Drug Delivery Systems: Covalent Interactions

The well-defined, multivalent surfaces of dendrimers are well-suited for the covalent attachment of drugs, particularly for the delivery of anticancer drugs which may benefit from the EPR effect. The desired drug loading can be controlled by varying the generation of the dendrimer, and drug release can be controlled by incorporating cleavable linkages between the drug and dendrimer.

Fréchet and co-workers attached the chemotherapeutic drug methotrexate (MTX) to ester-terminated polyether dendrimers (Figure 1.5).[29] The dendrimer esters were functionalized with hydrazide groups, which were then conjugated to the γ–carboxylic acid of MTX. A generation-2 dendrimer bearing 8 hydrazide groups bound only 4.7 molecules of MTX, as determined by ^{1}H NMR. Baker and coworkers used EDC coupling to attach four molecules of MTX to a generation-5 PAMAM amine- or hydroxyl-terminated dendrimer functionalized with folic acid (Figure 1.5) through either

amide or ester bonds.[30,31] The conjugates were over 100 times more cytotoxic to cells than free methotrexate, due in large part to increased cellular uptake from tumor cells that over-express folate receptors.[32] Generation-5 PAMAM conjugated with MTX and the monoclonal antibody cetuximab showed specific tumor targeting,[33] while a generation-2.5-MTX showed increased cytotoxicity to MTX-sensitive and resistant cell lines.[34]

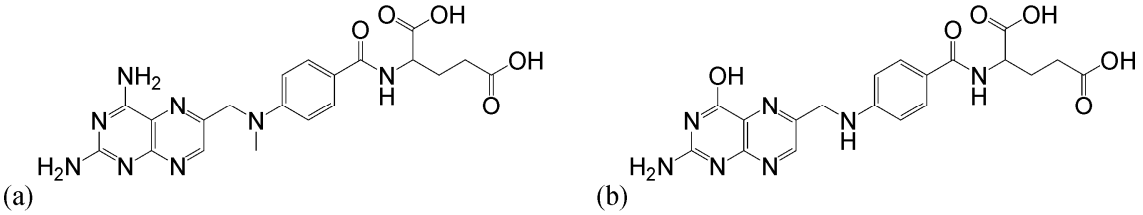

Figure 1.5. (a) Methotrexate and (b) folic acid.

Acetylated generation-4 and -5 PAMAM dendrimers with a core of 1,4,7,10-tetraazocyclododecane conjugated with 5-fluorouracil showed generation-dependent drug release in phosphate-buffered saline.[35]

Duncan and co-workers[36] synthesized conjugates of PAMAM dendrimers with the potent antitumor drug cisplatin that showed increased solubility, lower systemic toxicity, selective accumulation in tumors, and higher efficiency in the treatment of B16F10 melanoma compared to the free drug. Jansen et. al. synthesized a generation-1 poly(propylene imine) (PPI) dendrimer bound to four cisplatin molecules that showed binding to guanosinemonophosphate at the N^7 position, and decreased toxicity towards several cell lines.[37] Kapp et. al. also studied a generation-1 PPI dendrimer bearing four

platinum groups which showed 20 times higher transport to the cell than cisplatin, and 700 times higher DNA binding, but was not as cytotoxic.[38]

Ulbrich has done pioneering work in attaching the anticancer drug doxorubicin to *N*-(2-hydroxypropyl)methacrylamide (HPMA) copolymers through acid-labile hydrazine bonds that are stable at physiological pH (pH 7.4) but are degradable at endosomal pH (~5).[39-41] Wang extended this work by attaching doxorubicin-bound HPMA macromonomers to several generations of PAMAM dendrimer.[42] The doxorubicin (DOX) was bound through an enzyme-cleavable peptide, and the dendrimer conjugates showed slower drug release and cytotoxicity compared to free drug and to linear HPMA-DOX conjugates. Most recently doxorubicin was conjugated directly to generation -4.5 PAMAM dendrimers through amide (12 DOX/dendrimer) or hydrazone (14 DOX/dendrimer) bonds.[43] The amide-bound DOX was not released at physiological or acidic pH, whereas the hydrazone-bound DOX was released quickly at pH 4.5. The drug conjugates were administered along with a water-soluble sulfonated phthalocyanine, $AlPcS_{2a}$, to promote photochemical internalization (PCI) of the drug in the endosome. Application of light to the hydrazone-bound DOX mixture resulted in higher nuclear accumulation and cell death.

Dendrimers as Drug Delivery Systems: Polar Interactions

With their numerous ionizable surface groups, dendrimers are capable of multivalent interactions. Multivalency can result in an effect coined the 'cluster' or 'dendritic' effect that produces an increase in activity compared to a monomeric interaction.[44] In the dendritic effect, the simultaneous binding of *n* molecules to one

ligand results in a synergistic increase in the binding affinity of each substrate, with the maximum binding affinity $(K_a)^n$, that of the single binding affinity, K_a, raised to the power of *n*. Multivalency makes dendrimers very attractive for the complexation of small-molecule drugs and of DNA for gene therapy.

Ionizable groups in the interior of dendrimers can take part in electrostatic interactions as well. In seminal studies by Twyman and co-workers[45,46] small, weakly acidic molecules such as benzoic acid were associated with water-soluble PAMAM dendrimers end-functionalized with TRIS. The acidic molecules were ion paired with tertiary nitrogens in the interior of the dendrimers, and were precipitated at pH 2, at which the interior nitrogens are protonated. Several non-steroidal anti-inflammatory agents (NSAIDs) have been complexed with PAMAM dendrimers as well: ibuprofen,[47,48] ketoprofen,[49-52] flurbiprofen,[53] niclosamide,[54] and indomethacin (Figure 1.6).[55-57] All of these drugs, with the exception of niclosamide, contain carboxylic acids and are solubilized at neutral pHs through electrostatic interactions with the amines of PAMAM.

A G3 dendrimer with 32 surface amines binds 32 molecules of ibuprofen, while a G4 dendrimer with 64 surface amines binds 78 molecules of ibuprofen, suggesting that some interior encapsulation is occurring in the larger dendrimer.[47] The complexes showed facilitated entry and increased activity into A549 cells, relative to free drug.[48] Ketoprofen showed concentration- and generation-dependent solubilization with increasing PAMAM dendrimer concentration.[49] Complexes showed prolonged release

of ketoprofen *in vitro* and *in vivo*,[51] and in transdermal delivery, the dendrimer-ketoprofen complex showed 2.73 times higher bioavailability.[52]

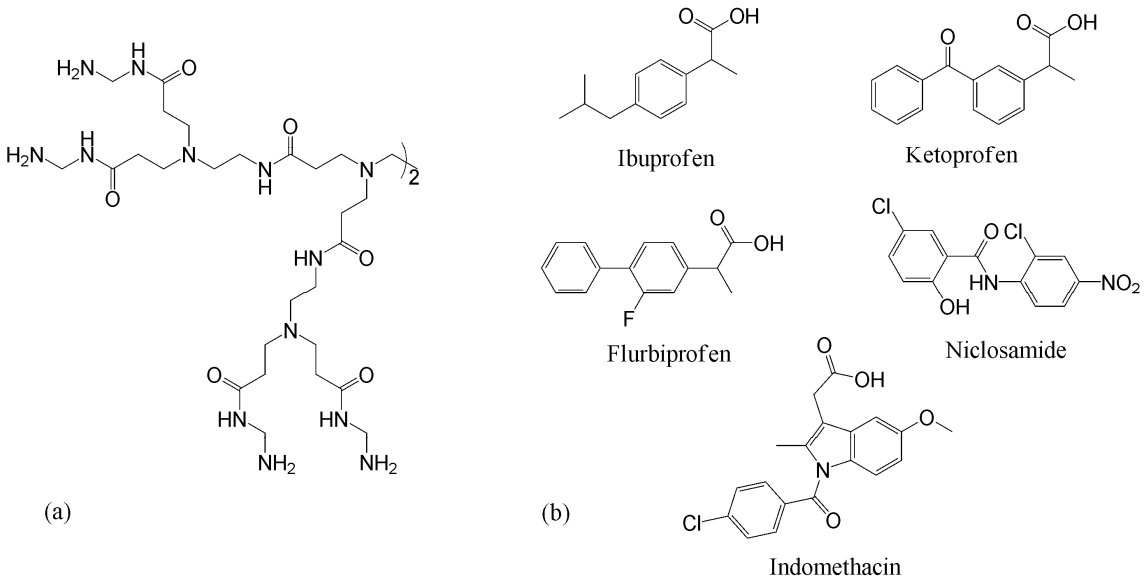

Figure 1.6. (a) G2-PAMAM dendrimer and (b) several drugs that it complexes.

Chauhan et al.[55] developed PAMAM complexes with indomethacin for transdermal delivery which showed an increase in the flux of drug across the skin *in vivo* and *in vitro*, with increased activity as well. Chandrasekar et al. increased indomethacin loading in G3.5 and G4 PAMAM dendrimers by forming dendrimer-folate[56] and dendrimer-folate-PEG[57] conjugates. The conjugates showed sustained release of indomethacin, as well as targeted delivery to inflamed areas.

Dendrimers as Drug Delivery Systems: Unimolecular Micelles

Dendrimers with a hydrophobic core and hydrophilic surface are referred to as 'unimolecular micelles' which lack a critical micellar concentration, and may be used to

solubilize hydrophobic guests in a polar environment. [2,58-60] The hydrophobic and hydrophilic properties, the branching and rotational angles, and the length of repeat units will collectively determine host-guest interactions.[61] PEG is often conjugated to the surface of a hydrophobic dendrimer to form unimolecular micelles that can solubilize hydrophobic drugs in the interior of the dendrimer or polar drugs in the PEG coat.

The increased solubility of water-insoluble drugs in PEGylated materials has been attributed to the structure-altering effects PEG has on water (hydrotropic solubilization).[62] Paclitaxel had a 10000-fold increase in solubility in a 80 wt% solution of polyglycerol dendrimer in water.[63] ^{1}H NMR data showed that the aromatic rings, methyne groups, and acetyl groups of paclitaxel are surrounded by the dendrimer and hydrogen-bonded to the terminal hydroxyl groups (Figure 1.7).[64]

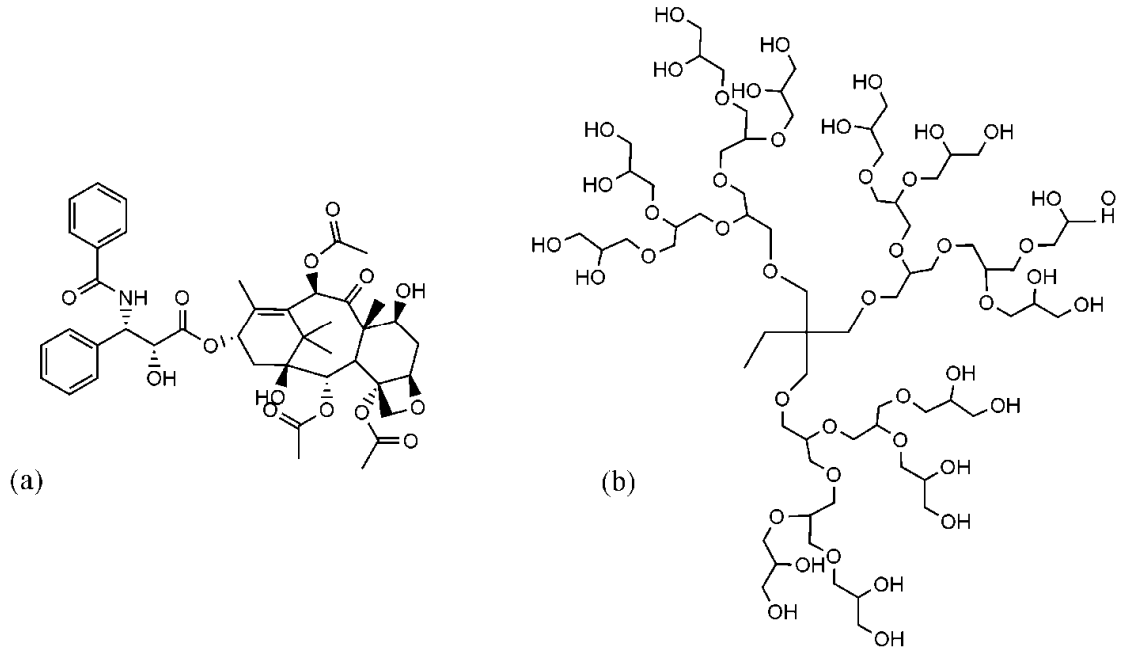

Figure 1.7. (a) Paclitaxel and (b) A generation-3 polyglycerol dendrimer.

PAMAM dendrimers functionalized with varying lengths of PEG showed increased encapsulation of MTX and DOX with both increasing dendrimer generation and increasing length of PEG.[65] A G4 dendrimer with PEG2000 grafts encapsulated 26 molecules of MTX or 6.5 molecules of DOX. The MTX complex showed sustained drug release in aqueous solutions of low isotonic strength, and rapid release in isotonic solutions. These results are similar to release of MTX from non-PEGylated PAMAM-folate conjugates.[31] Our own PEGylated triazine dendrimers can encapsulate three molecules of MTX in a generation-3 dendrimer, and when administered to mice the complexes showed attenuated liver toxicity.[66] Dendrimers with PEG in the interior can also solubilize MTX, with loading as high as 24.5% w/w.[67] These dendrimers show an initial burst release of drug, then sustained release. PEGylated dendrimers have been used to encapsulate many other drugs as well: 5-fluorouracil,[68] 10-hydroxycamptothecin,[69] chloroquine phosphate,[70] betamethasone corticosteroids,[71] 5-aminosalicylic acid, mefamic acid, and diclofenac.[72]

Photodynamic Therapy

Photodynamic therapy (PDT) is a treatment modality wherein a photosensitizer is administered to a patient, and after a predetermined amount of time the diseased area is exposed to light of a wavelength specific to the absorption of the photosensitizer. The sensitizer gets excited to its first triplet state, which can react with oxygen present in the cells to produce reactive oxygen species, such as singlet oxygen and superoxide anion radicals. These reactive oxygen molecules then react with electron-rich biomolecules to cause cellular destruction (Figure 1.8).[73]

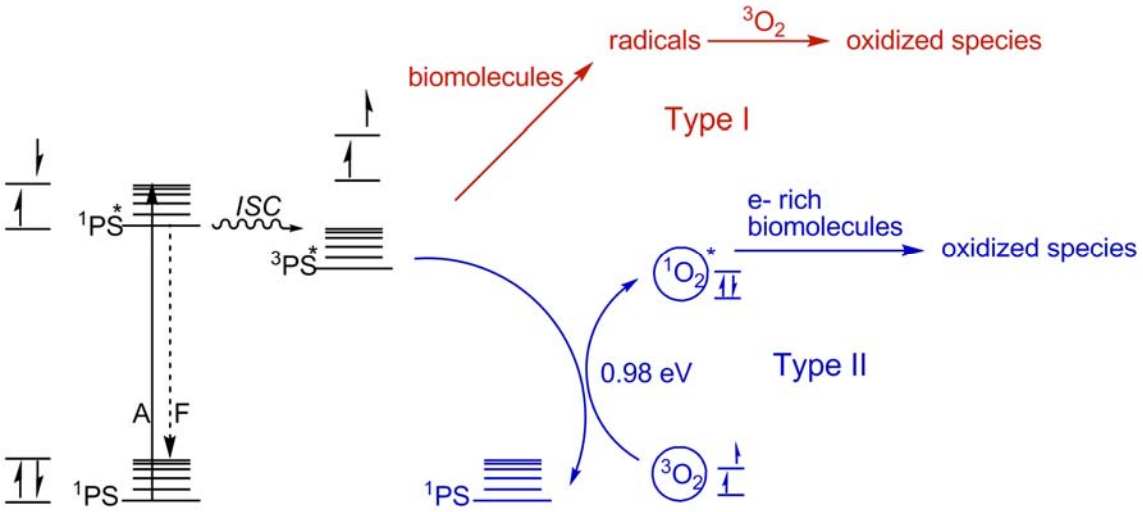

Figure 1.8. Overview of photosensitization for PDT.

There are two main prerequisites for an effective photosensitizer, in addition to the toxicity and biodistribution requirements of all drugs. First, the sensitizer must absorb light at a wavelength that will penetrate tissue without causing significant damage. There is an optical window from approximately 600-1300 nm where biomolecules such as water, hemoglobin, oxygen-bound hemoglobin, and melanin do not absorb. Within this window, the photosensitizer must have an absorption coefficient greater than the transmittance of skin.[74] The second requirement is that the triplet state must have at least 0.98 eV of energy to excite molecular oxygen to its singlet state. This requirement narrows the useful optical window to 600-900 nm. Of these requirements, only phthalocyanines and naphthalocyanines are ideally suited for PDT; however, they are notoriously insoluble which hinders their utility.

The use of porphyrins as photosensitizers has been widely explored, most notably with Photofrin, hematoporphyrin derivative (HpD), the first clinically used

porphyrin.[75] Although HpD has been effective at treating a variety of diseases, it has many characteristics that limit its usefulness. These include: its low absorptivity (600 nm, ε = 6000) at wavelengths that most easily penetrate tissue (700-900 nm), poor tumor selectivity, and lack of purity (it is a mixture of monomers and oligomers of ester- or ether-linked hematoporphyrins).[76,77] To overcome these disadvantages, many other porphyrinic compounds have been investigated.

Phthalocyanines (Pc) and azaporphyrins or porphyrazines (Pz) are porphyrin derivatives in which the *meso*-positions between pyrrole rings are nitrogen atoms, causing significantly different electronic properties compared to porphyrins. In azaporphyrins the Soret band is shifted to lower wavelengths and is less intense, while the Q bands are red-shifted to 600-800 nm and are often as intense as or more intense than the Soret band. The trend is the same for phthalocyanines, although the Q bands are even further red-shifted, to 700-900 nm, and are very intense.

Phthalocyanines have been evaluated for PDT since 1985.[78] Their intense absorption in the far red region of the spectrum, their purity, and their amenability to derivatization makes Pc good candidates for photosensitization, but their insolubility becomes the main issue to overcome. Most Pc-mediated photosensitization occurs through a type II mechanism in which the excited Pc reacts with molecular oxygen to form singlet oxygen, which is very reactive towards many key biomolecules. However, type I sensitization, and the more rare type II sensitization to form superoxide anion radicals, can occur depending on the Pc derivative.[73]

Several different techniques have been employed to enhance the delivery efficiency and specificity of Pc. Most Pc are hydrophobic molecules, and must be solubilized with a biologically compatible medium. Cremophor EL (CRM)[79] and liposomes[80-83] have been used extensively. Polyethylene glycol (PEG) and polyvinyl alcohol,[84] polymeric micelles,[85] nanospheres,[86] albumin,[87] cyclodextrins[88,89], and more recently, dendrimers[90-92] have also been examined.

Conclusions

The controlled manner in which dendrimers are synthesized allows for detailed control over their functionality, as well as unprecedented purity compared to traditionally synthesized linear polymers. These factors, as well as their multiple surface sites available for manipulation and unique globular shape, make dendrimers ideal candidates for macromolecular drug delivery devices, whether drugs are covalently bound to the surface or non-covalently encapsulated within the interior of the dendrimer. This dissertation describes the synthesis and characterization of several melamine-based dendrimers as potential candidates for drug delivery, as well as initial studies on the encapsulation of a hydrophobic phthalocyanine within a PEGylated dendrimer that may be used for PDT.

CHAPTER II

CONVERGENT, ORTHOGONAL SYNTHESIS AND CHARACTERIZATION OF A GENERATION-2 HYDRAZONE-BEARING DENDRIMER

Introduction

In the development of macromolecular drug delivery vehicles, it is usually advantageous to have a scaffold onto which several different moieties can be incorporated, such as drugs, targeting groups, and solubilizing groups.[93] Historically, dendrimers designed for these uses were synthesized divergently using known ratios of monomers to create a combinatorially-generated library.[94,95] However, dendrimers derived from a divergent strategy are often plagued by inseparable heterogeneities resulting from the statistical nature of their synthesis. Although typically more laborious, the convergent approach offers the opportunity for structural diversity with single-entity purity.

Our group is concerned with the synthesis and utilization of dendrimers based on triazines, particularly for drug delivery. Our dendrimers are built from the nucleophilic substitution of cyanuric chloride with various diamine linkers to provide branching points. The substitution of each chloride on cyanuric chloride subsequently decreases the reactivity towards substitution of the next chloride, which must be carried out at a higher temperature or with a more reactive amine.

Early dendrimers were synthesized using *p*-aminobenzylamine[96-101] as the two amines have very different reactivities, offering control over substitution. However, the instability of the linker to light and moisture incited us to examine the reactivity of other

diamines. A study of the reactivity of 6 different amines showed that anilines are the least reactive, followed by primary amines, and cyclic secondary amines are the most reactive.[96] Using this data, a rational choice of linker can be made based on the desired substitution pattern (i.e. first, second, or third).

The original dendrons discussed here were synthesized using a convergent approach with piperazine as the diamine linker and orthogonally-protected amines as surface groups. 1,7-*Bis*(Boc)diethylenetriamine **2.1** and 4-Dde-aminomethylpiperidine **2.2** were chosen based on previous group successes in post-synthetic attachment of both PEG for water solubility (after Boc deprotection) and thiopyridyl groups for drug delivery (after Dde deprotection).[102] 4-Dde-aminomethylpiperidine was later replaced as a surface group with 4-piperidone to synthesize a generation-2 dendrimer capable of covalently binding hydralazine, an antihypertensive drug, while eliminating the need for protecting group manipulation.

Hydralazine has been used as an antihypertensive drug since 1952, particularly in pregnant women with preeclampsia since it does not affect the fetal bloodstream.[103] Although it is particularly effective at reducing acute hypertension, there are several drawbacks to its use: it is unstable for storage in pharmaceutical formulations[104]; it is metabolized at different rates in different people, causing dosing problems; and it causes drug-induced lupus (DIL), an autoimmune disease indistinguishable from idiopathic lupus. Although the drug has been well-studied, the mechanism of its action is not known, but it is suggested that it may modulate the effect of purine-like compounds released from the sympathetic nervous system. It may also alter the Ca^{2+} balance in

vascular smooth muscle by blocking the inositol trisphosphate (IP3)-induced calcium release inhibiting calcium release from the sarcoplasmic reticulum.[105-108]

Hydralazine is administered orally, but bioavailability is low because the drug becomes inactivated as it is acetylated in the bowels and/or liver to 3-methyl-1,2,4-triazolo-(3,4a) phthalazine. There are slow acetylators, who have a reduction in the N-acetyltransferase enzyme NAT-2, and fast acetylators, making dosing difficult because fast acetylators will need a higher dose to achieve the desired effect.[109] It readily forms hydrazones with circulating α-keto acids, and the major plasma metabolite is pyruvic acid hydrazone. Other metabolites include (4-(2-acetylhydrazino) phthalazin-1-one, which is excreted in the urine and (3-hydroxymethyl-1,2,4-triazolo(3,4a) phthalazine. Systemic metabolism is dependent on hydroxylation followed by conjugation with glucoronic acid in the liver, which is not dependent on the rate of acetylation.[110]

Hydralazine is rarely administered systemically because the injectable solution degrades rapidly. It is believed to form polymeric products, it oxidizes rapidly in the presence of oxidizers, and it is a strong metal chelator, requiring strict exclusion from any metal contact. It is also difficult for hospital personnel to dilute the stock solutions without compromising the stock solution.[104]

Hydralazine is known to interact with chromatin and inhibit DNA methylation.[111] DNA methylation is important for gene expression, and changes in DNA methylation cause a deficit in receptor editing of self-reactive B cells, causing lupus.[112,113] Hydralazine also decreases signaling in the Erk pathway, which triggers anti-dsDNA antibodies, contributing to lupus.[113] These same mechanisms that cause so

many problems can be beneficial when applied to tumor treatment. Malignant tumors show regional hypermethylation that silences tumor suppressor genes. Hydralazine causes demethylation, which reactivates tumor suppressor genes, and it is currently under phase II studies as a treatment for solid tumors.[114]

Conjugating hydralazine to a biocompatible dendrimer could alleviate these negative effects, breathing new life into an old drug. When the hydrazine functionality is protected by forming a hydrazone, hydralazine shows no metal chelation, making it useful as a pharmaceutical composition.[104] Attaching the drug to the dendrimer through a hydrazone bond should have a similar effect. Delivered orally, the hydrazone bond would be hydrolyzed in the acidic stomach environment to release active drug. Based on previous studies[28], when injected systemically, a PEGylated dendrimer would be non-immunogenic, and may physically and chemically protect hydralazine from becoming acetylated. Once taken into the acidic endosome of a tumor cell, the hydrazone bond would be hydrolyzed, and the drug may be active to interact with DNA. This principle has been employed extensively in the delivery of doxorubicin.[26,39-41,115-121] The EPR effect may help in tumor targeting for anticancer application of hydralazine.

Results and Discussion

Synthesis of Dendrons and the Core. *Bis*(2-aminoethyl)amine and 4-(aminomethyl)piperidine were protected with BOC-ON and 2-acetyl dimedone, respectively, to provide intermediates **2.1** and **2.2** in 85% and 87.5% yields (Figure 2.1). Initial syntheses of monochlorotriazine **2.3** were carried out in a one-pot procedure in which amine **2.1** was added to cyanuric chloride at 0 °C and the reaction was carried to

completion as monitored by thin layer chromatography (TLC), after which amine **2.2** was added at room temperature. Dendron **2.4** was obtained by reaction of **2.3** with piperazine at room temperature (Figure 2.1).

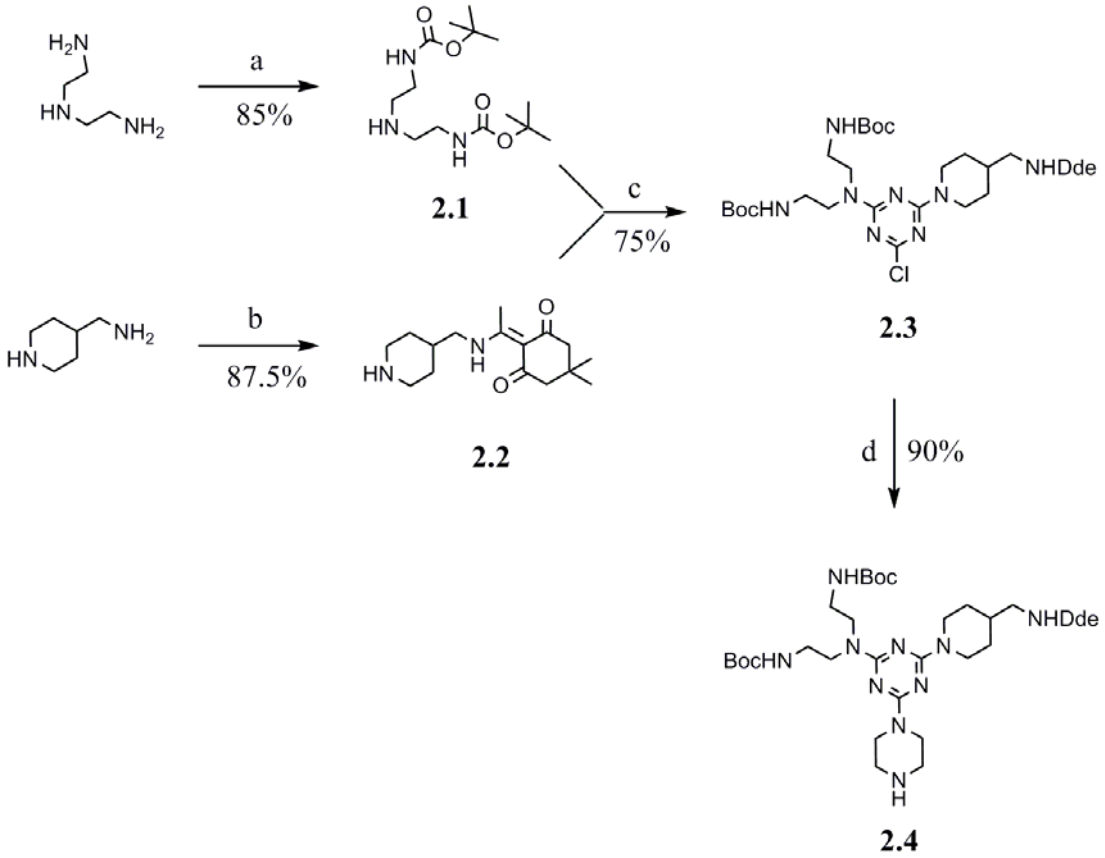

Figure 2.1. Synthesis of dendron **2.4**. (a) BOC-ON, THF, 0-25 °C (b) 2-acetyldimedone, EtOH, 120 °C (c) $C_3N_3Cl_3$, DIPEA, THF, 0-25 °C (d) piperazine, THF.

All materials appeared clean by TLC and NMR; however, a side product formed from disubstitution of Dde-amp on trace amounts of unreacted cyanuric chloride was observed by mass spectrometry, and persisted even after chromatography or precipitation. To remedy this situation, the dichloride intermediate **2.5** (Figure 2.2) was

isolated in 95% yield and purified by precipitation before addition of **2.2**, making disubstitution of Dde-amp impossible. Monochlorotriazine **2.3** was also isolated and purified by precipitation before addition of piperazine. Although column chromatography was necessary after the isolation of dendron **2.4** to remove dimers, by isolating dichlorotriazine **2.5**, one chromatographic step was eliminated while the overall yield remained the same (92%).

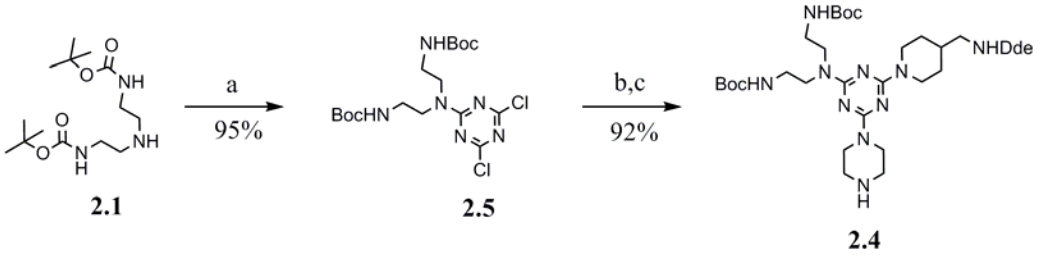

Figure 2.2. Alternate synthesis of dendron **2.4**. (a) DIPEA, THF, 0 °C (b)**2.2**, DIPEA, THF (c) piperazine, THF.

This strategy was extended to form a dendron bearing four Boc-protected amines (Figure 2.3). Monochlorotriazine **2.6** was obtained in 99% yield from reaction of amine **2.1** with cyanuric chloride without chromatography. Piperazine was added to form dendron **2.7** in 92% yield, which can be added to cyanuric chloride to form dichlorotriazine **2.8** in 58% yield after precipitation. The unusually low yield for this step is the result of the formation of a side product where dendron **2.7** has substituted cyanuric chloride twice; the addition of piperazine to cyanuric chloride is difficult to control, even at lowered temperatures. Finally, the generation-1 dendron **2.9** was obtained in 73% yield after addition of dendron **2.4** to dichlorotriazine **2.8**.

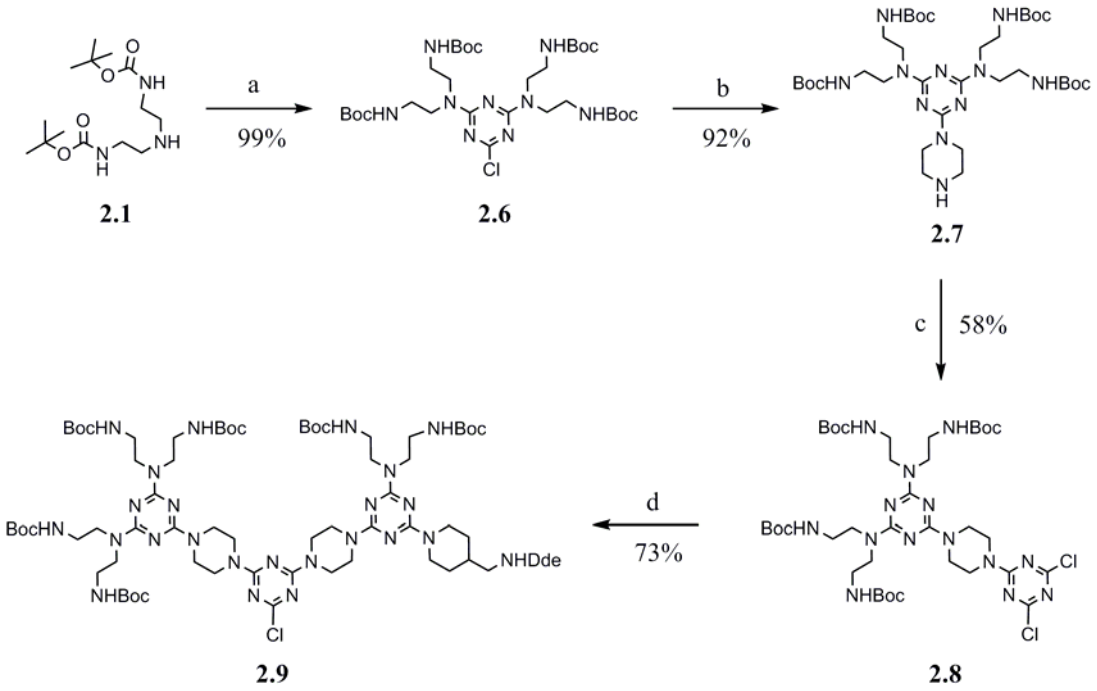

Figure 2.3. Synthesis of generation-1 dendron **2.9**. (a) $C_3N_3Cl_3$, DIPEA, THF (b) piperazine, THF (c) $C_3N_3Cl_3$, THF, 0 °C (d) **2.4**, DIPEA, THF.

In order to bind the drug hydralazine through a hydrazone bond, Dde-amp was replaced as a surface group with 4-piperidone. As the ketone is unreactive under dendrimer building conditions, this yields latent functionality without the need for a protecting group. Dendron **2.10** was obtained in two steps from the addition of 4-piperidone monohydrate hydrochloride to dichlorotriazine **2.5**, followed by the addition of piperazine (Figure 2.4). The monochlorotriazine intermediate was isolated and excess Et_3N and its salts removed with water washes, but it was not further purified. A side product resulting from two substitutions of piperidone to the triazine was observed by mass spectrometry (MS), but its polarity and solubility was too similar to the monochlorotriazine to be separated at this step. However, after the addition of

piperazine, dendron **2.10** is more polar than the impurity and can be purified by silica gel chromatography. The side product resulting from dimerization of the monochlorotriazine with piperazine was also removed during chromatography.

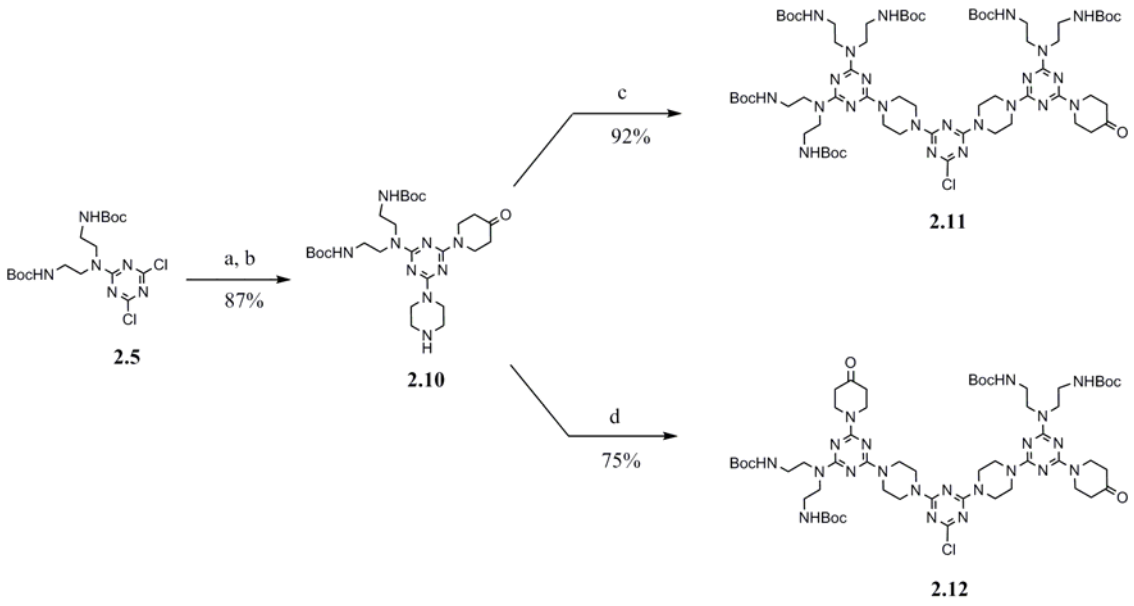

Figure 2.4. Synthesis of generation-1 dendrons **2.11** and **2.12**. (a) 4-piperidone.HCl.H_2O, Et_3N, THF/H_2O, 0-25 °C (b) piperazine, DIPEA, THF (c) **2.8**, DIPEA, THF (d) $C_3N_3Cl_3$, DIPEA, THF.

Two different generation-1 dendrons were synthesized by the addition of dendron **2.10** to either dichlorotriazine **2.8** (dendron **2.11**) or to cyanuric chloride (dendron **2.12**) (Figure 2.4). Although both reactions were carried out at room temperature, dendron **2.11** was obtained in high yield and purified only by precipitation, while an impurity later identified as tri-substituted triazine persisted in dendron **2.12** and had to be removed by column chromatography.

Synthesis of the Dendrimer and Hydralazine Conjugation. The dendrimer core with three Boc-protected amines was synthesized from Boc-piperazine and cyanuric chloride. The Boc groups were removed with trifluoroacetic acid to yield the active *tris*-piperazine core (Figure 2.5). Excess dendron **2.11** was reacted with the deprotected core at 80 ºC using BEMP resin (PS-2-tert-butylimino-2-dimethylamino-1,3-dimethylperhydro-1,3,2-diazaphosphorine) as a base. The reaction proceeded over 6 days until only three spots were seen by TLC, identified by MS as dendron **2.11**, the dendrimer product, and core with only two dendrons substituted. The reaction mixture was filtered, the solids discarded, and the filtrate evaporated. The filtrate was redissolved in THF, and a fresh batch of BEMP was added. After six more days of heating at 80 ºC, the 2-arm intermediate appeared to have reacted by TLC, and the dendrimer was separated from excess dendron **2.11** by column chromatography. Attempts towards the synthesis of a generation-3 dendrimer from six equivalents of dendron **2.11** and an expanded generation-1 hexapiperazine core were unsuccessful, presumably due to steric hindrance.

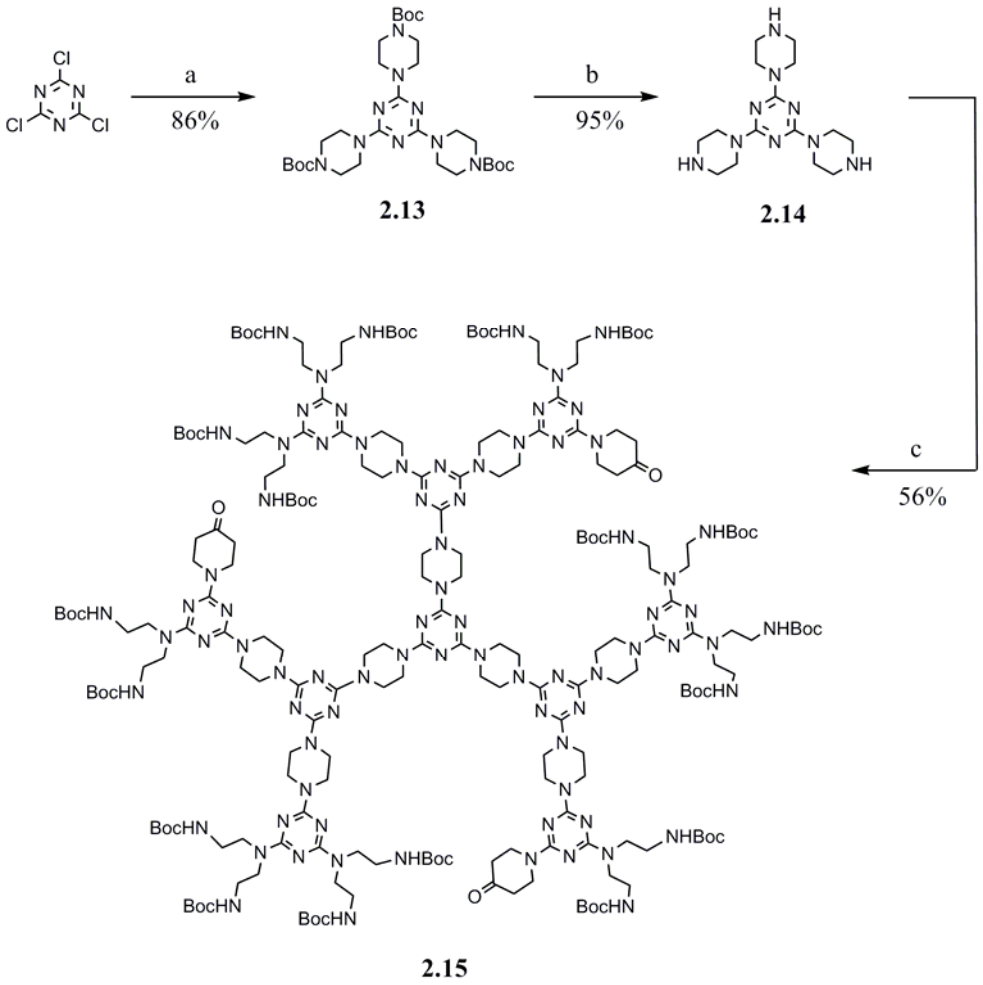

Figure 2.5. Synthesis of generation-2 dendrimer **2.15**. (a) Boc-piperazine, K_2CO_3, THF, 80 °C (b) TFA, DCM (c) **2.11**, BEMP, THF, 80 °C.

Model studies of the reaction of 4-nitro-benzoic hydrazide with dendron **2.10** were carried out to optimize the conditions for hydrazone formation with piperidone (Figure 2.6). Reactions carried out in MeOH with acetic acid or TFA, and in EtOH with HCl were not as effective as reactions carried out in MeOH without acid. Product **2.16** was formed, but the reaction was slow and unreacted ketone persisted in the reaction mixture. Reactions in neutral MeOH with 4Å molecular sieves proceeded faster than in acidic methanol, and the reaction in DMF with 4Å molecular sieves was most

successful, with a 98 % yield after purification by precipitation. These reactions cannot be monitored by TLC or purified by chromatography, as the hydrazone bond is unstable and hydrolyzes on the slightly acidic silica surface. The hydazones were characterized by ^{1}H and ^{13}C NMR spectroscopy and mass spectrometry.

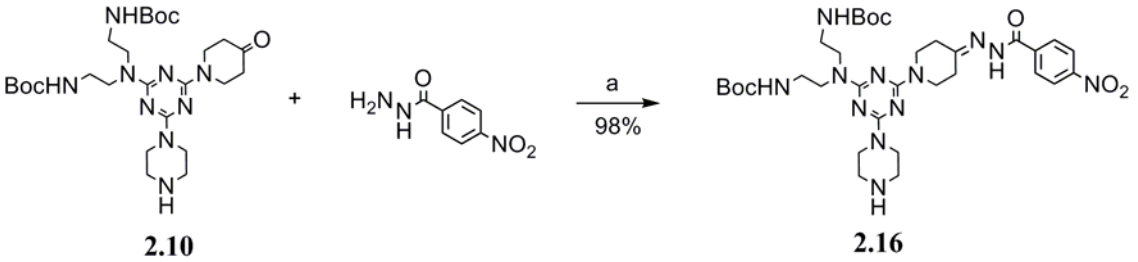

Figure 2.6. Synthesis of hydrazone **2.16**. (a) DMF, 25 °C.

Characterization

All materials were characterized by ^{1}H and ^{13}C NMR spectroscopy, and ESI or MALDI-TOF mass spectrometry (MS). ^{1}H NMR assignments are labeled in uppercase letters and are shown in red, while ^{13}C NMR assignments are labeled in lowercase letters and shown in blue throughout the following figures.

The ^{1}H NMR spectra of dendrons **2.4** and **2.10**, and dendrimer **2.15** are shown in figure 2.7, and are representative of the other intermediates not shown. The assignments of shifts from the Dde group were taken from HMQC spectra previously published.[102] The methyl groups **A** and **C** of the Dde groups appear as singlets at 0.88 and 2.41 ppm, respectively, while the methyl protons of the Boc group, **H**, appear at 1.25 ppm. The methylene protons **B** and **D** of the Dde group appear at and 2.22 and 3.11 ppm, respectively, where **D** overlaps with the peak for Boc methylene protons, **I**, at 3.17 ppm.

The axial and equatorial protons of the aminomethyl piperidine ring methylenes **F** and **G** each had unique shifts, although the peak for the equatorial protons **Fe** overlapped with the tertiary proton **E** centered at 1.71 ppm.

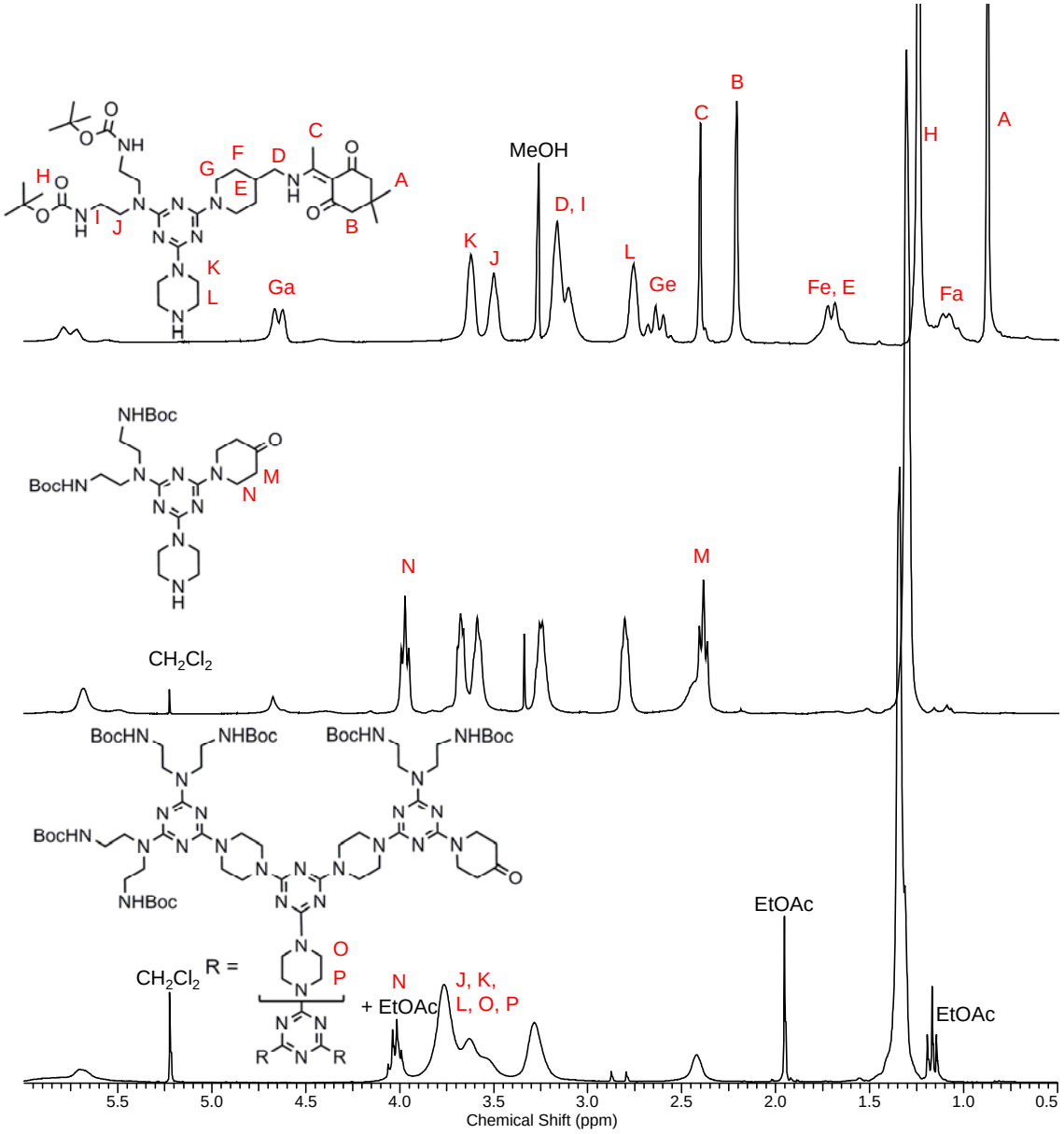

Figure 2.7. ^{1}H NMR spectra of dendrons **2.4** and **2.10**, and dendrimer **2.15**.

Dendron **2.10**, with piperidone in place of Dde-amp, has no overlapping peaks. The methylene protons of the piperidone ring have unique shifts, with **M** at 2.39 ppm and **N** at 3.98 ppm. Upon substitution of cyanuric chloride to form dendron **2.11**, and coupling to the core to form dendrimer **2.15**, the most notable change in the spectra is the shift of protons **L** from 2.81 ppm into the cluster of piperazine (and **J**) peaks from ~3.9-3.5 ppm. Confirmation of complete substitution on the dendrimer is offered by integration of this entire mass of peaks, which contains the core piperazine peaks (108 H), to the broad singlet for the Boc methyl protons (**H**) at 1.34 ppm (162 H). In the model hydrazone studies the most notable change to the spectrum of **2.10** upon conjugation of 4-nitro-benzoic hydrazide is the appearance of the benzoic protons at 8.15 and 7.98 ppm.

^{13}C NMR Spectroscopy. The ^{13}C NMR spectra for all intermediates appeared as expected. Characteristic peaks for the quaternary, allyl, vinyl, and methyl carbons of the Dde-amp and Boc groups were observed in the spectra for compounds **2.1-2.9** (Appendix A). The carbonyl carbons of Dde-amp appear at δ 198.98 and 196.79 ppm when attached to cyanuric chloride, while the carbonyl for piperidone appears at 208.9 ppm. The most notable changes in the spectra occur when a monochlorotriazine is substituted with piperazine. The monochlorotriazine carbon, which appears at ~169 ppm, disappears and a new peak at ~ 166 ppm appears. For example, when dendron **2.11** is attached to the piperazine core to form dendrimer **2.15**, the peak at 169.45 ppm disappears and a new peak at 166.83 ppm appears (Figure 2.8). All of the signals are

shifted downfield in the dendrimer as well. There are two distinct signals for the carbonyls of the Boc groups in the spectrum of **2.11**, as there are two chemically distinct Boc groups; however, there are three signals in the spectrum of **2.15**. The appearance of a third signal may be due to the presence of dendrimer rotamers. Unambiguous assignments cannot be made without 2D NMR characterization.

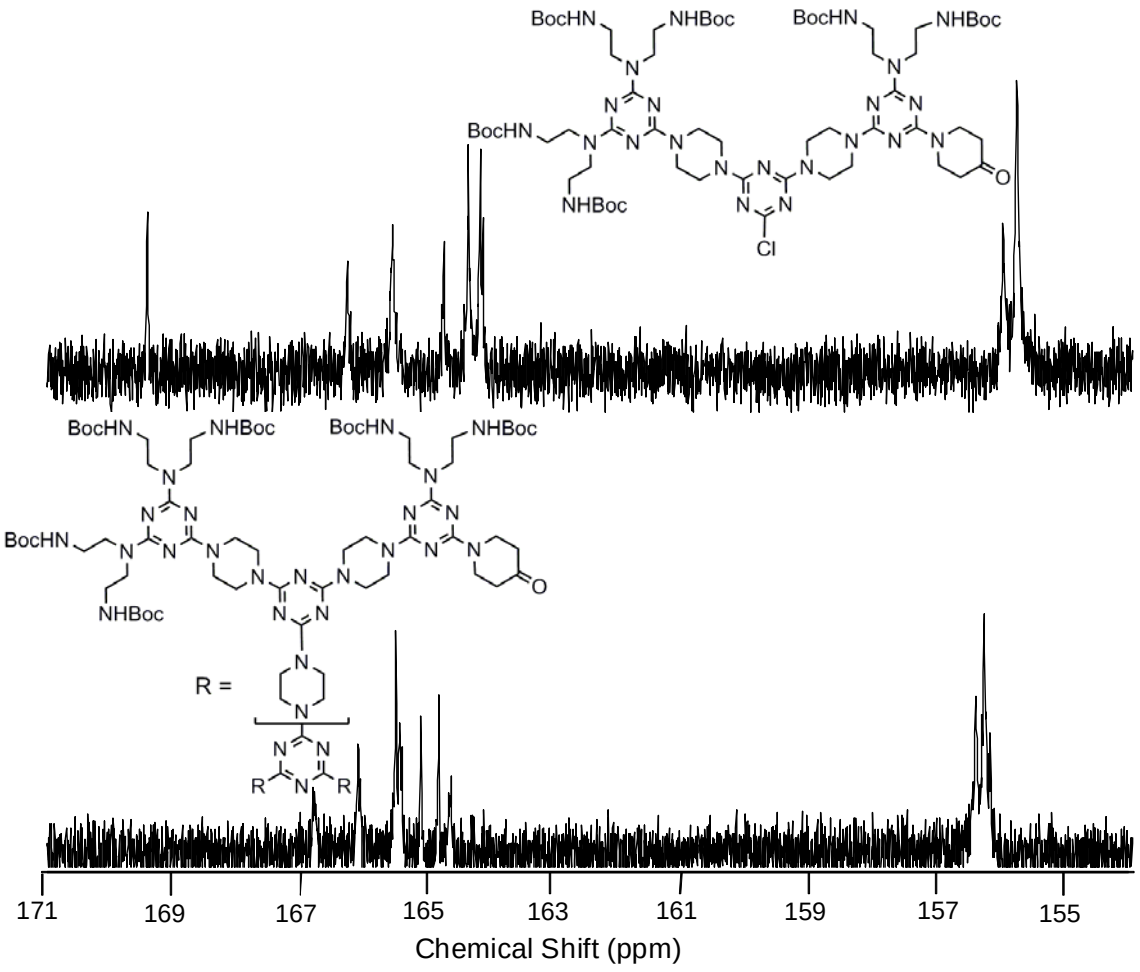

Figure 2.8. The downfield region of the ^{13}C NMRs of **2.11** and **2.15**.

The ^{13}C NMR spectrum of the model conjugate from **2.10** is most diagnostic, as the carbonyl peak at 208 ppm is gone and replaced with a peak at ~165 ppm, which is overlapped with triazine peaks, confirming hydrazone formation. Additional peaks at ~120-140 ppm are visible for the benzoic carbons.

Mass Spectrometry. Mass spectra for all compounds are provided in Appendix A. All spectra show single lines for $(M + H)^+$ as the parent ion, except intermediates **2.3** and **2.5** whose $(M + Li)^+$ is the parent ion. Dendrons containing chlorotriazines are often difficult to ionize using ESI, and lithium is added to facilitate ionization. Many spectra also have $(M + Li)^+$, $(M + Na)^+$, and/or $(M + K)^+$ peaks. Two intermediates, **2.1** and **2.8**, have peaks at -56 m/z, which are the result of the loss of isobutene, which is a common fragmentation for Boc-containing molecules. Loss of the entire Boc group during ionization is also common, particularly for larger molecules ionized using MALDI, as evidenced in the spectra for dendrons **2.9**, **2.11**, **2.12** (Appendix A), and dendrimer **2.15** (Figure 2.9).

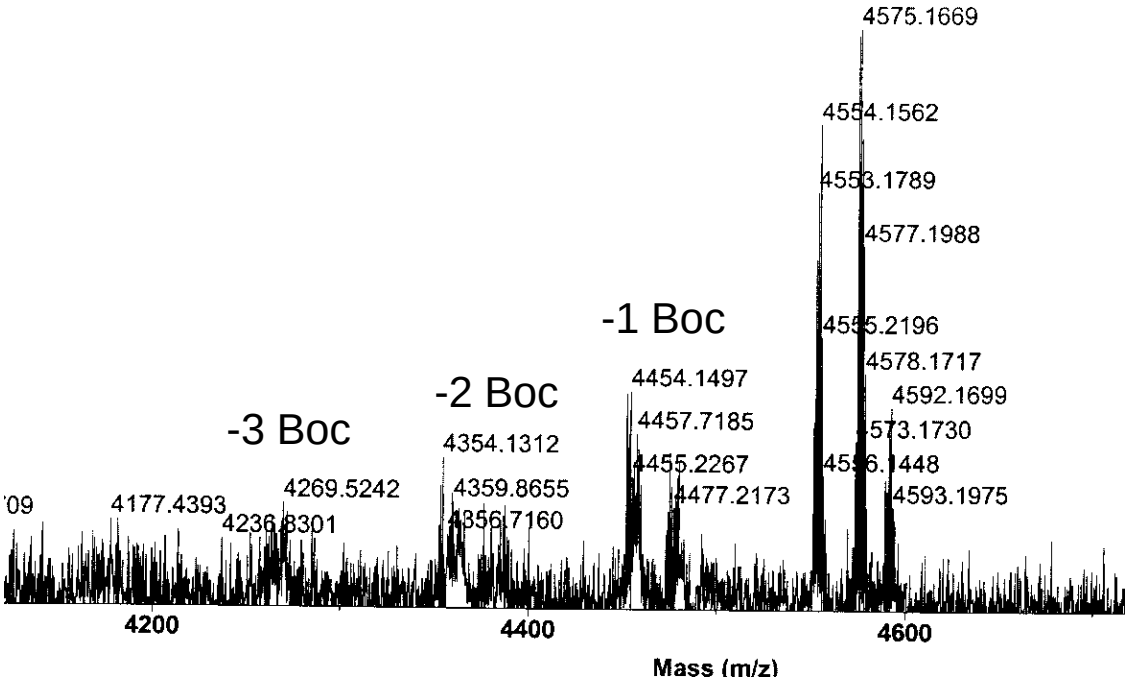

Figure 2.9. Mass spectrum of compound **2.15** showing loss of Boc.

Conclusions

Generation-1 dendrons with orthogonally-protected Boc- and Dde- surface amines were synthesized through a convergent protocol. The Dde-aminomethyl piperidine was replaced with piperidone, decreasing the number of protecting group manipulations necessary, and offering a handle for the conjugation of the antihypertensive drug hydralazine through a hydrazone bond. A generation-2 dendrimer was synthesized from the piperidone-containing dendron and a *tris*-piperazine core. The related generation-3 dendrimer was not successfully obtained due to steric encumbrance. The dendrimer and all intermediates were characterized by ^{1}H and ^{13}C NMR spectroscopy and mass spectrometry.

Future studies for this dendrimer include the conjugation of hydralazine and studies of the pH-dependency of hydrazone hydrolysis. Hydralazine is a strong nucleophile, and readily forms hydrazones under various conditions, including physiological.[122] Since the hydrazone bond is acid-labile, the Boc groups of the dendrimer must be removed prior to hydrazone formation. Hydralazine may then be reacted with the amine-terminated dendrimer (Figure 2.7) in methanol or DMF under water-free conditions to best ensure hydrazone formation (Figure 2.10).

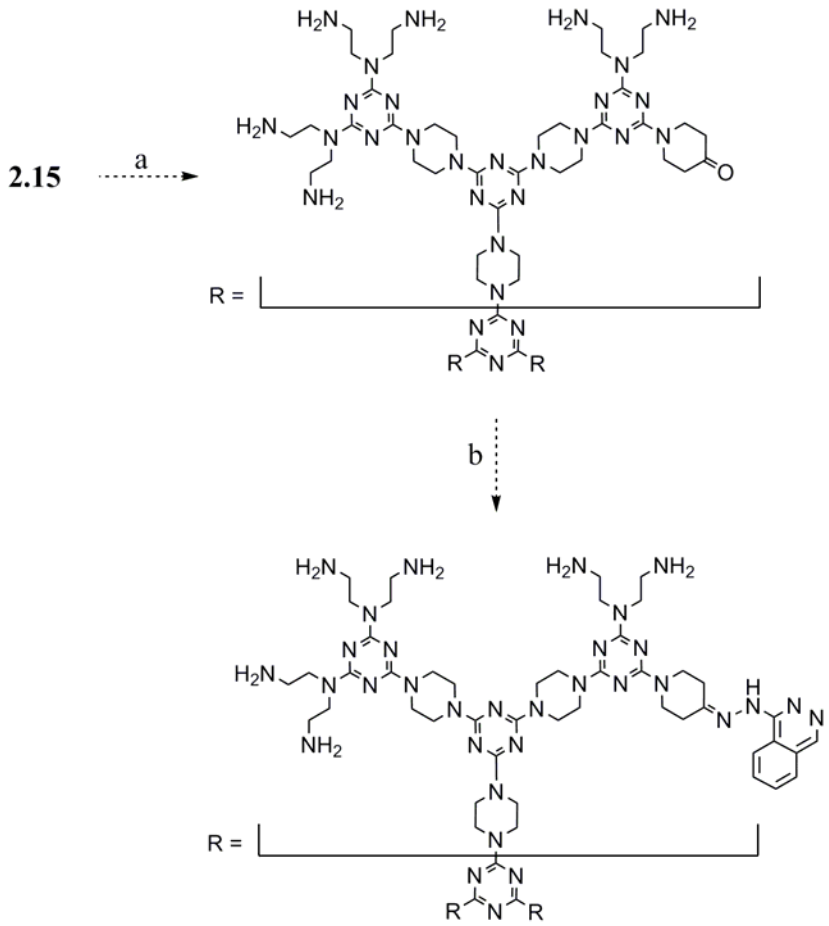

Figure 2.10. Proposed synthesis of a hydralazine conjugate. (a) MeOH, HCl (b) hydralazine, MeOH.

Experimental

All chemicals were purchased from Sigma-Aldrich or Acros and used without further purification. All solvents were ACS grade and used without further purification. Thin-layer chromatography was performed using EMD silica gel 60 F254 pre-coated glass plates (0.25 mm). Preparative column chromatography was performed using EMD silica gel 60 (0.040 mm particle size). ^{1}H and $^{13}C\{^{1}H\}$ NMR data were acquired on a Varian 300 MHz spectrometer at 25 °C unless otherwise indicated. ^{1}H and $^{13}C\{^{1}H\}$ NMR chemical shifts are listed relative to tetramethylsilane in parts per million, and were referenced to the residual proton or carbon peak of the solvent. All mass spectral analyses were carried out by the Laboratory for Biological Mass Spectrometry at Texas A&M University. MALDI-TOF mass spectra (in the positive mode) were acquired on a Voyager-DE STR mass spectrometer equipped with a pulsed nitrogen laser emitting at 337 nm. Samples were analyzed in linear mode using an extraction delay time set at 350 ns and an accelerating voltage operating at 25 kV utilizing trihydroxyacetophenone as the matrix. To improve the signal-to-noise ratio, 100 single shots were averaged for each mass spectrum, and typically, four individual spectra were accumulated to generate a summed spectrum. Electrospray mass spectra were acquired in the positive ion mode using a MDS Sciex API Qstar Pulsar using an Ionwerks time-to-digital converter, TDCx4, for data recording at 625 ps time resolution. Samples were electrosprayed from acetonitrile at 50 mM under the conditions listed next. The ion spray (needle) voltage was held constant at 4.5 kV. The nozzle skimmer potential was set to +10 V to minimize fragmentation in that region. TOF voltages were tuned to optimize the resolving power

over the mass range observed, but usually the following parameters were used: grid -338 V, plate +360 V, mirror +960 V, and liner +4000 V. Acquisition and data analysis were performed with the Analyst QS software.

1,7-Bis(Boc)diethylenetriamine (2.1). Diethylenetriamine (1.00 g, 9.70 mmol, 1.0 equiv) and triethylamine (2.94 g, 29.1 mmol, 3.0 equiv) were dissolved in 50 mL of THF and cooled in an ice bath. BOC-ON (4.78 g, 19.40 mmol, 2 equiv), dissolved in 20 mL THF, was added dropwise to this mixture, which was stirred for an hour in an ice bath and then at room temperature for another hour. The solvent was evaporated and the residue was dissolved in 100 mL dichloromethane. The mixture was washed with 5% NaOH. The product was purified by flash column chromatography (silica, 9:1 DCM:MeOH, 1% NH_4OH), to give 2.47 g (85 %). Rf = 0.63 (4:1 DCM:MeOH). ^1H NMR (300 MHz, $CDCl_3$) δ 3.19 (q, J = 5.7 Hz, 4H), 2.70 (t, J = 5.7 Hz, 4H), 1.85 (br, 2H) 1.30 (s, 18H). ^{13}C NMR (75 MHz, $CDCl_3$) δ 156.42, 79.43, 48.97, 40.43, 28.56. MS (ESI): Calcd, 304 (M^+); Found, 304.1 (M^+).

4-Dde-aminomethylpiperidine (2.2). 4-Aminomethylpiperidine (1.66 g, 14.5 mmol) and 2-acetyldimedone (2.64 g, 14.5 mmol) were dissolved in 100 mL absolute ethanol and were refluxed for three hours. The solvent was evaporated and the product was purified by flash column chromatography (silica, 4:1 DCM:MeOH, 1% NH_4OH), to give a yield of 3.50 g (87.5%). Rf = 0.075 (9:1 DCM:MeOH). ^1H NMR (500 MHz, CD_3OD) δ 3.27 (t, J = 6.0 Hz, 2H), 2.62 (m, 2H), 2.55 (s, 3H), 2.36 (br, 4H), 1.77 (m, 3H), 1.24 (m, 2H), 1.02 (s, 6H). ^{13}C NMR (125 MHz, CD_3OD) 199.96, 175.76, 108.88, 106.00, 53.55,

50.45, 46.66, 37.48, 32.01, 31.18, 28.54, 18.01. MS (ESI): Calcd, 279.21 (M^+); Found, 279.20 (M^+).

(Boc)$_2$-Dde-Cl (2.3). Cyanuric chloride (1.73 g, 9.38 mmol) and 3 mL DIPEA were dissolved in 100 mL THF and cooled to 0 °C. 1,7-*Bis*(Boc)diethylenetriamine (**1**) (2.85 g, 9.38 mmol) was dissolved in 50 mL THF and added dropwise to the cold solution of cyanuric chloride and DIPEA. After all of the amine had reacted, as monitored by thin layer chromatography, another 3mL of DIPEA and 4-Dde-amp (**2**) (2.61 g, 9.38 mmol) were added and the reaction mixture was stirred at room temperature overnight. The solvent was evaporated and the residue was dissolved in about 50 mL of CH_2Cl_2. The resulting solution was washed with water in three 100 mL portions. The CH_2Cl_2 layer was dried with $MgSO_4$ and the solvent was evaporated. The product was isolated by flash column chromatography (silica, 3:1 DCM:EtOAc) (4.87 g, 75%). Rf = 0.30 (3:1 DCM:EtOAc). ^{1}H NMR (500 MHz, CD_3OD) δ 4.77 (br, 2H), 3.65 (m, 4H), 3.46 (m, 2H), 3.31 (m, 4H), 2.93 (t, *J* = 12.5 Hz, 2H), 2.59 (s, 3H), 2.39 (s, 4H), 2.01 (br, 1H), 1.89 (d, *J* = 10.5 Hz, 2H), 1.42 (s, 18H), 1.30 (m, 2H), 1.05 (s, 6H). ^{13}C NMR (75 MHz, $CDCl_3$) δ 199.24, 196.81, 173.67, 169.40, 165.77, 163.93, 156.29, 156.04, 108.03, 79.30, 79.19, 53.51, 52.28, 48.92, 47.87, 47.52, 43.33, 39.49, 39.13, 36.42, 30.16, 29.88, 29.72, 28.63, 28.43, 28.38, 28.32,18.02. MS (ESI): Calcd, 693.39 (M^+); Found, 693.39 (M^+), 699.40 ($M + Li^+$), 715.37 ($M + Na^+$).

***(Boc)$_2$-Dde-piperazine (2.4)*.** (Boc)$_2$-Dde-Cl (**2.3**) (3.49 g, 5.04 mmol) and piperazine (2.17 g, 25.2 mmol) were dissolved in about 150 mL THF. The mixture was stirred at room temperature overnight. The solvent was evaporated and the product was obtained

by flash column chromatography (19:1 DCM:MeOH) (3.20 g, 90%). Rf = 0.33 (9:1 DCM:MeOH). ^{1}H NMR (500 MHz, $CDCl_3$) δ 5.79 (br, 1H), 5.69 (br, 1H), 4.78 (m, 2H), 3.74 (m, 4H), 3.64 (br, 4H), 3.30 (m, 6H), 2.89 (m, 4H), 2.75 (m, 2H), 2.55 (s, 3H), 2.36 (br, 4H), 1.88 (m, 3H), 1.39 (s, 18H), 1.22 (m, 2H), 1.02 (s, 6H). ^{13}C NMR (75 MHz, $CDCl_3$) δ 198.98, 196.79, 173.50, 166.50, 165.36, 165.07, 164.77, 164.50, 156.07, 107.88, 78.90, 68.05, 61.50, 53.28, 52.15, 49.00, 46.27, 45.51, 43.62, 39.98, 36.54, 29.75, 28.18, 17.88. MS: Calcd, 743.49 (M^+); Found (ESI), 743.46 (M^+).

(Boc)$_2$-Cl$_2$ (2.5). Cyanuric chloride (2.91g, 15.8 mmol) was dissolved in 100 mL of THF and cooled to 0 °C in an ice bath. DIPEA (4.25 ml, 23.7 mmol) was added to the cold solution. 1,7-*Bis*(Boc)diethylenetriamine **1** (4.8 g, 15.8 mmol) was dissolved in 100 mL of THF and added dropwise to the cold cyanuric chloride solution over 1 hour. The mixture was stirred at 0 °C for an additional 45 minutes. The solvent was removed *in vacuo* and the resulting solids dissolved in 50 mL dichloromethane. The solution was washed with 50 mL of water (2X) and with 50 mL of brine (1X). The organic layer was dried with Na_2SO_4, filtered, and the solvent was removed *in vacuo*. The resulting residue was dissolved in a minimal amount of dichloromethane, and 100 mL of hexanes was added slowly. The resulting precipitate was filtered and dried under vacuum overnight (6.814 g, 96%). Rf = 0.51 (3:2 DCM: EtOAc). ^{1}H NMR (300 MHz, $CDCl_3$) δ 5.27 (s, 0.5H), 5.02 (br, 1.5H), 3.71 (t, $^{3}J_{H\text{-}H}$ = 6Hz, 4H) 3.36 (m, 4H), 1.36 (s, 18H). ^{13}C NMR (75 MHz, $CDCl_3$) δ 170.20, 165.87, 156.29, 79.87, 48.87, 38.80, 28.48. MS: Calcd, 450.1549 (M^+); Found (ESI), 457.1625 $(M+Li)^+$.

(Boc)$_4$-Cl (2.6). Cyanuric chloride (0.260 g, 1.41 mmol) and 1,7-*Bis*(Boc)diethylenetriamine **2.1** (0.86 g, 2.83 mmol) were dissolved in 20 mL of THF. DIPEA (1.01 mL, 5.65 mmol) was added and the mixture was stirred at room temperature for 16 hours. The solvent was removed *in vacuo* and the residue dissolved in DCM. The organic layer was washed with 20 mL of water (2X) and with 20 mL of brine (1X). The organic layer was dried with Na_2SO_4, filtered, and the solvent was removed *in vacuo* to yield a white solid (0.9996 g, 99%). Rf = 0.44 (3:2 DCM:EtOAc). ^{1}H NMR (300 MHz, $CDCl_3$) δ 5.61 (br, 1.5 H), 5.20 (br, 1.5 H), 3.60 (m, 8H), 3.29 (m, 8H), 1.38 (s, 36H). ^{13}C NMR (75 MHz, $CDCl_3$) δ 169.13, 165.46, 156.43, 79.45, 48.15, 47.39, 39.65, 37.85, 28.62. MS: Calcd, 717.3940 (M^+); Found (ESI), 718.3982 $(M+H)^+$.

(Boc)$_4$-piperazine (2.7). Boc$_4$-Cl **6** (4.5 g, 6.26 mmol), and piperazine (2.698 g, 31.32 mmol) were dissolved in 180 mL THF and the solution was stirred at room temperature for 2 days. The solvent was removed *in vacuo* and the residue was purified by silica column chromatography with 4:1 DCM:MeOH. Rf = 0.65, 4.450 g, 92%. ^{1}H NMR (300 MHz, $CDCl_3$) δ 5.72 (br, 3H), 5.26 (s, 1H), 3.69 (br, 4H), 3.61 (br, 4H), 3.55 (br, 4H), 3.27 (br, 8H), 2.84 (br, 4H). NMR (75 MHz, $CDCl_3$) δ 166.10, 164.71, 156.44, 79.38, 47.52, 46.77, 46.00, 43.38, 40.84, 38.58, 28.64. MS: Calcd, 767.5018 (M^+); Found (ESI), 768.5382 $(M+H)^+$.

(Boc)$_4$-Cl$_2$ (2.8). Cyanuric chloride (1.07 g, 5.782 mmol) was dissolved in 50 mL of THF and cooled to 0 °C in an ice bath. Boc$_4$-piperazine **7** (3.7 g, 4.82 mmol) was dissolved in 50 mL of THF and added dropwise to the cold cyanuric chloride solution. The mixture was stirred at 0 °C for 4 hours and the solvent was removed *in vacuo*. The

residue was dissolved in dichloromethane and washed with three 50 mL portions of water. The organic layer was dried with Na_2SO_4, filtered, and the solvent removed *in vacuo*. The solids were dissolved in a minimal amount of DCM and hexanes was added to precipitate the product (2.566 g, 58% yield). ^{1}H NMR (300 MHz, $CDCl_3$) δ 5.58 (br, 3H), 5.29 (s, 1H), 3.91 (m, 4H), 3.84 (m, 4H), 3.65 (br, 4H), 3.58 (br, 4H), 3.32 (m, 8H), 1.40 (s, 36H). ^{13}C NMR (75 MHz, $CDCl_3$) δ 170.64, 165.99, 164.36, 156.49, 156.28, 79.49, 47.74, 47.05, 44.28, 43.10, 40.68, 38.46, 28.70, 28.65. MS: Calcd, 914.4409 (M^+); Found (MALDI-TOF), 915.2529 $(M+H)^+$, 937.2355 $(M+Na)^+$.

(Boc)$_6$-Dde-Cl (2.9). Boc_4-Cl_2 **2.8** (0.122 g, 0.1331 mmol) and $(Boc)_2$-Dde-piperazine **2.4** (0.099 g, 0.1331 mmol) were dissolved in 20 mL of THF. DIPEA was added (0.07 mL, 0.3993 mmol) was added and the mixture was stirred 16 hours at room temperature. The solvent was removed *in vacuo*. The resulting residue was dissolved in 15 mL of DCM and was washed with 10 mL of water (2X) and with 10 mL of brine (1X). The organic layer was dried with Na_2SO_4, filtered, and the solvent was removed *in vacuo*. The resulting residue was dissolved in a minimal amount of dichloromethane, and hexanes was added to form a precipitate (0.1575g, 73%). ^{1}H NMR (300 MHz, $CDCl_3$) δ 5.63 (br, 5H), 4.77 (d, $^3J_{H\text{-}H}$ = 12 Hz, 2H), 3.81 (br, 16H), 3.59 (br, 12H), 3.30 (br, 14H), 2.78 (t, 2H), 2.54 (s, 3H), 2.35 (s, 4H), 2.02 (br, 1H), 1.85 (d, 2H), 1.40 (br, 54H), 1.24 (br, 2H), 1.02 (s, 6H). ^{13}C NMR (75 MHz, $CDCl_3$) 199.22, 196.93, 173.82, 169.94, 166.03, 164.68, 156.44, 156.28, 108.20, 79.32, 53.66, 49.27, 47.65, 46.92, 46.71, 43.56, 43.19, 40.79, 40.53, 38.48, 36.80, 31.80, 30.34, 30.06, 28.64, 22.86, 18.21. MS: Calcd,

1620.9496 (M^+); Found (MALDI-TOF), 1621.6767 $(M+H)^+$, 1643.6596 $(M+Na)^+$, 1659.6321 $(M+K)^+$.

(Boc)$_2$-piperidone-piperazine (2.10). Boc_2-Cl_2 **2.5** (0.50 g, 1.108 mmol) was dissolved in 10 mL THF with Et_3N (1.6 mL, 11.08 mmol) and cooled to 0 ºC in an ice bath. 4-Piperidone·HCl·H_2O (0.170 g, 1.108 mmol) was dissolved in a minimal amount of H_2O and added to the cold THF solution. The reaction was stirred and allowed to come to room temperature over 3 hours. The reaction progress was monitored by TLC (3:2 DCM:EtOAc). The THF was removed *in vacuo*, and the residue taken up in 50 mL DCM. The organic layers were washed three times with 50 mL H_2O and once with 50 mL brine. The DCM was removed *in vacuo*, and the solids were dissolved in 30 mL THF. Piperazine (0.477 g, 5.5.4 mmol) and DIPEA (0.17 mL, 1.108 mmol) were added and the reaction was stirred at room temperature overnight. The THF was removed *in vacuo*, and the residue taken up in 50 mL DCM. The organic layers were washed three times with 50 mL H_2O and once with 50 mL brine. The DCM was removed *in vacuo*, and the solids purified by silica gel column chromatography. Rf = 0.26 (9:1 DCM:MeOH; 1% NH_4OH), 0.5436 g, 87% overall yield. ^{1}H NMR (300 MHz, $CDCl_3$) δ 5.68 (br, 1H), 3.98 (t, 4H), 3.68 (t, 4H), 3.59 (br, 4H), 3.25 (br, 4H), 2.81 (br, 4H), 2.39 (t, 4H), 1.32 (s, 18 H). ^{13}C NMR (75 MHz, $CDCl_3$) δ 208.90, 166.82, 165.10, 164.84, 156.33, 79.27, 46.62, 46.06, 44.44, 42.71, 41.39, 40.41, 28.58. MS: Calcd, 563.354 (M^+); Found (ESI), 564.3617 $(M+H)^+$.

(Boc)$_6$-piperidone-Cl (2.11). Boc_4-Cl_2 (0.854 g, 0.932 mmol) and Boc_2-pipd-pipz (0.526 g, 0.932 mmol) were dissolved in 10 mL THF with DIPEA (0.5 mL, 2.797 mmol)

and stirred at room temperature overnight. The THF was removed in vacuo and the solids were dissolved in 50 mL DCM. The organic layer was washed three times with 50 mL H_2O and once with 50 mL brine. The DCM was removed *in vacuo*, and the solids were purified by precipitation from a minimal amount of DCM with hexanes (1.238 g, 92% yield). ^{1}H NMR (300 MHz, $CDCl_3$) δ 5.67-5.57 (br, 6H), 3.98 (br, 4H), 3.76 (br, 16H), 3.58 (br, 8H), 3.50 (br, 4H), 3.24 (br, 12 H), 2.39 (br, 4H), 1.32-1.30 (br, 54H). ^{13}C NMR (75 MHz, $CDCl_3$) δ 208.18, 169.45, 166.31, 165.61, 164.81, 164.42, 164.24, 156.04, 155.82, 78.84, 47.20, 46.45, 43.08, 42.65, 42.29, 40.93, 40.37, 39.90, 38.00, 28.21, 28.17, 28.14. MS: Calcd, 1441.8185 (M^+); Found (MALDI-TOF), 1442.9251 $(M+H)^+$, 1464.9022 $(M+Na)^+$, 1480.8792 $(M+K)^+$.

(Boc)$_4$-(piperidone)$_2$-Cl (2.12). Boc_2-pipd-pipz (1.842 g, 3.26 mmol) and cyanuric chloride (0.3 g, 1.63 mmol) were dissolved in 50 mL THF with DIPEA (1.3 mL, 7.11 mmol) and stirred at room temperature for 4 days. The THF was removed *in vacuo*, and the residue taken up in 50 mL DCM. The organic layers were washed three times with 50 mL H_2O and once with 50 mL brine. The DCM was removed *in vacuo*, and the solids purified by silica gel column chromatography. Rf = 0.37 (19:1 DCM:MeOH), 1.524 g, 75% yield. ^{1}H NMR (300 MHz, $CDCl_3$) δ 5.56 (br, 4H), 4.04 (t, 8H), 3.82 (br, 16H), 3.65 (br, 8H), 3.32 (br, 8H), 2.46 (t, 8H), 1.36-1.35 (br, 36 H). ^{13}C NMR (75 MHz, $CDCl_3$) δ 208.61, 169.96, 166.80, 165.26, 164.88, 164.70, 156.24, 79.40, 46.84, 43.54, 43.34, 43.10, 42.74, 41.41, 40.37, 28.61. MS: Calcd, 1237.6712 (M^+); Found (MALDI-TOF), 1238.7128 $(M+H)^+$, 1260.6938$(M+Na)^+$, 1276.6722 $(M+K)^+$.

(Boc-pip)$_3$ triazine (2.13). Cyanuric chloride (0.85 g, 4.59 mmol) and mono(*t*-butoxycarbonyl)piperazine (2.65 g, 14.2 mmol) were dissolved in 100 mL THF in a round bottom flask and stirred at 80 °C in the presence of K_2CO_3 (5.7 g, 41.3 mmol) overnight. THF was removed *in vacuo* and the resulting residue was dissolved in dichloromethane. The mixture was washed with three 50-mL portions of water. The dichloromethane layer was dried with $MgSO_4$, and concentrated *in vacuo*. Flash column chromatography (silica, 4:1 DCM:EtOAc) of the residue gave 2.59 g of product (86 %). Rf = 0.64 (9:1 DCM:MeOH). ^{1}H NMR (500 MHz, $CDCl_3$) δ 3.72 (t, *J* = 5 Hz, 12H), 3.42 (t, *J* = 5 Hz, 12H), 1.46 (s, 27H). ^{13}C NMR (125 MHz, $CDCl_3$) 165.49, 154.98, 80.02, 76.24, 43.16, 28.58. MS: Calcd, 634.40 (M^+); Found (ESI), 634.40 (M^+).

(Pip)$_3$ triazine (2.14). Triazine *tris*(monoboc-piperazine) **13** (2.01 g, 3.18 mmol) was dissolved in 25 mL of 1:1 TFA:DCM solution and was stirred at room temperature for three hours. The solvent was evaporated and the residue was treated with 5M NaOH until highly basic (pH 14 using pH paper). The product was extracted with three 50-mL portions of chloroform. The organic layer was dried with $MgSO_4$ and chloroform was evaporated off. The residue was dried *in vacuo* giving 1.01 g of the amine (95 %). ^{1}H NMR (300 MHz, CD_3OD) δ 4.04 (t, *J* = 5.3 Hz, 12H), 3.23 (t, *J* = 5.1 Hz, 12H). ^{13}C NMR (75 MHz, CD_3OD) 166.61, 44.43, 41.16. MS: Calcd, 334.25 (M^+); Found (ESI), 335.25 (M^+).

G2-(Boc)$_{18}$(Piperidone)$_3$ (2.15). $(Pip)_3$ triazine (0.036 g, 0.107 mmol) and BEMP resin (PS-2-tert-butylimino-2-dimethylamino-1,3-dimethylperhydro-1,3,2-diazaphosphorine; 0.73 g, 1.60 mmol) were dissolved in 20 mL THF. Boc_4-pipd-Cl (0.773 g, 0.536 mmol)

was dissolved in 20 mL THF and added to the core solution. The reaction was stirred at 80 °C for 6 days, after which the solids were removed by filtration, and the filtrate was collected and the THF removed *in vacuo*. The residue was then redissolved in 20 mL THF, BEMP resin (0.773 g, 0.536 mmol) was added, and the reaction stirred at 80 °C for an additional 6 days. The solids were removed by filtration and the filtrate was collected and the THF removed *in vacuo*. The mixture was purified by silica gel column chromatography. Rf = 0.44 (8:2 (9:1 DCM:MeOH; 1% NH_4OH):EtOAC), 0.273 g, 56% yield. ^{1}H NMR (300 MHz, $CDCl_3$) δ 6.0-5.3 (br, 18H), 4.04 (t, 12H), 3.76-3.52 (br, 108 H), 3.28 (br, 36 H), 2.42 (br, 12 H), 1.34-1.31 (br, 162 H). ^{13}C NMR (75 MHz, $CDCl_3$) δ: 208.72, 166.83, 166.14, 165.56, 165.50, 165.16, 164.89, 164.70, 156.47, 156.34, 79.25, 79.10, 47.56, 46.82, 43.29, 42.73, 41.41, 40.94, 40.44, 38.43, 28.65. MS: Calcd, 4550.7646 (M^+); Found (MALDI-TOF), 4551.1562 $(M+H)^+$, 4573.1730 $(M+Na)^+$, 4590.1311 $(M+K)^+$.

Model hydrazone (2.16). Dendron **2.10** (0.20 g, 0.354 mmol) and 4-nitro-benzoic hydrazide (0.064 g, 0.354 mmol) were dissolved in dimethylformamide (DMF, 20 mL) with 4 molecular sieves. The reaction was stirred at room temperature for 10 days. The DMF was removed in vacuo and the residue purified by precipitation from DCM with hexanes to yield **2.16** (0.2530 g, 98%). ^{1}H NMR (300 MHz, $CDCl_3$) δ: 8.15-7.98 (br, 4H), 3.94-3.55 (multiple peaks, 12H), 3.20 (br, 4H), 2.86-2.76 (br, 4H), 2.51-2.37 (br, 4H), 1.28 (br s, 18 H). ^{13}C NMR (75 MHz, $CDCl_3$) δ: 166.52, 164.82, 156.67, 149.71, 139.31, 129.06, 123.72, 79.52, 46.95, 45.59, 44.00, 43.45, 42.61, 41.29, 39.92. MS (ESI): calcd, 726.3925 (M^+); found, 727.3919 $(M + H)^+$.

CHAPTER III

A DIVERGENT ROUTE TOWARDS SINGLE-CHEMICAL ENTITY TRIAZINE DENDRIMERS WITH OPPORTUNITIES FOR STRUCTURAL DIVERSITY

Introduction

The convergent route of dendrimer synthesis has been used extensively by our group to generate dendrimers that present one surface group[21,66,69,97,100,123,124] or those with diverse, orthogonally-functional surfaces.[5,6,99,101,102,125-127] Dendrimers displaying up to six different surface groups (free hydroxyls, levulinic acid ester-protected alcohols, *tert*-butyldiphenylsilyl protected alcohols, thiopyridyl-protected thiols, Boc-protected amines, and monochlorotriazines) were obtained.[6] Although reasonable quantities of the dendrimers discussed were obtained, the synthetic burden of purification using the convergent route is great. In addition, the multimerizations of each generation building step results in a decrease in the number of moles of product by $1/n$ for AB_n monomers such that three moles of AB_3 monomer results in 1 mole of dendrimer. Finally, the highest generation attainable was generation-3, due to the steric restraints of attaching large dendrons onto a small core.

Divergent strategies, when perfectly efficient, boast mole conservation – that is the number of moles of product obtained is equal to the number of moles of initial reagents. These reactions occur on the periphery of the molecule, allowing for the synthesis of higher generations, but the structural defects common to this strategy make isolation of a truly monodisperse dendrimer difficult. The ease of synthesis and

purification with which dichlorotriazine **2.5** was isolated led our group to pursue a divergent dendrimer synthesis based on dichlorotriazine monomers.[128] Generation-2 and -3 dendrimers were built from three different dichloride monomers and the *tris*-piperazine core. While the dendrimers showed radial symmetry with the same monomer used within a generation, a different monomer was used in each generation-building step, yielding dendrimers with diversity (hydroxyls, amines, and monochlorotriazines). Because the monomers used in this strategy are large (compared to ethylene diamine, the monomer for PAMAM dendrimers, for example) the side products resulting from over- or under-substitution are readily identified and removed. The main drawback to the strategy presented was that dendrimers of generation higher than 3 were not accessible due to insolubility caused by hydrogen bonding of the hydroxyl groups.[128]

In order to probe the limits of the new divergent strategy, a new scheme in which the same dichlorotriazine monomer is used for each generation was employed, and is described in this chapter.[129] The general route is described in figure 3.1.

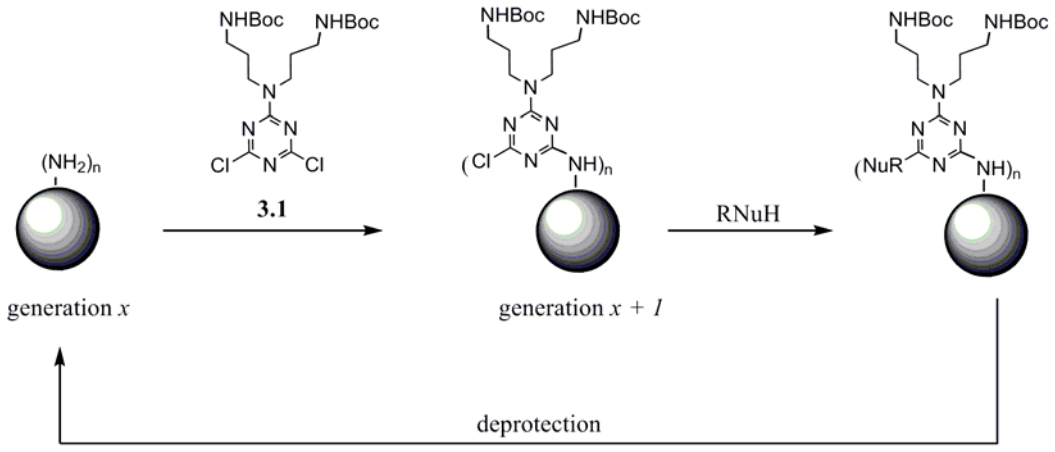

Figure 3.1. General divergent route.

The dichlorotriazine monomer **3.1** is installed onto a poly(amine) dendrimer of generation *x* to produce a dendrimer of generation *x*+1, the remaining poly(monochlorotriazine) is capped with a nucleophilic amine, piperidine here, and the resulting dendrimer is deprotected to repeat the cycle. Dendrimers will be referred to by their generation, G*n*, and functional group, -Cl, -pip, or $–NH_2$; for example, **G1-Cl** is a generation-1 poly(monochlorotriazine) dendrimer.

Results and Discussion

Synthesis. The dichlorotriazine monomer **3.1** was obtained from reaction of *bis*(Boc-dipropylenetriamine) with cyanuric chloride at 0 ºC and purified by precipitation. Dipropylenetriamine was used instead of the diethylenetriamine described in the previous chapter to afford higher solubility in organic solvents. All **G*n*-Cl** were capped with piperidine as the nucleophile because it promotes solubility in organic solvents, and it is a strong nucleophile that readily substitutes the third chloride at room temperature. The synthesis of fifteen dendrimers from G1-G5 is outlined in figure 3.2. The first step of each cycle is the only problematic one, and begins with the addition of monomer **3.1** to the *tris*-piperazine core described in the previous chapter. Reactions proceed overnight in most cases, although **G5-Cl** took several days. The reaction progress is monitored by TLC for the disappearance of the polyamine core. Although **G*n*-Cl** dendrimers have a significantly different retention factor (Rf) than **G*n*-pip**, partially-substituted intermediates are not seen, as all polyamines remain at the origin. The reaction solvent had to be evaluated and changed at almost every generation due to the solubility of the **G*n*-NH_2** dendrimers. The yields for this step also decrease at each

generation. They start at 93% for both **G1-Cl** and **G2-Cl**, and decrease to 78% for **G3-Cl**, 69% for **G4-Cl**, and finally, 25% for **G5-Cl**.

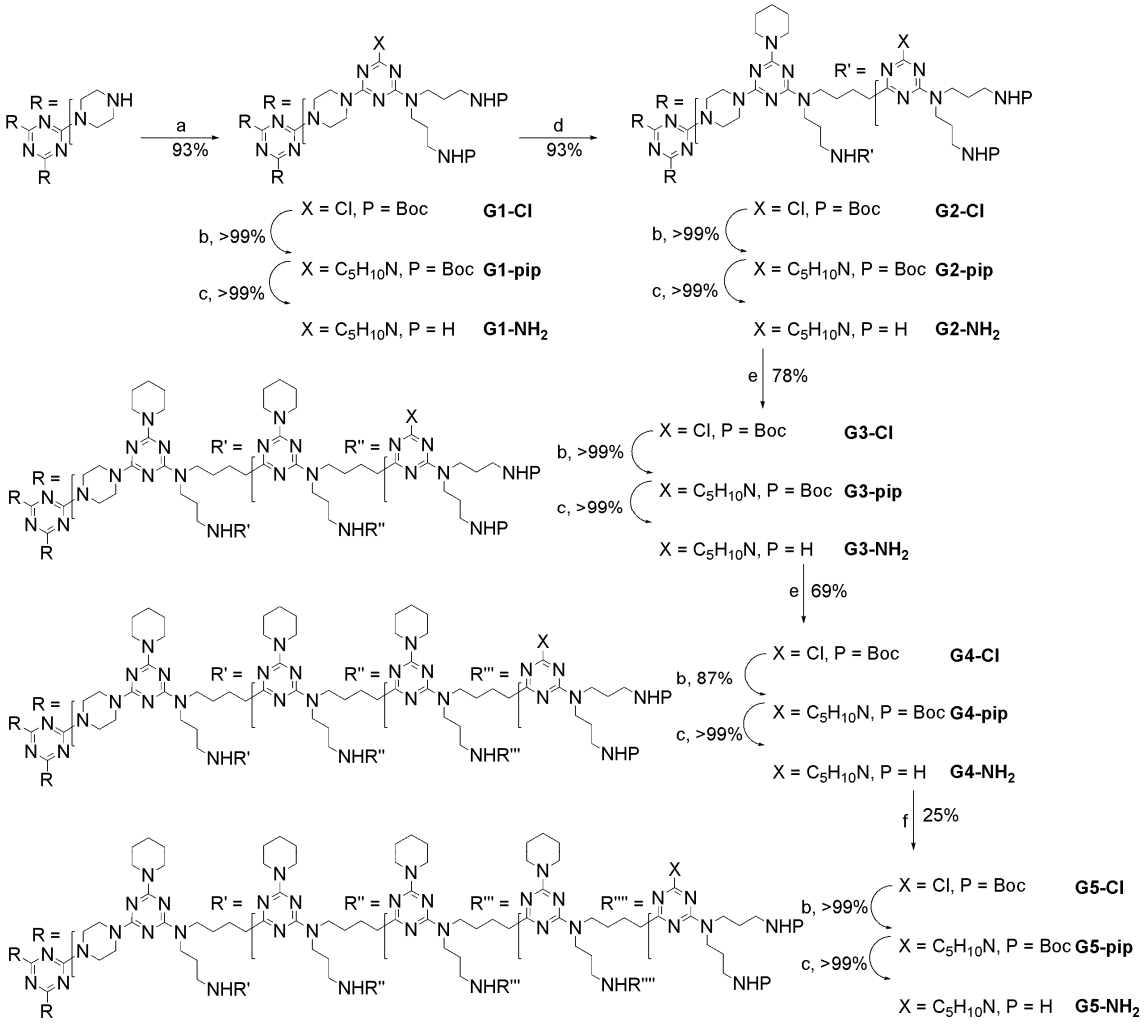

Figure 3.2. Synthesis of **G1-G5** dendrimers. (a) **3.1**, DIPEA, THF, 0-25 ºC, 15 h; (b) piperidine, THF, 25 ºC, 12-16 h; (c) 5 M HCl-MeOH, 25 ºC, 15 h; (d) **3.1**, DIPEA, THF-water, 0-25 ºC, 15 h; (e) **3.1**, DIPEA, EtOAc-DCM-water, 25 ºC; (f) **3.1**, DIPEA, $CHCl_3$, 25 ºC, 5 d.

The decline in yield is attributed to an increasing amount of dendrimers with incomplete substitutions, which remain at the origin in TLC and chromatography, and

possibly to incomplete solubilization of the **G*n*-NH$_2$** species during reaction. Tetrahydrofuran was initially chosen as a solvent because it typically solubilizes triazines well, and is more environmentally friendly than other organic solvents. However, it was necessary to move to dichloromethane and eventually chloroform for **G5-Cl**. The volley of ineffective solvents tested includes dimethylformamide, dimethylacetamide, dimethyl sulfoxide, methanol, water, THF/water with and without sodium dodecyl sulfate, and the ionic liquid octylmethylimidazolium tetrafluoroborate. The addition of heat would increase the solubility of the **G*n*-NH$_2$** cores, but it would also increase the likelihood of impurities caused by two substitutions on the monomer (Figure 3.3).

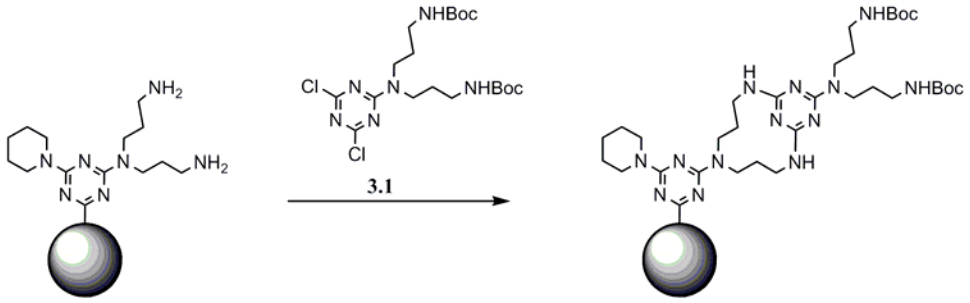

Figure 3.3. An unlikely side product becomes possible when heated.

Carrying out the reaction at room temperature prevents the formation of any impurities other than under-substituted dendrimer, as the third chloride will not react with a primary amine at room temperature. Excess monomer **3.1** was used in each generation to promote full substitution, and was removed by filtration through a silica

plug; reprecipitation from DCM with hexanes removed any residual monomer. Only **G2-Cl** required purification by column chromatography.

Throughout the generations the conditions for capping the **G*n*-Cl** dendrimers and deprotecting the **G*n*-pip** dendrimers remained constant. An excess of piperidine was used, and reactions proceeded at room temperature overnight. Especially for smaller generation dendrimers, the reaction is most likely complete well before 16 hours, but it is impossible to follow the reaction by TLC as the **G*n*-Cl** and **G*n*-pip** dendrimers have very similar polarities, and any dendrimers with incomplete substitutions are indistinguishable. Excess piperidine is removed by filtration of the reaction mixture through silica, after which the THF is removed and the residue taken up in DCM. The DCM is washed with water to remove any remaining piperidine or its salts. The products were obtained by either simply removing the DCM *in vacuo*, or reducing the DCM *in vacuo* followed by precipitation with hexanes. The precipitation protocol is more effective at reducing the amount of solvent that remains encapsulated in the dendrimer interior; however, an effective precipitation protocol for **G5-pip** could not be found – it remained as a residue which was subjected to vacuum to remove entrapped solvent.

Deprotection of **G*n*-pip** was carried out using 5 M HCl in methanol with a slight amount of DCM. Reactions were stirred at room temperature overnight, although they are most likely complete within hours. The reaction cannot be followed by TLC as the partially deprotected dendrimers adhere to silica, and cannot be distinguished from the

fully deprotected products. The dendrimer is isolated by extraction with $CHCl_3$, and not further purified.

Characterization

Materials were characterized by NMR spectroscopy, mass spectrometry (MS), HPLC, and/or GPC (Appendix B). Although the assessment of purity for G4 and G5 dendrimers may be slightly imprecise, the lower generations can be confidently labeled as pure within the standards of conventional organic chemistry (>97%). They are certainly at least as pure as, if not more so, other dendrimers in the literature.

NMR Spectroscopy. Except for G1, NMR spectroscopy is of somewhat limited use, as the lines become very broad and overlapped. Fortunately, in the ^{1}H NMR spectra of **G*n*-Cl** and **G*n*-pip** the C***H***$_2$NHBoc peak stands alone at ~3 ppm, and can be integrated with respect to the mass of peaks from ~3.8-3.2 ppm, which contains the cyclic and acyclic methylene protons α to triazine-bound nitrogens (Figure 3.4). The extent of substitution can be observed by defining the integration of the C***H***$_2$NHBoc peak, and comparing the expected and observed values of the integration for the α-protons. G1-G4 appear to be completely substituted, while the integration for **G5-Cl** is slightly lower than expected, suggesting incomplete substitution. The integration for **G5-pip** matched the expected value; however, this is rather coincidental as the observed integration is higher than it should be due to the presence of THF.

^{1}H NMR spectroscopy of **G*n*-NH$_2$** dendrimers is useful to confirm complete Boc-deprotection by the disappearance of the *tert*-butyl protons at 1.4 ppm and the upfield shift of the C***H***$_2$NHBoc; for example the peak shifts from 3.07 to 2.68 ppm when

G1-pip is deprotected to reveal **G1-NH_2**. These spectra lack the resolution of the **G*n*-Cl** and **G*n*-pip** dendrimers, especially at higher generations, due to their insolubility.

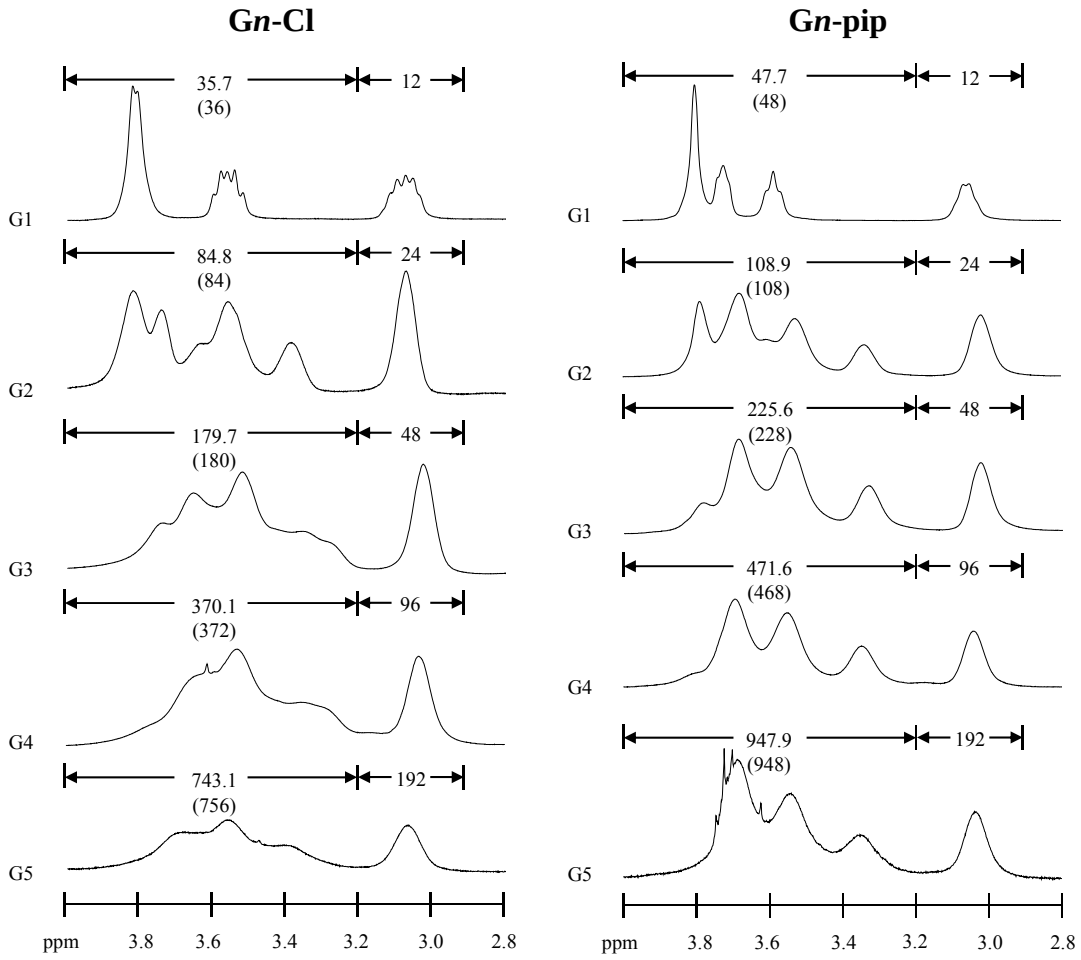

Figure 3.4. ^{1}H NMR spectra of the aliphatic region of **G*n*-Cl** and **G*n*-pip**. The integration regions are indicated with arrows. The integration of the upfield peak is assigned, and the expected (in parentheses) and observed values for the downfield region are shown.

The ^{13}C NMR spectra are mostly unremarkable except for two features. The monochlorotriazine peak at ~169 in **G*n*-Cl** dendrimers moves to ~167 upon substitution

with piperidine, and the peaks from the Boc group at ~156, 79, and 28 ppm are not present in **G*n*-NH$_2$** spectra.

Mass Spectrometry. MS confirms the purity of G1-G3 dendrimers at isotopic resolution, with no lines seen for partially substituted intermediates (Appendix B). Peaks showing losses of Boc during ionization are common in all **G*n*-Cl** and **G*n*-pip** spectra. The trace for **G4-Cl** (Figure 3.5) shows a tailing at the molecular ion peak and in the doubly-charged M^{2+} peak that is attributed to loss of Boc, as lines are evenly spaced at 100 *m/z* values apart. Although these lines are not the result of impurities, they obscure the possible presence of under-substituted intermediates. The spectrum for **G4-pip** does not show this tailing, offering additional confirmation that the tailing is an artifact of loss of Boc during ionization. The spectrum for **G4-NH$_2$** is broader, and extends to both higher and lower m/z values than the calculated mass, making interpretation difficult. Spectra for **G5-Cl** and **G5-pip** are also very broad and appear at lower *m/z* than expected, which may be caused by impurities or simply the limitations of the instrument. **G5-NH$_2$** was not soluble enough to obtain a spectrum.

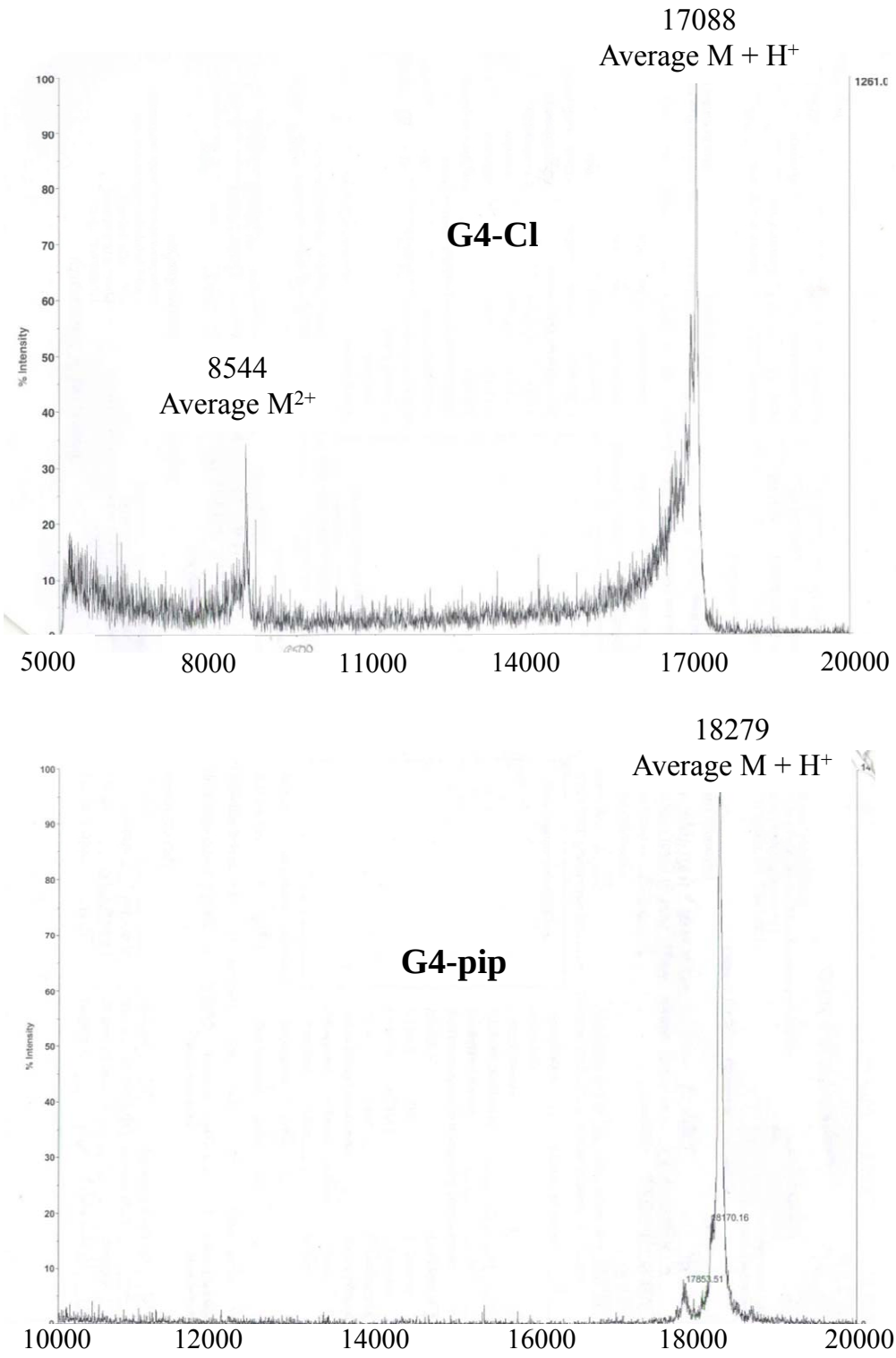

Figure 3.5. MALDI-TOF mass spectra of **G4-Cl** and **G4-pip**.

Chromatography. **G*n*-Cl** dendrimers were analyzed by both reverse phase high performance liquid chromatography (HPLC) and gel permeation chromatography (GPC), and **G*n*-pip** were analyzed by HPLC. With both techniques G5 dendrimers did not elute from the columns. **G1-Cl** through **G3-Cl** showed sharp HPLC traces, but **G4-Cl** showed tailing, and was significantly broader than the lower generations (Figure 3.6).

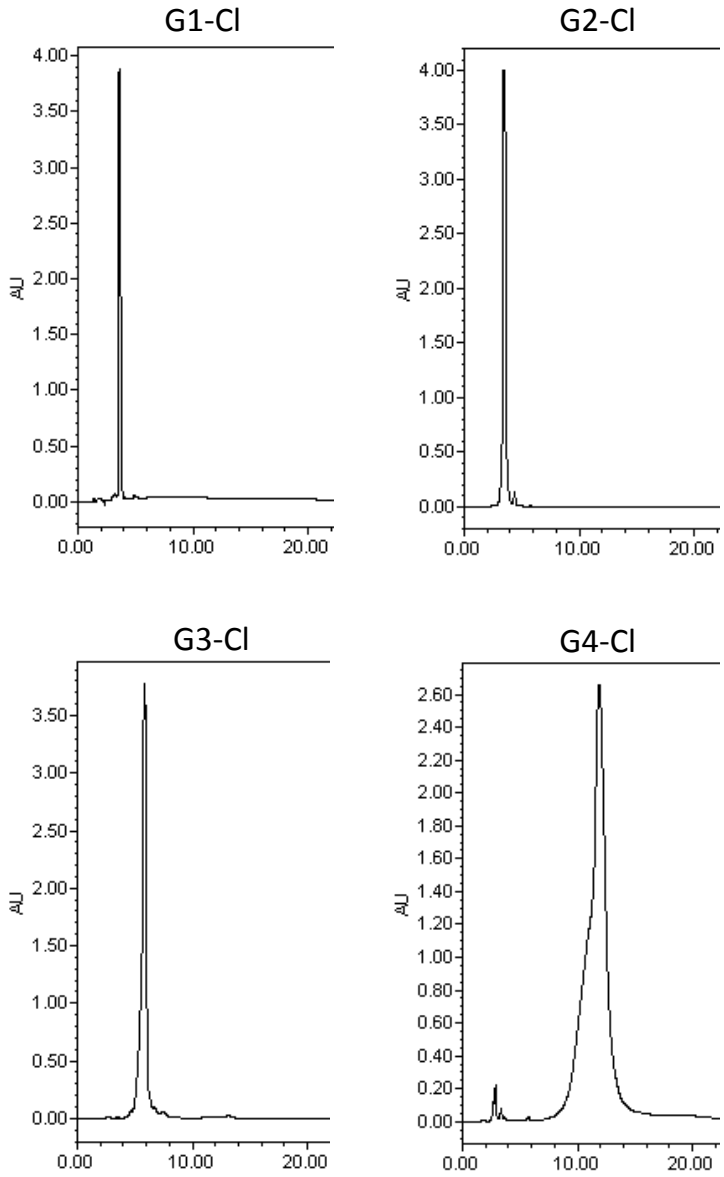

Figure 3.6. HPLC traces of **G1-Cl** through **G4-Cl.**

The traces for **G1-pip** through **G3-pip** were also very sharp, and the trace for **G4-pip** was much sharper than **G4-Cl** and did not show tailing. Interestingly, the **G*n*-pip** dendrimers were retained much longer in the HPLC column; a column with a 300 Å pore size (in place of 100 Å pore size) had to be used in order to elute all **G1-pip** to **G4-pip**.

The GPC traces of **G1-Cl** through **G3-Cl** are symmetric and have similar peak widths at half-height and at the base (Table 3.1), but the trace for **G4-Cl** shows some tailing (Figure 3.7). Although the peak width at half-height is only slightly larger than **G3-Cl**, the width at the base is significantly larger, again suggesting the presence of some impurities.

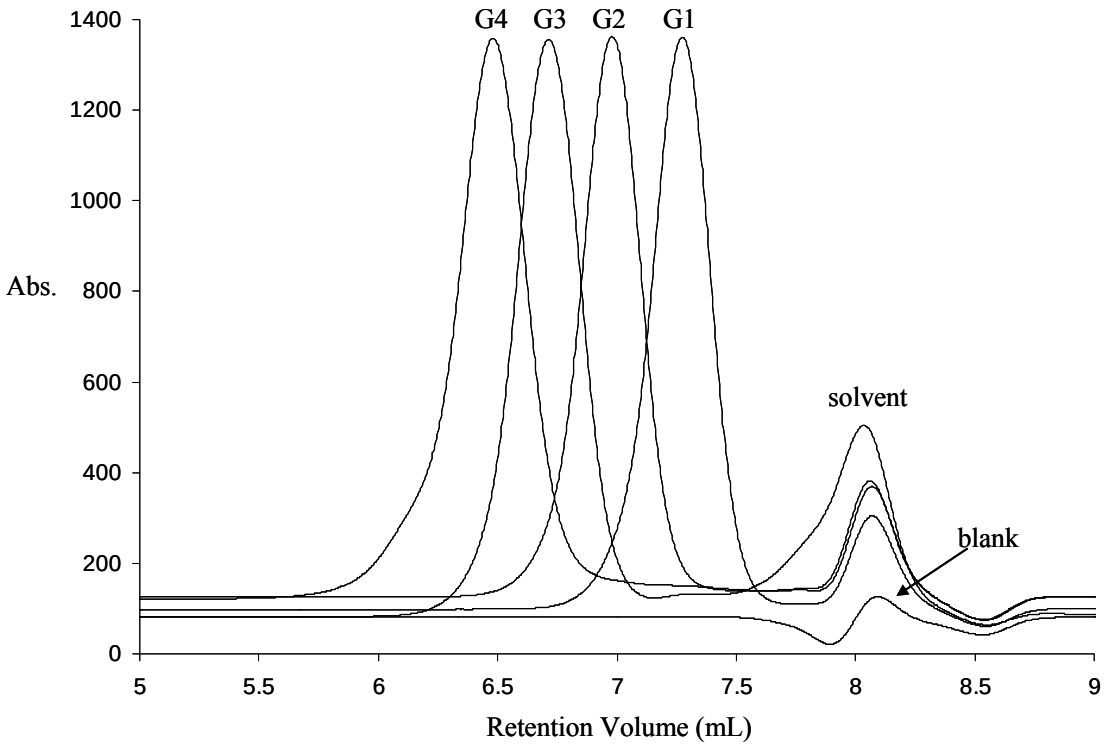

Figure 3.7. GPC traces of **G1-Cl** through **G4-Cl** and a blank.

Table 3.1. The peak widths of GPC traces of **G1-Cl** through **G4-Cl** are reported in terms of retention volume (mL).

Generation	Peak width at half-height (mL)	Peak width at base (mL)
1	0.2934	1.3740
2	0.2977	1.2367
3	0.3200	1.0900
4	0.3433	1.9533

Computational Models. Gas-phase computational models of **G*n*-pip** dendrimers show the formation of globular structures for G4 and G5 (Figure 3.8). In smaller generations the three arms of the dendrimer (colored in red, blue, and green) interact with each other and are bent towards one side of the dendrimer, and the core (colored in purple) is on the other side. These dendrimers are not sterically hindered enough to segregate into specific regions. However, in G4 and particularly in G5 the core is internalized, and the arms each occupy a specific region of space. **G1-pip** measures approximately 20 Å in diameter, while **G5-pip** measures 50 Å. Even though the dendrimers will behave differently in solution, these calculations provide a first approximation of the three-dimensional structures.

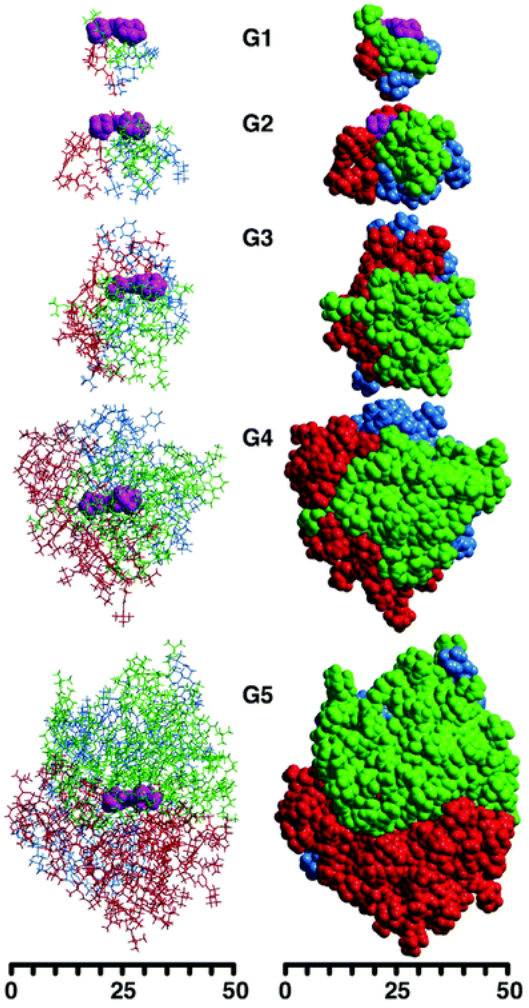

Figure 3.8. Computational models of **G1-pip** through **G5-pip**. The core is shown in purple and the three arms of the dendrimer are shown in red, blue, and green.

Conclusions

The synthesis and characterization of a series of fifteen dendrimers of generations 1-5 was accomplished. The divergent route used offers a facile synthesis and purification of dendrimers of higher generations than the convergent route previously employed by our group, while maintaining excellent purity. The differential reactivity of cyanuric chloride towards amines provides a means to control reactions and

prevent side products by controlling the temperature of reaction. Although piperidine was the only nucleophile used here, the general route is amenable to the addition of diversity through use of some other functionalized nucleophile, and possibly using different nucleophiles at each generation.

^{1}H NMR spectroscopy indicates that reactions are complete up to **G4-NH$_2$** by integration, and mass spectroscopy confirms that assignment. HPLC and GPC of **G*n*-Cl** dendrimers show sharp peaks for G1-G3, but **G4-Cl** appears to have a small amount of impurities that are similar in size and polarity to the fully-substituted dendrimer. The G1-G3 dendrimers can be confidently assigned as pure by conventional organic chemistry standards, but the assignment of purity to higher generations remains tentative. The reliance on NMR, a somewhat insensitive technique, combined with broad yet appropriately centered peaks in MS, allows us only to confirm that these larger dendrimers are at least as pure as commercially available dendrimers of equal generation.

Experimental

All chemicals were purchased from Sigma-Aldrich or Acros and used without further purification. All solvents were ACS grade and used without further purification.

Computational results were obtained using the software package Cerius2 4.9 by Accelrys Inc. Minimization and dynamics calculations were performed with the Open Force Field (OFF) program, using the pcff second-generation force field. The dendrimer was initially drawn and minimized in a fully extended conformation. Constant volume and temperature (NVT) molecular dynamics (MD) calculations were then performed on

the minimized structure via simulated annealing. The simulated annealing was carried out for 560.0 ps, over a temperature range of 300–1000 K, with DT = 50 K, using the T-Damping temperature thermostat, a relaxation time of 0.1 ps, and a time step of 0.001 ps. The dendrimer was minimized after each annealing cycle, resulting in 200 structures

Thin-layer chromatography was performed using EMD silica gel 60 F254 pre-coated glass plates (0.25 mm). Preparative column chromatography was performed using EMD silica gel 60 (0.040 mm particle size). ^{1}H and $^{13}C\{^{1}H\}$ NMR data were acquired on a Varian 300 MHz spectrometer at 25 °C unless otherwise indicated. ^{1}H and $^{13}C\{^{1}H\}$ NMR chemical shifts are listed relative to tetramethylsilane in parts per million, and were referenced to the residual proton or carbon peak of the solvent. MS analyses were performed by the Laboratory for Biological Mass Spectrometry at Texas A&M University. MALDI-TOF mass spectra were obtained on an Applied Biosystems voyager-DE STR Biospectrometry workstation. Samples were diluted to 0.1 mg ml^{-1} and mixed with 2,4,6-trihydroxyacetophenone at 20 mg ml^{-1} in a 1 : 5 analyte : matrix ratio. HPLC analyses were performed on a Waters Delta 600 system with a Waters 2487 dual wavelength absorbance detector at 240 nm. A Waters Symmetry C18 silica-based RP-HPLC column (4.6 x 250 mm, 5 mm, 100A˚) was used with a mobile phase of 70 : 30 acetonitrile–THF at a flow rate of 1 mL min^{-1}. Injection volumes were 40 mL at a concentration of 0.5 mg mL^{-1}. Analyses were performed using Empower Pro software. GPC analyses were performed using a Viscotek VE3210 UV/Vis detector at 260 nm and 30 °C. A Visco- GEL mixed bed I-MBMMW-3078 GPC column (7.8 mm x 30 cm) was

used with a mobile phase of THF at a flow rate of 1mL min^{-1}. Injection volumes were 100 mL at a concentration of 1 mg mL^{-1}.

$C_3N_3[N(CH_2CH_2CH_2NHBoc)_2]Cl_2$ (3.1). A solution of cyanuric chloride (5.586 g, 30.34 mmol) in THF (200 mL) was cooled to 0 ºC. A clear solution of $HN(CH_2CH_2CH_2NHBoc)_2$ (9.578 g, 28.9 mmol) in THF (150 mL) was added dropwise to the cyanuric chloride solution, followed by dropwise addition of a solution of DIPEA (8.8 mL, 57.8 mmol) in THF (100 mL). The solution was stirred at 0 ºC for 1 h, then warmed gradually to 25 °C and stirred for an additional 12 h. The solvent was removed *in vacuo*, and then the residue was taken up in CH_2Cl_2 (200 mL). The solution was washed with water (3 x 300 mL), and then dried with $MgSO_4$. Following filtration, the solvent was removed *in vacuo*. The product was obtained as a pure white solid by reprecipitation with hexanes from a clear solution of EtOAc. Yield: 11.9 g (86%). ^1H NMR (300 MHz, $CDCl_3$) δ: 5.02 (br, 2H), 3.61 (t, $^3J_{H-H}$ = 7 Hz, 4H), 3.12 (m, 4H), 1.77 (p, $^3J_{H-H}$ = 7 Hz, 4H), 1.43 (s, 18H). $^{13}C\{^1H\}$ NMR (75.5 MHz, $CDCl_3$) δ: 170.1 , 164.7, 156.0 , 79.3 , 44.9 , 37.3 , 28.3 , 27.7 . MS (ESI): calcd 478.1862 (M^+); found 479.1992 ($M + H^+$).

G1-Cl_3Boc_6. Solutions of $C_3N_3(piperazine)_3$ (1.21 g, 3.63 mmol) and $C_3N_3[N(CH_2CH_2CH_2NHBoc)_2]Cl_2$ (6.09 g, 12.7 mmol) were dissolved separately in THF (100 mL each) to give a slurry and a clear solution, respectively. DIPEA (6.5 mL, 36 mmol) was added to the solution of $C_3N_3(piperazine)_3$, and then both solutions were cooled to 0 °C. The mixture was added dropwise to the $C_3N_3[N(CH_2CH_2CH_2NHBoc)_2]Cl_2$ solution, and the slurry was stirred at 0°C for 1 h.

The solution was warmed gradually to 25 °C and stirred for an additional 15 h. The mixture was filtered through Celite, and then the solvent was removed *in vacuo*. The residue was dissolved in CH_2Cl_2 (150 mL), and this solution was washed with water (3 x 200 mL). The organic phase was dried with $MgSO_4$. Excess $C_3N_3[N(CH_2CH_2CH_2NHBoc)_2]Cl_2$ was removed by filtration of the organic phase through a silica plug. The product was reprecipitated from CH_2Cl_2 with hexanes to afford a white solid. Yield: 5.63 g (93%). ^{1}H NMR (300 MHz, $CDCl_3$) δ: 5.59 (br, 3H), 4.83 (br, 3H), 3.82 (br, 24H), 3.56 (m, 12H), 3.08 (m, 12H), 1.73 (m, 12H), 1.424 (s, 27H), 1.420 (s, 27H). ^{13}C{^{1}H} NMR (75.5 MHz, $CDCl_3$) δ: 169.2, 165.2, 164.9, 164.2, 156.1, 155.8 , 79.2, 78.8, 43.8, 43.3, 42.9, 42.6, 37.7, 36.7, 28.4, 28.3, 27.8 , 27.7. MS (MALDI): calcd 1662.2559 (M^+); found 1663.0484 ($M + H^+$).

G1-Piperidine$_3$Boc$_6$. A clear solution of Cl_3Boc_6 (2.53 g, 1.52 mmol) and piperidine (1.52 mL, 15.2 mmol) was prepared in THF (50 mL). The mixture was stirred at 25 °C for 16 h, and the resulting slurry was filtered through silica to give a clear solution. The solvent was removed *in vacuo*. The residue was dissolved in CH_2Cl_2 (20 mL), and this solution was washed with water (3 x 50 mL). The organic phase was dried with Na_2SO_4. Following filtration, the solvent was removed *in vacuo* to afford the product as a white powder. (Yield: 2.79 g, >99%) ^{1}H NMR (300 MHz, $CDCl_3$) δ: 5.27 (br, 6H), 3.80 (br, 24H), 3.72 (br, 12H), 3.96 (br, 12H), 3.07 (br, 12H), 1.70 (br, 12H), 1.62 (br, 6H), 1.55 (br, 12H), 1.42 (s, 54H). ^{13}C NMR (75.5 MHz, $CDCl_3$) δ: 166.1, 165.5, 165.1, 156.2, 79.2, 44.4, 43.4, 43.3, 42.0, 37.4, 37.3, 28.7, 27.9, 26.0, 25.1. MS (MALDI): calcd 1807.2050 (M^+); found 1808.3271 ($M + H^+$).

G1-Piperidine$_3$(NH$_2$)$_6$. 5 M HCl (35 mL) was added to a clear solution of Piperidine$_3$Boc$_6$ (2.75 g, 1.52 mmol) in CH_2Cl_2 (3 mL) and MeOH (70 mL), and the solution was stirred at 25 °C for 15 h. The volatile components were concentrated *in vacuo* until only *ca.* 15 mL of water remained. The solution was made basic (pH = 14) with 40 mL of 5 M NaOH (aq) solution. The resulting milky suspension was extracted with $CHCl_3$ (5 x 250 mL). The combined organic phases were dried with Na_2SO_4. Following filtration, the solvent was removed *in vacuo* to afford the product as a white solid. Yield: 1.845 g, >99%. ^{1}H NMR (300 MHz, $CDCl_3$) δ: 3.79 (br, 24H), 3.71 (br, 12H), 3.63 (br t, $^3J_{H\text{-}H}$ = 7 Hz, 12H), 2.68 (br t, $^3J_{H\text{-}H}$ = 7 Hz, 12H), 1.73 (br m, 12H), 1.62 (br, 6H), 1.54 (br, 24H). $^{13}C\{^1H\}$ NMR (75.5 MHz, $CDCl_3$) δ: 165.5, 165.2, 164.8, 44.0, 43.0, 42.4, 39.1, 39.0, 31.3, 25.7, 24.9. MS (MALDI): calcd 1206.8904 (M^+); found 1207.9496 ($M + H^+$).

G2-Piperidine$_3$Boc$_{12}$Cl$_6$. A solution of Pip$_3$(NH$_2$)$_6$ (889 mg, 0.74 mmol), DIPEA (2.1 mL, 12.5 mmol) and $C_3N_3[N(CH_2CH_2CH_2NHBoc)_2]Cl_2$ (2.99 g, 6.21 mmol) was prepared in a THF:water mixture (200:10 mL) to give a slurry. The solution was stirred at 25 °C for 16 h, and then filtered through Celite. The solvent was removed *in vacuo*. Purification was achieved using column chromatography on silica gel (40:1 CH_2Cl_2:MeOH; R_f = 0.19 using 20:1 CH_2Cl_2:MeOH as the developing solvent) to afford the product as a white solid. Yield: 2.66 g (93%). The excess/unreacted $C_3N_3[N(CH_2CH_2CH_2NHBoc)_2]Cl_2$ may also be recovered from this purification (R_f = 0.50 using 20:1 CH_2Cl_2:MeOH as the developing solvent). ^{1}H NMR (300 MHz, $CDCl_3$) δ: 6.08 (br, 2H) 5.61 (br, 8H), 5.44 (br, 2H), 4.98 (br, 6H), 3.82 (br, 24H), 3.74 (br,

12H), 3.64-3.56 (br, 36H), 3.39 (br, 12H), 3.08 (br, 24H), 1.85 (br, 12H), 1.73 (br, 30H), 1.58 (br, 12H), 1.43(s, 54H), 1.41 (s, 54H). $^{13}C\{^{1}H\}$ NMR (75.5 MHz, $CDCl_3$) δ: 169.2, 168.4, 165.4, 165.1, 164.9, 164.6, 156.0, 155.7, 78.9, 78.6, 44.0, 43.1, 37.6, 36.6, 28.2, 27.7, 25.6, 24.8. MS (MALDI): calcd 3865.2622 (M^+); found 3868.2945.

G2-Piperidine$_9$Boc$_{12}$. A clear solution of Piperidine$_3$Boc$_{12}$Cl$_6$ (168 mg, 4.3 x 10^{-5} mol) and piperidine (0.1 mL, 1.0 mmol) was prepared in THF (10 mL). The mixture was stirred at 25 °C for 12 h, and the resulting slurry was filtered through silica to give a clear solution. The solvent was removed *in vacuo*. The solid was washed with hexanes and dried *in vacuo* to afford the product as a white powder. Yield: 180 mg (99%). ^{1}H NMR (300 MHz, $CDCl_3$) δ: 6.70-5.49 (br, 18H), 3.79 (br, 24H), 3.68 (br, 36H), 3.53 (br, 36H), 3.34 (br, 12H), 3.02 (br, 24H), 1.80 (br, 12H), 1.66 (br, 24H), 1.58 -1.52 (br, 54 H), 1.39 (s, 108H). $^{13}C\{^{1}H\}$ NMR (75.5 MHz, $CDCl_3$) δ: 165.9, 165.6, 165.2, 165.0, 156.0, 79.0, 44.3, 43.3, 42.2, 37.3, 28.7, 27.9, 26.0, 25.1. MS (MALDI): calcd 4157.3818 (M^+); found 4158.6648 ($M + H^+$).

G2-Piperidine$_9$(NH$_2$)$_{12}$. Concentrated aqueous HCl (15 mL) was added to a solution of Piperidine$_9$Boc$_{12}$ (1.35 g, 0.32 mmol) in MeOH (40 mL), and the clear solution was stirred at 25 °C for 16 h. The volatile components were concentrated *in vacuo* until only *ca.* 5 mL of water remained. The residue was made basic (pH = 14) with 25 mL of 1 M NaOH (aq) solution, and the resulting milky suspension was extracted with $CHCl_3$ (5 x 250 mL). The organic extractions were combined, and then the solvent was removed *in vacuo* to afford the product as a white solid. Yield: 959 mg, >99%. ^{1}H NMR (300 MHz, $CDCl_3$ with trace CD_3OD) δ: 5.24 (br, 6H), 3.80 (br, 24H), 3.73 (br, 12H), 3.65

(br, 36H), 3.57 (br, 24H), 3.32 (br, 12H), 2.64 (br, 24H), 1.81 (br, 12H), 1.70 (br, 24H), 1.58-1.51 (br, 54H). $^{13}C\{^{1}H\}$ NMR (75.5 MHz, $CDCl_3$ with trace CD_3OD) δ: 165.8, 165.4, 165.2, 165.1, 165.0, 164.6, 164.3, 43.8, 42.8, 41.7, 38.1, 37.3, 30.3, 27.7, 25.5, 24.6. MS (MALDI): calcd 2954.1932 (M^+); found 2955.0237 ($M + H^+$).

G3-Piperidine$_9$Boc$_{24}$Cl$_{12}$. A solution of $Pip_9(NH_2)_{12}$ (1.00 g, 0.34 mmol), DIPEA (2.3 mL, 13.5 mmol) and $C_3N_3[N(CH_2CH_2CH_2NHBoc)_2]Cl_2$ (2.43 g, 5.1 mmol) was prepared in a THF:water mixture (200:10 mL) to give a slurry. The solution was stirred at 25 °C for 16 h, and then filtered through Celite. The solvent was removed *in vacuo*. Purification was achieved using column chromatography on silica gel (20:1 CH_2Cl_2:MeOH) to elute the excess starting material (R_f = 0.5), and to afford the product as a white solid (R_f = 0.19). Yield: 1.913 g (68%). ^{1}H NMR (300 MHz, $CDCl_3$) δ: 9.33, 5.62, 4.98 (br, 42H), 3.75 (br, 24H), 3.65-3.52 (br, 120H), 3.36-3.29 (br, 36H), 3.03 (br, 48H), 1.89 (br, 12H), 1.79 (br, 24H), 1.68 (br, 48H), 1.49 (br, 54H), 1.39 (s, 108H), 1.37 (s, 108H). $^{13}C\{^{1}H\}$ NMR (75.5 MHz, $CDCl_3$) δ: 169.7, 168.8, 168.2, 165.9, 165.6, 165.3, 165.1, 164.8, 156.4, 156.1, 79.2, 79.0, 44.4, 43.7, 43.6, 43.3, 39.0, 38.8, 38.1, 37.1, 28.6, 28.1, 27.9, 26.0, 25.2. MS (MALDI): calcd 8271.27 (average M^+); found 8272.27 (average $M + H^+$).

G3-Piperidine$_{21}$Boc$_{24}$. A clear solution of $Piperidine_9Boc_{24}Cl_{12}$ (0.66 g, 0.0797 mmol) and piperidine (0.316 mL, 3.19 mmol) was prepared in THF (30 mL). The mixture was stirred at 25 °C for 12 h, and the resulting slurry was filtered through silica to give a clear solution. The solvent was removed *in vacuo*. The solid was washed with hexanes and dissolved in 50 mL CH_2Cl_2. The solution was washed with water (2 x 50 mL) and

brine (1 x 50 mL). The organic phases were dried with Na_2SO_4 and the solvent was removed *in vacuo*. The residue was reprecipitated from CH_2Cl_2 with hexanes to afford the product as a white powder. Yield: 721 mg (>99%). ^{1}H NMR (300 MHz, $CDCl_3$) δ: 7.00-5.00 (br, 42H), 3.78 (br, 24H), 3.68 (br, 84H), 3.53 (br, 84H), 3.32 (br, 36H), 3.02 (br, 48H), 1.78 (br, 36H), 1.65 (br, 48H), 1.50 (br, 126H), 1.40 (s, 108H), 1.39 (s, 108H). ^{13}C{^{1}H} NMR (75.5 MHz, $CDCl_3$) δ: 165.9, 165.6, 165.2, 164.6, 155.9, 78.7, 43.9, 42.9, 41.7, 33.9, 28.3, 27.5, 25.7, 24.8. MS (MALDI): calcd 8855.5141 (average M^+); found 8856.89 (average $M + H^+$).

G3-Piperidine$_{21}$(NH$_2$)$_{24}$. 5 M HCl (25 mL) was added to a solution of Piperidine$_{21}$Boc$_{24}$ (706 mg, .0797 mmol) in MeOH (70 mL), and the clear solution was stirred at 25 °C for 16 h. The volatile components were concentrated *in vacuo* until only *ca.* 5 mL of water remained. The residue was made basic (pH = 14) with 26 mL of 5 M NaOH (aq) solution, and the resulting milky suspension was extracted with $CHCl_3$ (5 x 150 mL). The organic extractions were combined, dried with Na_2SO_4, and then the solvent was removed *in vacuo* to afford the product as a white solid. Yield: 520 mg, >99%. ^{1}H NMR (300 MHz, $CDCl_3$) δ: 7.00-5.00 (br, 18H), 3.76 (br, 24H), 3.62 (br, 84H), 3.53 (br, 84H), 3.27 (br, 36H), 2.61 (br, 48H), 1.99 (br, 48H), 1.66 (br, 84H), 1.54 (br, 42H), 1.47 (br, 84H). ^{13}C{^{1}H} NMR (75.5 MHz, $CDCl_3$) δ: 166.0, 165.9, 165.3, 165.1, 164.8), 164.6, 164.5, 43.8, 42.9, 42.2, 38.9, 37.4, 31.1, 27.9, 25.6, 24.8. MS (MALDI): calcd 6448.7990 (M^+); found 6471.9424 ($M + Na^+$).

G4-Piperidine$_{21}$Boc$_{48}$Cl$_{24}$. A clear solution of Pip$_{21}$(NH$_2$)$_{24}$ (0.94 g, 0.146 mmol) in H_2O (15 mL) and EtOAc (80 mL) was added to a clear solution of

$C_3N_3[N(CH_2CH_2CH_2NHBoc)_2]Cl_2$ (5.03 g, 10.49 mmol) in CH_2Cl_2 (90 mL) with DIPEA (4.79 mL, 31.47 mmol) and stirred at room temperature for 16 hours. The solvents were removed *in vacuo* and the residue taken up in 20 mL CH_2Cl_2. The solution was washed with water (3 x 100 mL) and brine (1 x 100 mL). The organic phases were filtered through silica to remove excess starting material. The solvent was removed *in vacuo* and any residual starting materials were removed by reprecipitation from CH_2Cl_2 with hexanes to afford the product as a white solid. Yield: 1.718 g, 69%. ^{1}H NMR (300 MHz, $CDCl_3$) δ: 9.39, 5.65, 5.03 (br, 90H), 3.79-3.53 (br, 288H), 3.35-3.30 (br, 84H, C**H**$_2$NH-C_3N_3), 3.04 (br, 96H), 1.88-1.69 (br, 180H), 1.58-1.47 (br, 126H), 1.38 (bs, 432H). ^{13}C{^{1}H} NMR (75.5 MHz, $CDCl_3$) δ: 168.8, 168.2, 166.4, 165.9-165.8, 165.6, 165.4-165.3, 165.1, 164.9, 156.4, 156.1, 79.3, 79.0, 44.5-44.3, 43.7-43.5, 38.9, 38.0-37.8, 37.2-37.0, 28.6, 28.1, 26.1, 25.2. MS (MALDI): calcd 17083.3001 (average M^+); found 17088.03 (~average M + H^+).

G4-Piperidine$_{45}$Boc$_{48}$. A clear solution of $Pip_{21}Boc_{48}Cl_{24}$ (284 mg, 0.0166 mmol) and piperidine (0.14 mL, 1.394 mmol) was prepared in THF (16 mL). The mixture was stirred at 25 °C for 16 h, and the resulting slurry was filtered through silica to give a clear solution. The solvent was removed *in vacuo*. The solid was washed with hexanes and dissolved in 50 mL CH_2Cl_2. The solution was washed with water (2 x 50 mL) and brine (1 x 50 mL). The organic phases were dried with Na_2SO_4 and the solvent was removed *in vacuo*. The residue was reprecipitated from CH_2Cl_2 with hexanes to afford the product as a white powder. Yield: 265 mg (87%). ^{1}H NMR (300 MHz, $CDCl_3$) δ: 7.12-5.08 (br, 90H), 3.78-3.69 (br, 204H), 3.56 (br, 180H, C**H**$_2$, NC**H**$_2$), 3.35 (br, 84H),

3.02 (br, 96H), 1.83 (br, 84H), 1.65 (br, 96H), 1.50 (br, 270H), 1.41 (s, 432H). $^{13}C\{^{1}H\}$ NMR (75.5 MHz, $CDCl_3$) δ: 166.0-165.7, 164.9, 156.2, 79.1, 44.3, 43.3, 42.2, 38.9, 37.3, 28.7, 27.9, 26.0, 25.1. MS (MALDI): calcd 18251.78 (average M^+); found 18279.01 (~average M + Na^+).

G4-Piperidine$_{45}$(NH$_2$)$_{48}$. A clear solution of $Pip_{45}Boc_{48}$ (480 mg, 0.0263 mmol) in CH_2Cl_2 (15 mL) and MeOH (90 mL) was prepared. 5 M HCl (aq) (24 mL) was added and the reaction was stirred at room temperature for 16 hours. The volatile components were concentrated *in vacuo* until only *ca.* 5 mL of water remained. The residue was made basic (pH = 14) with 26 mL of 5 M NaOH (aq) solution, and the resulting milky suspension was extracted with $CHCl_3$ (5 x 100 mL). The organic extractions were combined, dried with Na_2SO_4, and the solvent was removed *in vacuo* to afford the product as a white solid. Yield: 429 mg (>99%). ^{1}H NMR (300 MHz, CD_3OD) δ: 3.65, 3.04, 2.04, 1.56. MS (MALDI): calcd 13446.22 (average M^+); found 13453.87.

G5-Piperidine$_{45}$Boc$_{96}$Cl$_{48}$. A clear solution of $Pip_{45}(NH_2)_{48}$ (0.175 g, 0.013 mmol) in 35 mL $CHCl_3$ with DIPEA (0.57 mL, 3.74 mmol) was prepared and concentrated *in vacuo* to *ca*. 10 mL. $C_3N_3[N(CH_2CH_2CH_2NHBoc)_2]Cl_2$ was added and the solution was stirred at 25 °C for 5 days. $CHCl_3$ (50 mL) was added and the solution was washed with water (3 x 75 mL) and brine (1 x 75 mL). The organic layers were filtered through silica to remove excess $C_3N_3[N(CH_2CH_2CH_2NHBoc)_2]Cl_2$. Portions containing the product and an impurity were filtered through silica again and the product was retrieved as a white solid. Yield: 0.111 g (25%). ^{1}H NMR (300 MHz, $CDCl_3$) δ: 7.70, 7.23, 5.67, 5.03, 3.65-3.36 (br, 756 H), 3.06 (br, 192 H), 1.84-1.47 (br, 642H), 1.40 (br, 864H). $^{13}C\{^{1}H\}$

NMR (75.5 MHz, $CDCl_3$) δ: 165.9-164.6, 163.5, 156.4, 156.2, 79.2, 79.0, 44.3, 43.7, 38.9, 37.9, 37.1, 28.7, 28.0, 27.9, 26.0, 25.6. MS (MALDI): calcd 34707.36 (average M^+); found 32932.41, 15823.00.

G5-Piperidine$_{93}$Boc$_{96}$. A clear solution of $Pip_{45}Boc_{96}Cl_{48}$ (0.0523 g, 0.0015 mmol) in THF (5 mL) was prepared. Piperidine (0.022g, 0.216 mmol) was added and the solution was stirred at room temperature for 16 hours. The cloudy solution was filtered through silica to remove excess piperidine. The solvents were removed *in vacuo* to yield a white solid. Yield: 0.059 g (>99%). ^{1}H NMR (300 MHz, $CDCl_3$) δ: 3.68, 3.54 (br, 372H), 3.36 (C**H**$_2$), 3.04 (br, 192H), 1.68-1.52 (br, 930H), 1.41 (s, 864H). MS (MALDI): calcd 37044.33 (average M^+); found 33010.74.

G5-Piperidine$_{93}$(NH$_2$)$_{96}$. A clear solution of $Pip_{93}Boc_{96}$ (0.0556 g, 0.0015 mmol) in CH_2Cl_2 (3 mL) and MeOH (9 mL) was prepared. 5 M HCl (aq) (3 mL) was added and the solution was stirred at room temperature for 2 days. The volatile components were concentrated *in vacuo* until only *ca.* 1 mL of water remained. The residue was made basic (pH = 14) with 5 mL of 5 M NaOH (aq) solution, and the resulting milky suspension was extracted with $CHCl_3$ (5 x 15 mL). The organic extractions were combined, dried with Na_2SO_4, and the solvent was removed *in vacuo* to afford the product as a white solid. Yield: mg (>99%). ^{1}H NMR (300 MHz, CD_3OD) δ: 3.73, 3.13, 2.08, 1.61.

CHAPTER IV

SYNTHESIS OF AN IMIDAZOLE-CONTAINING DENDRIMER AND STUDIES OF Zn-PHTHALOCYANINE ENCAPSULATION AND WATER SOLUBILIZATION

Introduction

Due to their intense absorbance in the 700-900 nm range, phthalocyanines (Pc) are promising candidates for photodynamic therapy (PDT). Unfortunately, their tendency to aggregate even in organic solvents and their insolubility in water limit their usefulness. There are a few examples of Pc currently in various stages of clinical trials for PDT, namely ZnPc, $AlPcS_n$, Pc4, and PcS_4 (Figure 4.1).[73]

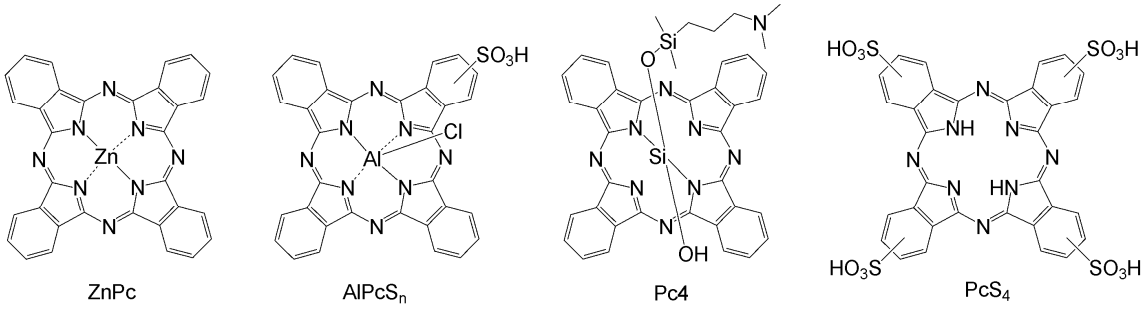

Figure 4.1. Phthalocyanine photosensitizers for PDT.

ZnPc is delivered via liposomes, $AlPcS_n$ is water-soluble, but has different biodistribution and cellular uptakes dependent on the degree of sulfonation, Pc4 is delivered via liposomes or Cremophor EL emulsion, and PcS_4 is water soluble.

Although liposomal and Cremophor drug delivery are commonplace, the delivery of Pc by dendrimer would offer the advantages of a chemically well-defined and stable system that may target tumor cells passively through the EPR effect, or through an active targeting system such as proteins or antibodies, if so functionalized.

The conjugation of porphyrinic molecules to the surface of a dendrimer is rare. Hackbarth *et al.* report the attachment of Pheophorbide a (Pheo) to diaminobutane (DAB) dendrimers of generation 0-4 through an amide bond (Figure 4.2).[130] Steric hindrance and stacking became a problem at higher generations; only 13 chromophores are conjugated to G3-DAB, which has 16 reactive amines. Materials were characterized only by MALDI mass spectroscopy and infrared spectroscopy to confirm covalent conjugation through the amide bond.[131]

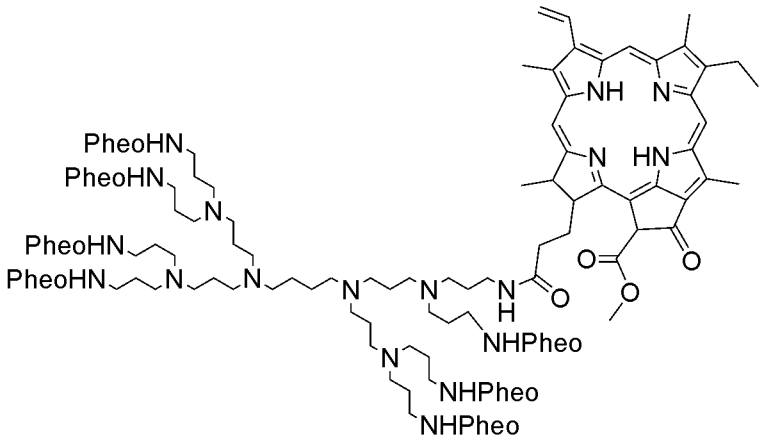

Figure 4.2. A generation-2 DAB dendrimer conjugated with Pheophorbide a (Pheo).

Although the absorption spectra for the dendrimer conjugates are not significantly different from free Pheo, the fluorescence quantum yields and singlet oxygen quantum yields are significantly decreased, to 0.5% and 8%, respectively, of those yields for free

Pheo in solution. This quenching is due to the presence of intramolecular dimers bound to a single dendrimer. Monomeric dye molecules can undergo Förster energy transfer several times, until the energy reaches a dimer, where it is quenched. Just one dimer on a dendrimer will quench enough of the energy to cause the observed reductions in fluorescence and singlet oxygen quantum yields. However, excitation of the dendrimer-Pheo conjugate in the presence of oxygen led to the destruction of the dendrimer into fragments carrying only one or two Pheo molecules, which remain monomeric in solution, so that the fluorescence and singlet oxygen quantum yields approximate those of free Pheo.[131]

The formation of dendrimers with porphyrins as the core is fairly common, with some recent examples given here. Kataoka *et al*. have built core-shell polyion complex (PIC) micelles based on a benzyl ether dendrimer with a porphyrin core that show unusual stability towards high salt concentrations and dilution.[132] These PIC micelles have shown enhancement of transfection[133] and treatment of choroidal neovascularization,[134,135] an ophthalmic disease. Shinoda has developed several "patched dendrimers" in which unsymmetrical dendrons are introduced onto a porphyrin core in a formation that allows for supramolecular recognition of other molecules or macromolecules.[136,137]

Phthalocyanines have also been incorporated into dendrimers as a peripherally-substituted core,[138-142] or as dendritic axial substituents on Si-centered Pc.[142,143] Pc have been solubilized in water by incorporation as a core into benzyl ether dendrimers terminated with carboxylates.[90-92] Many of these reports refer to the porphyrins and Pc

as "encapsulated", a term usually referring to noncovalent interactions. However, the photosensitizers are covalently bound, and there are no reports of phthalocyanines encapsulated by noncovalent means in a dendrimer.

In the first report of a phthalocyanine covalently bound to a triazine, two equivalents of a siloxy phthalocyanine were added to a dichlorotriazine bearing a protected benzyl alcohol (Figure 4.3).[144] The benzyl group was removed and the alcohol coupled to 1,3,5-benzenetricarboxylic acid to form a dendrimer with six Pc.

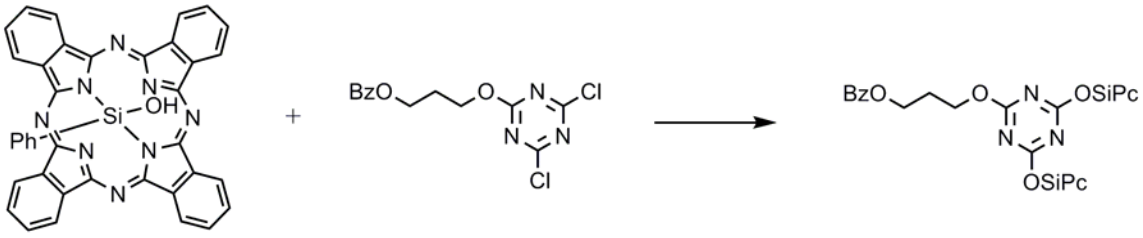

Figure 4.3. Substitution of cyanuric chloride with a siloxy phthalocyanine.

Cyanuric chloride has also been substituted with Pc through oxygen,[145] nitrogen,[146,147] and ethenyl bonds (Figure 4.4).[148] In this chapter, efforts towards the covalent attachment of a phthalocyanine and a porphyrazines (Pz) to triazine dendrimers will be presented, as well as the synthesis of an imidazole-containing dendrimer and the encapsulation and water solubilization of Zn-tetra(*tert*-butyl)phthalocyanine.

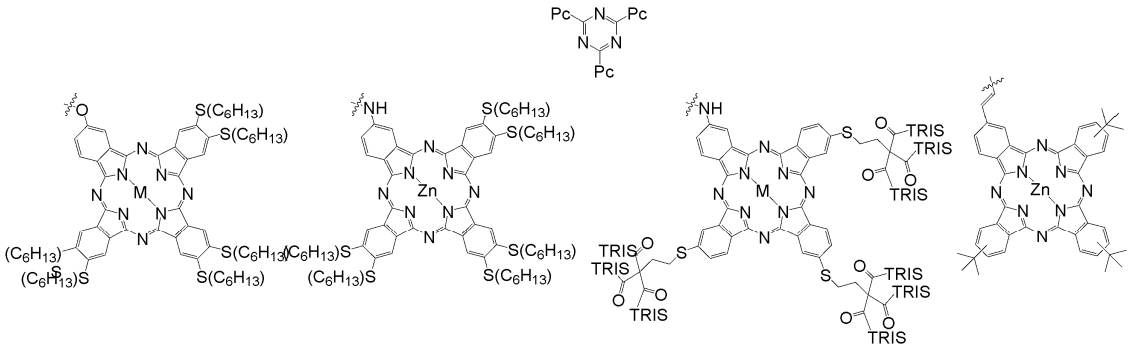

Figure 4.4. Several tri-Pc substituted triazines.

Results and Discussion

Phthalocyanine-Dichlorotriazine Monomers. Zn-4-amino-tri(*tert*-butyl)phthalocyanine **4.1** ($ZnPc\text{-}NH_2$) was synthesized from the statistical condensation of 4-amino-pththalonitrile with 4-*tert*-butyl-phthalonitrile in the presence of $ZnCl_2$ (Figure 4.5).

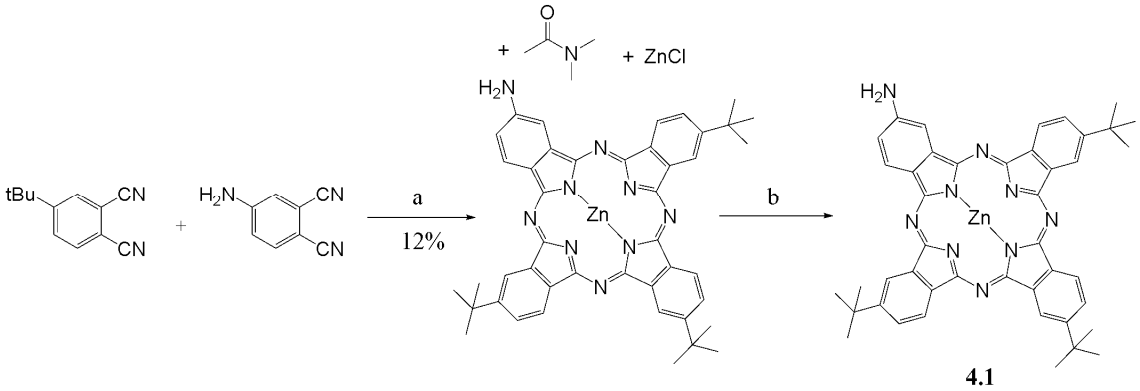

Figure 4.5. Synthesis of $ZnPc\text{-}NH_2$ **4.1**. (a) octanol, Et_3N, $ZnCl_2$, DMA, 130 °C, 2 d. (b) HCl, 16 h.

The resulting mixture was purified by column chromatography, and three bands were isolated. The first band contained Zn-tetra(*tert*-butyl)phthalocyanine, the second band contained the desired product, and the third band contained the remaining products and

any linear polymer that formed. Upon closer inspection the second band actually consisted of three products that were isolated by precipitation and filtration through a silica plug and identified as metal-free 4-amino-tri(*tert*-butyl) phthalocyanine, the desired ZnPc-NH_2 **4.1**, and the major fraction contained a product that, by mass spectral analysis, appears to have extra Zn, Cl, and DMA. This blue-green product was stirred in DCM with TFA overnight causing the solution to turn green, presumably due to the loss of zinc; however, the solution turns blue-green again when washed with water. The mixture was stirred overnight with concentrated HCl (causing it to turn green again), then washed with a saturated solution of $NaHCO_3$ and ethylene diamine tetra-acetic acid (EDTA). The product was obtained in only 12% total yield, but given the statistical nature of the reaction, with five possible products the maximum theoretical yield was 20%.

The mass spectrum of the product originally isolated from the purification of ZnPc-NH_2 **4.1** had a parent ion peak at 945.3237 *m/z* with an isotope distribution pattern that indicated the presence of two zinc atoms in the molecule (Figure 4.6). After stirring the product with acid, the expected parent ion (760.9832 g/mol) appears in the MS, as well as a small peak for completely demetallated Pc at 698.0972 g/mol.

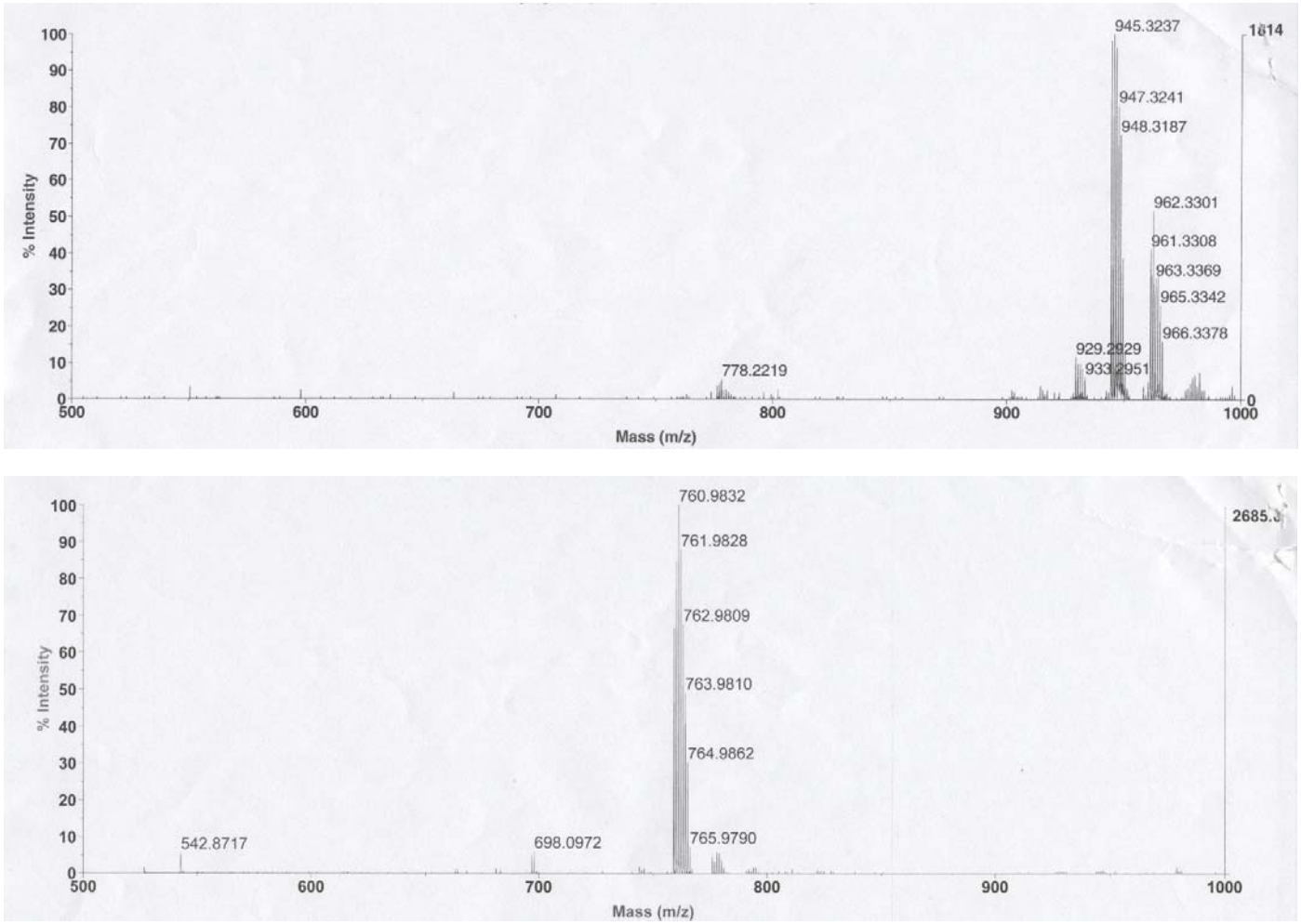

Figure 4.6. MS showing ZnPc-NH_2 **4.1** before (top) and after (bottom) stirring with HCl.

Although ZnPc-NH_2 is reported in the literature,[149] no NMR data was reported. ^{1}H NMR spectroscopy confirms the identity of the product, although only two peaks are seen in the aromatic region (integrating for 12 total protons) where at least three different peaks were expected. Only one peak for the *tert*-butyl protons was present at 1.368 ppm. Only the proton-bearing carbons were seen in the ^{13}C NMR spectrum, as the sample was too dilute to see any quaternary carbons.

ZnPc-NH_2 **4.1** was reacted with cyanuric chloride to form a ZnPc-dichlorotriazine to be used as a monomer in dendrimer formation. Following the reaction by TLC, two new products with similar polarity were formed and the starting material depleted; however, the isolated products could not be identified.

A new route based on the silanol-centered phthalocyanine strategy used by Kraus[144] was explored, where SiPc(CH_3)(OH) was reacted with cyanuric chloride to form a dichlorotriazine monomer (Figure 4.7); however, the reaction progress could not be monitored by TLC, and MS analysis of the rather insoluble product did not indicate the presence of product.

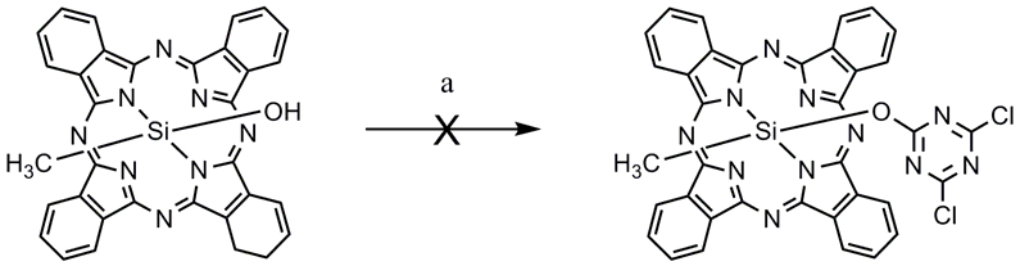

Figure 4.7. Synthesis of a SiPc-dichlorotriazine monomer. (a) NaH, THF, 0 °C.

The MS of the reaction mixture from the addition of $SiPc(CH_3)OH$ to cyanuric chloride contained three peaks: 543.0917 m/z, for $SiPcH_2$; 557.0911 m/z, for $SiPc(CH_3)H$; and 1068.3119, for the dimer formed by the reaction of the two former Pc (Figure 4.8). There was no indication of the formation of the desired product.

Direct Conjugation of a Phthalocyanine to G2-Cl. A new approach to form a phthalocyanine with a more reactive amine through conjugation of isonipecotic acid to ZnPc-NH_2 **4.1** was undertaken. Initial attempts to couple Boc-protected isonipecotic acid to **4.1** using PyBOP/HOBt or CDI were unsuccessful. To facilitate the reaction, Boc-isonipecotic acid was activated by forming the NHS-ester, after which the activated ester was reacted with ZnPc-NH_2 **4.1** (Figure 4.9). After stirring for several days, the reaction did not go to completion, and the product could not be separated from the starting material, as their polarities were very similar. The entire reaction mixture was stirred with concentrated HCl to remove the Boc group, after which the deprotected product could be separated from unreacted starting material by filtration through a silica plug and elution with increasing amounts of methanol. The product, **4.4**, was obtained in 70% overall yield after deprotection. The identification of ZnPc-isonipecotic acid **4.4** rests on the presence of the expected molecular ion peak in the MS of the isolated product, and of the formerly Boc-protected product in the MS of the crude reaction mixture.

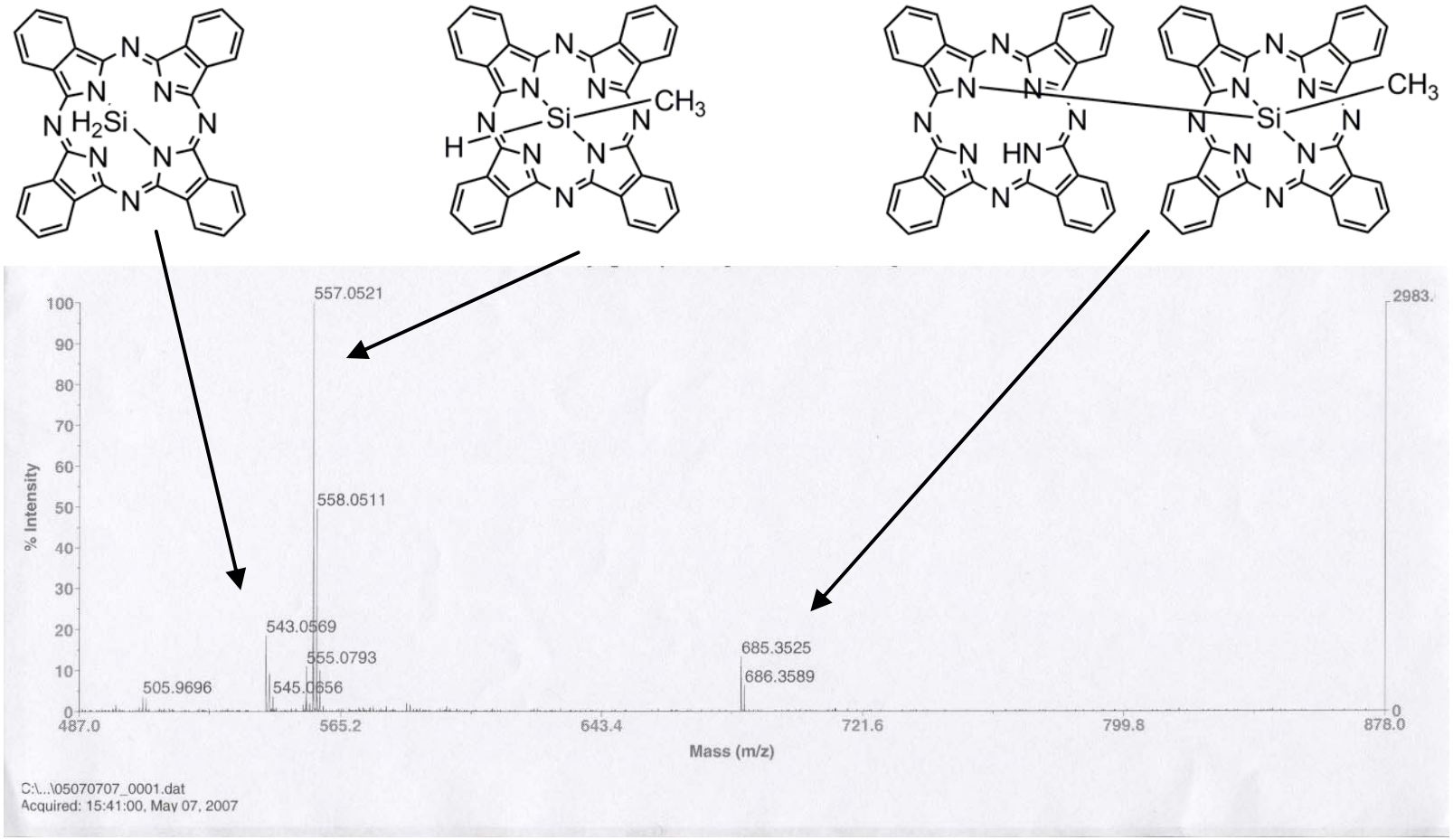

Figure 4.8. MS showing the crude mixture from the reaction of $SiPc(CH_3)OH$ with cyanuric chloride.

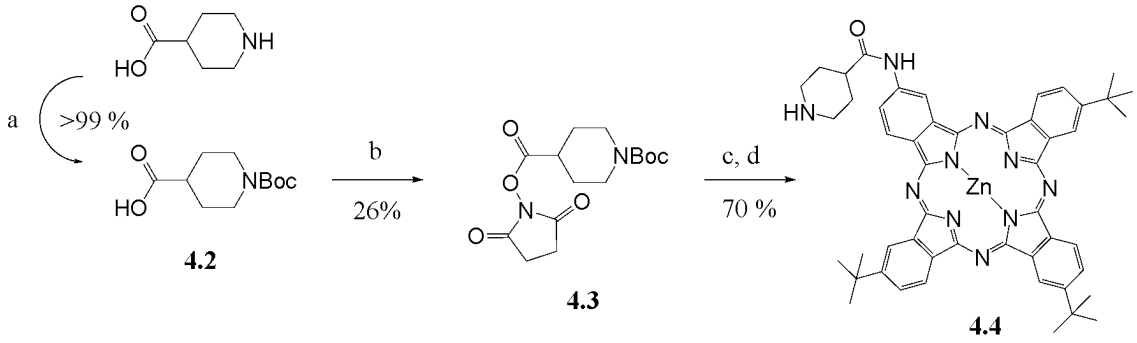

Figure 4.9. Synthetic route to ZnPc-isonipecotic acid **4.4**. (a) BOC-ON, Et_3N, THF, 16 h. (b) DSC, DMF, pyridine, 16 h. (c) **4.1**, Et_3N, DCM, 3 d. (d) HCl, DCM/MeOH.

ZnPc-isonipecotic acid **4.4** was added to G2-Cl to form a dendrimer with six covalently-bound phthalocyanines. The secondary amine of **4.4** should be nucleophilic enough to react with a monochlorotriazine at room temperature; however, after stirring at room temperature for two days, only small amounts of new phthalocyanine-containing products with Rfs lower than the dendrimer and higher than **4.4** were formed, as monitored by TLC. The reaction was heated to 50 °C for several more days, after which a large blue (phthalocyanine) spot appeared at the same Rf as the G2-Cl dendrimer. These products could not be separated by chromatography or precipitation, and mass spectral analysis of the crude mixture showed a peak only for the G2-Cl, and no Pc-substituted product or intermediates. Mass spectroscopy is an unreliable tool, as visualization of peaks is dependent upon ionization, and products that are indeed present may not appear as peaks in the spectrum. However, more reliable methods, such as NMR spectroscopy, could not be used in this situation since the product could not be separated from the starting material.

Amine-Functionalized Porphyrazines. An alternate route to a photosensitive dendrimer through conjugation of porphyrazines (Pz) was also explored concurrently with the Pc-dendrimer route. Tetra(*tert*-butyl)porphyrazine was purchased as a mixture of three regioisomers (the fourth possible isomer is not formed due to sterics, figure 4.10) which were separated by silica gel column chromatography with toluene as the eluent and their identity was confirmed by ^{1}H NMR spectroscopy, which matched with the literature.[150]

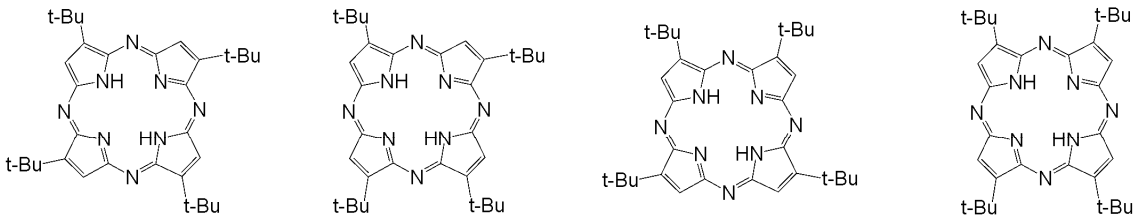

Figure 4.10. The four possible regioisomers of tetra(*tert*-butyl)porphyrazine.

Regioisomer II was the major isomer, and was iodinated with phenyl iodine *bis*(trifluoroacetic acid) (PIFA) (Figure 4.11). The reaction proceeded in only 46% yield due to the formation of di-iodinated side product, which also left some unreacted starting material; the product **4.5** was easily separated from the side products by column chromatography.

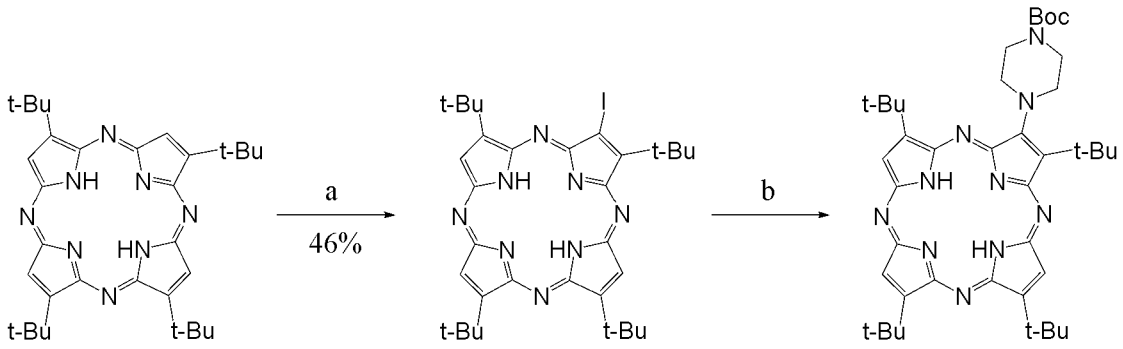

4.5

Figure 4.11. Iodination and substitution of tetra(*tert*-butyl)porphyrazine. (a) phenyl iodine *bis*(trifluoroacetic) acid, I_2, pyridine, $CHCl_3$, 50 °C. (b) Boc-piperazine, DMF, 100 °C.

.

Upon iodination of regioisomer II, the NMR spectra become more complicated due to the formation of regioisomers that are present in different amounts (Figure 4.12). The two peaks in the aromatic region of the starting Pz become six peaks whose integration totals 3H, with respect to the inner pyrrole N*H*'s (2H) seen at -2.37 ppm. The *tert*-butyl protons that appear as a multiplet in the unsubstituted Pz appear as 9 broad peaks from ~2.4-2.2 ppm in the iodinated product. The sum of the integrals for these peaks is 36H, as expected, with respect to the pyrrole N*H*'s. 2-Dimensional NMR would be necessary to make unambiguous peak assignments.

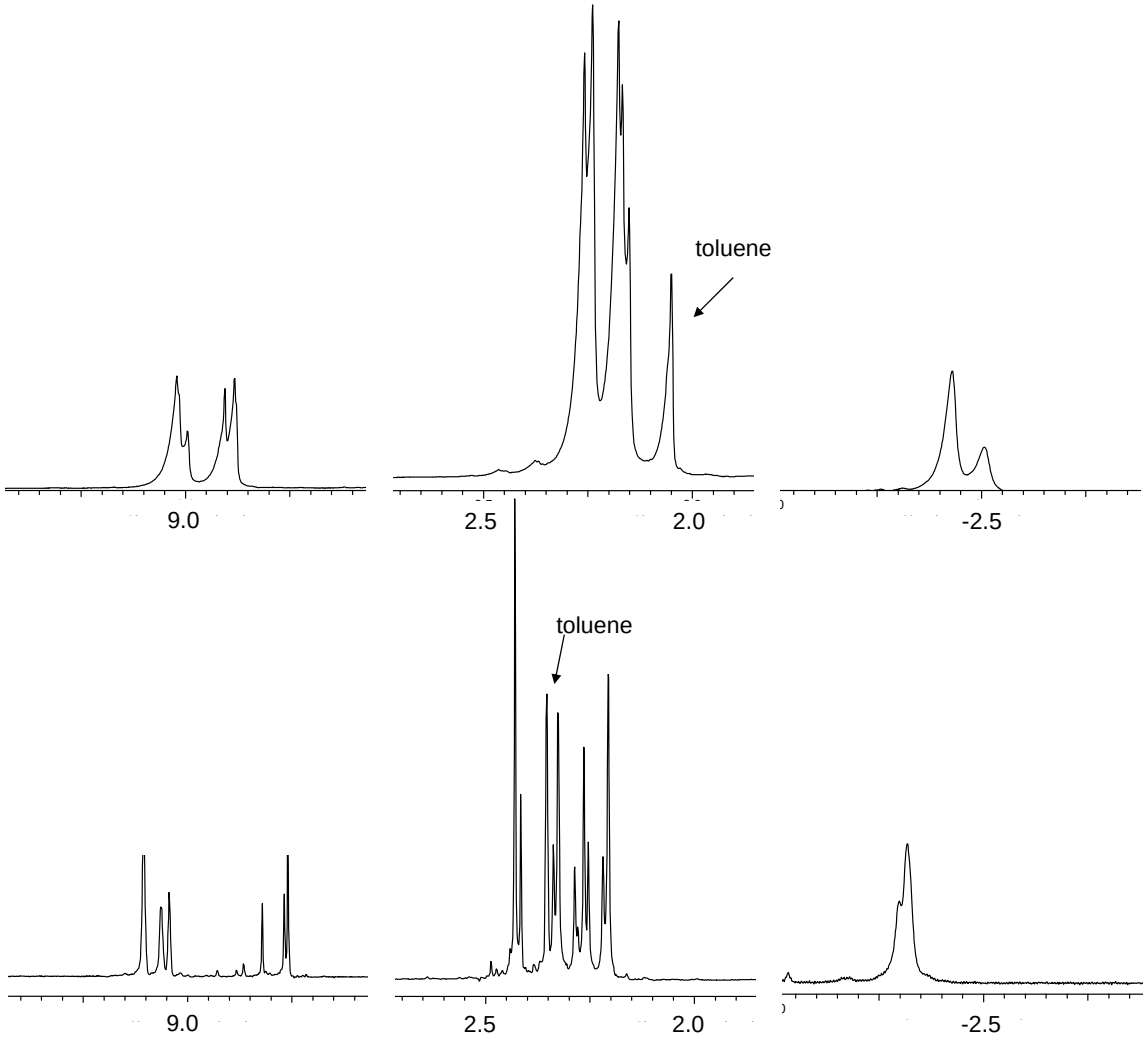

Figure 4.12. ^{1}H NMRs of tetra(tert-butyl)porphyrazine in C_6D_6 (top) and Pz-I **4.5** in $CDCl_3$ (bottom).

The MALDI-TOF mass spectrum of Pz-I **4.5** showed only the $(M + H)^+$ peak at 665.2016 *m/z*, and peaks for losses of methyl groups at -15 *m/z*, which presumably occur during ionization.

Iodo-Pz **4.5** was reacted with Boc-piperazine at elevated temperatures (Figure 4.11), and although only one new product seemed to have formed (by TLC) with no

apparent starting material, mass spectral analysis indicated the presence of **4.5** and unsubstituted porphyrazine, as well as product. However, the peak for the unsubstituted Pz at 537.1216 *m/z* is may be the result of the loss of iodine during ionization. ^{1}H NMR spectroscopy was inconclusive. At this point, a more attractive approach wherein phthalocyanines are non-covalently encapsulated in the dendrimer through Zn-imidazole interactions was initiated.

A Water-Soluble Imidazole-Bearing Dendrimer. A generation-1 dendrimer bearing three imidazole groups (**4.6**) was synthesized by the addition of 1-(3-aminopropyl)imidazole to **G1-Cl** in dioxane (Figure 4.13).

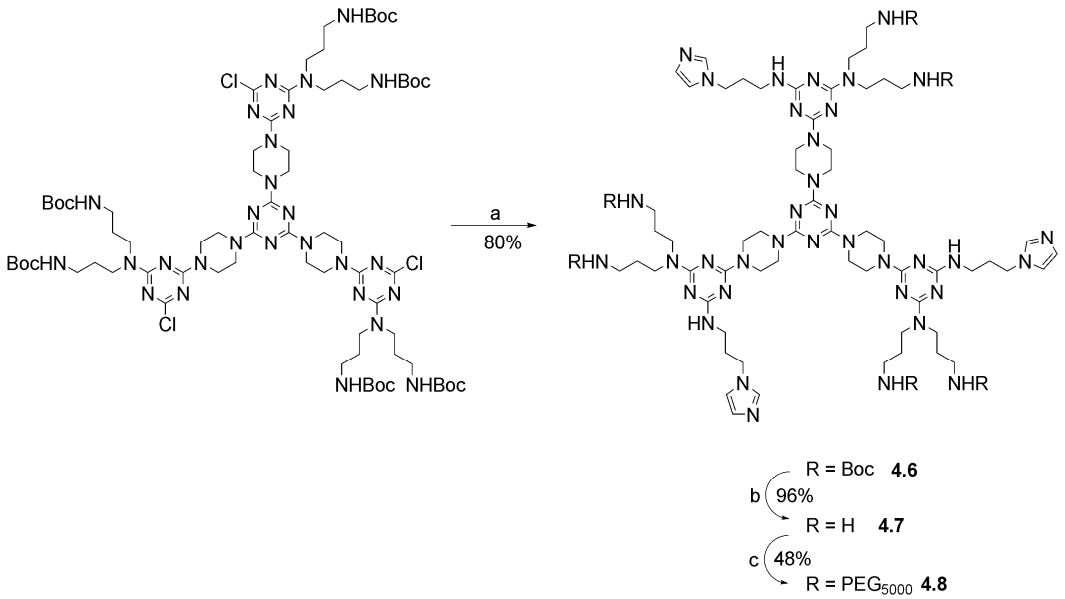

Figure 4.13. Synthesis of a G1 water-soluble dendrimer **4.8**. (a)1-(3-aminopropyl)imidazole, DIPEA, THF/dioxane, 100 C. (b) DCM/MeOH, HCl, 6 h. (c) NHS-PEG_{5000}, MeOH/DCM, 14 d.

Although the third substitution of a primary amine with a triazine is unfavorable, the product was formed in 80% yield at elevated temperatures (100 °C). A small amount of **G1-Cl** still remained after heating for two days, which was removed by column chromatography, along with dendrimer with only two imidazoles substituted.

. The ^{1}H and ^{13}C NMR spectra for G1-Boc_6Im_3 **4.6** and their peak assignments are presented in Figure 4.14. All of the expected peaks are present and integrate correctly, with no impurities other than solvent. The MS was quite clean as well, with peaks only for $(M + H)^+$ at 1928.5465 *m/z*, $(M + Na)^+$, $(M + K)^+$, and small peaks corresponding to losses of Boc during ionization.

G1-$(Boc)_6Im_3$ **4.6** was deprotected with HCl to yield G1-$(NH_2)_6Im_3$ **4.7** (Figure 4.13). Upon deprotection, the ^{1}H NMR spectrum of G1-$(NH_2)_6Im_3$ **4.7** shows complete loss of the *tert*-butyl protons, evidence which is corroborated by MS (Appendix C). A ^{13}C NMR spectrum could not be obtained due to the low solubility of the deprotected dendrimer.

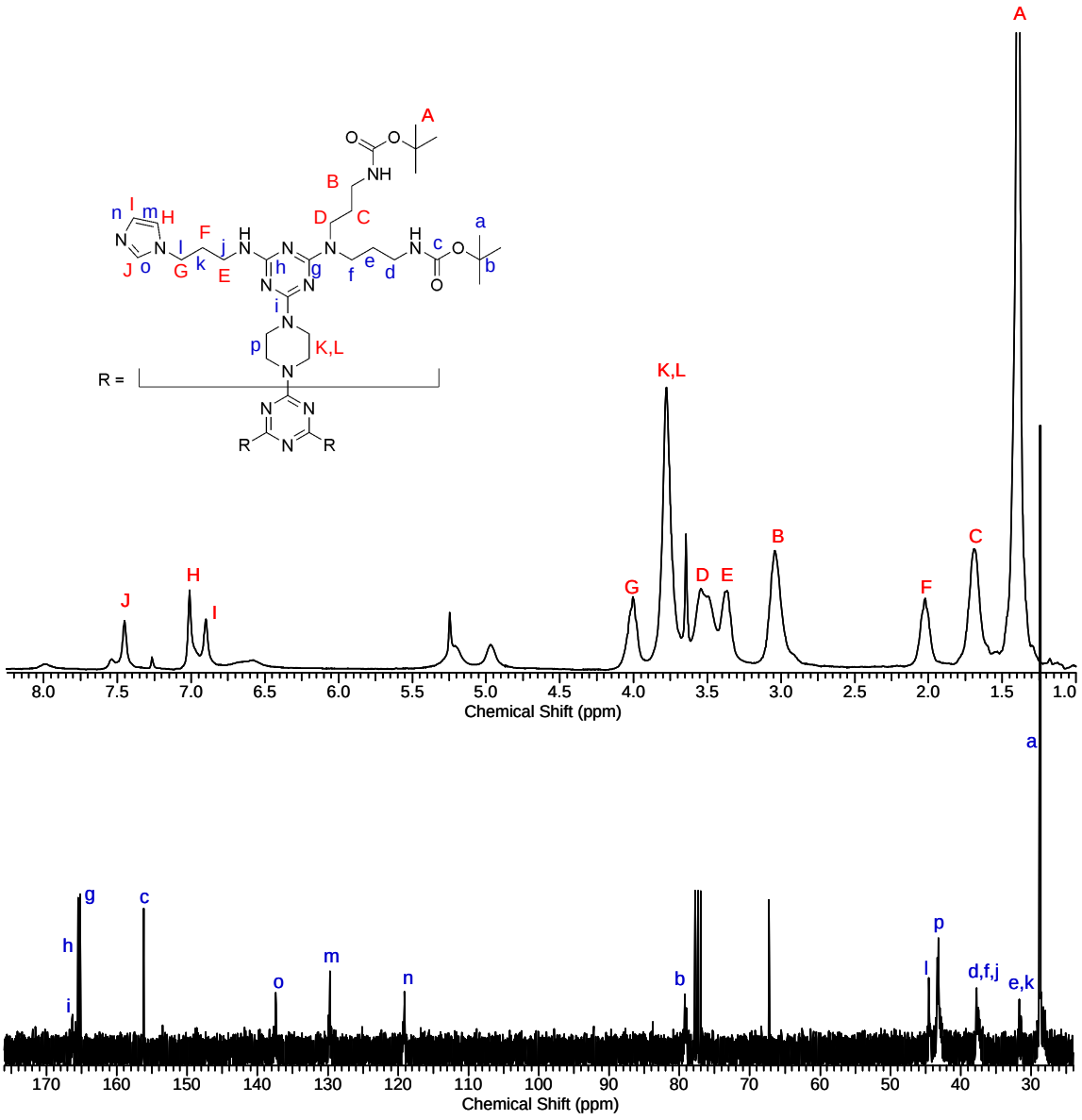

Figure 4.14. Assigned NMR spectra for G1-Boc_6Im_3 **4.6** in $CDCl_3$.

G1-$(NH_2)_6Im_3$ **4.7** was then reacted with NHS-activated PEG_{5000} to form a water-soluble dendrimer **4.8** (Figure 4.13). The PEGylation reaction was followed over time with MS. No peaks other than free PEG_{5000} were seen until day 9 (Figure 4.15).

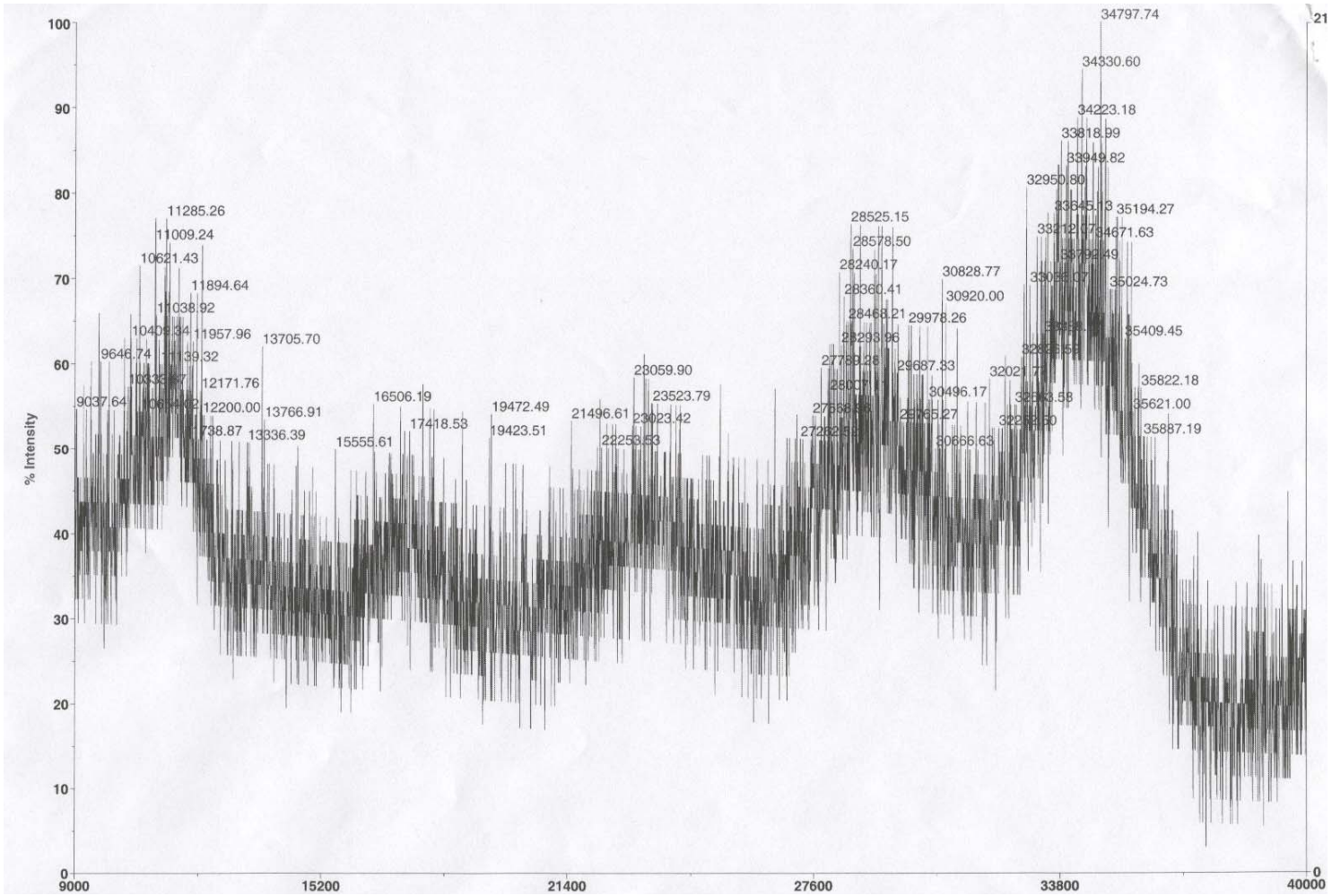

Figure 4.15. MS of the crude PEGylation reaction at day 9.

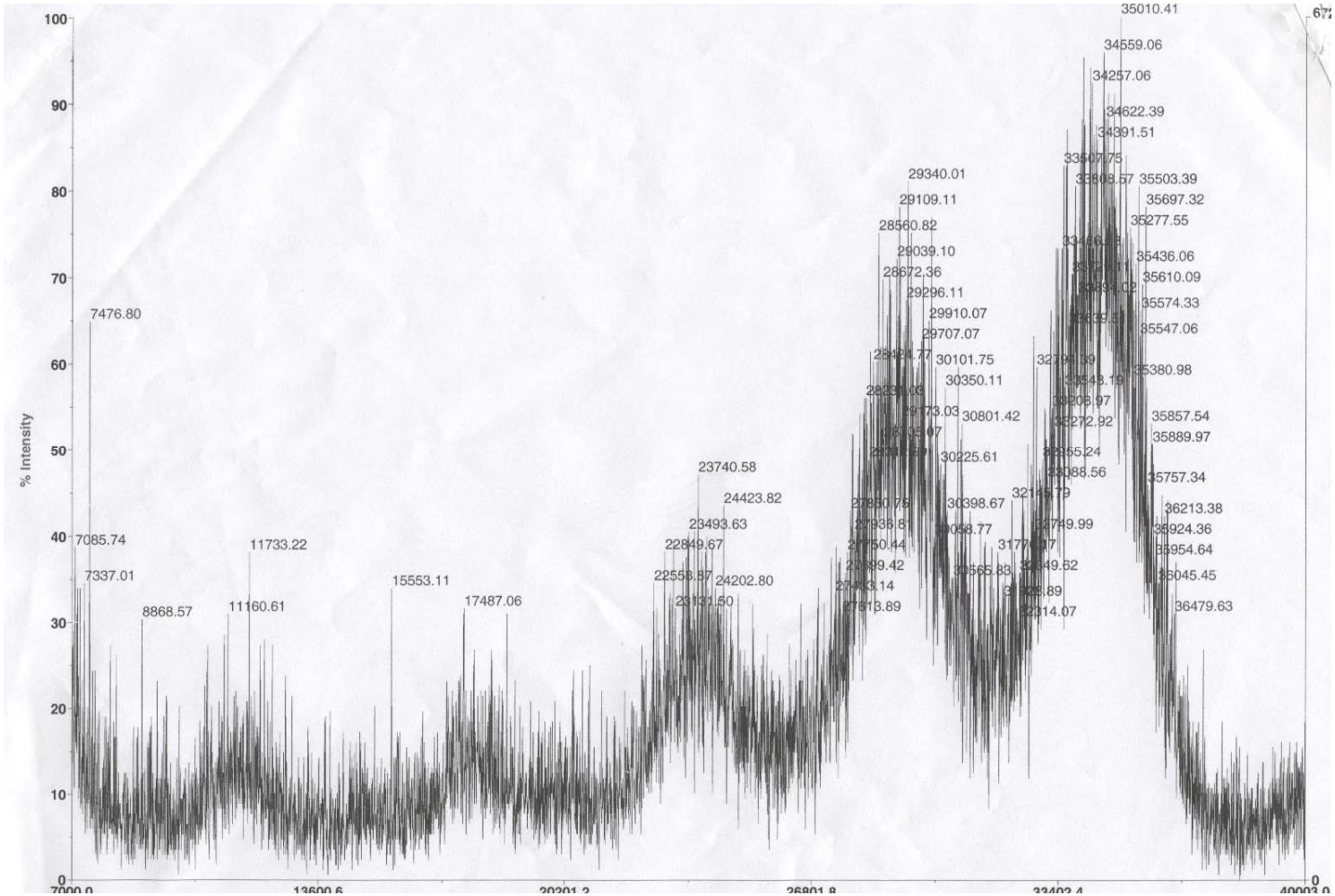

Figure 4.16. MS of the crude PEGylation reaction at day 13.

The spectrum from day 13 (Figure 4.16) shows the two major products as dendrimer with 5 and 6 PEG chains (at ~29000 and 35000, respectively) as well as small peaks for dendrimer with 4, 3, and 2 substitutions. The PEGylated dendrimer was purified by dialysis using 25,000 MW cutoff cellulose ester membranes, which should have removed free PEG and dendrimers with less than 5 PEG chains. Unfortunately, after dialysis, a mass spectrum could not be obtained, but the dendrimer was characterized by ^{1}H NMR spectroscopy.

^{1}H NMR spectroscopy analysis of the PEGylated dendrimer **4.8** is difficult due to the small amount of imidazole present and the presence of some as yet unidentified peaks (Figure 4.17). The imidazole proton that appears at ~7.5 ppm in the Boc-protected dendrimer is obscured by one of two peaks at 7.60 and 7.45 ppm that have not been identified.

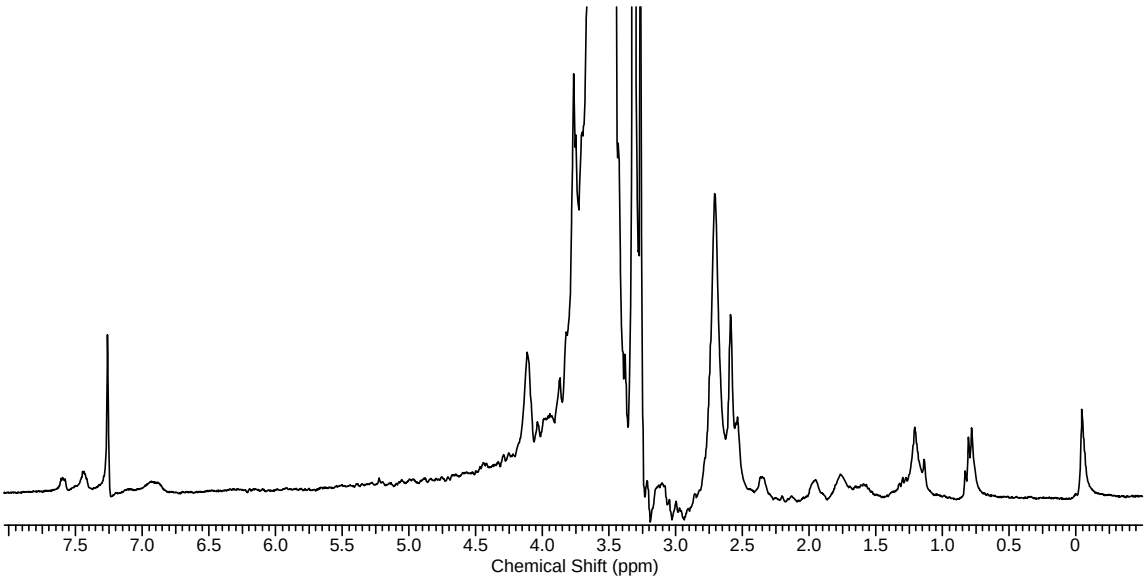

Figure 4.17. ^{1}H NMR spectrum of **4.8** in $CDCl_3$.

The broad peak from 7.02-6.80 ppm contains the two other imidazole protons. Two peaks for the propyl protons can be identified at 4.11 and 1.96 ppm, while the third peak at ~3.4 ppm is partially overlapped with the PEG protons. When the integration for the two imidazole protons at 7.02-6.80 is set to 6H, the PEG protons integrate for only 468H, suggesting a very low degree of PEGylation; however, the integration is not reliable as applying different pulse widths can change the integration by hundreds of protons.

Encapsulation

The encapsulation and water-solubilization of Zn-tetra(*tert*-butyl)phthalocyanine (ZnPc) by the PEGylated dendrimer was probed using increasing amounts of ZnPc (Table 4.1). The molecular weight used to calculate amounts of dendrimer (29208 g/mol) was a weighted average of the peaks present in the MS from day 13 (Figure 4.15). Ratios of ZnPc:dendrimer of 1:1, 2:1, 3:1. 6:1, and 9:1 were co-dissolved in DCM and evaporated to dryness three times. The mixtures were then dissolved in water to yield blue aqueous solutions. Mixtures with 6:1 and 9:1 ZnPc:dendrimer ratios did not show complete solvation of ZnPc, as evidenced by blue flakes that do not dissolve in water even after sonication. As a control, ZnPc was co-dissolved with 6 equivalents of free PEG_{5000} under the same conditions, but showed no water solubilization, indicating that the solubilization seen in the dendrimer is not merely a hydrophobic effect. A conjugate formed from the addition of PEG_{5000} to 1-(3-aminopropyl)imidazole (**4.9**) also did not solubilize ZnPC in water. However, the conjugate was not purified, and any succinimide present could possibly inhibit the binding of Zn to the imidazole.

Table 4.1. Summary of encapsulation experiments.

Mixture	Ratio	result
ZnPc alone	--	ppt.
PEG_{5000}+ZnPc	6:1	ppt.
PEG_{5000}-im **4.9**+ZnPc	1:1	ppt.
dendrimer **4.8**+ZnPc	1:1	sol'n.
dendrimer **4.8**+ZnPc	1:2	sol'n.
dendrimer **4.8**+ZnPc	1:3	sol'n.
dendrimer **4.8**+ZnPc	1:6	sol'n. + ppt.
dendrimer **4.8**+ZnPc	1:9	sol'n + ppt.

Further analyses of the dendrimer/ZnPc mixtures by ^{1}H NMR may help determine how/if the Pc are bound to imidazole, as the shifts for the imidazole hydrogens should shift upon binding of zinc. Additional control studies of encapsulation in a PEGylated dendrimer without imidazoles will also help determine what role the imidazoles and the dendrimer structure play in the solubilization.

Conclusions

Although there was some literature precedence for the covalent conjugation of photosensitizers to dendrimers, the results here were rather unsuccessful. The inability to obtain single compounds, coupled with the unreliablility of mass spectrometry, made the identification of products difficult. If conjugation were successful, it is possible that the phthalocyanines would interact with other phthalocyanines on the same dendrimer, or on another dendrimer in solution. This aggregation would most likely be remedied by PEGylation of the dendrimer, which would be necessary for water-solubilization as well.

Given the difficulties in the covalent route, as well as the synthetic burden, the non-covalent strategy presented is much more appealing.

The initial encapsulation studies with the PEGylated imidazole dendrimer gave promising results, but the dendrimer is poorly characterized, making it difficult to obtain quantifiable results. This situation may be remedied in the future by more rigorous characterization of the dendrimer by gel permeation chromatography (GPC) and 2-D NMR spectroscopy.

Future studies include the synthesis of an alternative imidazole dendrimer that is functionalized with *tris*(hydroxymethyl)amino methane (TRIS) for water-solubility (Figure 4.17). While this dendrimer will not have the high molecular weight desirable for *in vivo* application for PDT, the characterization will be greatly simplified in comparison to the PEGylated dendrimer. Quantification of its ability to encapsulate phthalocyanine, as well as the kinetics of its release will also be studied.

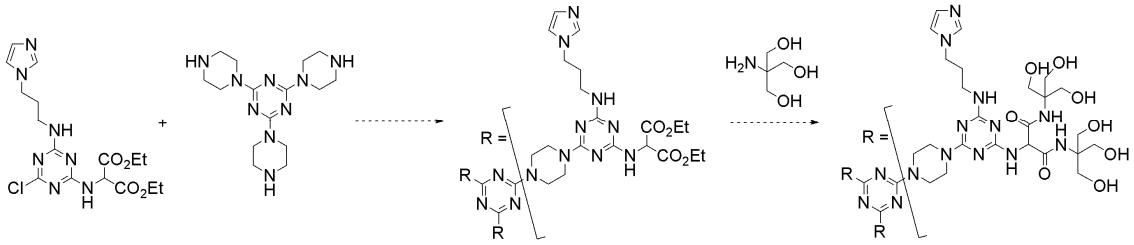

Figure 4.18. Proposed synthesis of a water-soluble imidazole-bearing dendrimer.

Experimental

All chemicals were purchased from Sigma-Aldrich or Acros and used without further purification. All solvents were ACS grade and used without further purification. Thin-layer chromatography was performed using EMD silica gel 60 F254 pre-coated glass plates (0.25 mm). Preparative column chromatography was performed using EMD silica gel 60 (0.040 mm particle size). ^{1}H and $^{13}C\{^{1}H\}$ NMR data were acquired on a Varian 300 MHz spectrometer at 25 °C unless otherwise indicated. ^{1}H and $^{13}C\{^{1}H\}$ NMR chemical shifts are listed relative to tetramethylsilane in parts per million, and were referenced to the residual proton or carbon peak of the solvent. All mass spectral analyses were carried out by the Laboratory for Biological Mass Spectrometry at Texas A&M University. MALDI-TOF mass spectra (in the positive mode) were acquired on a Voyager-DE STR mass spectrometer equipped with a pulsed nitrogen laser emitting at 337 nm. Samples were analyzed in linear mode using an extraction delay time set at 350 ns and an accelerating voltage operating at 25 kV utilizing trihydroxyacetophenone as the matrix. To improve the signal-to-noise ratio, 100 single shots were averaged for each mass spectrum, and typically, four individual spectra were accumulated to generate a summed spectrum. Electrospray mass spectra were acquired in the positive ion mode using a MDS Sciex API Qstar Pulsar using an Ionwerks time-to-digital converter, TDCx4, for data recording at 625 ps time resolution. Samples were electrosprayed from acetonitrile at 50 mM under the conditions listed next. The ion spray (needle) voltage was held constant at 4.5 kV. The nozzle skimmer potential was set to +10 V to minimize fragmentation in that region. TOF voltages were tuned to optimize the resolving power

over the mass range observed, but usually the following parameters were used: grid -338 V, plate +360 V, mirror +960 V, and liner +4000 V. Acquisition and data analysis were performed with the Analyst QS software.

Zn-4-amino-tris(tert-butyl)phthalocyanine (4.1). 4-Amino-phthalonitrile (0.518 g, 3.62 mmol) and 4-*tert*-butyl-phthalonitrile (2.0 g, 10.86 mmol) were dissolved in 3.6 mL degassed DMA with octanol (0.572 mL, 3.62 mmol), Et_3N (0.47 mL, 3.62 mmol), and $ZnCl_2$ (0.49 g, 3.62 mmol) to give a light yellow solution. The reaction mixture was stirred at 130 °C for 2 days and the reaction progress was monitored by TLC. The DMF, now a dark blue solution, was removed *in vacuo*, and the blue solids were dissolved in DCM and washed with water (3 x 100 mL) and brine (1 x 100 mL). The organic fractions were combined and the DCM removed *in vacuo*. The solids were purified by column chromatography (19:1 DCM: MeOH) to yield several products ranging in color from blue to green and in Rf from 0.54 to 0. The blue-green fractions containing the product and two other spots were further purified by precipitation from acetone with water. The acetone was removed *in vacuo*, and the products were dissolved in DCM/MeOH and stirred in concentrated HCl overnight. The acid was slowly neutralized with $NaHCO_3$, then the reaction mixture was washed with a solution of $NaHCO_3$ and ethylene diamine tetra-acetic acid (EDTA) and extracted with DCM. The organic fractions were filtered through a silica plug to isolate two bands: free-base Pc-NH_2 and the product, ZnPc-NH_2 (0.3407 g, 12% yield). ^{1}H NMR (300 MHz, $CDCl_3$) δ: 7.88 (m, 5H), 7.76 (m, 7H), 1.37 (s, 27H). ^{13}C NMR (75.5 MHz, $CDCl_3$) δ: 131.58,

123.61, 120.92, 31.35 (br). MS (MALDI-TOF): calcd, 759.2776 (M^+); found, 760.2983 $(M + H)^+$.

Boc-isonipecotic acid (4.2). Isonipecotic acid (1.0 g, 7,74 mmol) and BOC-ON (1.91 g, 7.74 mmol) were dissolved in 10 mL THF with Et_3N (2 mL, 15.48 mmol) and stirred at room temperature overnight. The THF was removed *in vacuo* and the residue dissolved in DCM (50 mL) and washed with 5% NaOH (3 x 50 mL). The organic layers were collected and filtered through silica. The filtrate was collected and removed *in vacuo* to yield 1.77g (>99% yield) of product as a white solid. ^1H NMR (300 MHz, $CDCl_3$) δ: 11.27 (s, 1H), 3.93 (br, 2H), 2.78 (br, 2H), 2.38 (br, 1H), 1.79 (br, 2H), 1.56 (br, 2H), 1.38 (s, 9H). ^{13}C NMR (75.5 MHz, $CDCl_3$) δ: 180.01, 155.04, 80.05, 43.25, 41.20, 28.58, 28.00. MS (ESI): calcd, 229.1314 (M^+); found, 230.1420 $(M + H)^+$, 252.1225 $(M + Na)^+$.

NHS-Boc-isonipecotic acid (4.3). Boc-isonipecotic acid 4.2 (0.5 g, 2.18 mmol) and disuccinimidyl carbonate (0.838 g, 3.27 mmol) were dissolved in 5 mL dry DMF with pyridine (0.25 mL, 3.27 mmol). The reaction was stirred at 50 °C for 1 hour, then 25 °C overnight. Water (50 mL) was added to the reaction mixture, which was extracted with DCM (3 x 50 mL). The DCM was reduced *in vacuo*, and the product was obtained by precipitation with hexanes (0.237 g, 26% yield, first crop). ^1H NMR (300 MHz, $CDCl_3$) δ: 3.92 (m, 2H), 2.91 (m, 2H), 2.77 (bs, 4H), 1.93 (br, 3H), 1.74 (m, 2H), 1.39 (s, 9H). ^{13}C NMR (75.5 MHz, $CDCl_3$) δ: 169.93, 169.37, 154.70, 79.97, 42.80, 38.66, 28.56, 27.85, 25.78. MS(ESI): calcd, 326.1487 (M+); found, 327.1568 $(M + H)^+$, 349.1341 $(M + Na)^+$.

ZnPc-isonipecotic acid (4.4). ZnPc-NH_2 **4.1** (0.125 g, 0.1638 mmol) and **4.3** (0.053 g, 0.1638 mmol) were dissolved in DCM (10 mL) with Et_3N (0.02 mL, 0.1638 mmol) and stirred at room temperature for 4 days. The reaction solution was washed with water (3 x 20 mL) and the organic portions were removed in vacuo. The solids were dissolved DCM/MeOH (1mL:5mL) with 5M HCl (5 mL). The reaction was stirred for 6 hours, then filtered through a silica plug. The filtrate was removed to yield the product as a blue-green solid (0.10 g, 70% yield). MS (MALDI): calcd, 870.3461 (M^+); found, 871.4258 $(M + H)^+$.

Iodo-tetra(tert-butyl)azaporphyrin (4.5). Tetra(*tert*-butyl)azaporphyrin (0.101 g, 0.1967 mmol) was dissolved in 12 mL $CHCl_3$. Pyridine (~0.2 mL) was added dropwise to a solution of phenyliodine *bis*(trifluoroacetate) (PIFA, 0.127 g, 0.295 mmol) and crushed iodine (0.025 g, 0.0983 mmol) in 3 mL $CHCl_3$ until it became a light yellow color. The PIFA solution was added dropwise to the azaporphyrin solution and the mixture was stirred at room temperature for 2 days. The reaction solution was washed with a saturated solution of $Na_2S_2O_3$ (3 x 50 mL), and the organic layers were reduced *in vacuo*. The residue was redissolved in 10 mL $CHCl_3$ with PIFA (0.127 g, 0.295 mmol) and crushed I_2 (0.025 g., 0.0983 mmol) and stirred at 50 °C overnight. The reaction solution was washed with a saturated solution of $Na_2S_2O_3$ (3 x 50 mL), and the $CHCl_3$ was removed *in vacuo*. The solids were dissolved in hexanes and filtered through a silica plug, then washed with 15:1 hexanes:toluene increasing to 1:1 hexanes:toluene. The product was collected in the first band (Rf = 0.93 in toluene, 0.060 g, 46% yield), with unreacted starting material in the second band (Rf = 0.42 in toluene). ^1H NMR

(300 MHz, $CDCl_3$) δ: 9.103, 9.063, 9.043, 8.820, 8.767, 8.759 (3H total); 2.429, 2.414, 2.337, 2.326, 2.285, 2.264, 2.253, 2.218, 2.206 (36H total). ^{13}C NMR (75.5 MHz, $CDCl_3$) δ: 161.708, 157.809, 157.566, 156.834, 130.886, 130.716, 130.609, 127.701, 127.527, 127.162, 126.897, 126.703, 126.460, 36.520, 35.453, 35.142, 34.949, 34.861, 33.935, 33.669, 32.610, 32.561, 32.352, 32.314, 32.227. MS (MALDI-TOF): calcd, 664.2499 (M^+); found, 665.2016 $(M + H)^+$.

G1-Boc$_6$Im$_3$ (4.6). **G1-Cl** (1.34 g, 0.806 mmol) and 1-(3-aminopropyl)imidazole (0.866 mL, 7.25 mmol) were dissolved in 3 mL THF and 10 mL dioxane with DIPEA (1 mL, 7.25 mmol) and stirred at 100 °C for 2 days. The solvents were removed *in vacuo* and the solids dissolved in DCM (50 mL) and washed with water (3 x 50 mL). The DCM was removed *in vacuo* and the product isolated by silica gel column chromatography (19:1 $CHCl_3$:MeOH, 1.246 g, 80% yield). ^1H NMR (300 MHz, $CDCl_3$) δ: 7.99 (br, 1H), 7.45 (s, 3H), 7.01 (s, 3H), 6.90 (s, 3H), 6.59 (br, 3H), 5.21 (br, 2H), 4.97 (br, 3H), 4.00 (br, 6H), 3.78 (br, 24H), 3.54 (br, 12H), 3.38 (br, 6H), 3.04 (br, 12H), 2.02 (br, 6H), 1.69 (br, 12H), 1.39 (s, 54H). ^{13}C NMR (75.5 MHz, $CDCl_3$) δ: 166.30, 165.49, 165.20, 156.18, 137.39, 129.71, 119.08, 79.23, 44.54, 43.20, 37.78, 31.67, 28.73. MS (MALDI-TOF): calcd, 1927.2234 (M^+); found, 1928.5465 $(M + H)^+$.

G1-(NH$_2$)$_6$Im$_3$ (4.7). **G1-Boc$_6$Im$_3$** (0.663 g, 0.344 mmol) was dissolved in 3 mL DCM with 3 mL MeOH. 5M HCl (3 mL) was added and the reaction stirred at room temperature for 6 hours. The organic solvents were removed *in vacuo*, and the remaining solution was made basic (pH = 14) with 5 M NaOH. The product precipitated as a residue in the flask, and the basic solution was poured off. The residue was

dissolved in DCM (100 mL) and washed with water (3 x 50 mL). The DCM was removed *in vacuo* to yield a white solid (0.439 g, 96% yield). ^{1}H NMR (300 MHz, CD_3OD) δ: 7.65 (s, 3H), 7.14 (s, 3H), 6.97 (s, 3H), 4.07 (br, 6H), 3.74 (br, 24H), 3.58 (br, 12H), 3.31 (br, 6H), 2.58 (br, 12H), 2.02 (br, 6H), 1.74 (br, 12H).

G1-(PEG$_{5000}$)$_6$Im$_3$ (4.8). **G1-(NH$_2$)$_6$Im$_3$** (0.039 g, 0.0297 mmol) was dissolved in 0.5 mL MeOH and diluted with 8 mL DCM. NHS-activated polyethylene glycol (5000 g/mol, 2.0 g, 0.4 mmol) and DIPEA (0.06 mL, 0.40 mmol) were added and the reaction was stirred at room temperature under nitrogen for 14 days. The solvents were removed in vacuo and the white solids were dissolved in water and filtered through 0.45 μm mixed cellulose ester microfiltration cartridges. The filtrate was dialyzed in 25,000 molecular weight cutoff cellulose ester dialysis tubing for 7 days. The water was removed from the dialyzed product *in vacuo* to yield the product as a white solid (0.4253 g, 48% yield). ^{1}H NMR (300 MHz, $CDCl_3$) δ: 7.60, 7.50, 7.45, 6.99-6.82 (br, 6H), 4.11 (br, 6H), 3.53-3.32 (br, 468 H), 3.13 (br, 12 H), 2.71, 2.35, 1.96 (br, 6H), 1.76 (br, 12H). MS (MALDI-TOF): calcd, 30127 (average M^+); found, 35010, 29340, 23740.

PEG$_{5000}$-Im. NHS-activated PEG_{5000} (0.25 g, 0.1 mmol) and 1-(3-aminopropyl)imidazole (0.006 mL, 0.1 mmol) were dissolved in 2 mL $CHCl_3$ with DIPEA (0.0025 mL, 0.3 mmol) for 1 week. The solvent was removed *in vacuo* and the solids were not further purified. ^{1}H NMR (300 MHz, $CDCl_3$) δ: 7.30 (s, 1H), 6.83 (s, 1H), 6.75 (s, 1H), 3.86 (t, 2H), 3.45 (s, 36H), 2.50 (t, 2H), 1.70 (p, 2H). ^{13}C NMR (75.5 MHz, $CDCl_3$) δ:137.22, 129.32, 118.99, 70.60, 44.44, 38.79, 34.36.

CHAPTER V

SUMMARY

Dendrimers are unique branched macromolecular structures that are well-suited for drug delivery,[47-57, 70-72] particularly anti-tumor drugs.[29-38, 43, 63, 65-69] Unlike traditional linear and hyperbranched polymers, dendrimers are generated from step-wise organic synthesis, leading to greater control over their structure and functionalization. Dendrimers synthesized from a convergent route may display a diverse periphery with a very low polydispersity index, but they are often limited to lower generations due to steric hindrance at the reaction focal site.[4-6] Dendrimers synthesized from a divergent protocol traditionally reach larger generations, but often present only one type of surface group and are plagued by impurities resulting from small amounts of under-substituted materials.[1-3]

The convergent approach was originally used here to synthesize a generation-2 dendrimer functionalized with hydrazone groups. Initially, orthogonally-protected Boc- and Dde- amines were used as surface groups, with piperazine as a linker, to form a generation-1 dendron **2.9** with six Boc-protected amines and one Dde-protected amine. During the course of this synthesis it became apparent that isolating dichlorotriazine intermediates produced from the first substitution of cyanuric chloride resulted in cleaner materials than previously used one-pot methods. The dichlorotriazines are isolated in high yields by precipitation, eliminating column chromatography that is typically necessary in our convergent syntheses.

4-piperidone was chosen as an alternative to the Dde-protected amine as it offers a reactive handle for hydrazone chemistry and eliminates the protecting group manipulations. The generation-1 dendron **2.11** was attached to a tris(piperazine) core to yield a generation-2 dendrimer with 3 hydrazones. The antihypertensive drug hydralazine will be conjugated to the deprtoected dendrimer through the formation of a hydrazone bond, and studies of the release of hydralazine in acidic solutions will be carried out.

The facile isolation of dichlorotriazines led us to devise a divergent route towards higher-generation dendrimers using a dichlorotriazine with Boc-protected amines as a monomer. The substitution of an amine core with the dichlorotriazine monomer **3.1** gave a poly(monochlorotriazine) dendrimer (G*n*-Cl), which was capped with piperidine (G*n*-pip) then deprotected to give a new polyamine core (G*n*-NH_2). This sequence was repeated to synthesize dendrimers from generation-1 through generation-5. The solvents for the reactions building G*n*-Cl dendrimers were changed at each generation due to the decreasing solubility of the G*n*-NH_2 dendrimers. The conditions for the capping and deprotection steos were universal, and proceeded in quantitative yields. The G*n*-Cl dendrimers were purified by precipitation and the G*n*-pip dendrimer were purified by filtration through a silica plug to remove excess piperidine. All dendrimers were characterized by ^{1}H and ^{13}C NMR spectroscopy, mass spectrometry, and either HPLC or GPC. The lower generations (1-3) were pure within small molecule organic synthesis standards (>97%). Analysis of generations 4 and 5 suggest that there may be small

impurities, but these dendrimers are still at least as pure as commercially-available dendrimers of complemetary generation and functionality.

Finally, the synthesis of a photoactive dendrimer was undertaken. Attempts to synthesize a phthalocyanine dichlorotriazine monomer using either ZnPc-NH_2 **4.1** or siloxy-centered pthalocyanines were unsuccessfull, as were attempts to conjugate amino-phthalocyanines and porphyrazines to a G2-Cl dendrimer. A generation-1 dendrimer functionalized with three imidazoles was synthesized by the substitution of G1-Cl with 1-(3-aminopropyl) imidazole. The dendrimer was deprotected, and then conjugated with six PEG_{5000} chains to form a water-soluble dendrimer **4.8**.

The PEGylated dendrimer encapsulated and solubilized in water up to three molecules of Zn-tetra(*tert*-butyl)phthalocyanine. A more detailed quantification of the encapsulation studies is difficult due to the inaccurate molecular weight of the dendrimer resulting from the polydispersity of the PEG_{5000}. Control studies with PEG_{5000} and a PEG_{5000}-imidazole conjugate **4.9** did not reveal any water-solubilization. Further control studies of encapsulation in a PEGylated non-imidazole dendrimer will be completed.

This dissertation has described two different synthetic pathways for melamine dendrimers, and studies into possible biological uses for these dendrimers have been initiated.

REFERENCES

(1) Buhleier, E.; Wehner, W.; Vogtle, F. *Synthesis* **1978**, 155-158.

(2) Newkome, G. R.; Yao, Z.-q.; Baker, G. R.; Gupta, V. K. *J. Org. Chem.* **1985**, *50*, 2003-2004.

(3) Tomalia, D. A.; Baker, H.; Dewald, J.; Hall, M.; Kallos, G.; Martin, S.; Roeck, J.; Ryder, J.; Smith, P. *Polym. J.* **1985**, *17*, 117-132.

(4) Hawker, C. J.; Frechet, J. M. J. *J. Am. Chem. Soc.* **1990**, *112*, 7638-7647.

(5) Lim, J.; Simanek, E. E. *Mol. Pharmaceutics* **2005**, *2*, 273-277.

(6) Steffensen, M. B.; Simanek, E. E. *Angew. Chem., Int. Ed.* **2004**, *43*, 5178-5180.

(7) Wooley, K. L.; Hawker, C. J.; Frechet, J. M. J. *J. Am. Chem. Soc.* **1991**, *113*, 4252.

(8) Khandare, J. J.; Minko, T. *Prog. Polym. Sci.* **2006**, *31*, 359.

(9) Singh, S. K.; Sirohi, S.; Verma, S.; Kumar, S. G. V.; Mishra, D. N. *Pharma. Review* **2005**, *3*, 29.

(10) Svenson, S.; Tomalia, D. A. *Adv. Drug Deliv. Rev.* **2005**, *57*, 2106.

(11) Yang, H.; Kao, W. J. *J.Biomater. Sci., Polym. Ed.* **2006**, *17*, 3-19.

(12) Matsumura, Y.; Maeda, H. *Cancer Res.* **1986**, *6*, 6387-6392.

(13) Duncan, R. *Pharmaceutical Science and Technology Today* **1999**, *2*, 441-449.

(14) Duncan, R. *Nature* **2003**, *2*, 347.

(15) Hobbs, S. K.; Monsky, W. L.; Yuan, F.; Roberts, W. G.; Griffith, L.;

Torhcilin, V. P.; Jain, R. K. *Proc. Natl. Acad. Sci. U.S.A.* **1998**, *95*, 4607-4612.

(16) Iyer, A. K.; Khaled, G.; Fang, J.; Maeda, H. *Drug Discovery Today* **2006**, *11*, 812-818.

(17) Maeda, H.; Matsumura, Y. *Critical Reviews in Therapeutic Drug Carrier Systems* **1989**, *6*.

(18) Jevprasesphant, R.; Penny, J.; Attwood, D.; McKeown, N. B.; D'Emanuele, A. *Pharm. Res.* **2003**, *20*, 1543.

(19) Metullio, L.; Ferrone, M.; Coslanich, A.; Fuchs, S.; Fermeglia, M.; Paneni, M. S.; Pricl, S. *Biomacromolecules* **2004**, *5*, 1371 - 1378.

(20) Duncan, R.; Malik, N.; Lorenz, K.; Weener, J. W.; Paulus, W. *J. Controlled Release* **2000**, *65*, 133.

(21) Chen, H.-T.; Neerman, M. F.; Parrish, A. R.; Simanek, E. E. *J. Am. Chem. Soc.* **2004**, *126*, 10044-10048.

(22) Hong, S.; Bielinska, A. U.; Mecke, A.; Keszler, B.; Beals, J. L.; Shi, X.; Balogh, L.; Orr, B. G.; James R. Baker, J.; Holl, M. M. B. *Bioconjugate Chem.* **2004**, *15*, 774-782.

(23) Hong, S.; Leroueil, P. R.; Janus, E. K.; Peters, J. L.; Kober, M.-M.; Islam, M. T.; Orr, B. G.; James R. Baker, J.; Holl, M. M. B. *Bioconjugate Chem.* **2006**, *17*, 728-734.

(24) Stiriba, S.-E.; Frey, H.; Haag, R. *Angew. Chem., Int. Ed.* **2002**, *41*, 1329.

(25) Duncan, R.; Izzo, L. *Adv. Drug Deliv. Rev.* **2005**, *57*, 2106.

(26) Padilla De Jesus, O. L.; Ihre, H. R.; Gagne, L.; Frechet, J. M. J.; Szoka, F. C. J. *Bioconjugate Chem.* **2002**, *13*, 453.

(27) Purohit, G.; Sakthivel, T.; Florence, A. T. *Int. J. Pharm.* **2003**, *254*, 37.

(28) Jevprasesphant, R.; Penny, J.; Jalal, R.; Attwood, D.; McKeown, N. B.; D'Emanuele, A. *Int. J. Pharm.* **2003**, *252*, 263.

(29) Kono, K.; Liu, M.; Frechet, J. M. J. *Bioconjugate Chem.* **1999**, *10*, 1115-1121.

(30) Quintana, A.; Raczka, E.; Piehler, L.; Lee, I.; Myc, A.; Majoros, I.; Patri, A. K.; Thomas, T.; Mule´, J.; James R. Baker, J. *Pharm. Res.* **2002**, *19*, 1310-1316.

(31) Patri, A. K.; Kukowska-Latallo, J. F.; Baker, J., R. Jr. *Adv. Drug Deliv. Rev.* **2005**, *57*, 2203-2214.

(32) Sudimack, J.; Lee, R. J. *Adv. Drug Deliv. Rev.* **2000**, *41*, 147-162.

(33) Wu, G.; Barth, R. F.; Yang, W.; Kawabata, S.; Zhang, L.; Green-Church, K. *Mol. Cancer Ther.* **2006**, *5*, 52-59.

(34) Gurdag, S.; Khandare, J.; Stapels, S.; Matherly, L. H.; Kannan, R. M. *Bioconjugate Chem.* **2006**, *17*, 275-283.

(35) Zhuo, R. X.; Du, B.; Lu, Z. R. *J. Cont. Rel.* **1999**, *57*, 249-257.

(36) Malik, N.; Evagorou, E. G.; Duncan, R. *Anticancer Drugs* **1999**, *10*, 767-776.

(37) Jansen, B. A. J.; van der Zwan, J.; Reedijk, J.; den Dulk, H.; Brouwer, J. *Eur. J. Inorg. Chem.* **1999**, 1429-1433.

(38) Kapp, T.; Dullin, A.; Gust, R. *J. Med. Chem.* **2006**, *49*, 1182-1190.

(39) Etrych, T.; Jelinkova, M.; Rihova, B.; Ulbrich, K. *J. Cont. Rel.* **2001**, *73*, 89-102.

(40) Chyrtry, V.; Ulbrich, K. *J. Bioact. Compat. Polym.* **2001**, *16*, 427-440.

(41) Etrych, T.; Chytil, P.; Jelinkova, M.; Rihova, B.; Ulbrich, K. *Macromol. Biosci.* **2002**, *2*, 43-52.

(42) Wang, D.; Kopeckova, P.; Minko, T.; Nanayakkara, V.; Kopecek, J. *Biomacromolecules* **2000**, *1*, 313-319.

(43) Lai, P.-S.; Lou, P.-J.; Peng, C.-L.; Pai, C.-L.; Yen, W.-N.; Huang, M.-Y.; Young, T.-H.; Shieh, M.-J. *J. Cont. Rel.* **2007**, *122*, 39-46.

(44) Boas, U.; Heegaard, P. M. H. *Chem. Soc. Rev.* **2004**, *33*, 43.

(45) Twyman, L. J.; Beezer, A. E.; Esfand, R.; Hardy, M. J.; Mitchell, J. C. *Tetrahedron Lett.* **1999**, *40*, 1743.

(46) Beezer, A. E.; King, A. S. H.; Martin, I. K.; Mitchell, J. C.; Twyman, L. J.; Wain, C. F. *Tetrahedron* **2003**, *59*, 3873.

(47) Kolhe, P.; Misra, E.; Kannan Rangaramanujam, M.; Kannan, S.; Lieh-Lai, M. *In.t J. Pharm.* **2003**, *259*, 143-60.

(48) Kannan, S.; Kolhe, P.; Raykova, V.; Glibatec, M.; Kannan Rangaramanujam, M.; Lieh-Lai, M.; Bassett, D. *J. Biomater. Sci., Polym. Ed.* **2004**, *15*, 311-30.

(49) Yiyun, C.; Tongwen, X. *Eur. J. Med. Chem.* **2005**, *40*, 1188-92.

(50) Yiyun, C.; Tongwen, X.; Rongqiang, F. *Eur. J. Med. Chem.* **2005**, *40*,

1390-1393.

(51) Na, M.; Yiyun, C.; Tongwen, X.; Yang, D.; Xiaomin, W.; Zhenwei, L.; Zhichao, C.; Guanyi, H.; Yunyu, S.; Longping, W. *Eur. J. Med. Chem.* **2006**, *41*, 670-4.

(52) Cheng, Y.; Man, N.; Xu, T.; Fu, R.; Wang, X.; Wang, X.; Wen, L. *J. Pharm. Sci.* **2007**, *96*, 595-602.

(53) Asthana, A.; Chauhan, A. S.; Diwan, P. V.; Jain Narendra, K. *AAPS Pharm. Sci. Technol.* **2005**, *27*, 536.

(54) Devarakanda, B.; Hill, R. A.; Liebenberg, W.; Brits, M.; de Villiers, M. M. *Int. J. Pharm.* **2005**, *304*, 193.

(55) Chauhan, A. S.; Sridevi, S.; Chalasani, K. B.; Jain, A. K.; Jain, S. K.; Jain, N. K.; Diwan, P. V. *J. Controlled Release* **2003**, *90*, 335-343.

(56) Chandrasekar, D.; Sistla, R.; Ahmad, F. J.; Khar, R. K.; Diwan, P. V. *Biomaterials* **2007**, *28*, 504-512.

(57) Chandrasekar, D.; Sistla, R.; Ahmad, F. J.; Khar, R. K.; Diwan, P. V. *J. Biomed. Mat. Res., Part A* **2007**, *82A*, 92-103.

(58) Tomalia, D. A.; Berry, V.; Hall, M.; Hedstrand, D. M. *Macromolecules* **1987**, *20*, 1164.

(59) Hawker, C. J.; Wooley, K. L.; Frechet, J. M. J. *J. Chem. Soc. Perkin. Trans.* **1993**, *1*, 1287.

(60) Newkome, G. R.; Moorefield, C. N.; Baker, G. R.; Saunders, M. J.;

Grossman, S. H. *Angew. Chem. Int. Ed.* **1991**, *30*, 1178.

(61) Esfand, R.; Tomalia, D. A. *Drug Discovery Today* **2001**, *6*, 427.

(62) Sato, T.; Niwa, H.; Chiba, A. *J. Chem. Phys.* **1998**, *108*, 4138.

(63) Ooya, T.; Lee, J.; Park, K. *J. Cont. Rel.* **2003**, *93*, 121.

(64) Ooya, T.; Lee, J.; Park, K. *Bioconjugate Chem.* **2004**, *15*, 1221.

(65) Kojima, C.; Kono, K.; Maruyama, K.; Takagishi, T. *Bioconjugate Chem.* **2000**, *11*, 910-917.

(66) Neerman, M. F.; Chen, H.-T.; Parrish, A. R.; Simanek, E. E. *Mol. Pharmaceutics* **2004**, *1*, 390-393.

(67) Dhanikula, R. S.; Hildgen, P. *Biomaterials* **2007**, *28*, 3140-3152.

(68) Bhadra, D.; Bhadra, S.; Jain, S.; Jain, N. K. *Int. J. Pharm.* **2003**, *257*, 111.

(69) Zhang, W.; Jiang, J.; Qin, C.; Perez, L. M.; Parrish, A. R.; Safe, S. H.; Simanek, E. E. *Supramol. Chem.* **2003**, *15*, 607-616.

(70) Bhadra, D.; Bhadra, S.; Jain Narendra, K. *Pharm. Res.* **2006**, *23*, 623.

(71) Sideratou, Z.; Tsiourvas, D.; Paleos, C. M. *J. Colloid Interf. Sci.* **2001**, *242*, 272.

(72) Namazi, H.; Adeli, M. *Biomaterials* **2005**, *26*, 1175.

(73) Ben-hur, E.; Chan, W.-S.; in *The Porphyrin Handbook*; Kadish, K. M., Smith, K. M., Guillard, R., Eds.; Academic Press:New York, NY, 2003; Vol. 19, 1-35.

(74) Castano, A. P.; Demidova, T. N.; Hamblin, M. R. *Photodiagnosis and Photodynamic Therapy* **2004**, *1*, 279.

(75) Bonnett, R. *Chem. Soc. Rev.* **1995**, 19-33.

(76) Vesper, B. J.; Lee, S.; Hammer, N. D.; Elseth, K. M.; Barrett, A. G. M.; Hoffman, B. M.; Radosevich, J. A. *J. Photochem. Photobiol. B.* **2006**, *82*, 180.

(77) Morgan, A. R.; Petousis, N. H.; van Lier, J. E. *Eur. J. Med. Chem.* **1997**, *32*, 21.

(78) Ben-Hur, E.; Rosenthal, I. *Int. J. Radiat. Biol.* **1985**, *47*, 145.

(79) Ben-Hur, E.; Zuk, M. M.; Chin, S.; Banerjee, D.; Kenney, M. E.; Horowitz, B. *Photochem. Photobiol.* **1995**, *62*, 575.

(80) Rensen, P. C.; Love, W. G.; Taylor, P. W. *J. Photochem. Photobiol. B.* **1994**, *26*.

(81) Versluis, A. J.; Rensen, P. C.; Kuipers, M. E.; Love, W. G.; Taylor, P. W. *J. Photochem. Photobiol. B.* **1994**, *23*, 141.

(82) Isele, U.; van Hoogevest, P.; Hilfiker, R.; Capraro, H. G.; Schieweck, K.; Leunberger, H. *J. Pharm. Sci.* **1994**, *83*, 1608.

(83) Maman, N.; Dhami, S.; Phillips, D.; Brault, D. *Biochim. Biophys. Acta* **1999**, *1420*, 168.

(84) Brasseur, N.; Ouellet, R.; La Madeleine, C.; van Lier, J. E. *Br. J. Cancer* **1999**, *80*, 1533.

(85) Taillefer, J.; Jones, M. C.; Brasseur, N.; van Lier, J. E.; Leroux, J. C. *J. Pharm. Sci.* **2000**, *89*, 52.

(86) Labib, A.; Lenaerts, V.; Chouinard, F.; Leroux, J. C.; Ouellet, R.; van

Lier, J. E. *Pharm. Res.* **1991**, *8*, 1027.

(87) Larroque, C.; Pelegrin, A.; van Lier, J. E. *Br. J. Cancer* **1996**, *7*, 1886.

(88) Ruebner, A.; Yang, Z.; Leung, D.; Breslow, R. *Proc. Natl. Acad. Sci. U.S.A.* **1999**, *96*, 14692.

(89) Baugh, S. D. P.; Yang, Z.; Leung, D. K.; Wilson, D. M.; Breslow, R. *J. Am. Chem. Soc.* **2001**, *123*, 12488-12494.

(90) Li, X.-y.; He, X.; Ng, A. C. H.; Wu, C.; Ng, D. K. P. *Macromolecules* **2000**, *33*, 2119-2123.

(91) Ng, A. C. H.; Li, X.-y.; Ng, D. K. P. *Macromolecules* **1999**, *32*, 5292-5298.

(92) Ng, D. K. P. *C. R. Chim.* **2003**, *6*, 903-910.

(93) Ihre, H. R.; Padilla De Jesus, O. L.; Szoka, F. C. J.; Frechet, J. M. J. *Bioconjugate Chem.* **2002**, *13*, 443-452.

(94) Newkome, G. R.; Childs, B. J.; Rourk, M. J.; Baker, G. R.; Moorefield, C. N. *Biotechnol. Bioeng.* **1999**, *61*, 243-253.

(95) Newkome, G. R.; Soo Yoo, K.; Hwang, S.-H.; Moorefield, C. N. *Tetrahedron* **2003**, *59*, 3955-3964.

(96) Steffensen, M. B.; Simanek, E. E. *Org. Lett.* **2003**, *5*, 2359-2361.

(97) Zhang, W.; Simanek, E. E. *Org. Lett.* **2000**, *2*, 843-845.

(98) Zhang, W.; Simanek, E. E. *Tetrahedron Lett.* **2001**, *42*, 5355-5357.

(99) Zhang, W.; Nowlan, D. T., III; Thomson, L. M.; Lackowski, W. M.; Simanek, E. E. *J. Am. Chem. Soc.* **2001**, *123*, 8914-8922.

(100) Zhang, W.; Gonzalez, S. O.; Simanek, E. E. *Macromolecules* **2002**, *35*, 9015-9021.

(101) Zhang, W.; Tichy, S. E.; Perez, L. M.; Maria, G. C.; Lindahl, P. A.; Simanek, E. E. *J. Am. Chem. Soc.* **2003**, *125*, 5086-5094.

(102) Umali, A. P.; Crampton, H. L.; Simanek, E. E. *J. Org. Chem.* **2007**, *72*, 9866-9874.

(103) Powers, D. R.; Papadakos, D. J.; Wallin, J. D. *J. Emerg. Med.* **1998**, *16*, 191-196.

(104) Barbeau, D. L.; (USA). Application: WO WO, 2003, p 62 pp.

(105) Ellershaw, D. C.; Gurney, A. M. *Br. J. Pharmacol.* **2001**, *134*, 621-631.

(106) Jacobs, M. *Biochem. Pharmacol.* **1984**, *33*, 2915-2919.

(107) Bang, L.; Nielsen-Kudsk, J. E.; Gruhn, N.; Trautner, S.; Theilgaard, S. A.; Olesen, S.-P.; Beosgaard, s.; Aldershville, J. *Eur. J. Pharmacol.* **1998**, *361*, 43-49.

(108) Gurney, A. M.; Allan, M. *Br. J. Pharmacol.* **1995**, *114*, 238-244.

(109) Koch-Weser, J. *New Eng. J. Med.* **1976**, *295*, 320-323.

(110) Grahame-Smith, D. G.; Aronson, J. K. *Oxford Textbook of Clinical Pharmacology and Drug Therapy,* 2nd ed.; Oxford University Press: New York, NY, 1992.

(111) Cornacchia, E.; Golbus, J.; Maybaum, J.; Strahler, J.; Hanash, S.; Richardson, B. *J. Immunol.* **1988**, *140*, 2197-2200.

(112) Huck, S.; Zouali, M. *Clin. Immunol. Immunopathol.* **1996**, *80*, 1-8.

(113) Mazari, L.; Ouarzane, M.; Zouali, M. *Proc. Natl. Acad. Sci. U.S.A.* **2007**, *104*, 6317-6322.

(114) Arce, C.; Segura-Pacheco, B.; Perez-Cardenas, E.; Taja-Chayeb, L.; Candelaria, M.; Duennas-Gonzalez *J.Transl. Med.* **2006**, *4*, 10.

(115) Willner, D.; Trail, P. A.; Hofstead, S. J.; King, H. D.; Lasch, S. J.; Braslawsky, G. R.; Greenfield, R. S.; Kaneko, T.; Firestone, R. A. *Bioconjugate Chem.* **1993**, *4*, 521-527.

(116) Kratz, F.; Beyer, U.; Roth, T.; Tarasova, N.; Collery, P.; Lechenault, F.; Cazabat, A.; Schumacher, P.; Unger, C.; Falken, U. *J. Pharm. Sci.* **1998**, *87*, 338-346.

(117) King, H. D.; Yurgaitis, D.; Willner, D.; Firestone, R. A.; Yang, M. B.; Lasch, S. J.; Hellstrom, K. E.; Trail, P. A. *Bioconjugate Chem.* **1999**, *10*, 279-288.

(118) Langer, M.; Kratz, F.; Rothen-Rutishauser, B.; Wunderli-Allenspach, H.; Sickinger, A. G. B. *J. Med. Chem.* **2001**, *44*, 1341-1348.

(119) Kratz, F.; Warneke, A.; Scheuermann, K.; Stockmar, C.; Schwab, J.; Lazar, P.; Druckes, P.; Esser, N.; Drevs, J.; Rognan, D.; Bissantz, C.; Hinderling, C.; Folkers, G.; Fichtner, I.; Unger, C. *J. Med. Chem.* **2002**, *45*, 5523-5533.

(120) Yoo, H. S.; Lee, E. A.; Park, T. G. *J. Cont. Rel.* **2002**, *82*, 17-27.

(121) King, H. D.; Dubowchik, G. M.; Mastalerz, H.; Willner, D.; Hofstead, S.

J.; Firestone, R. A.; Lasch, S. J.; Trail, P. A. *J. Med. Chem.* **2002**, *45*, 4336-4343.

(122) Liu-Snyder, P.; Borgens, R. B.; Shi, R. *J. Neurosci. Res.* **2006**, *84*, 219-227.

(123) Acosta, E. J.; Deng, Y.; White, G. N.; Dixon, J. B.; McInnes, K. J.; Senseman, S. A.; Frantzen, A. S.; Simanek, E. E. *Chem. Mater.* **2003**, *15*, 2903-2909.

(124) Neerman, M. F.; Zhang, W.; Parrish, A. R.; Simanek, E. E. *Int. J. Pharm.* **2004**, *281*, 129-132.

(125) Bell, S. A.; McLean, M. E.; Oh, S.-K.; Tichy, S. E.; Zhang, W.; Corn, R. M.; Crooks, R. M.; Simanek, E. E. *Bioconjugate Chem.* **2003**, *14*, 488-493.

(126) Umali, A. P.; Simanek, E. E. *Org. Lett.* **2003**, *5*, 1245-1247.

(127) Lim, J.; Simanek, E. E. *Abstracts, 62nd Southwest Regional Meeting of the American Chemical Society, Houston, TX, United States, October 19-22* **2006**, SRM-589.

(128) Hollink, E.; Simanek, E. E. *Org. Lett.***2006**, *8*, 2293-2295.

(129) Crampton, H.; Hollink, E.; Perez, L. M.; Simanek, E. E. *New J. Chem.* **2007**, *31*, 1283-1290.

(130) Hackbarth, S.; Ermilov, E. A.; Roder, B. *Opt. Commun.* **2005**, *248*, 295.

(131) Hackbarth, S.; Horneffer, V.; Wiehe, A.; Hillenkamp, F.; Roder, B. *Chem. Phys.* **2001**, *269*, 339.

(132) Stapert, H. R.; Nishiyama, N.; Jiang, D.-L.; Aida, T.; Kataoka, K. *Langmuir* **2000**, *16*, 8182-8188.

(133) Arnida; Nishiyama, N.; Kanayama, N.; Jang, W.-D.; Yamasaki, Y.; Kataoka, K. *J. Controlled Release* **2006**, *115*, 208-215.

(134) Nishiyama, N.; Jang, W.-D.; Kataoka, K. *New J. Chem.* **2007**, *31*, 1074-1082.

(135) Jang, W.-D.; Nishiyama, N.; Kataoka, K. *Supramol. Chem.* **2007**, *19*, 309-314.

(136) Shinoda, S. *J. Incl. Phenom. Macrocycl. Chem.* **2007**, *59*, 1-9.

(137) Shinoda, S.; Ohashi, M.; Tsukube, H. *Chemistry* **2007**, *13*, 81-9.

(138) Leclaire, J.; Coppel, Y.; Caminade, A.-M.; Majoral, J.-P. *J. Am. Chem. Soc.* **2004**, *126*, 2304-2305.

(139) Leclaire, J.; Dagiral, R.; Fery-Forgues, S.; Coppel, Y.; Donnadieu, B.; Caminade, A.-M.; Majoral, J.-P. *J. Am. Chem. Soc.* **2005**, *127*, 15762-15770.

(140) Leclaire, J.; Dagiral, R.; Pla-Quintana, A.; Caminade, A.-M.; Majoral, J. P. *Eur. J. Inorg. Chem.* **2007**, 2890-2896.

(141) Brewis, M.; Helliwell, M.; McKeown, N. B.; Reynolds, S.; Shawcross, A. *Tetrahedron Lett.* **2001**, *42*, 813-816.

(142) Brewis, M.; Helliwell, M.; McKeown, N. B. *Tetrahedron* **2003**, *59*, 3863-3872.

(143) El-Khouly, M. E.; Kang, E. S.; Kay, K.-Y.; Choi, C. S.; Aaraki, Y.; Ito,

O. *Chem. Eur. J.* **2007**, *13*, 2854-2863.

(144) Kraus, G. A.; Louw, S. V. *J. Org. Chem.* **1998**, *63*, 7520-7521.

(145) Ceyhan, T.; Korkmaz, M.; Kutluay, T.; Bekaroglu, O. *J. Porphyrins and Phthalocyanines* **2004**, *8*, 1383-1389.

(146) Ozan, N.; Bekaroglu, O. *Polyhedron* **2003**, *22*, 819-823.

(147) Suelue, M.; Altindal, A.; Bekaroglu, O. *Synthetic Metals* **2005**, *155*, 211-221.

(148) Quintiliani, M.; Garcia-Frutos, E. M.; Gouloumis, A.; Vazquez, P.; Ledoux-Rak, I.; Zyss, J.; Claessens, C. G.; Torres, T. *Eur. J. Org. Chem.* **2005**, 3911-3915.

(149) González-Cabello, A.; Vázquez, P.; Torres, T.; Guldi, D. M. *J. Org. Chem.* **2003**, *68*, 8635.

(150) Kopranenkov, V. N.; Askerov, D. B.; Shul'ga, A. M.; Luk'yanets, E. A. *Khimiya Geterotsiklicheskikh Soedinenii* **1988**, *9*, 1261-1263.

APPENDIX A

^{1}H NMR, ^{13}C NMR, AND MASS SPECTRA FOR COMPOUNDS DESCRIBED IN CHAPTER II

^{1}H NMR spectrum of intermediate **2.1** in $CDCl_3$.

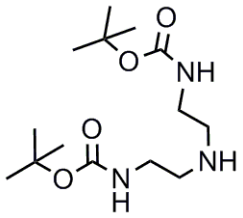

^{13}C NMR spectrum of intermediate **2.1** in $CDCl_3$.

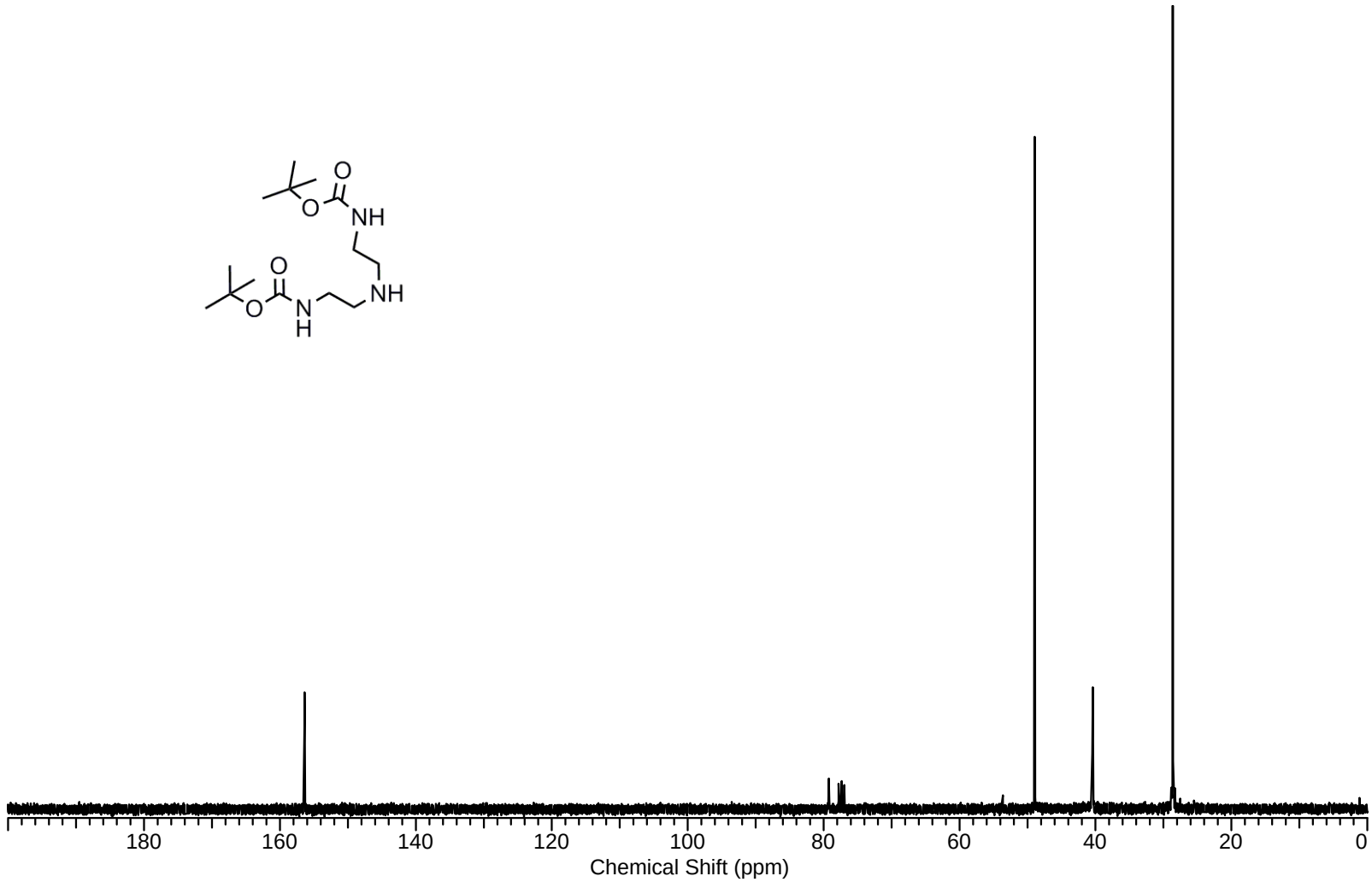

Mass spectrum (ESI) of intermediate **2.1**.

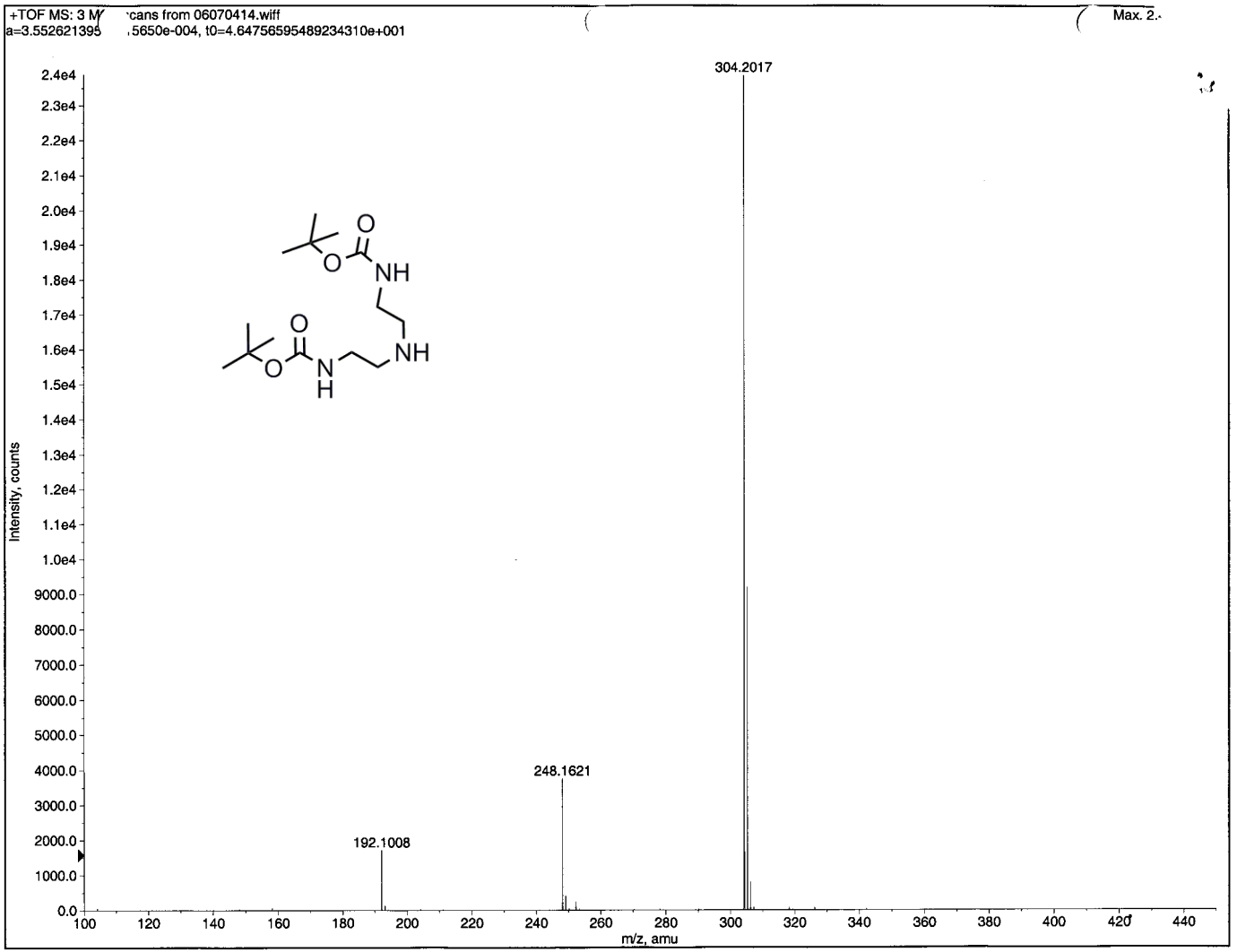

^{1}H NMR spectrum of intermediate **2.2** in $CDCl_3$.

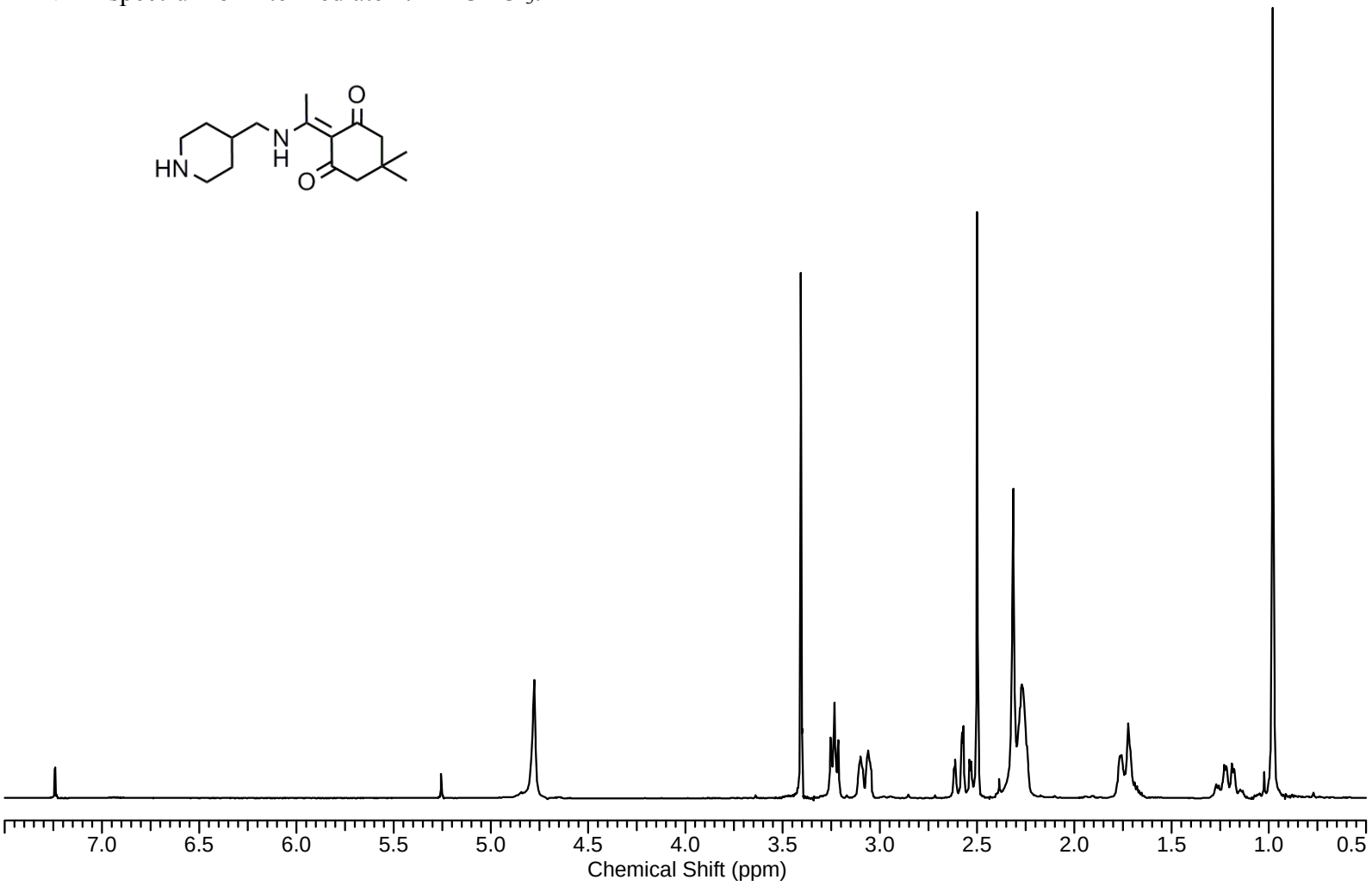

^{13}C NMR spectrum of intermediate **2.2** in $CDCl_3$.

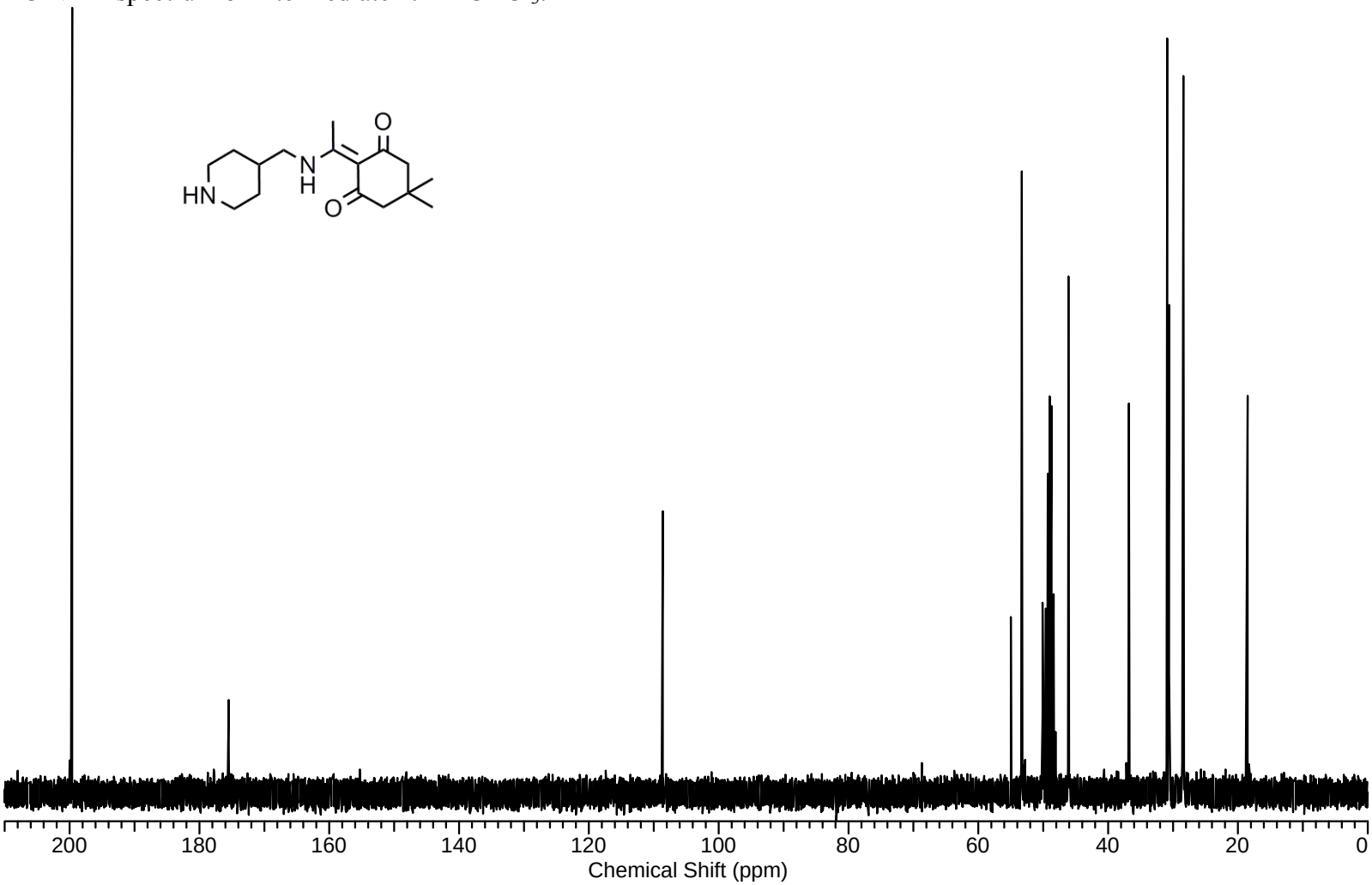

Mass spectrum (ESI) of intermediate **2.2**.

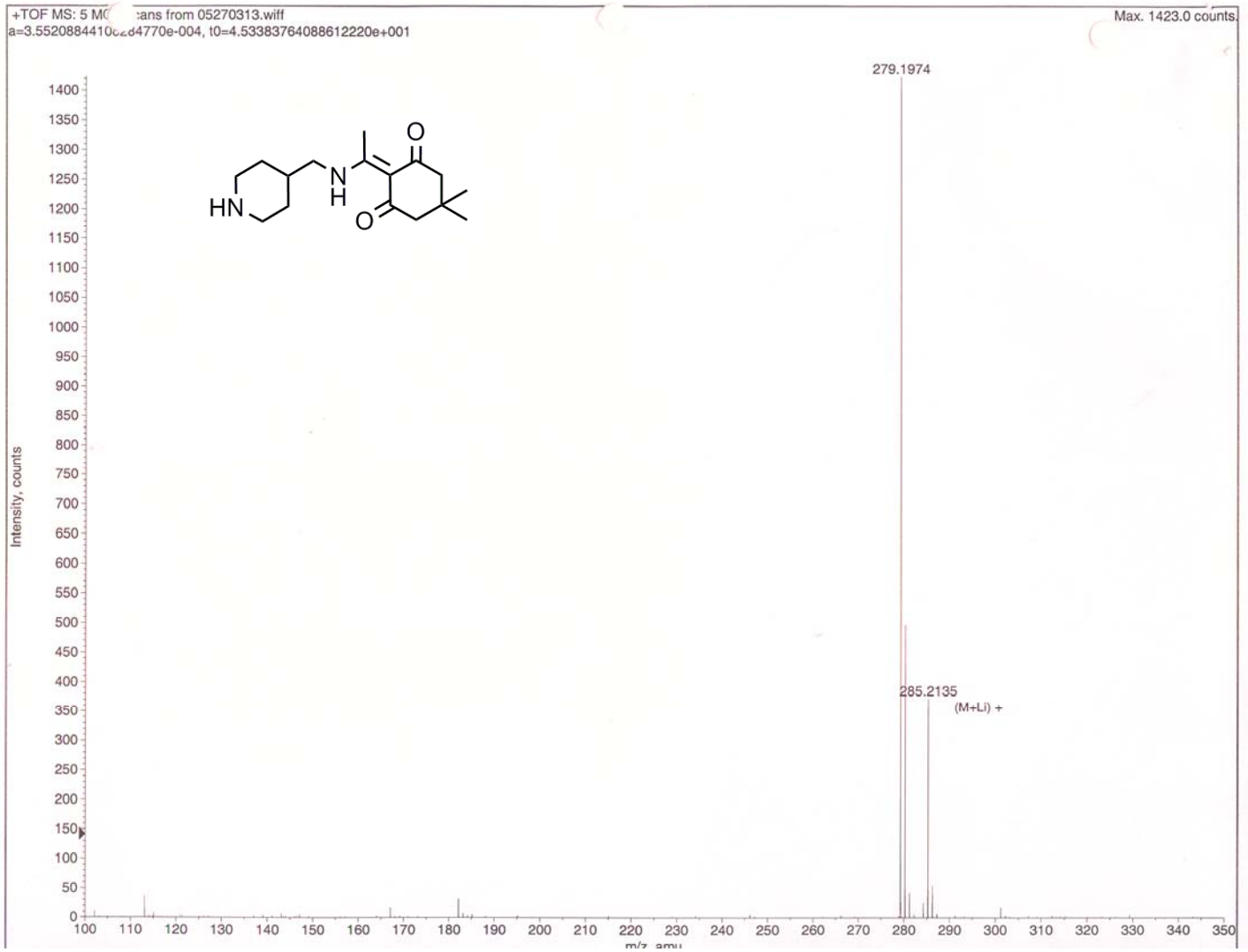

^{1}H NMR spectrum of monochlorotriazine **2.3** in $CDCl_3$.

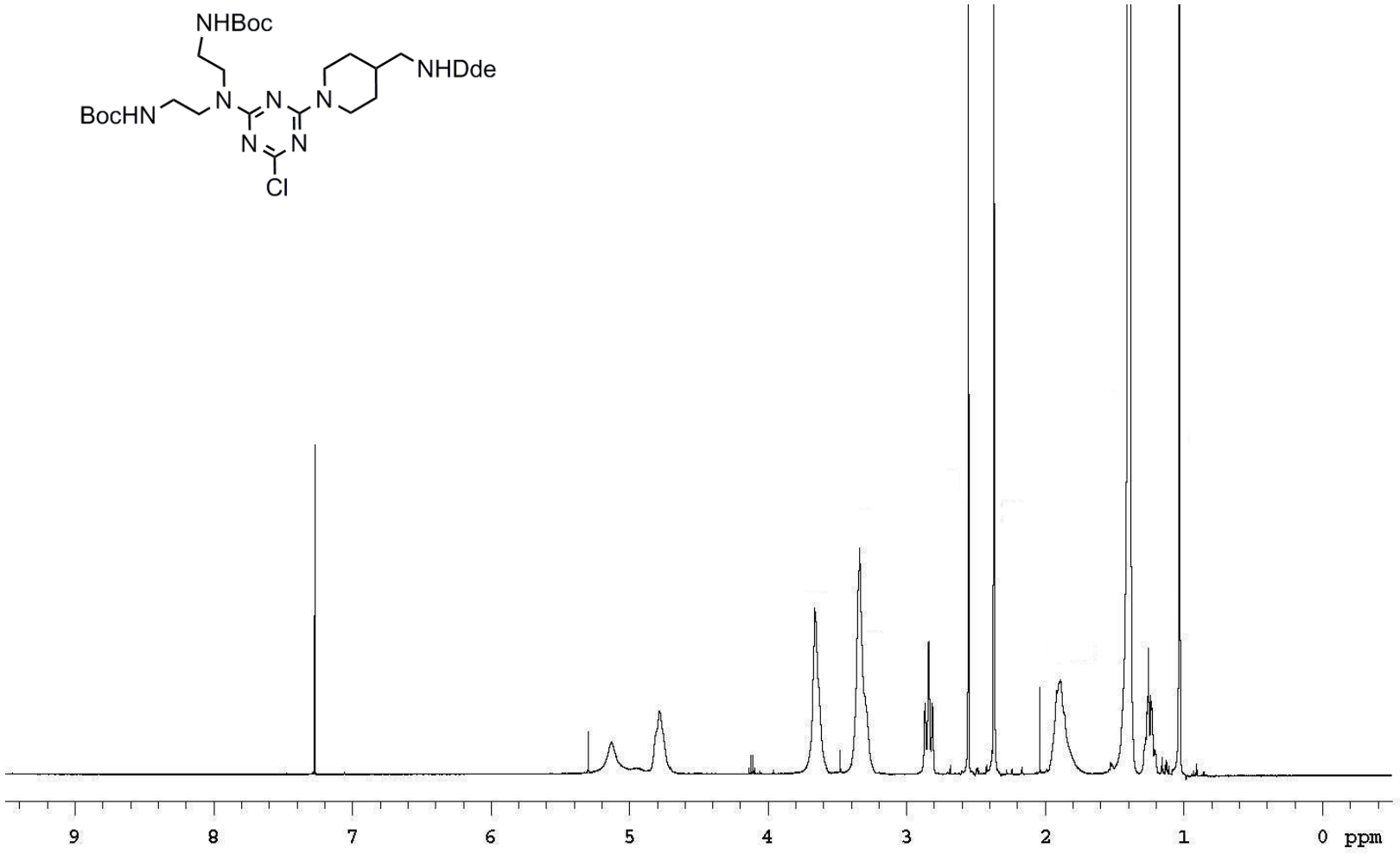

^{13}C NMR spectrum of monochlorotriazine **2.3** in $CDCl_3$.

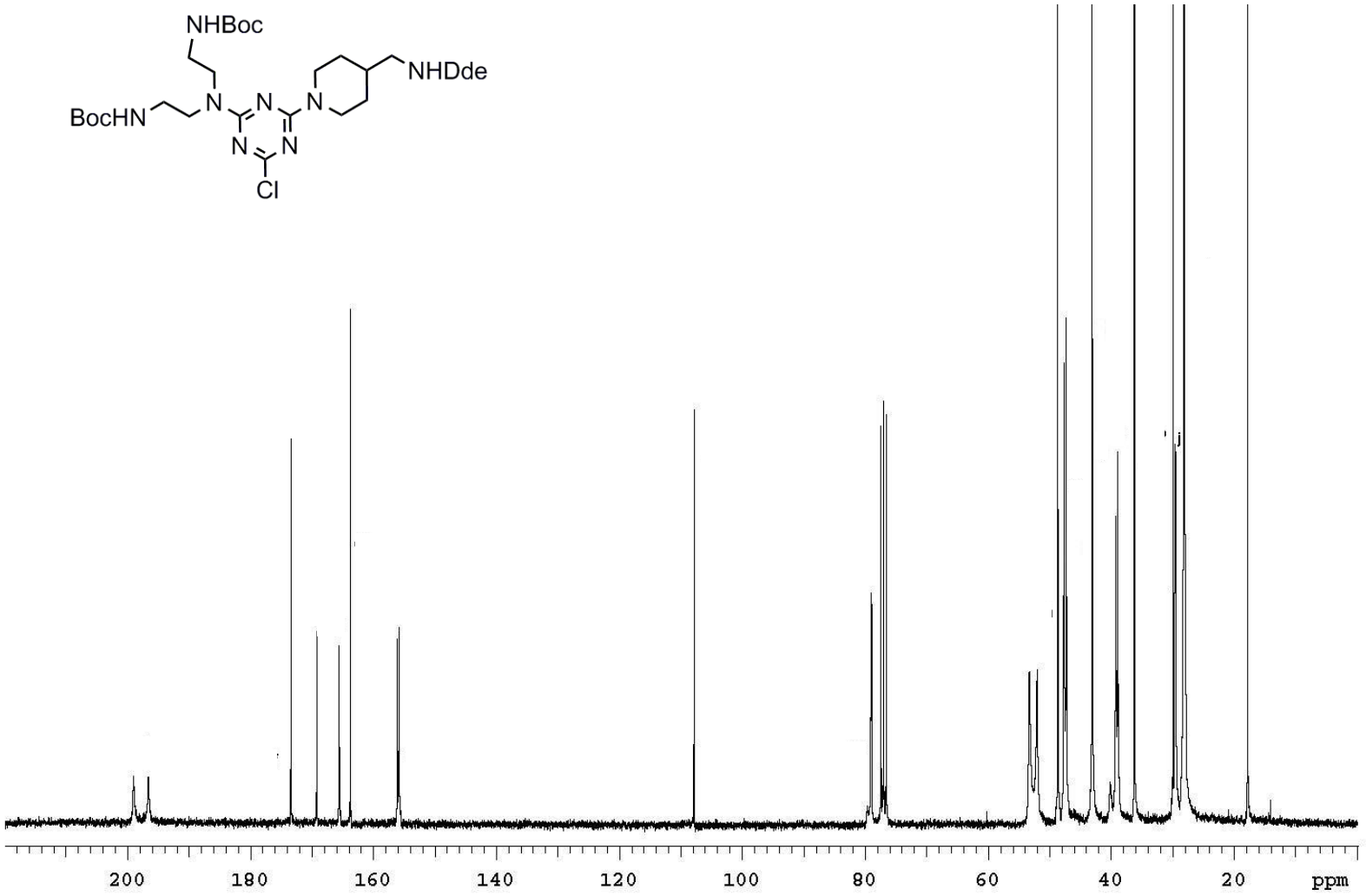

Mass spectrum (ESI) of monochlorotriazine **2.3**.

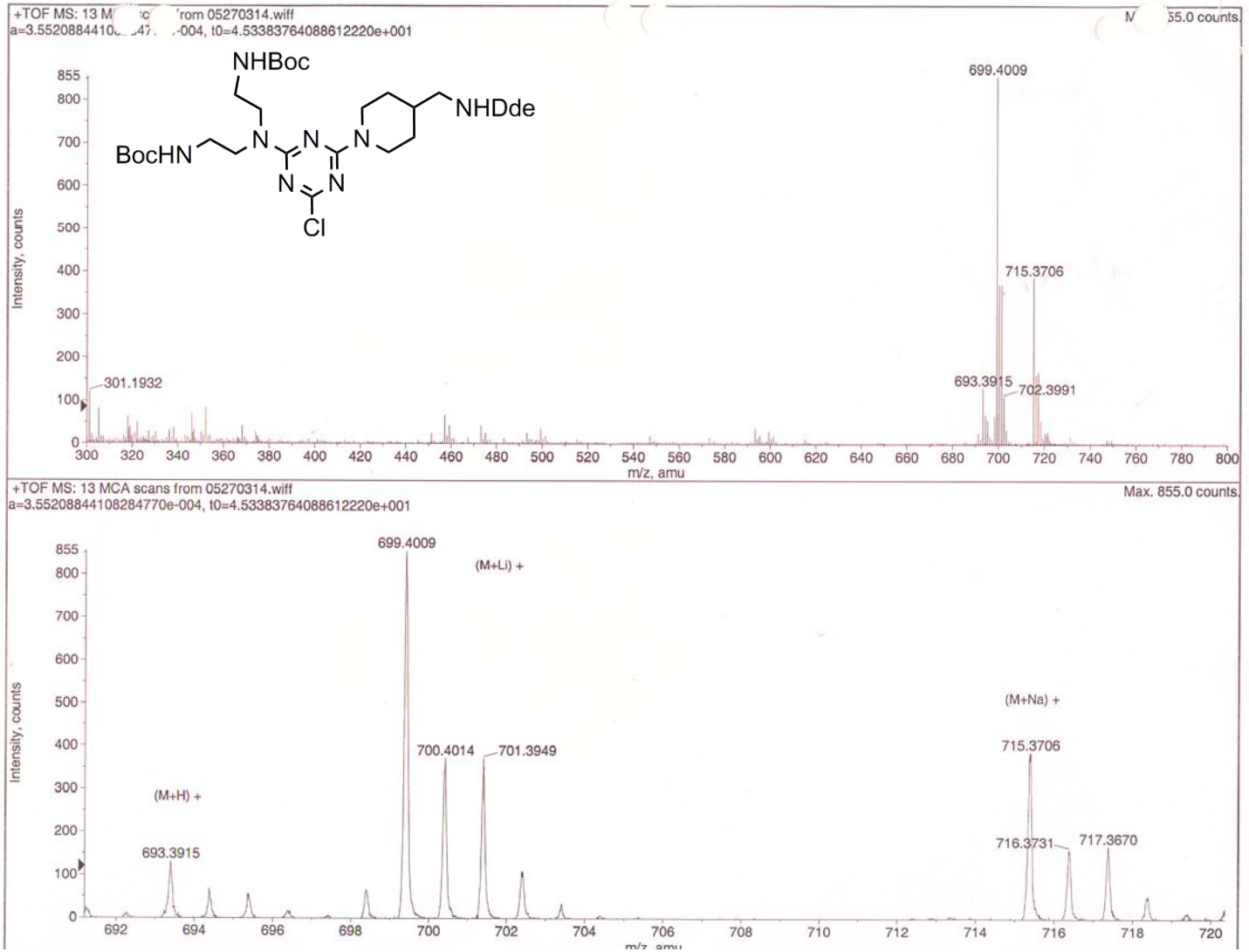

^{1}H NMR spectrum of dendron **2.4** in $CDCl_3$.

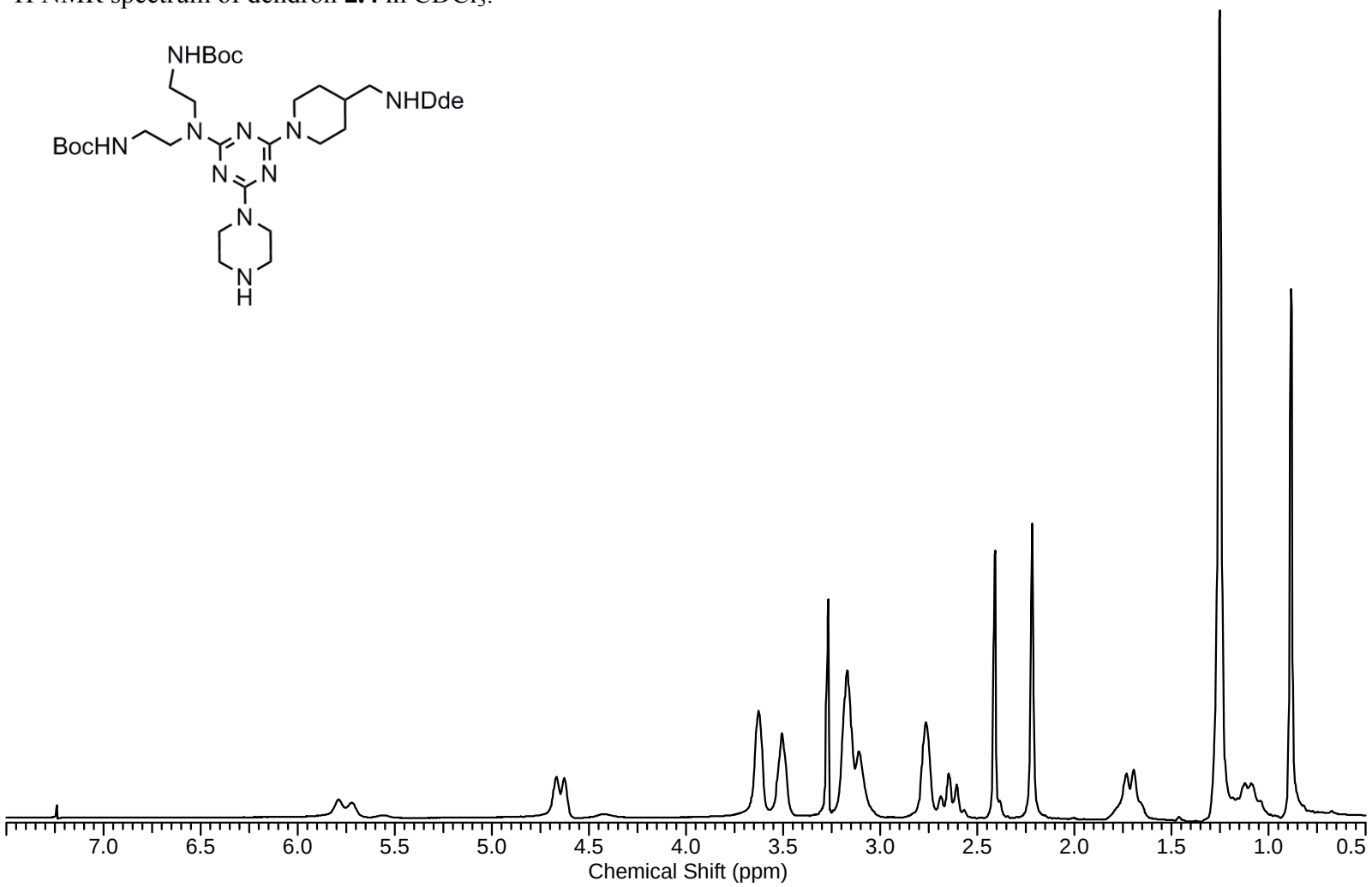

^{13}C NMR spectrum of dendron **2.4** in $CDCl_3$.

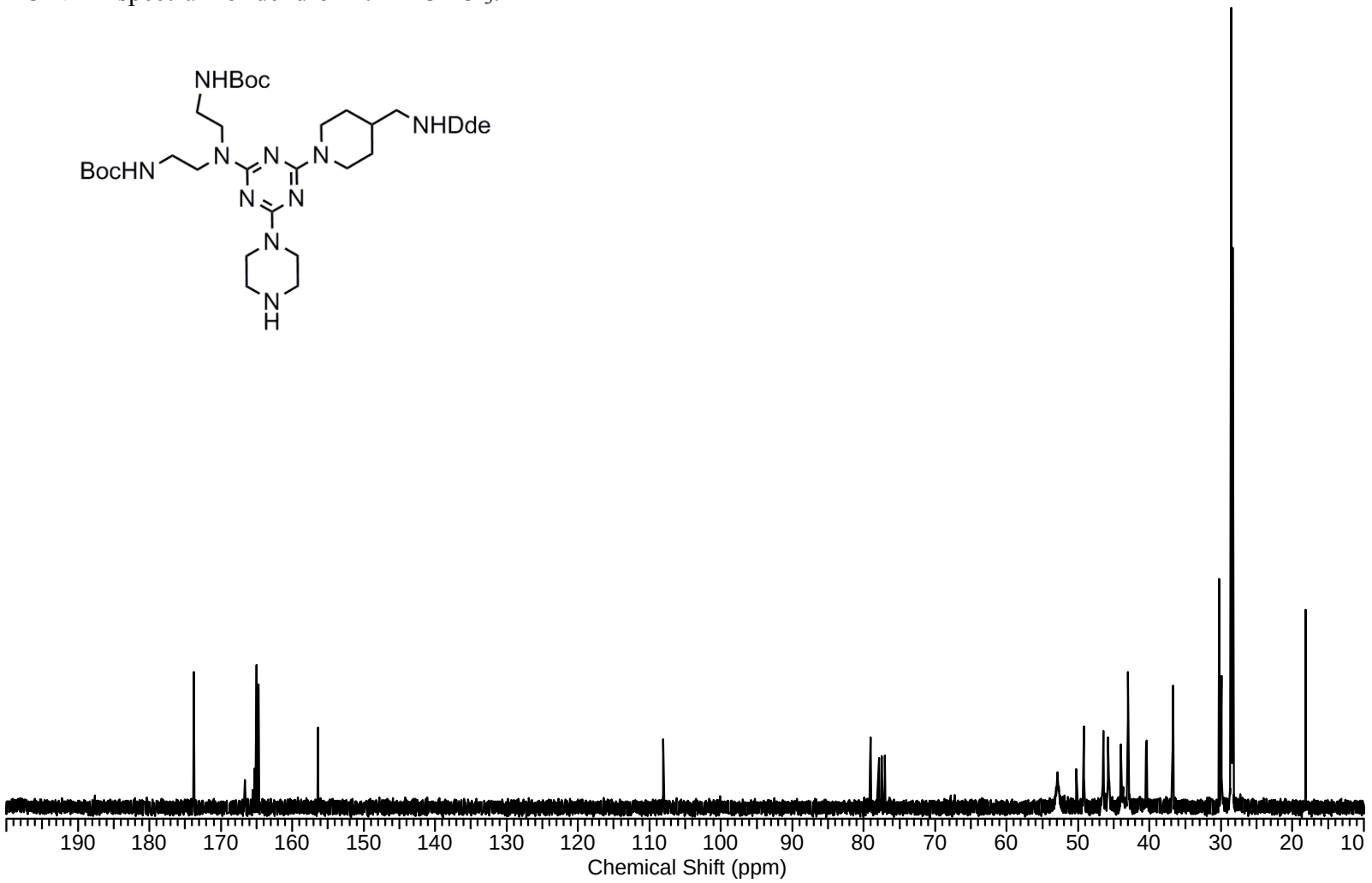

Mass spectrum (ESI) of dendron **2.4**.

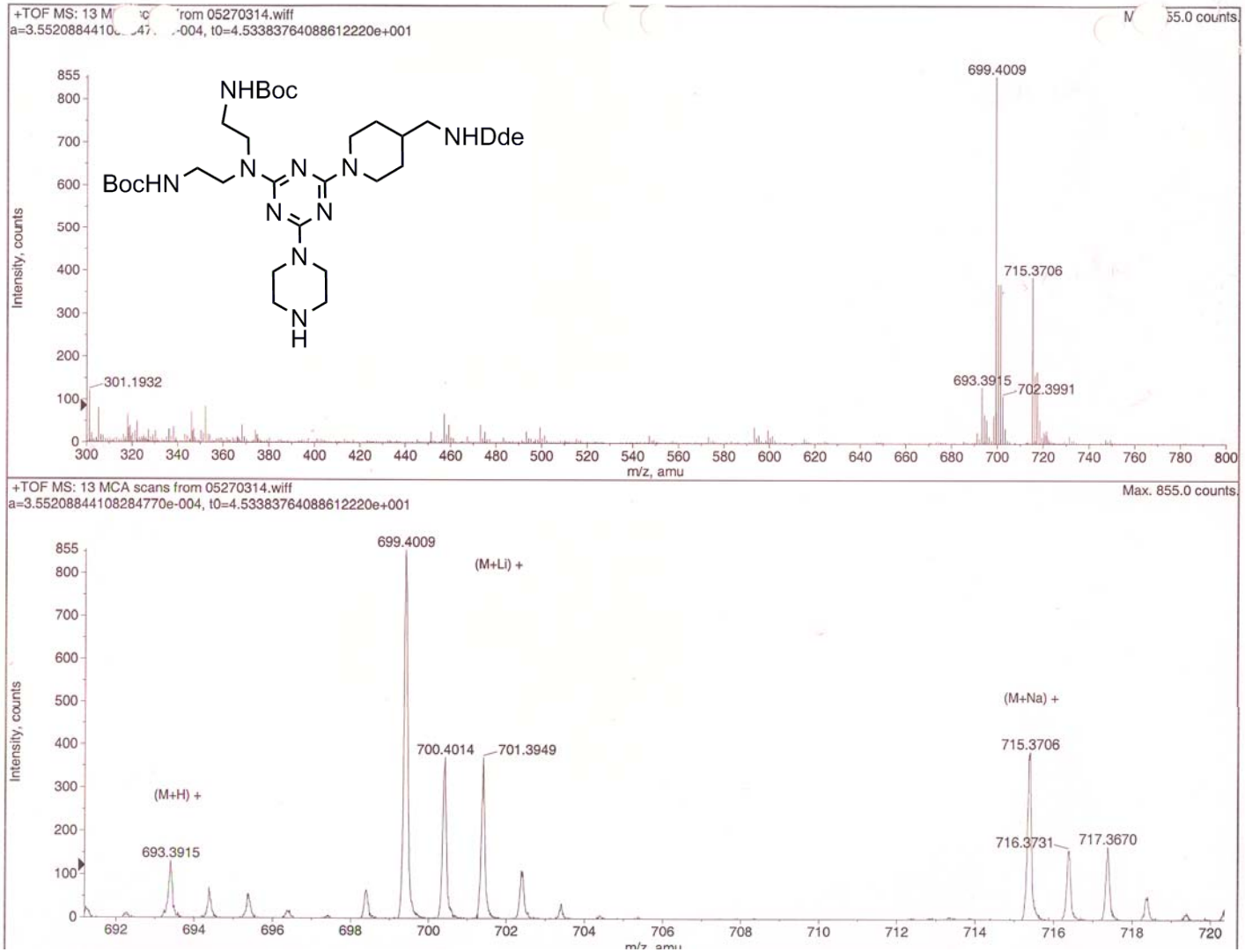

^{1}H NMR spectrum of dichlorotriazine **2.5** in $CDCl_3$.

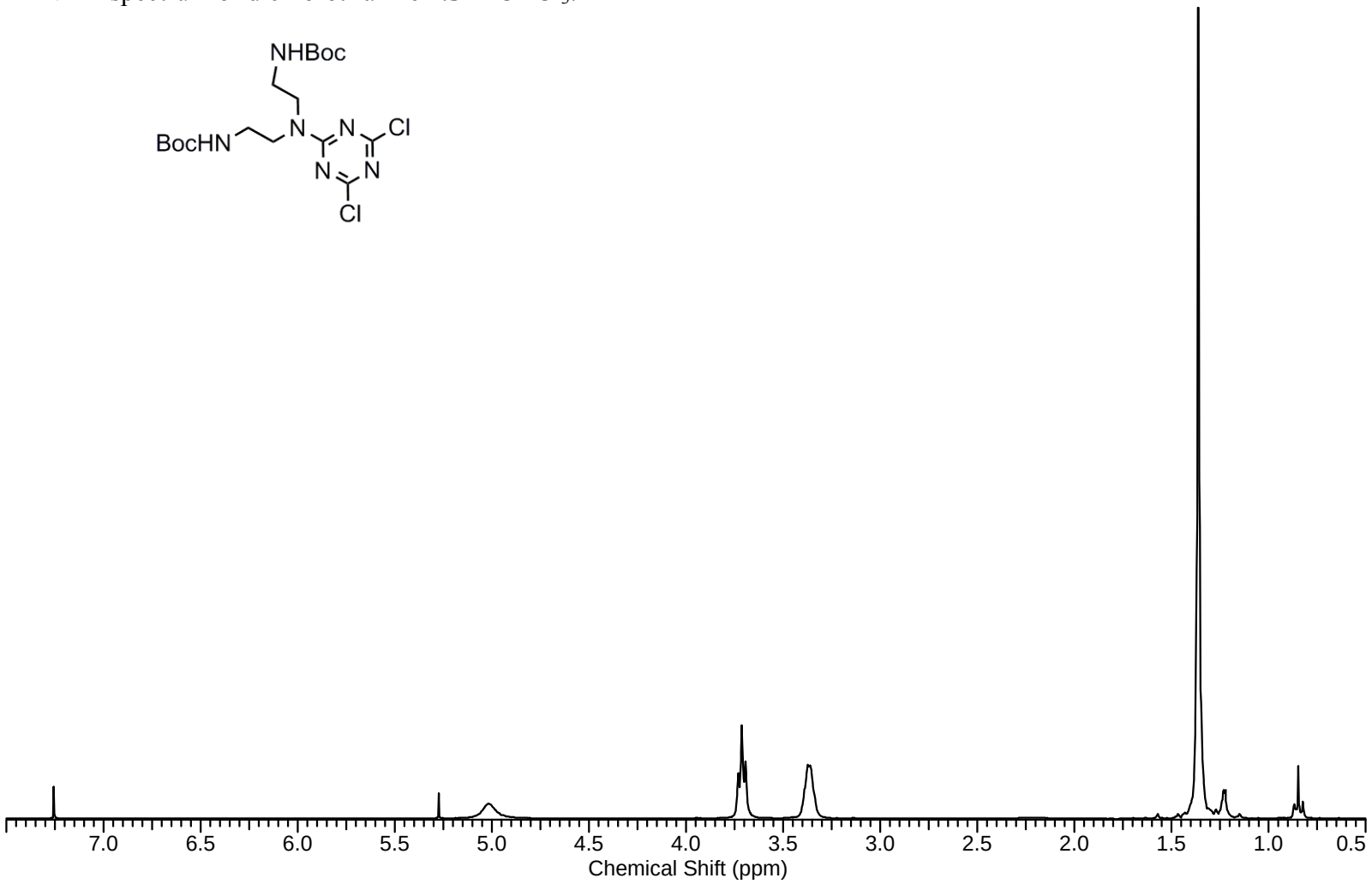

^{13}C NMR spectrum of dichlorotriazine **2.5** in $CDCl_3$.

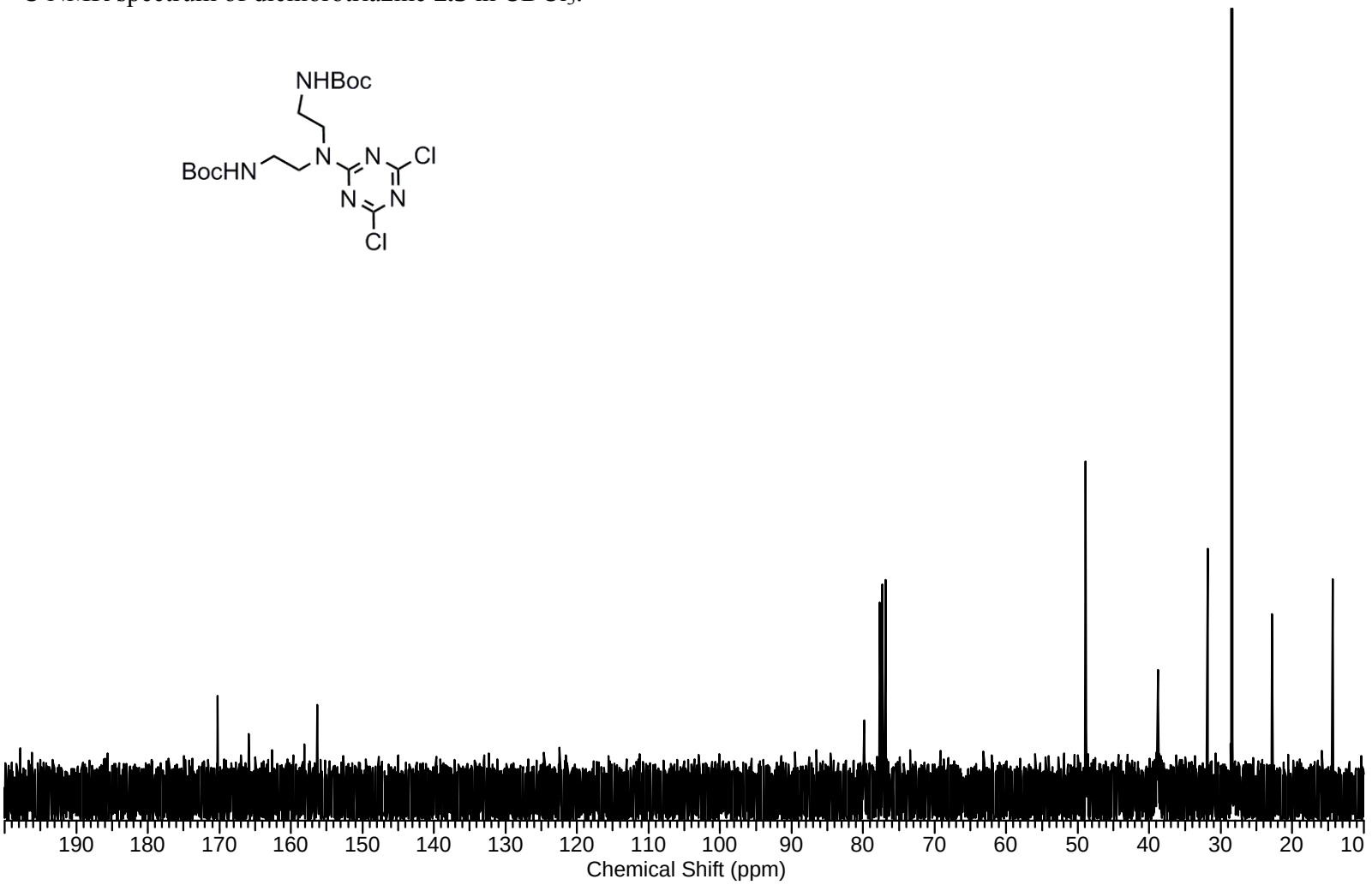

Mass spectrum (ESI) of dichlorotriazine **2.5.**

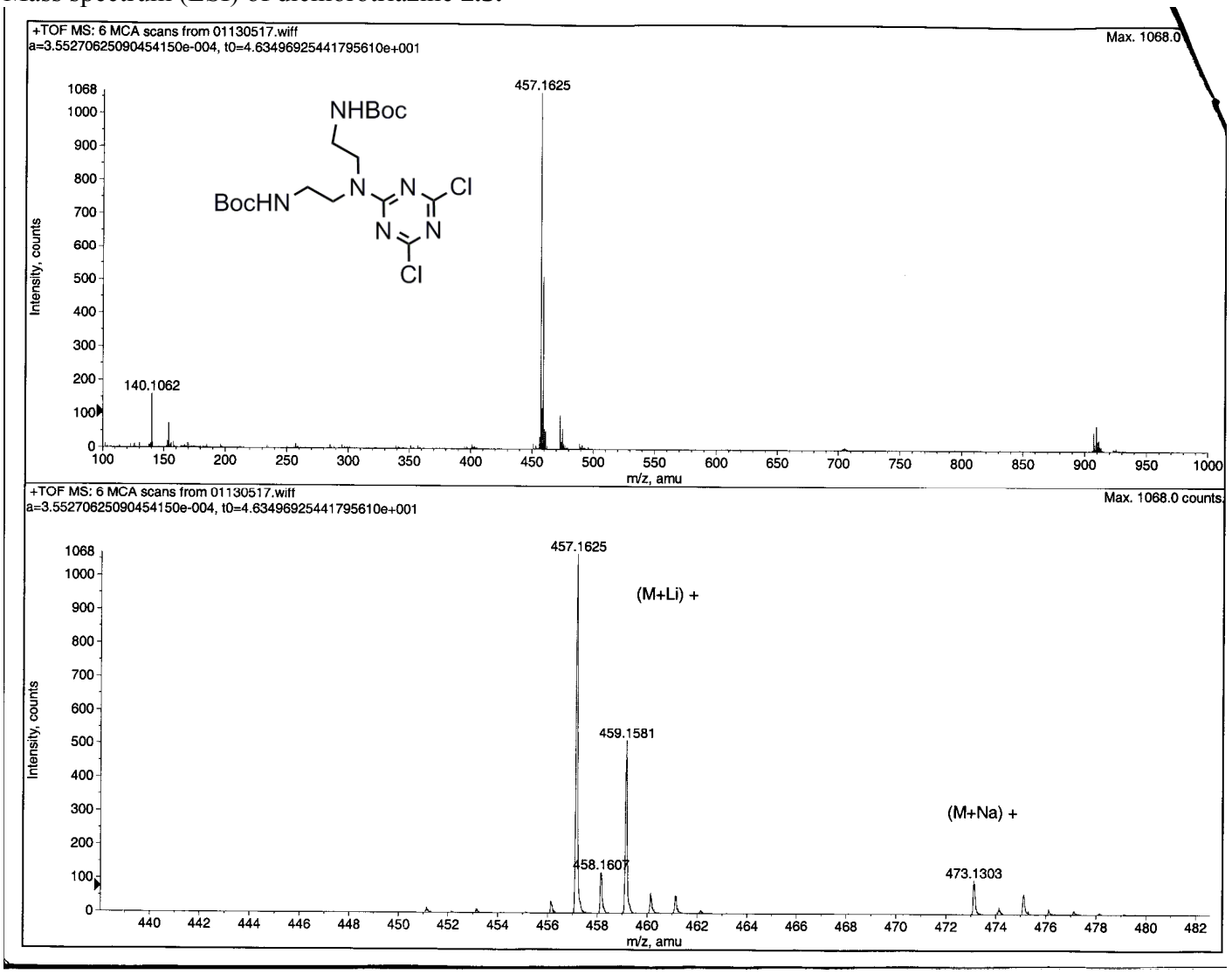

^{1}H NMR spectrum of monochlorotriazine **2.6** in $CDCl_3$.

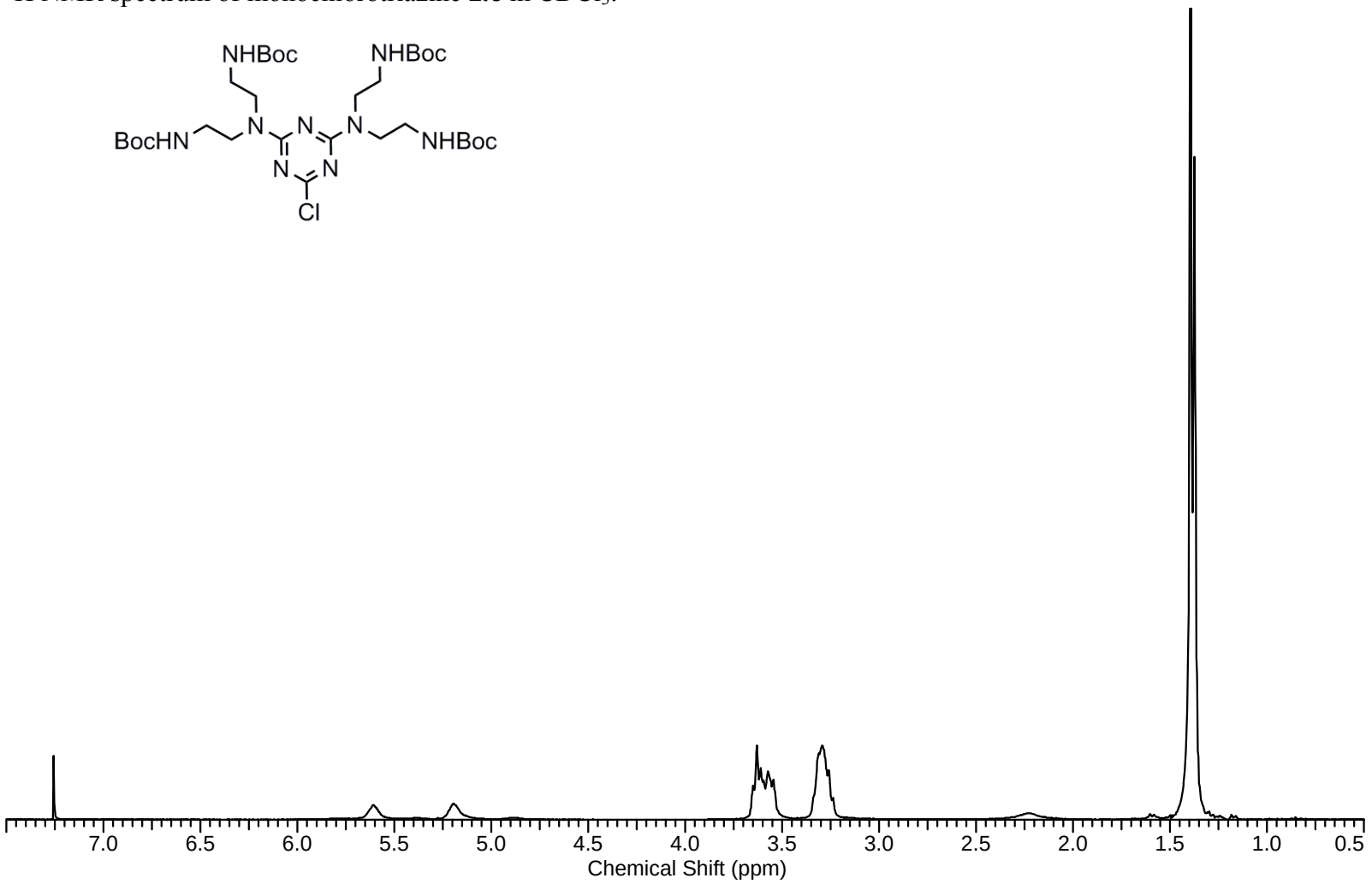

^{13}C NMR spectrum of monochlorotriazine **2.6** in $CDCl_3$.

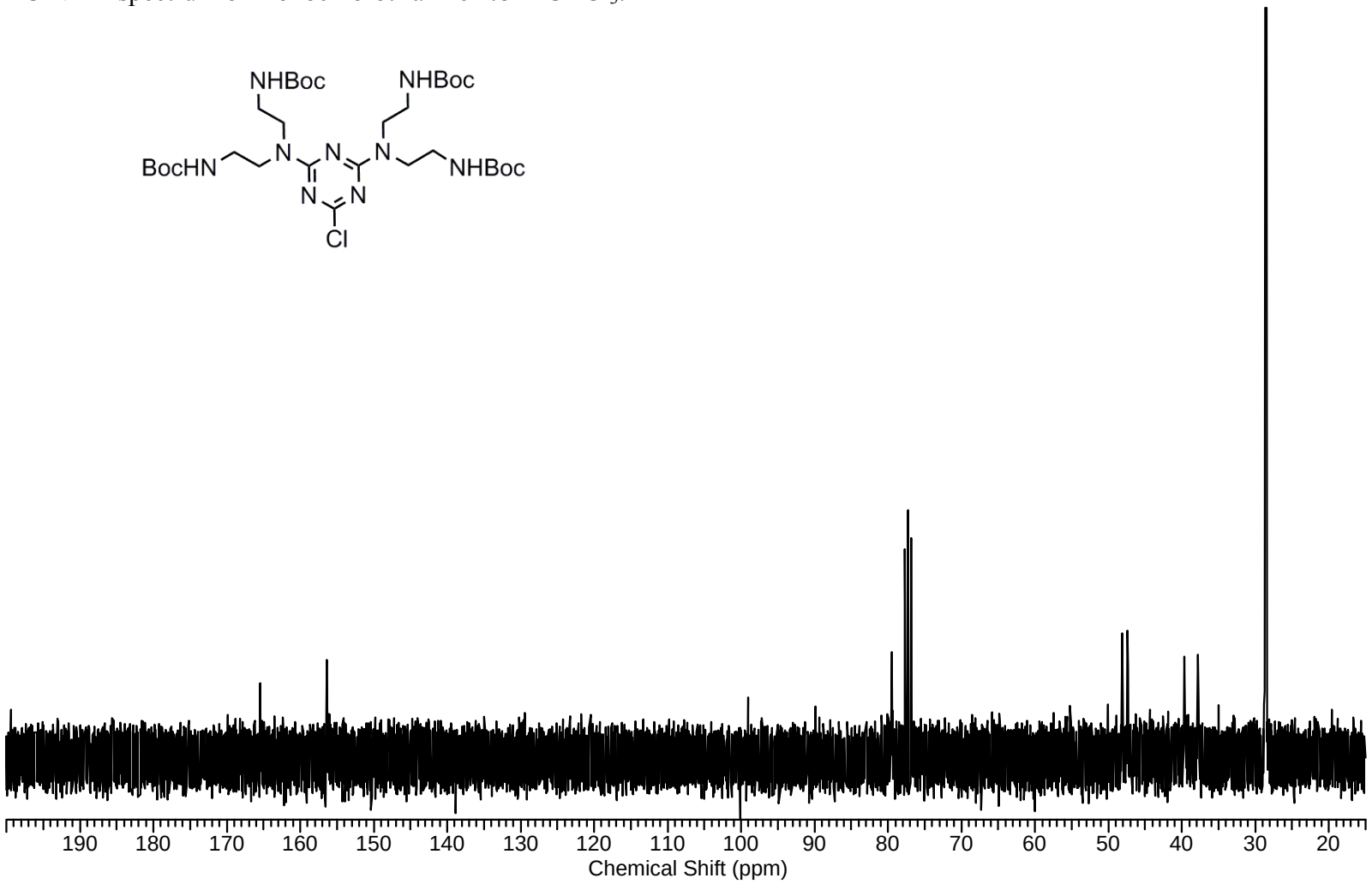

Mass spectrum (ESI) of monochlorotriazine **2.6.**

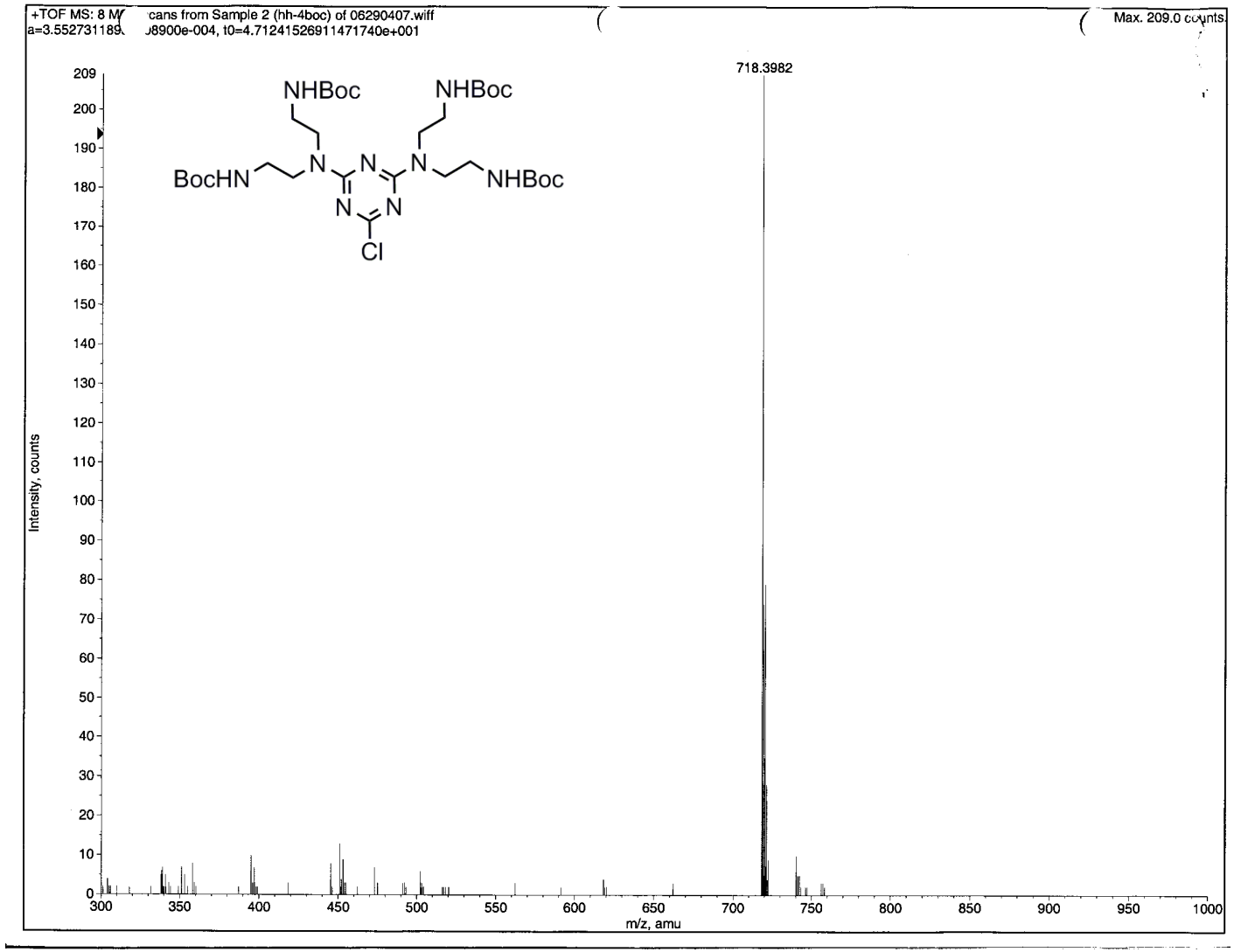

^{1}H NMR spectrum of dendron **2.7** in $CDCl_3$.

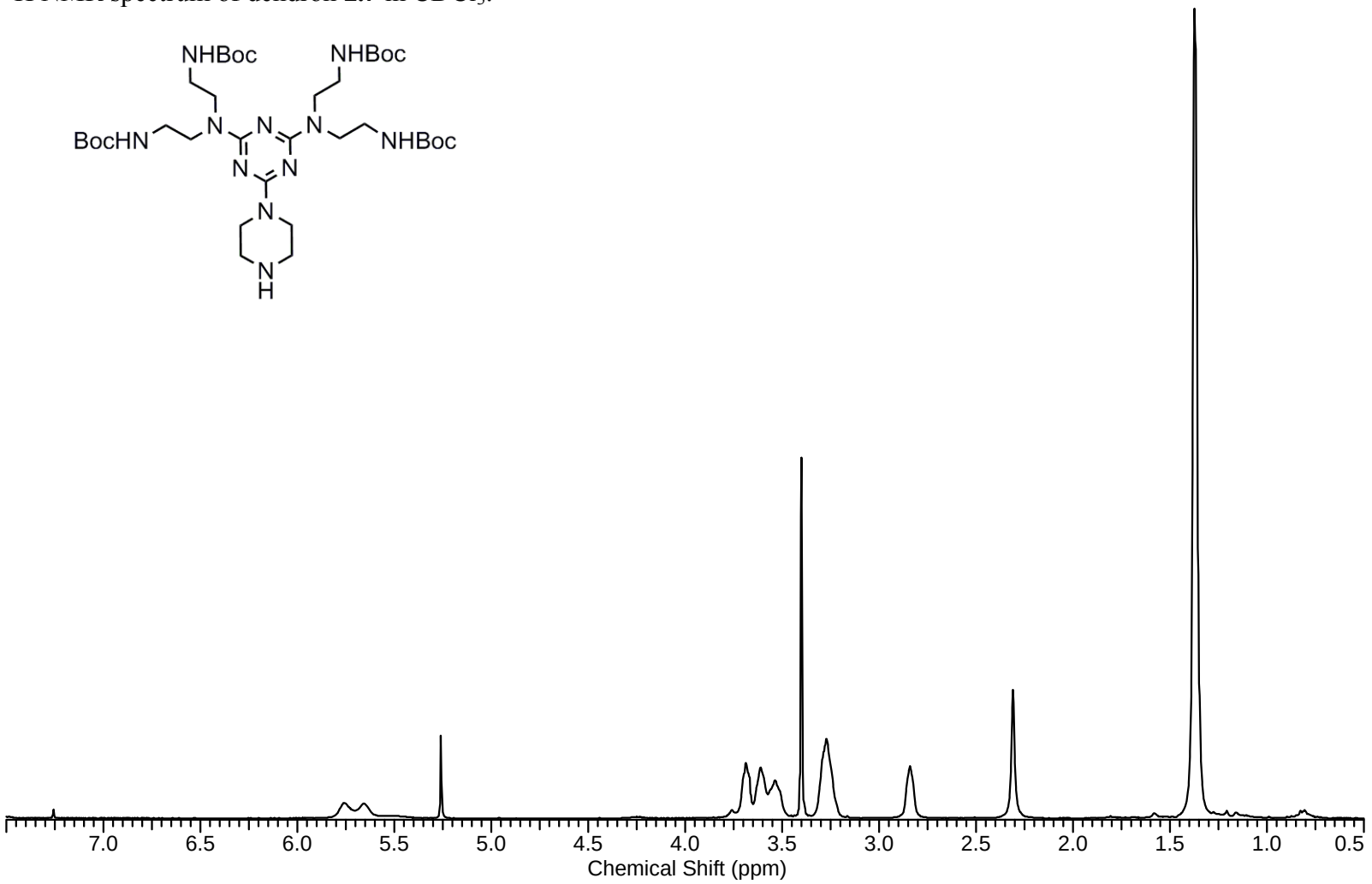

^{13}C NMR spectrum of dendron **2.7** in $CDCl_3$.

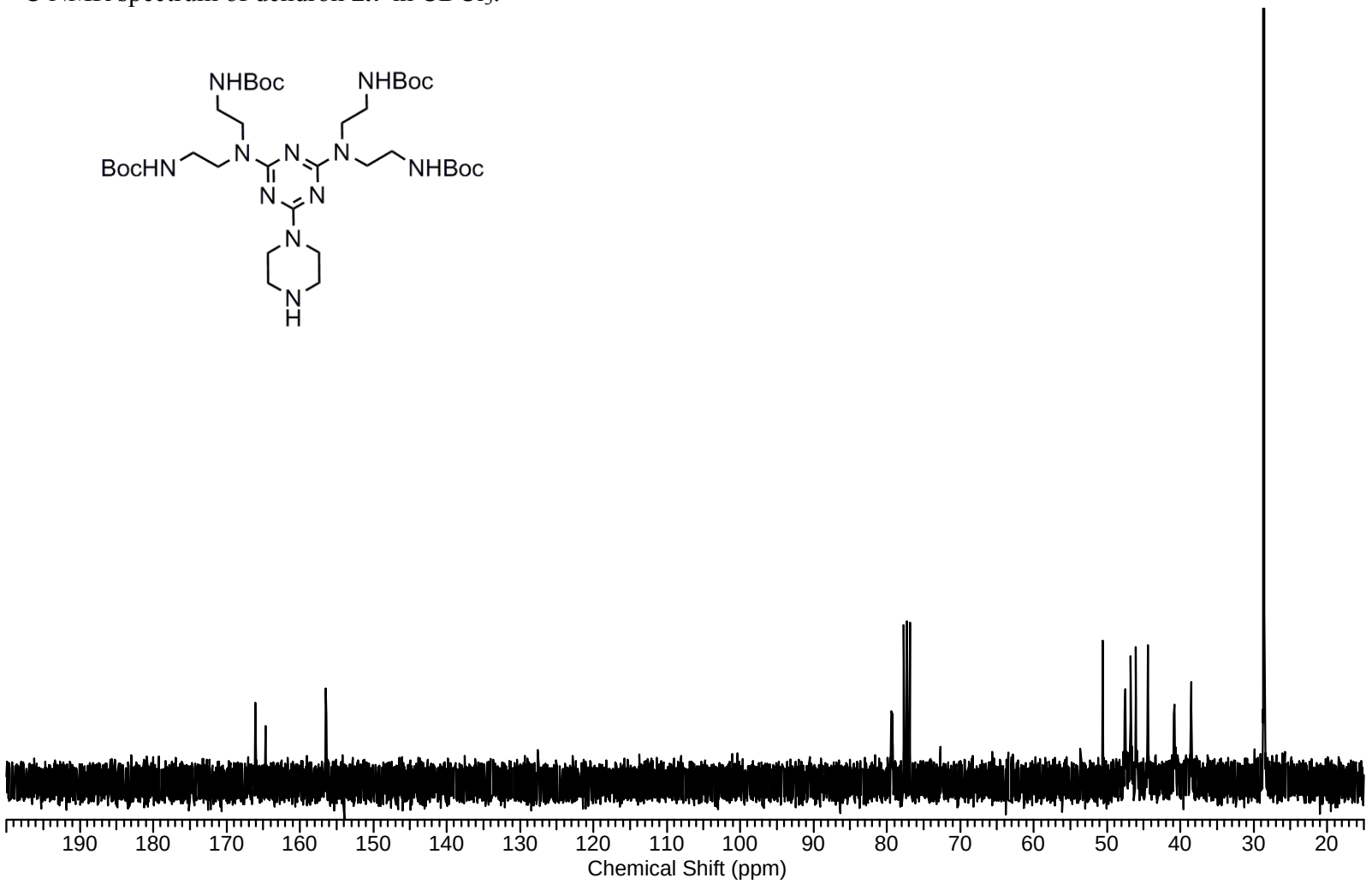

Mass spectrum (ESI) of dendron **2.7.**

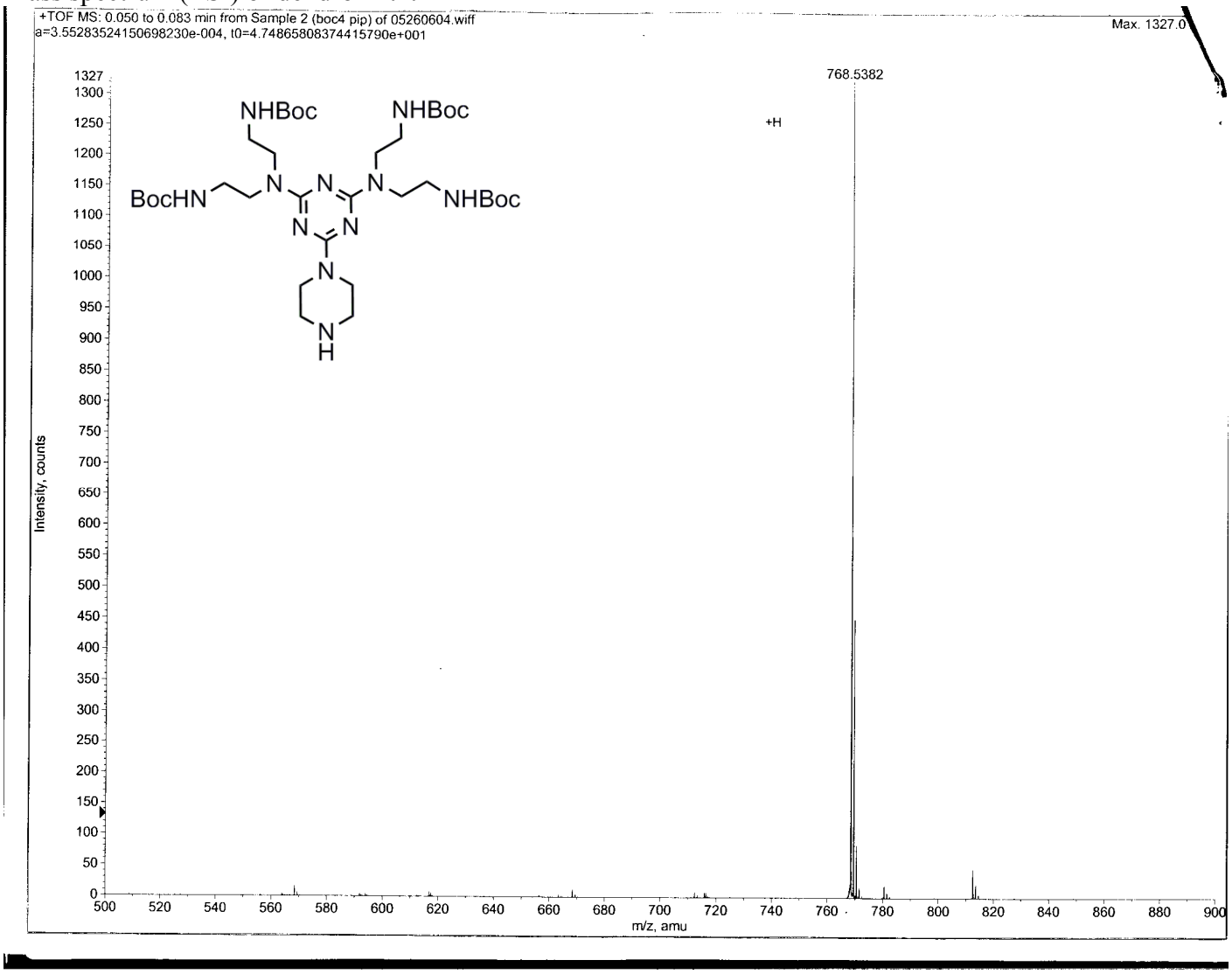

^{1}H NMR spectrum of dichlorotriazine **2.8** in $CDCl_3$.

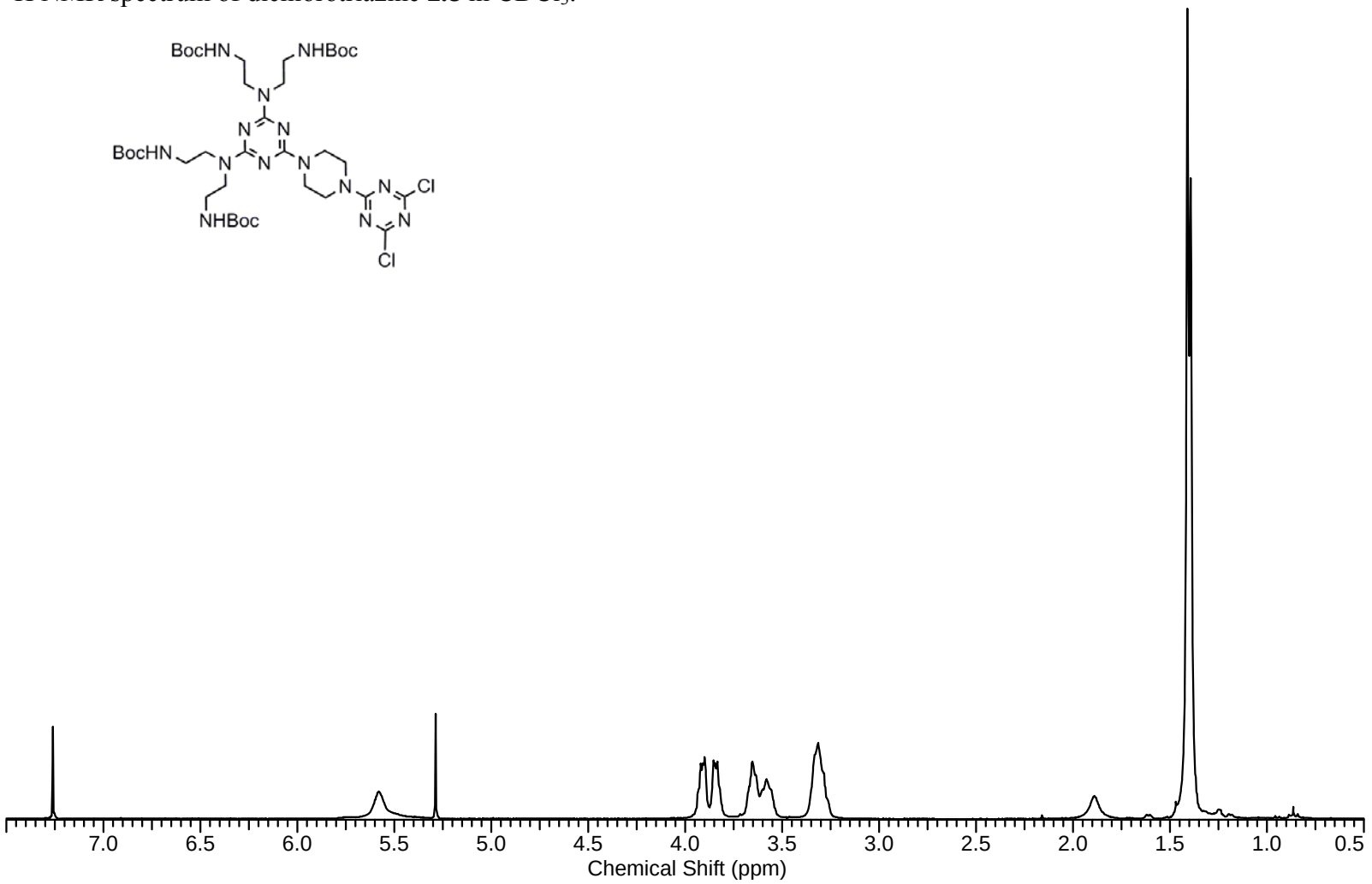

^{13}C NMR spectrum of dichlorotriazine **2.8** in $CDCl_3$.

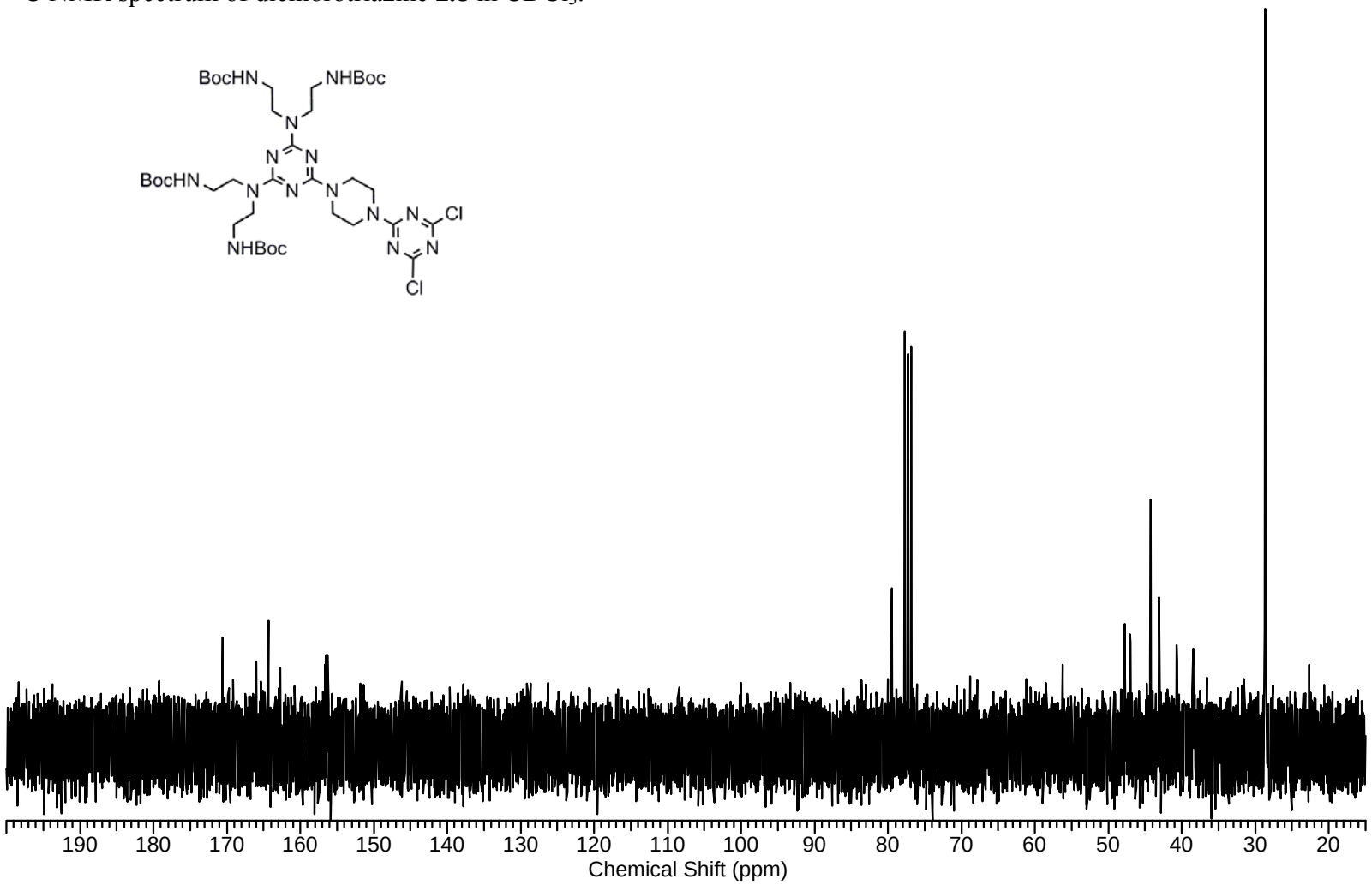

Mass spectrum (MALDI-TOF) of dichlorotriazine **2.8.**

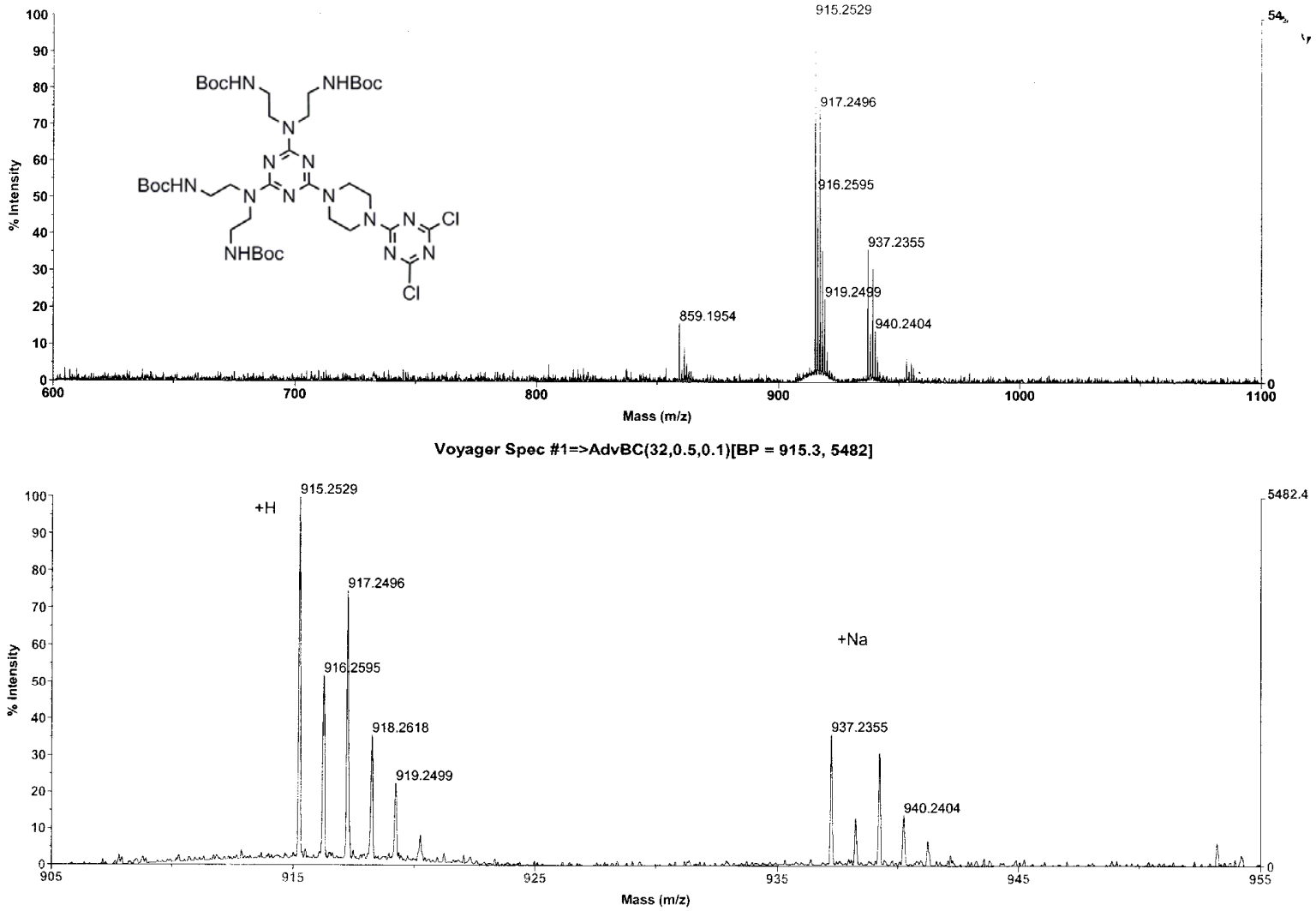

^{1}H NMR spectrum of generation-1 dendron **2.9** in $CDCl_3$.

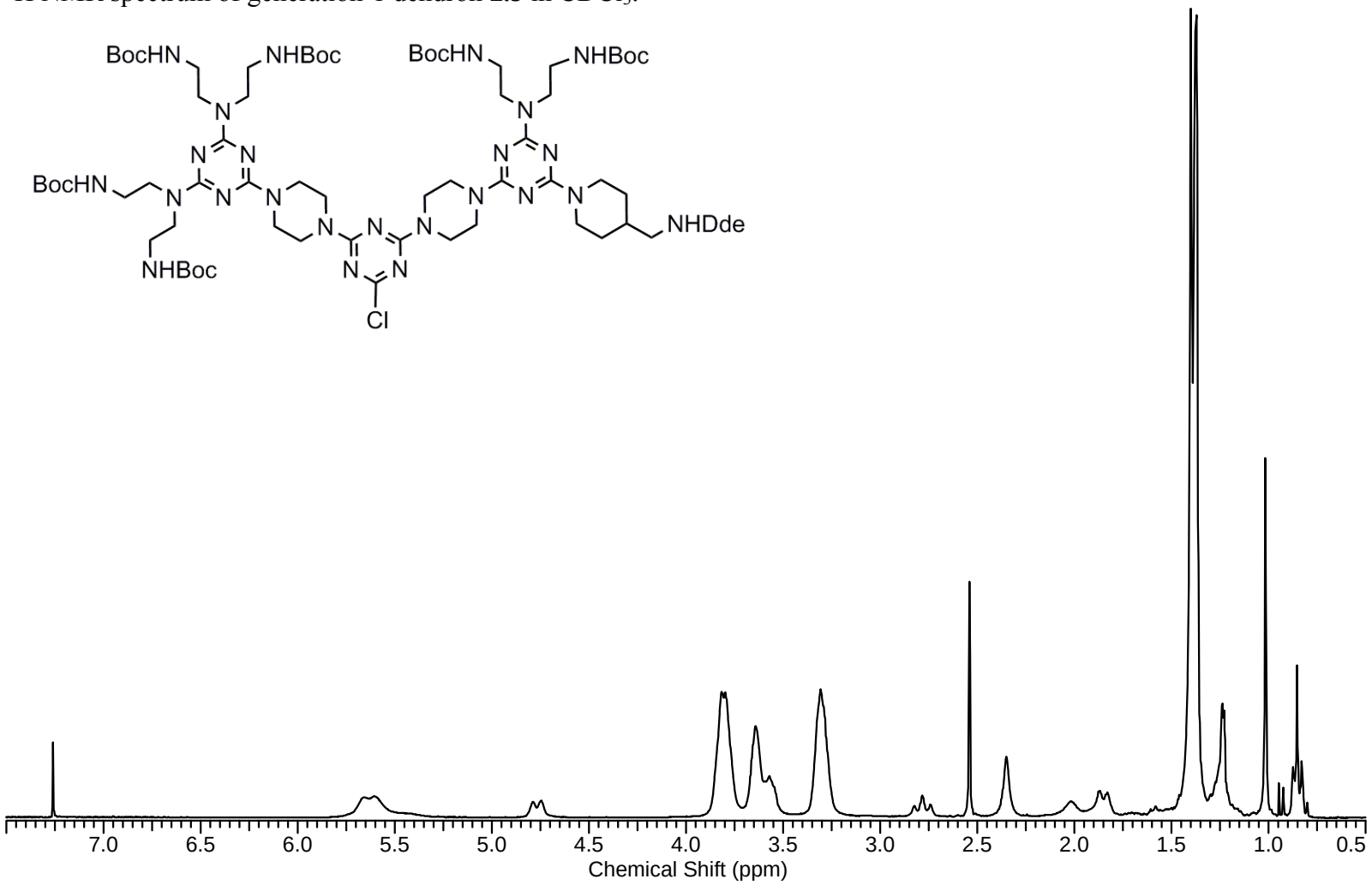

^{13}C NMR spectrum of generation-1 dendron **2.9** in $CDCl_3$.

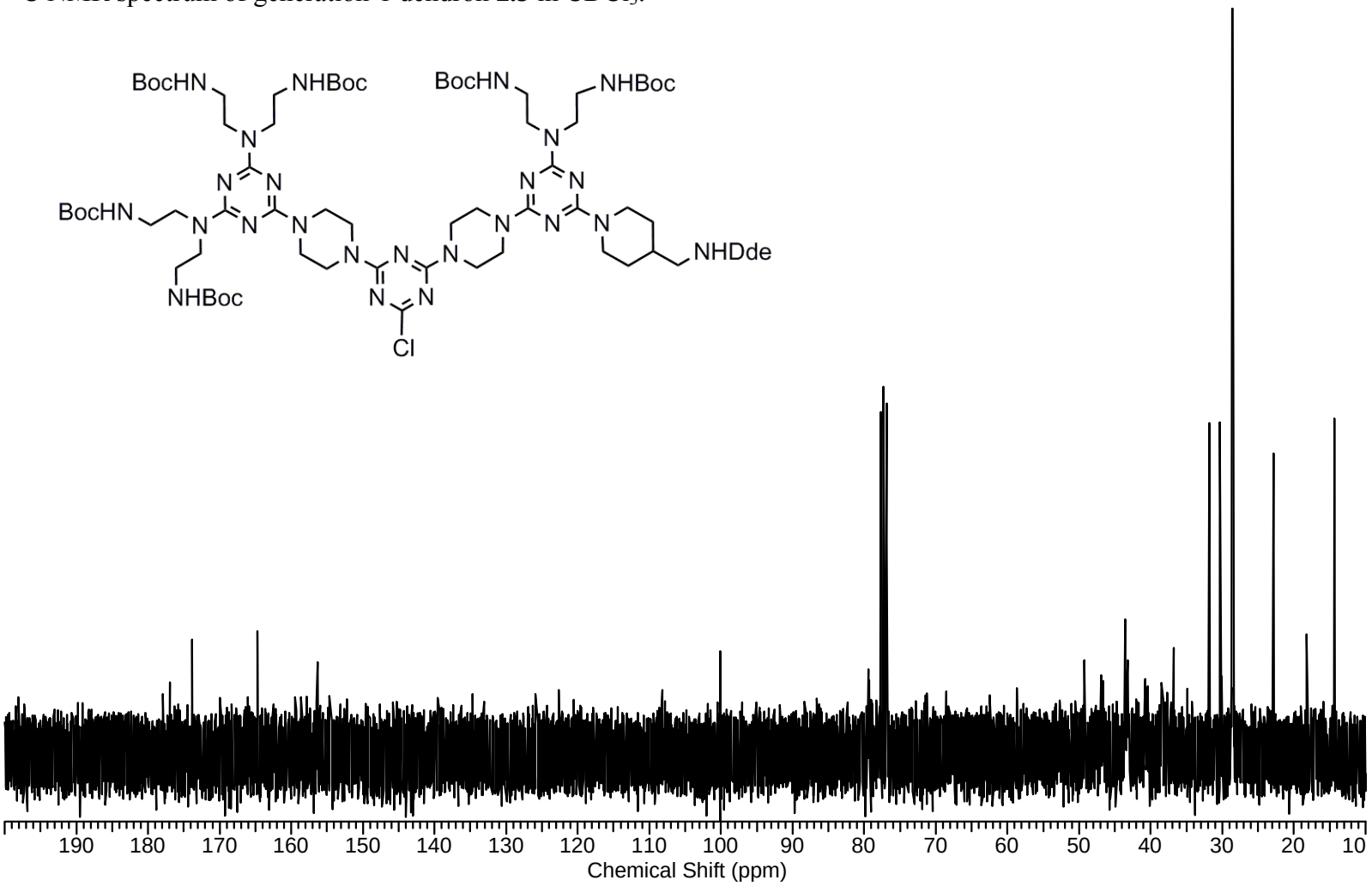

Mass spectrum (MALDI-TOF) of generation-1 dendron **2.9**.

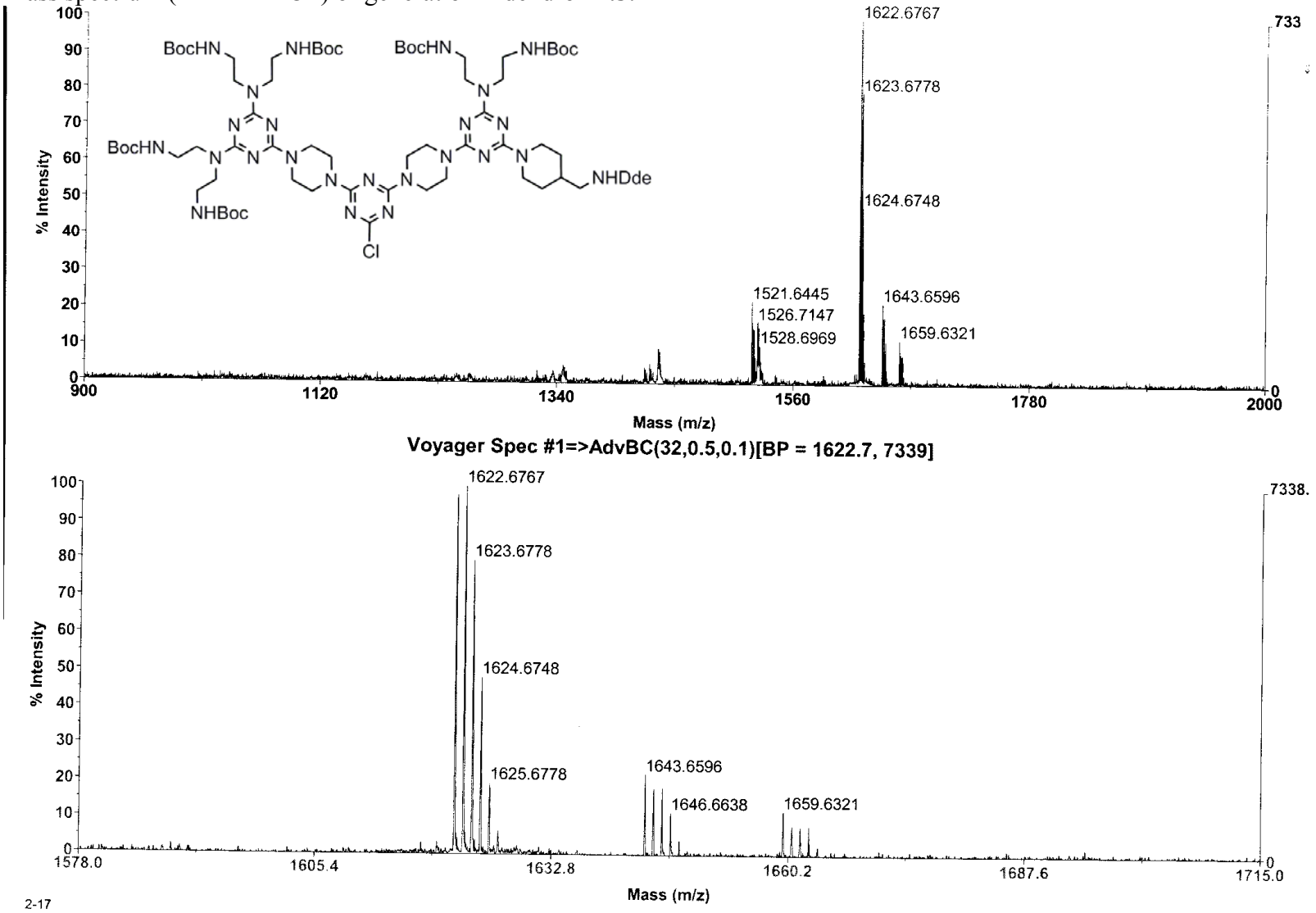

^{1}H NMR spectrum of dendron **2.10** in $CDCl_3$.

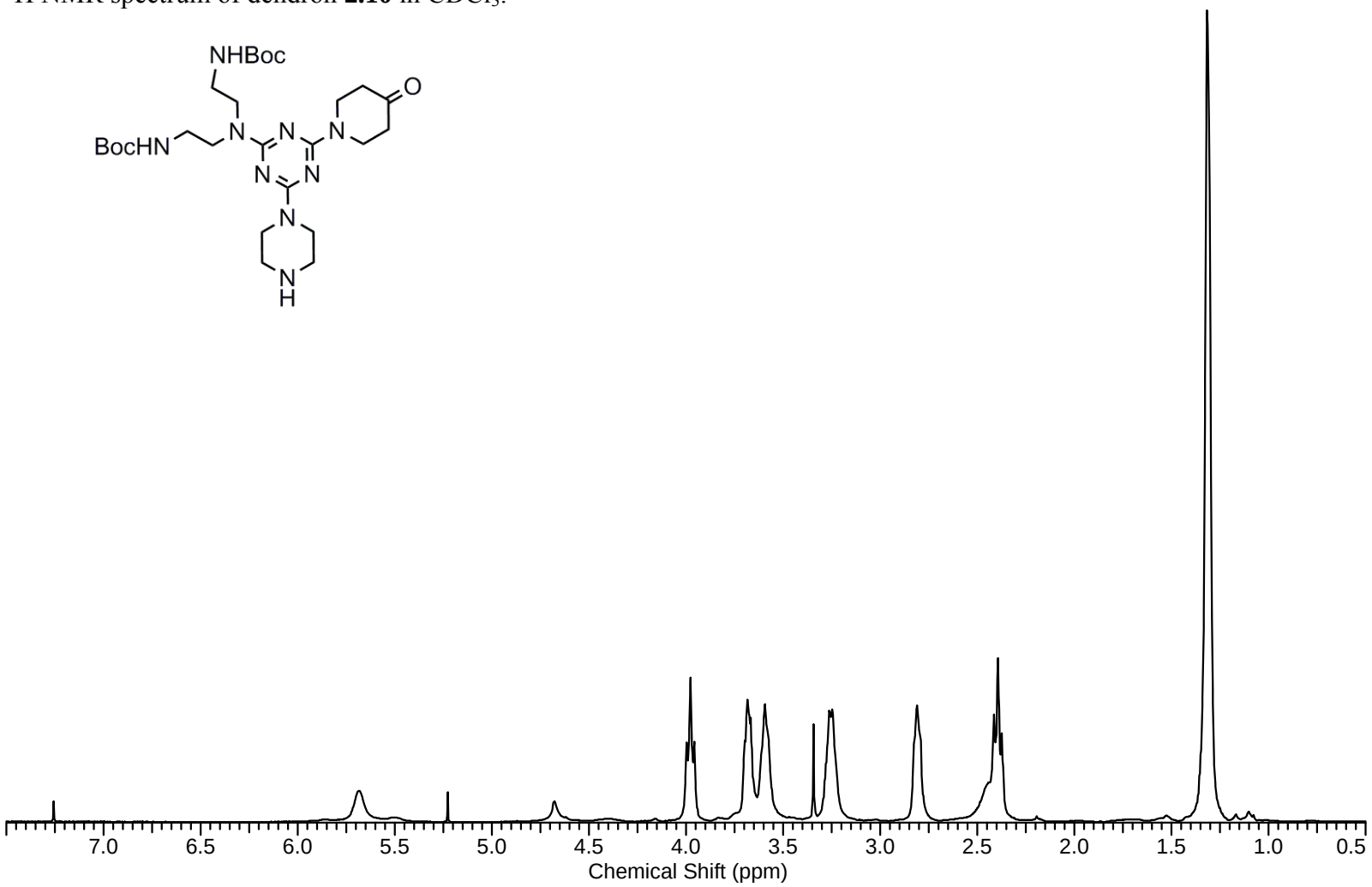

^{13}C NMR spectrum of dendron **2.10** in $CDCl_3$.

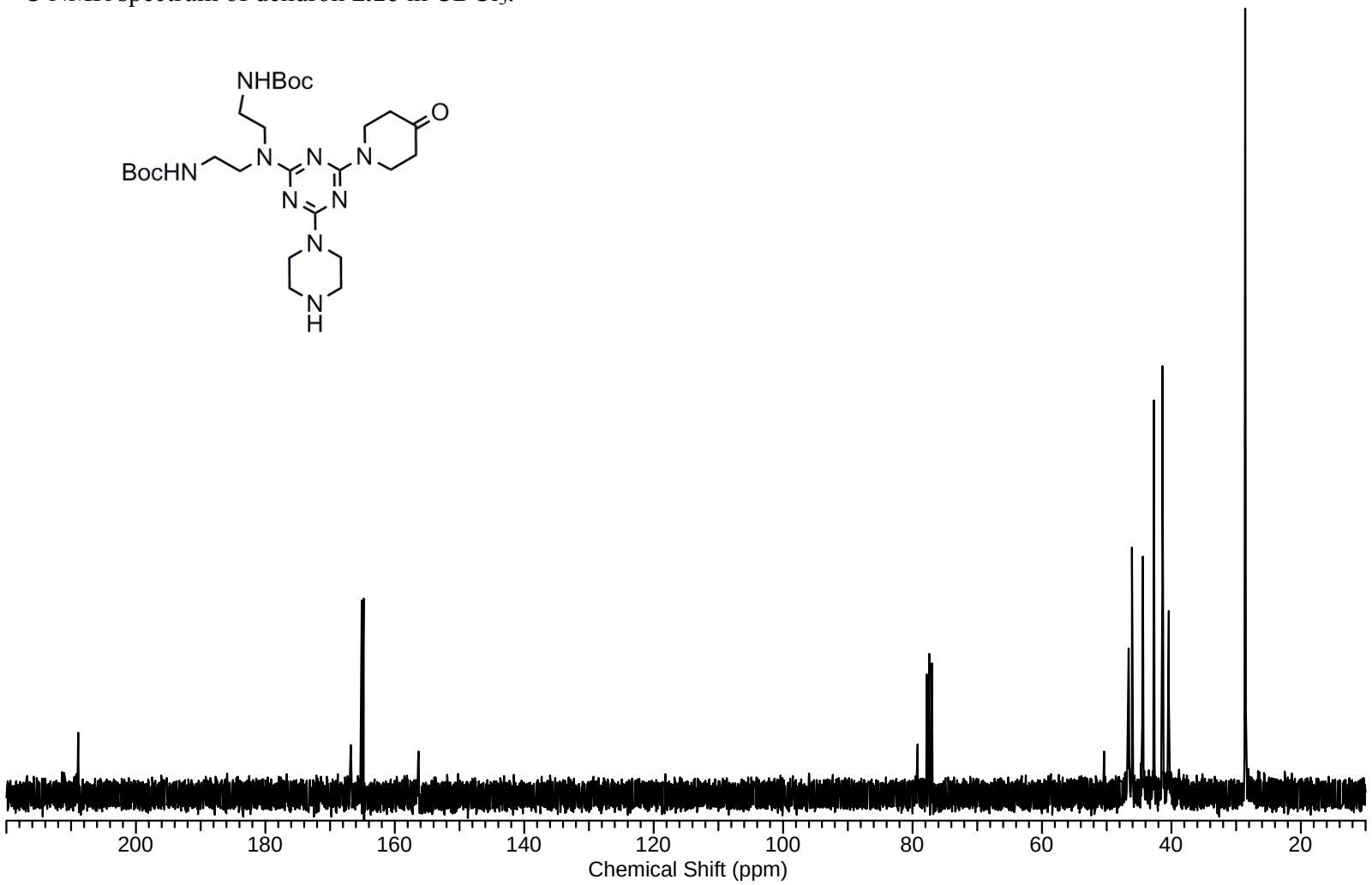

Mass spectrum (ESI) of dendron **2.10**.

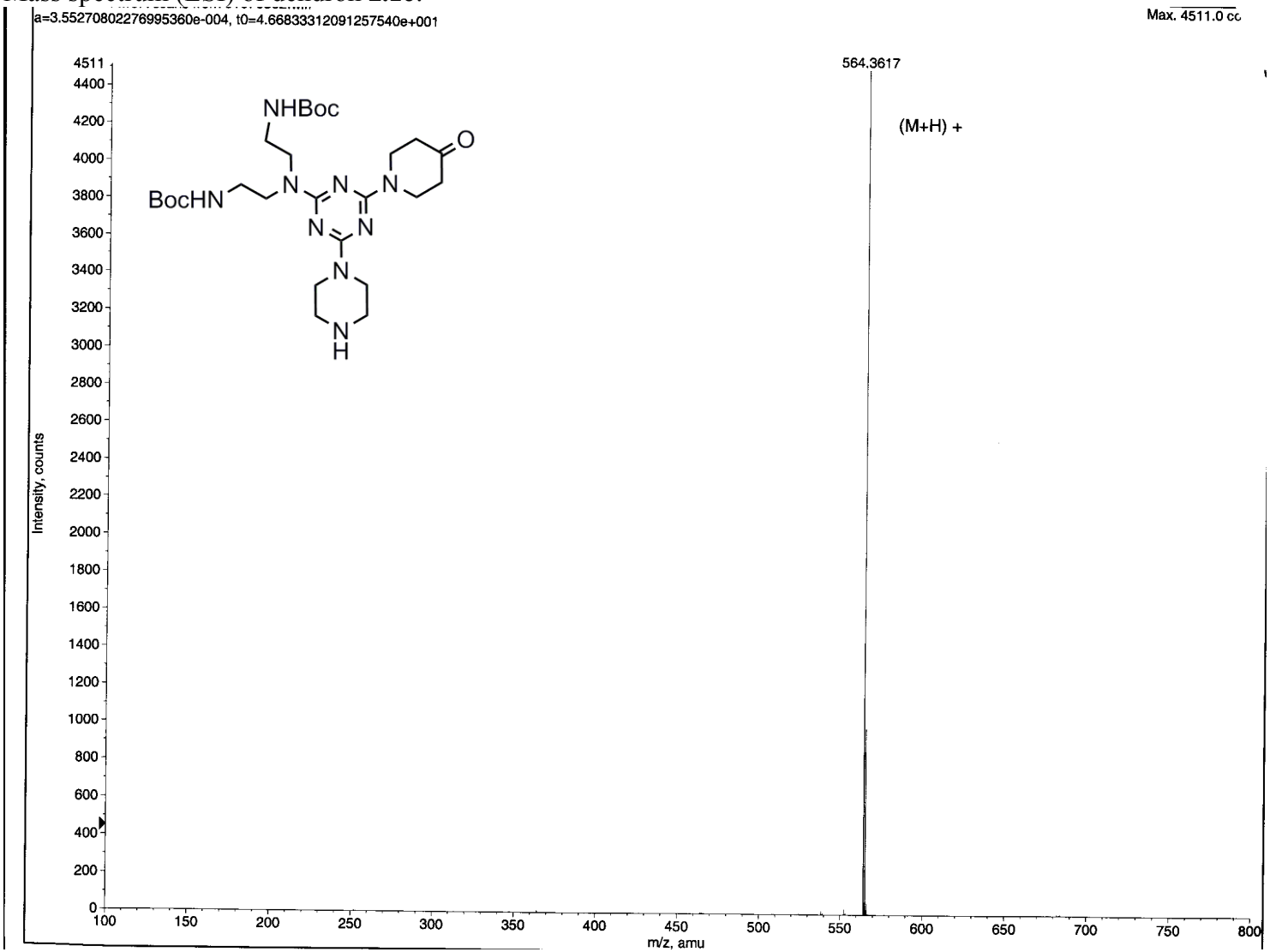

^{1}H NMR spectrum of generation-1 dendron **2.11** in $CDCl_3$.

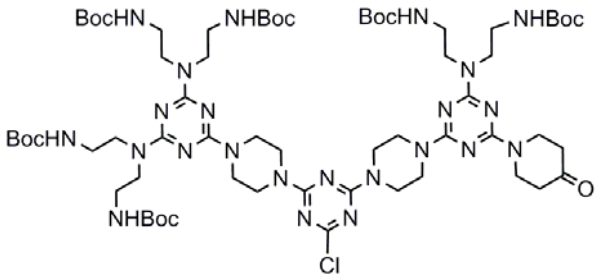

^{13}C NMR spectrum of generation-1 dendron **2.11** in $CDCl_3$.

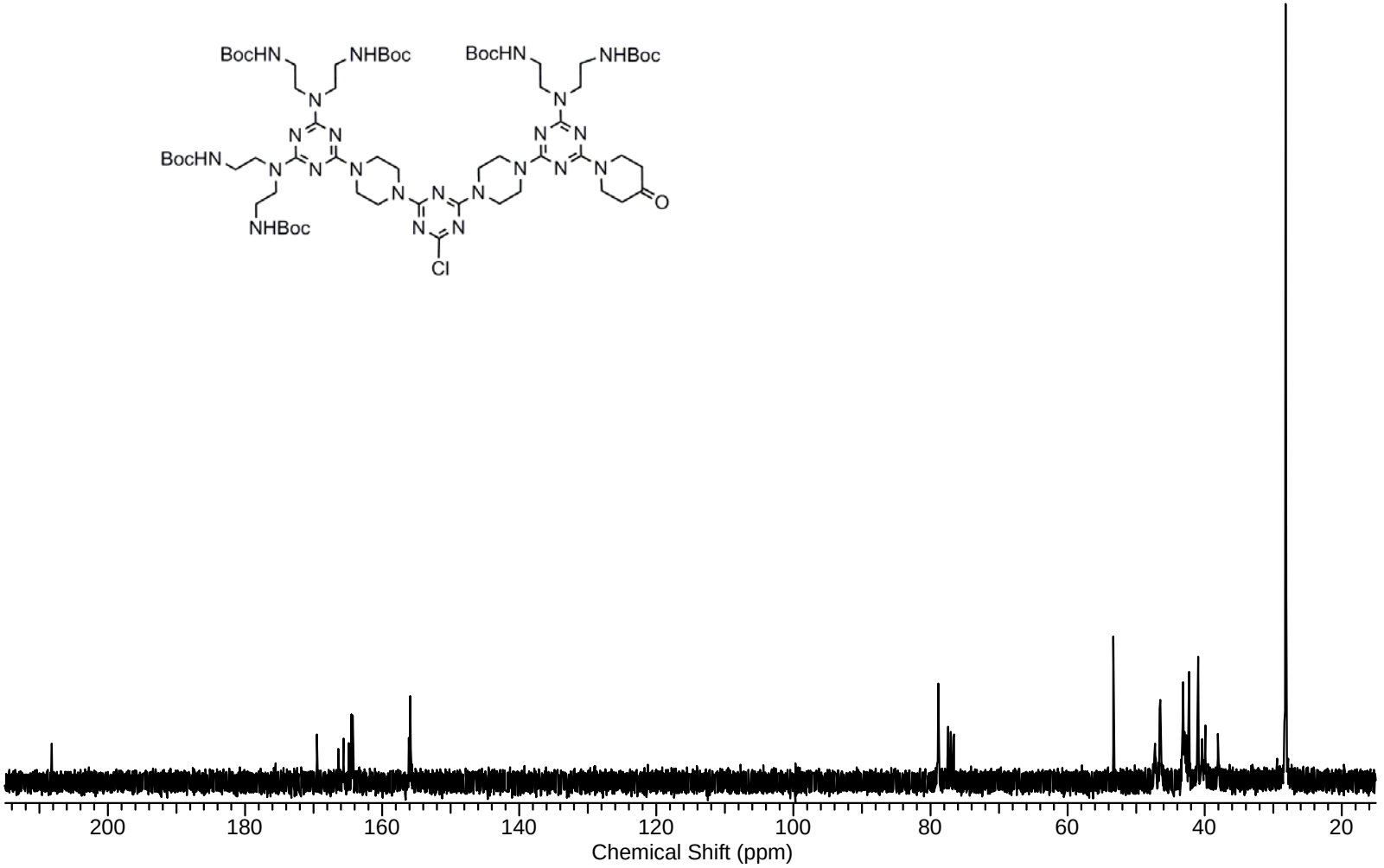

Mass spectrum (MALDI-TOF) of generation-1 dendron **2.11**.

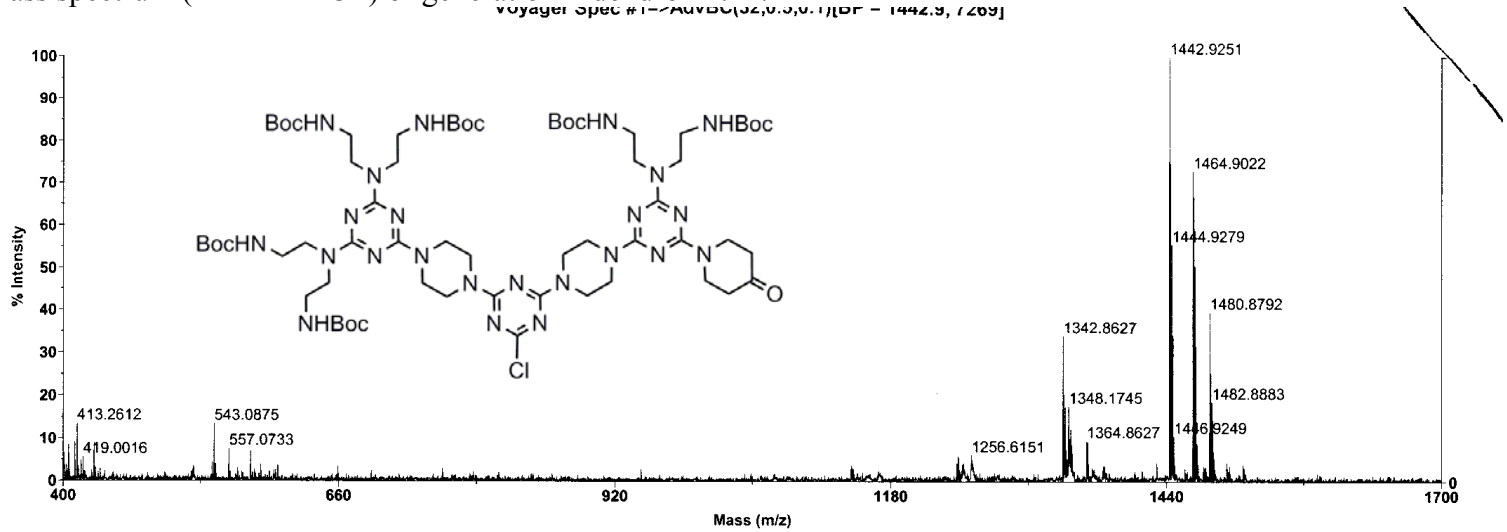

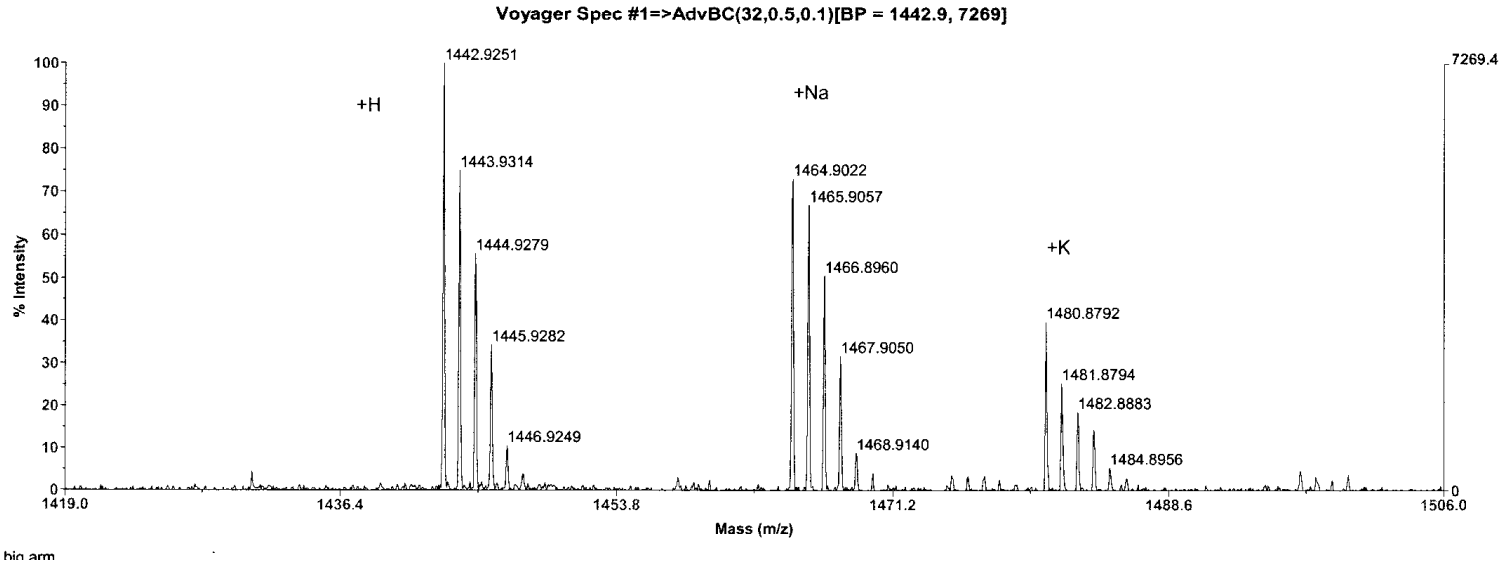

bio arm

^{1}H NMR spectrum of generation-1 dendron **2.12** in $CDCl_3$.

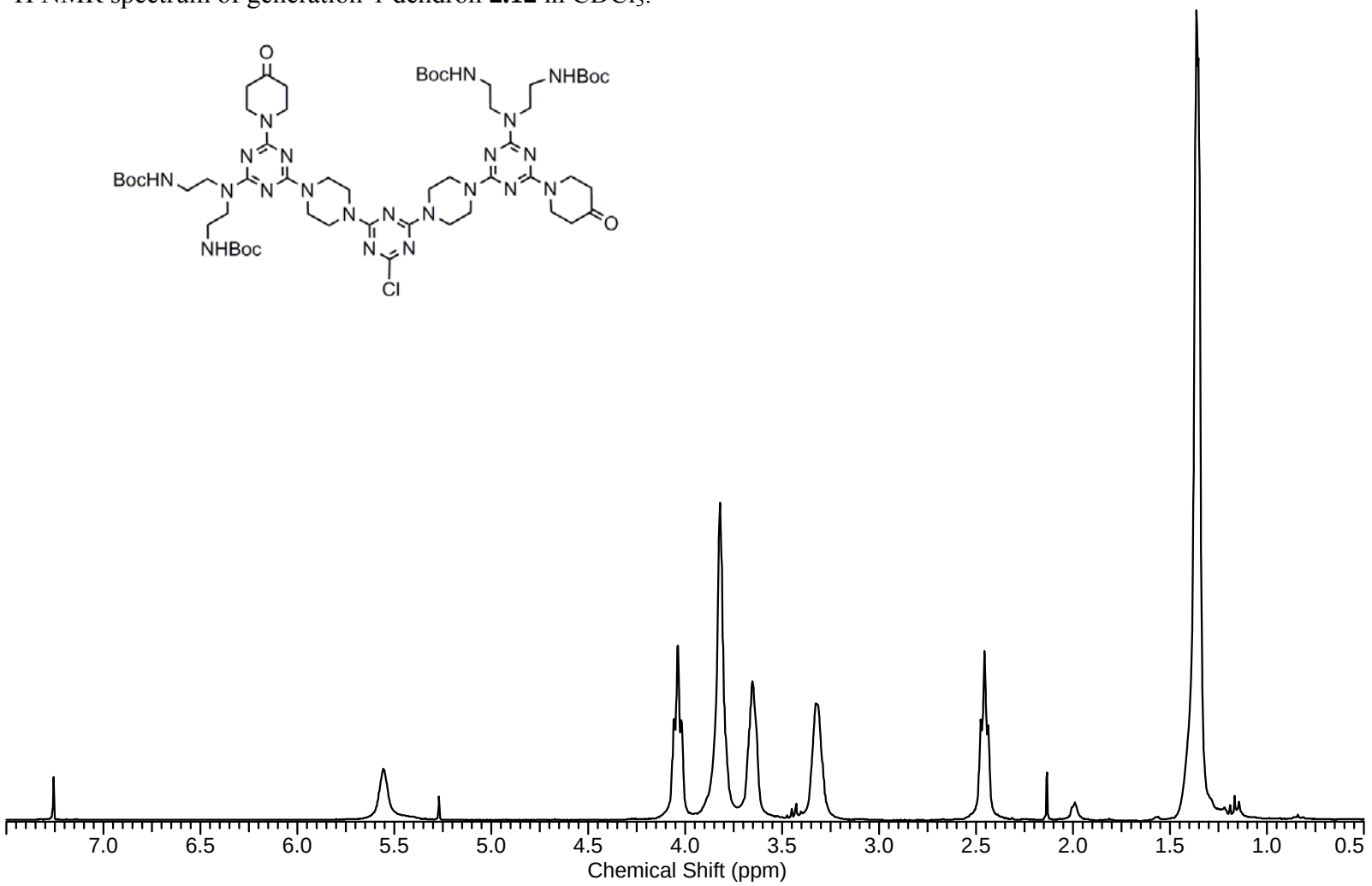

^{13}C NMR spectrum of generation-1 dendron **2.12** in $CDCl_3$.

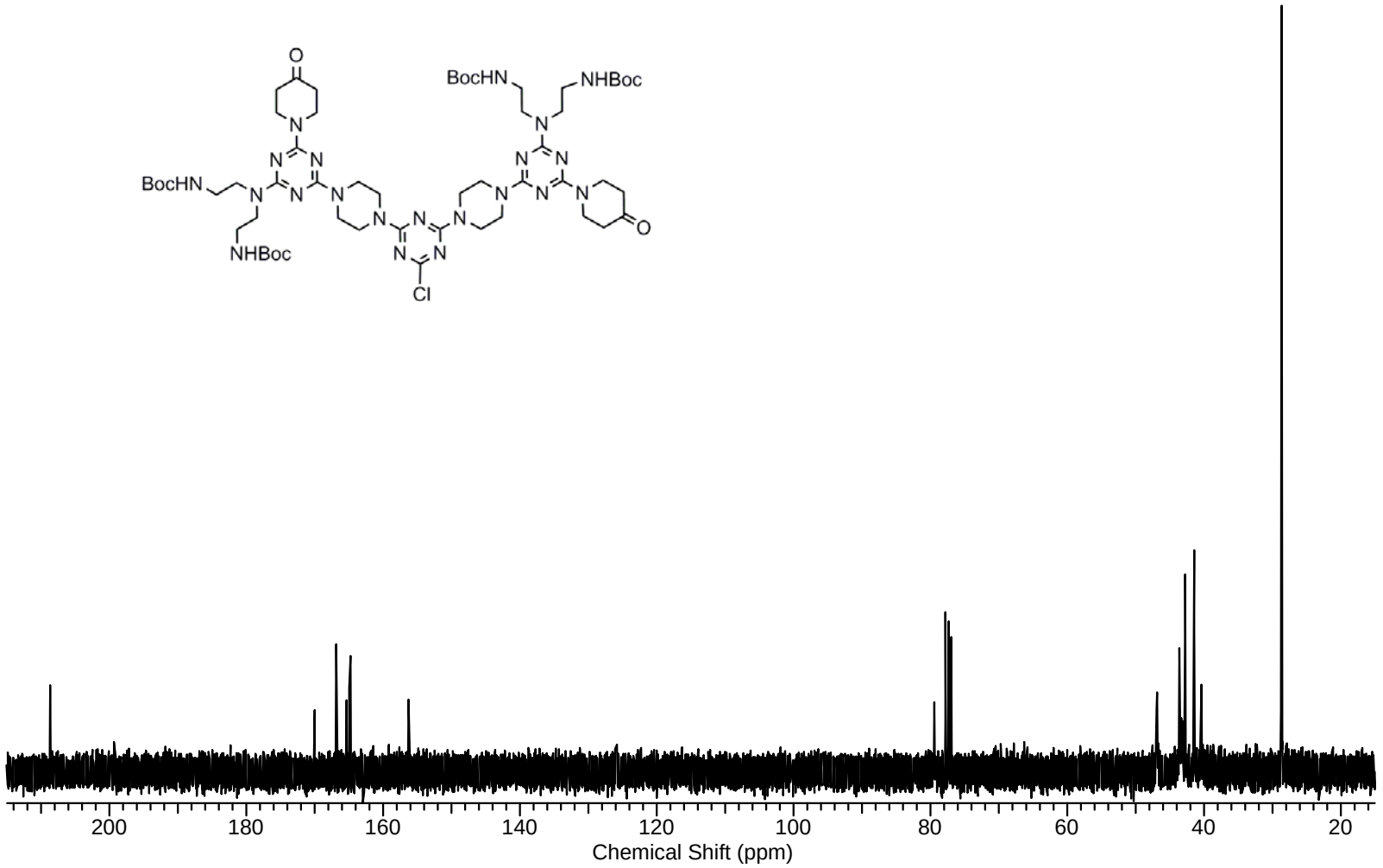

Mass spectrum (MALDI-TOF) of generation-1 dendron **2.12**.

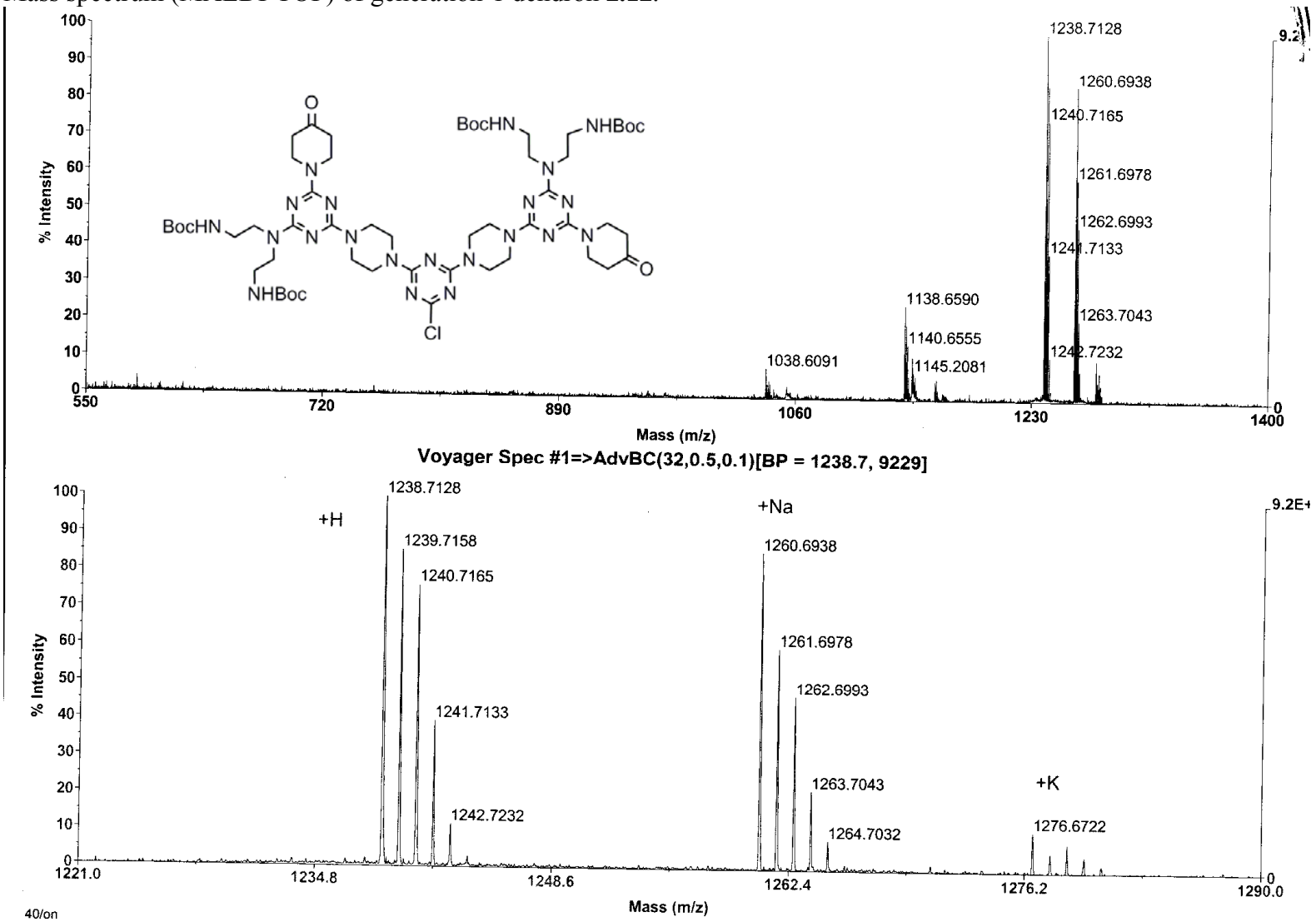

^{1}H NMR spectrum of protected core **2.13** in $CDCl_3$.

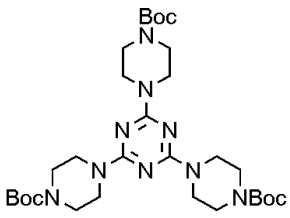

^{13}C NMR spectrum of protected core **2.13** in $CDCl_3$.

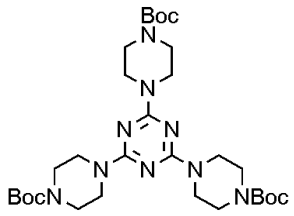

Mass spectrum (ESI) of protected core **2.13.**

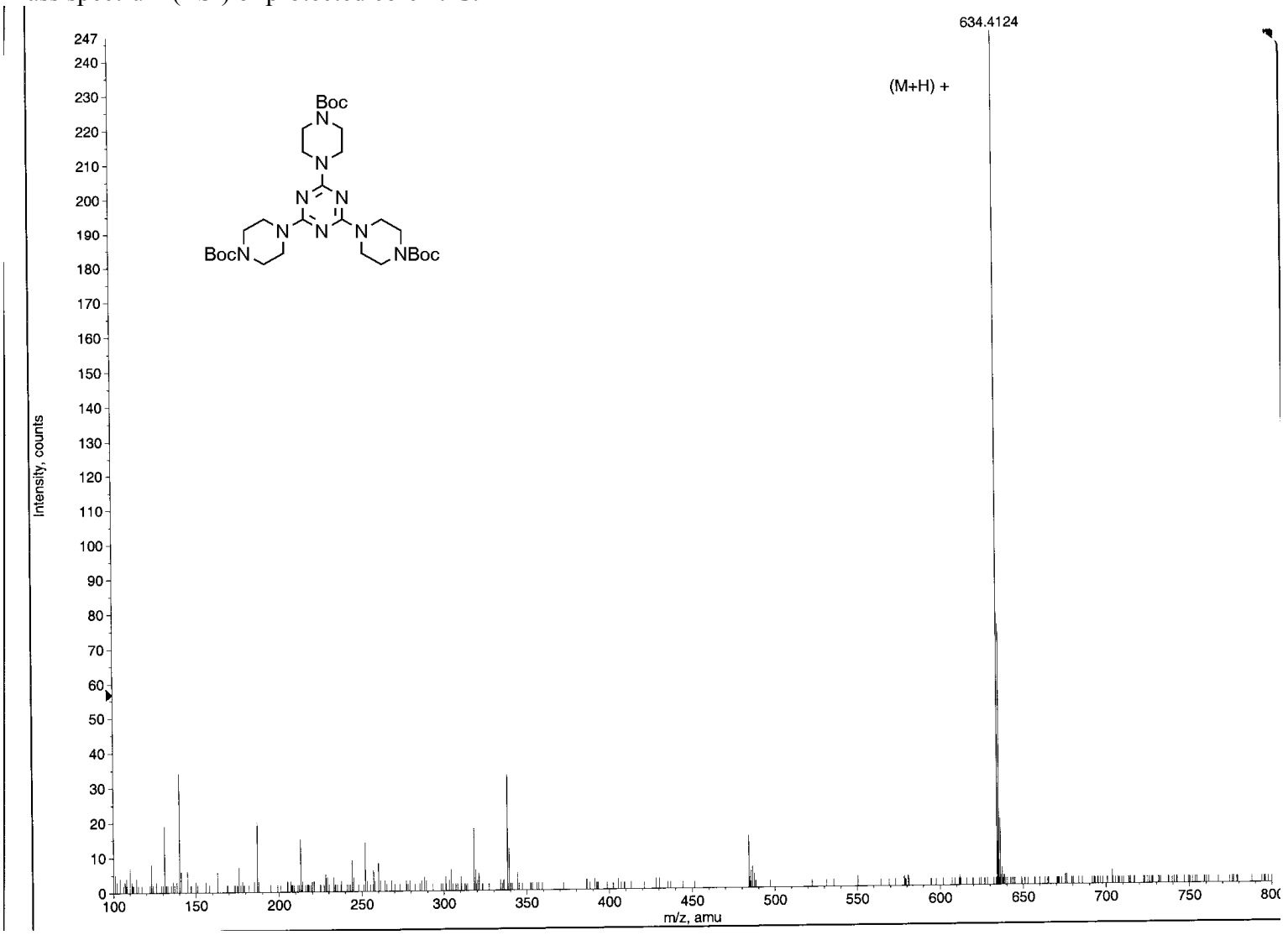

^{1}H NMR spectrum of amine core **2.14** in $CDCl_3$.

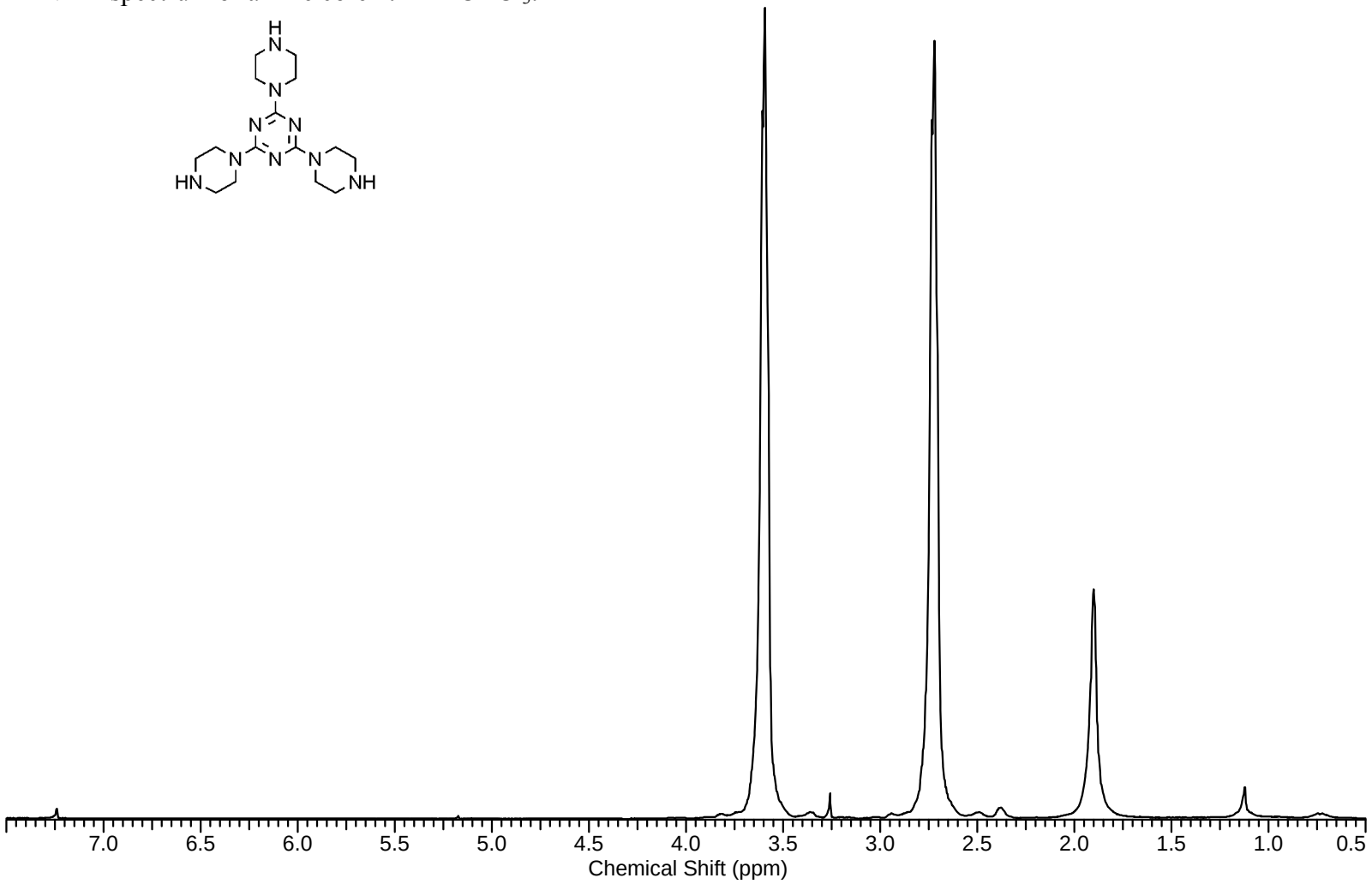

^{13}C NMR spectrum of amine core **2.14** in $CDCl_3$.

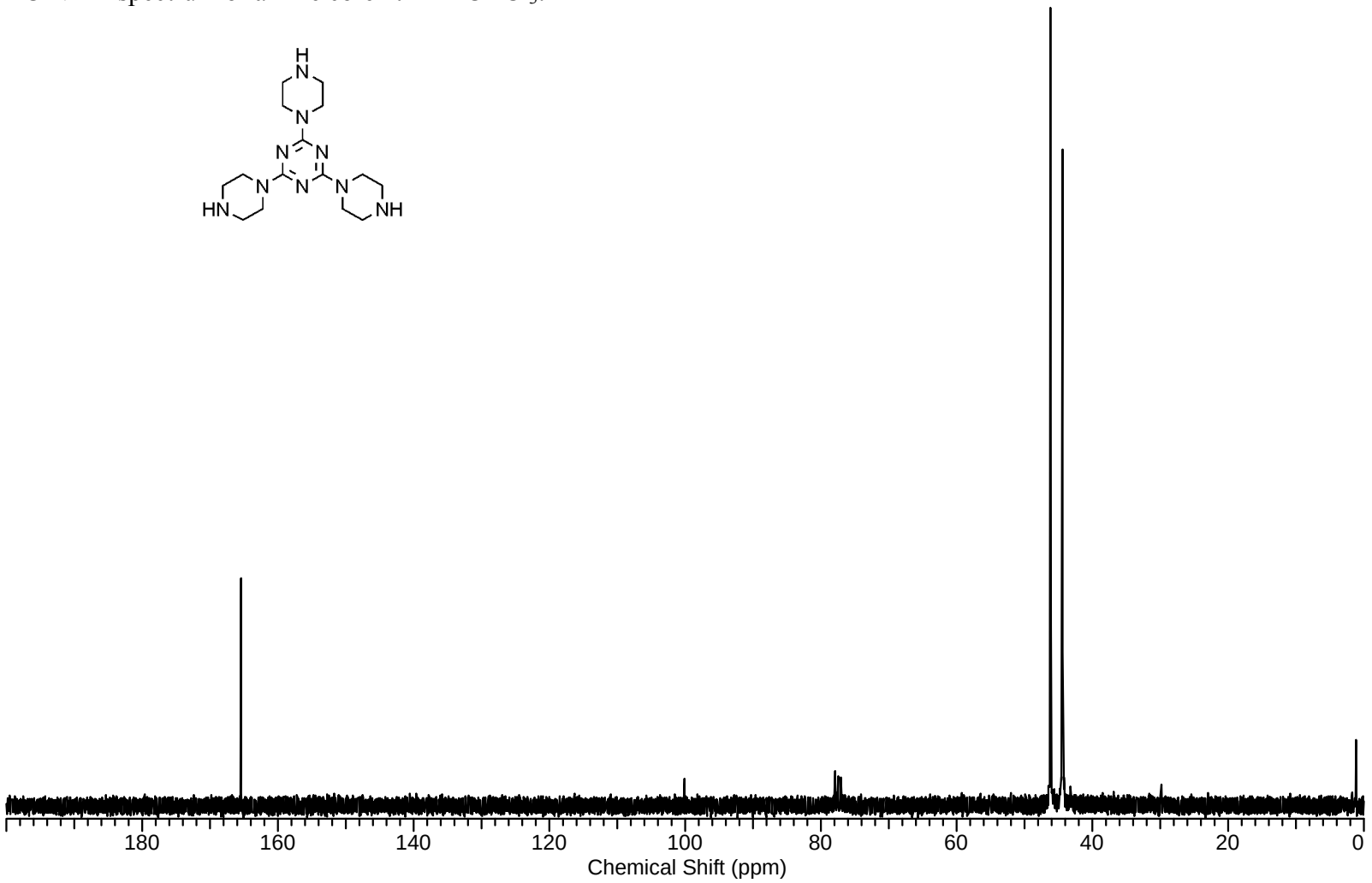

Mass spectrum (ESI) of amine core **2.14.**

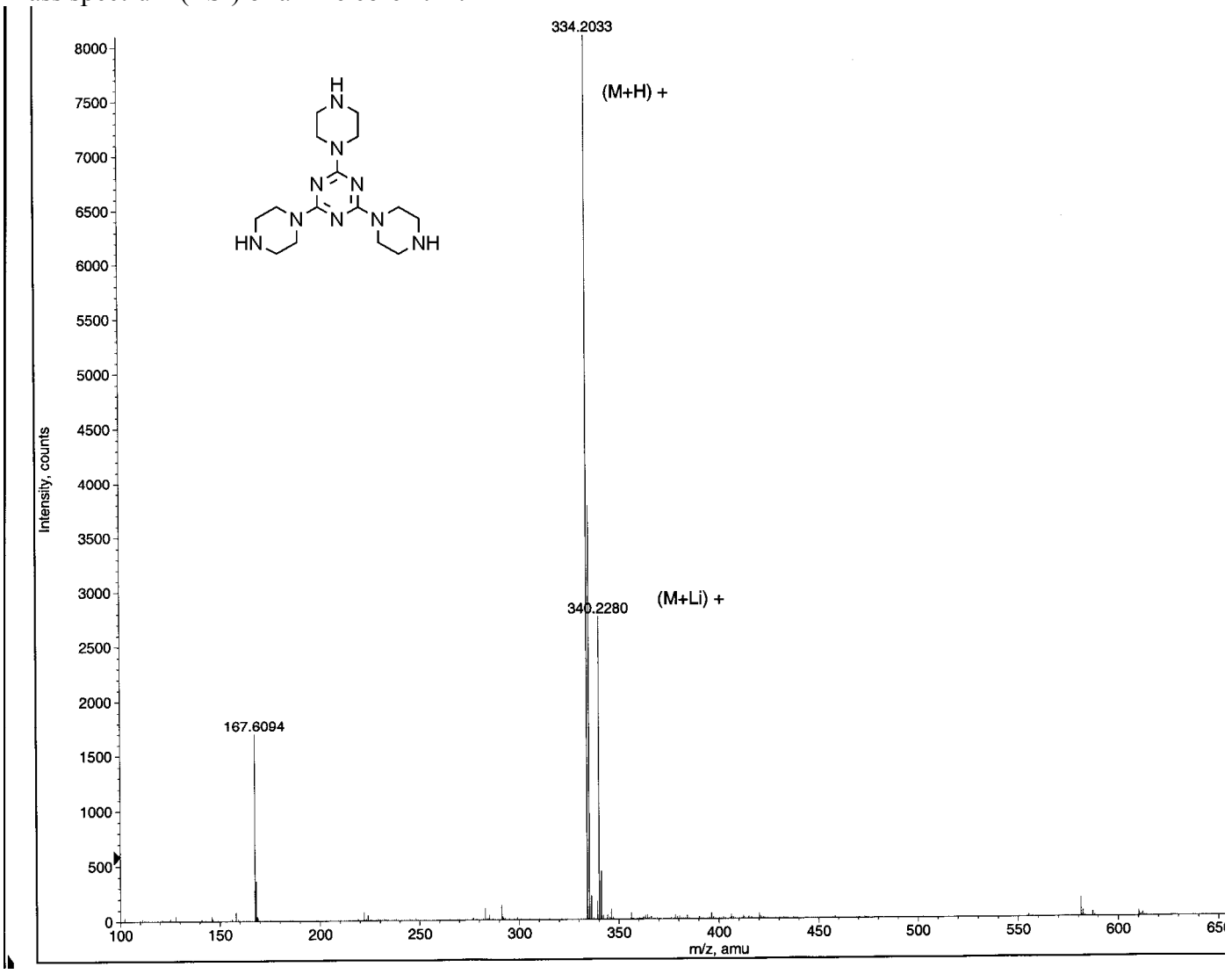

^{1}H NMR spectrum of generation-2 dendrimer **2.15** in $CDCl_3$.

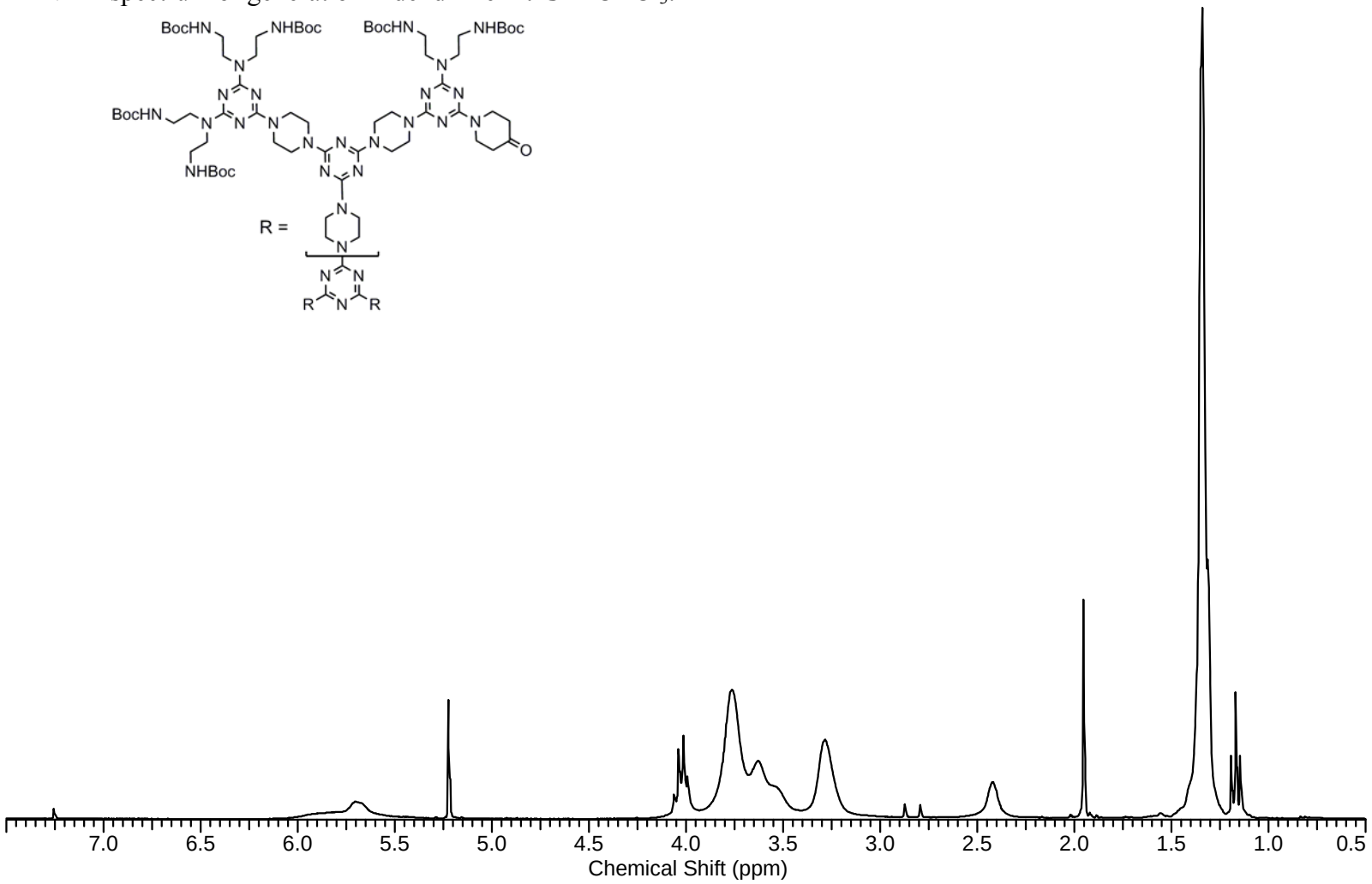

^{13}C NMR spectrum of generation-2 dendrimer **2.15** in $CDCl_3$.

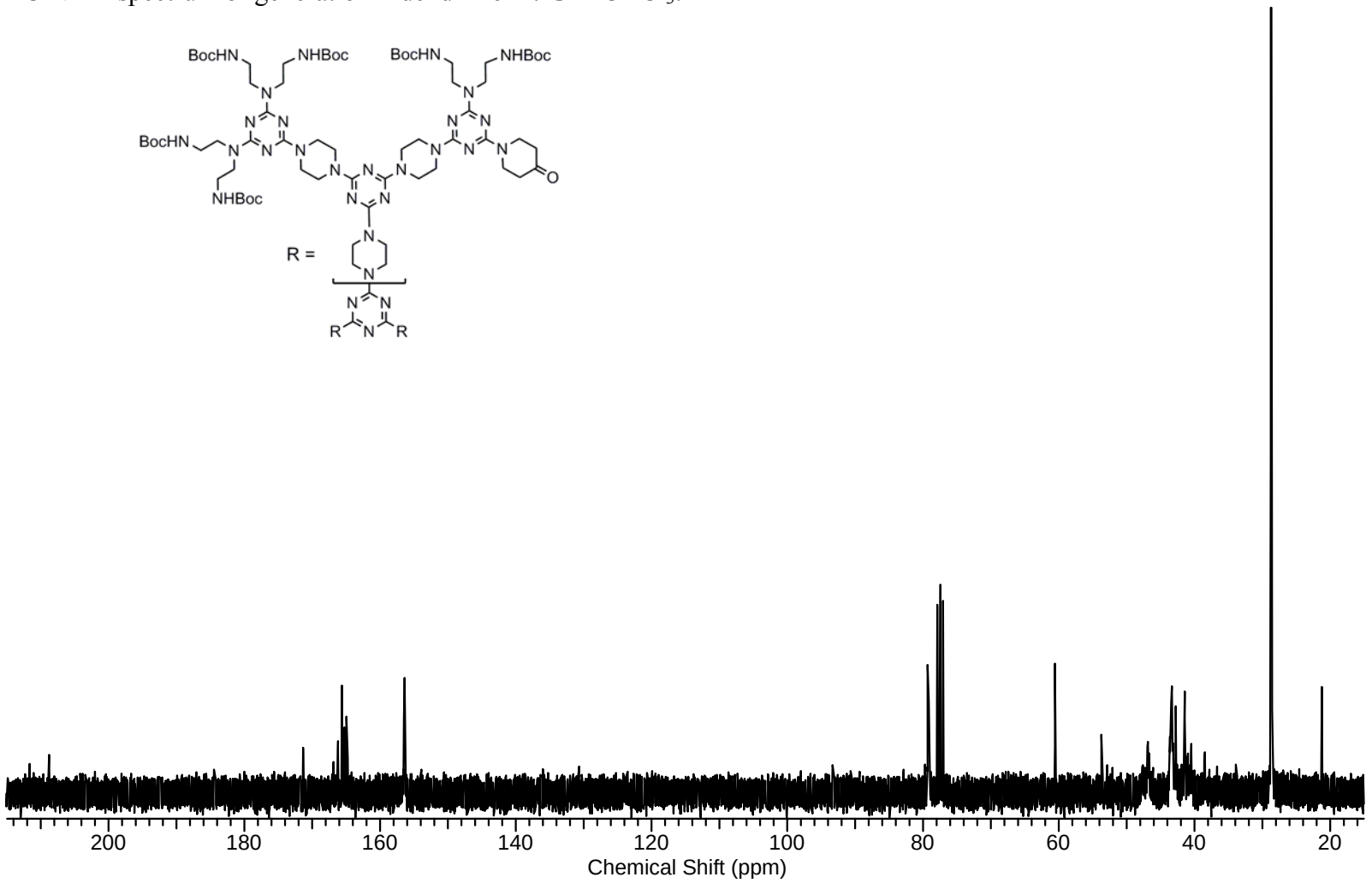

Mass spectrum (MALDI-TOF) of generation-2 dendrimer **2.15.**

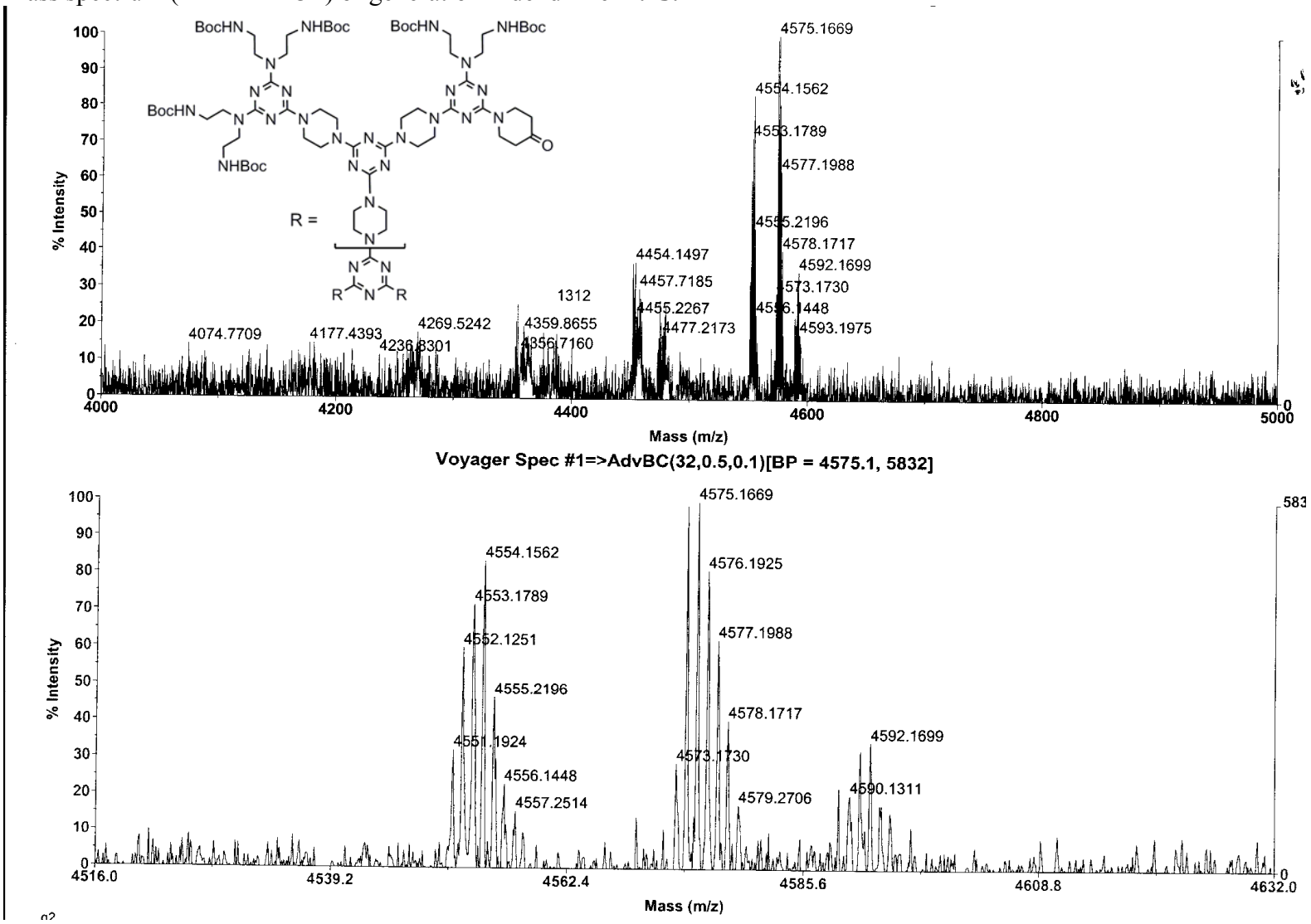

^{1}H NMR spectrum of hydrazone **2.16** in $CDCl_3$.

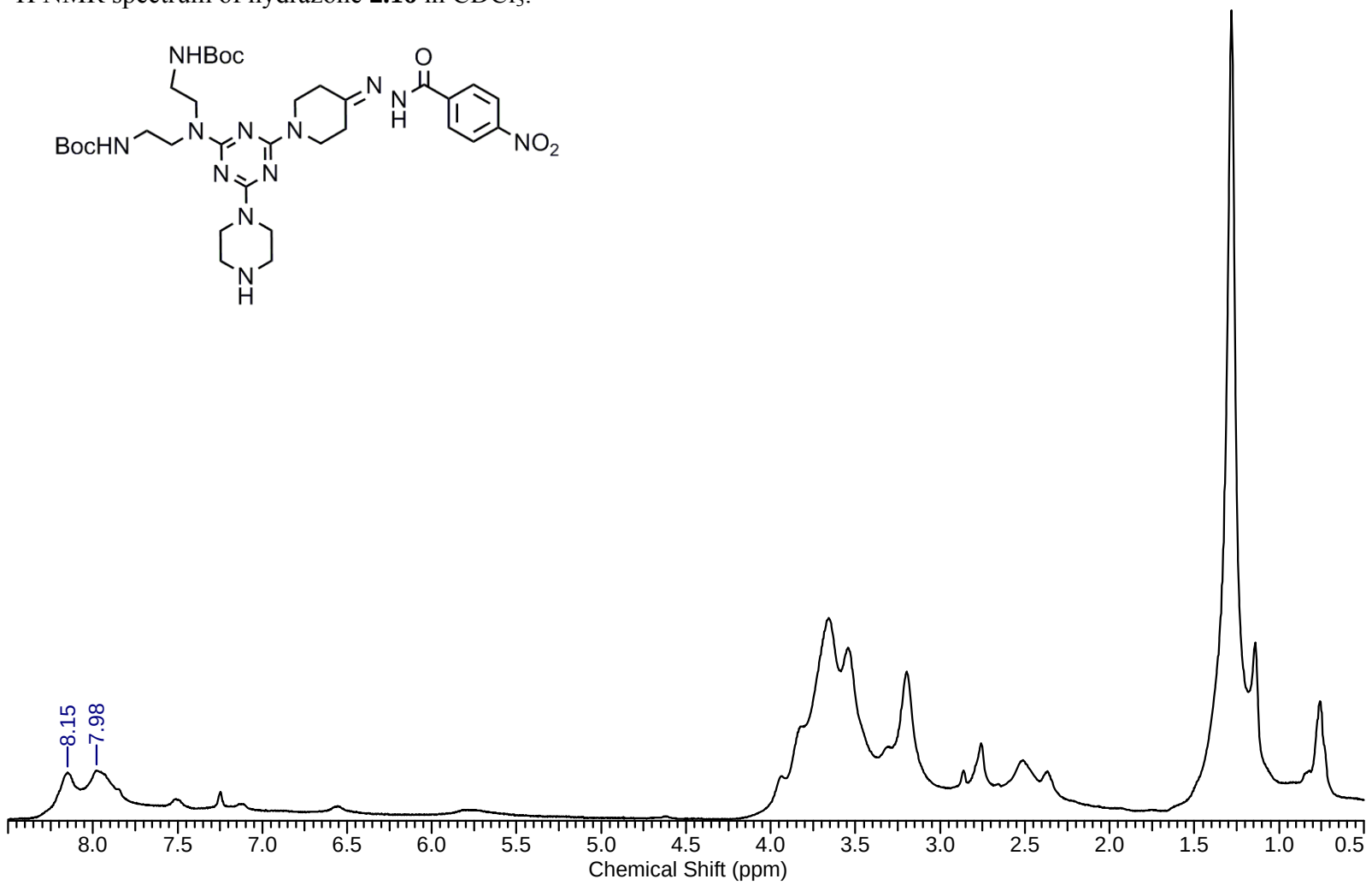

^{13}C NMR spectrum of hydrazone **2.16** in $CDCl_3$.

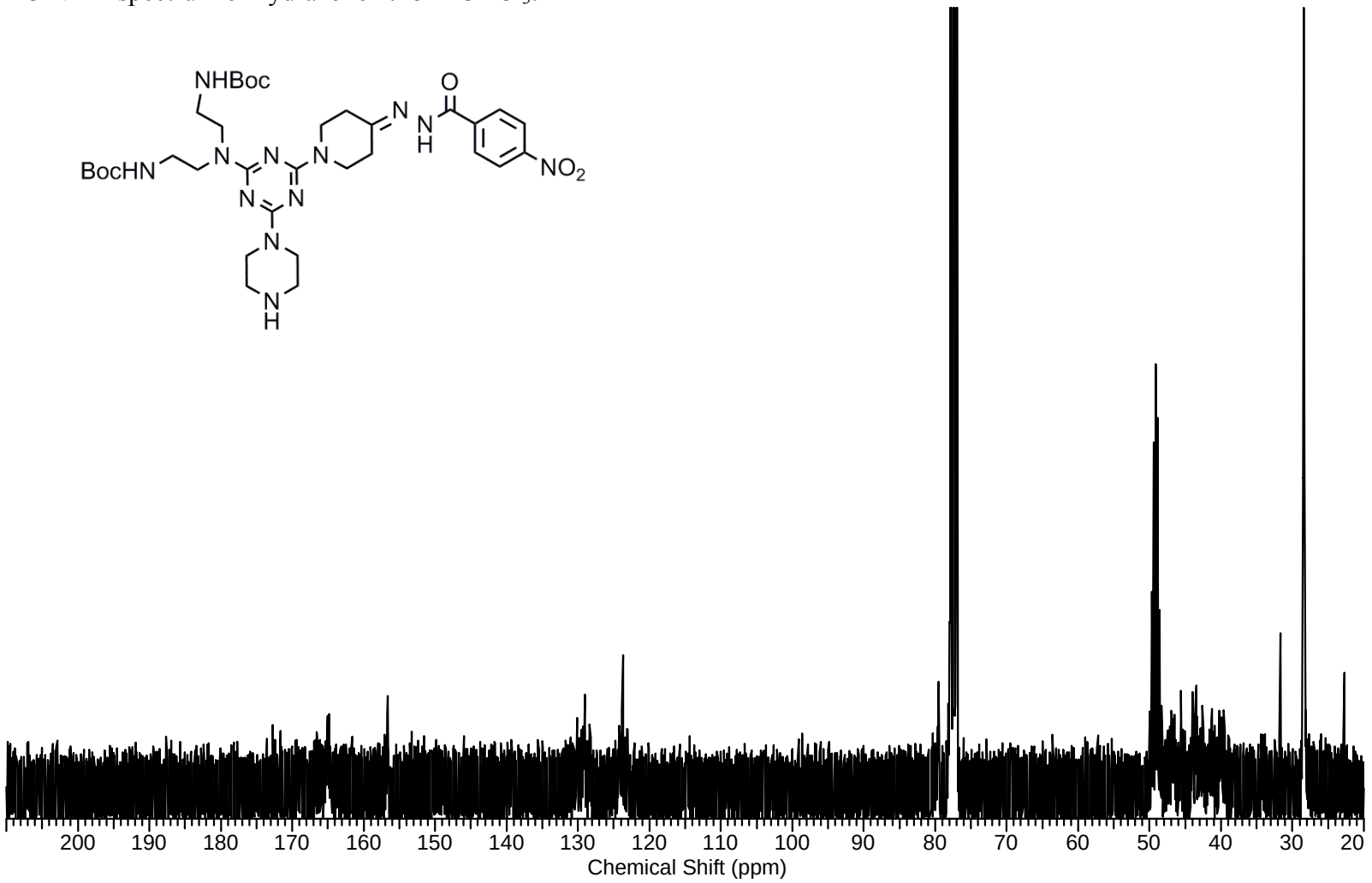

Mass spectrum (ESI) of hydrazone **2.16.**

APPENDIX B

^{1}H NMR, ^{13}C NMR, AND MASS SPECTRA FOR COMPOUNDS DESCRIBED IN CHAPTER III

^{1}H NMR spectrum of **3.1** in $CDCl_3$.

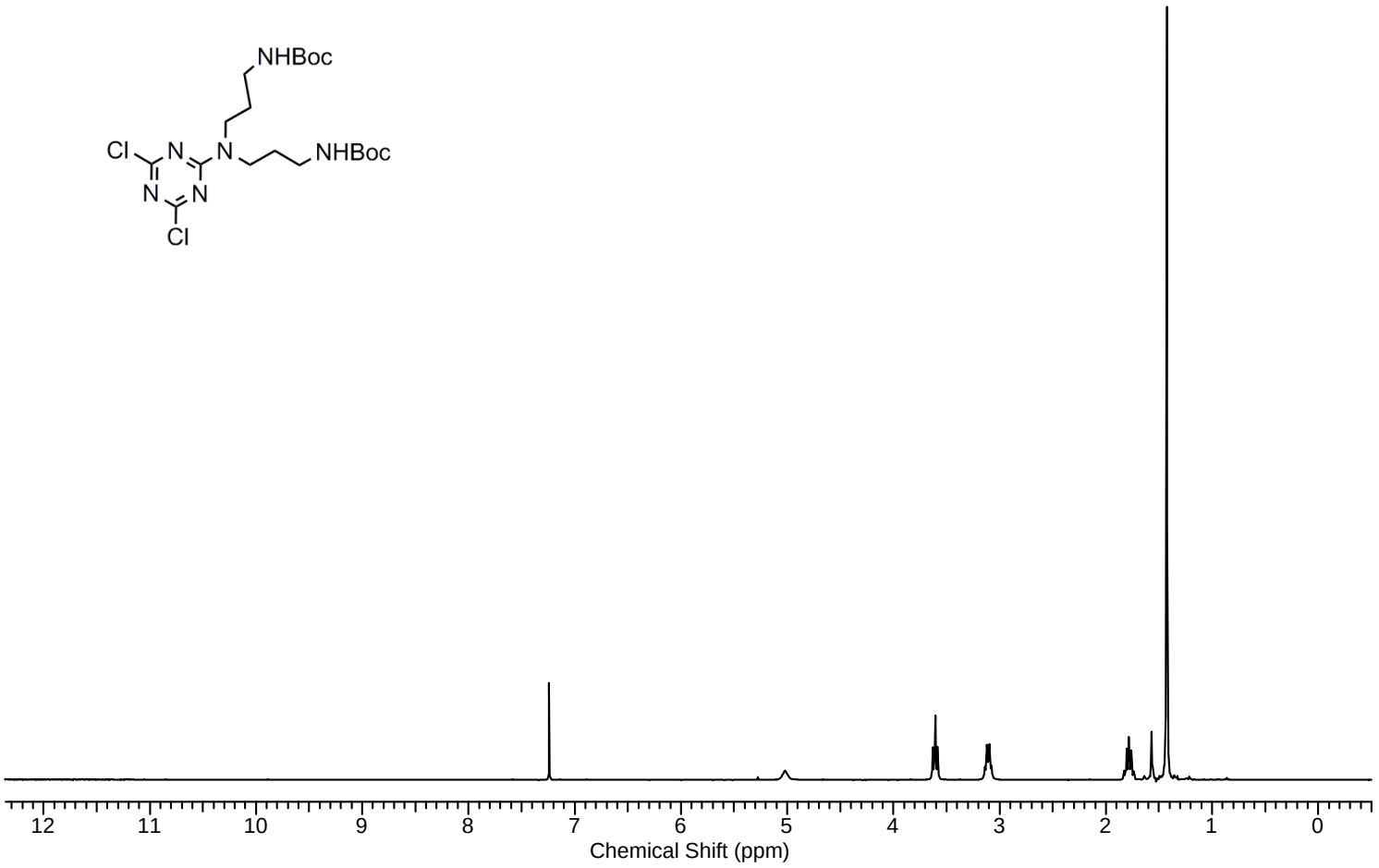

^{1}H NMR spectrum of **3.1** in $CDCl_3$.

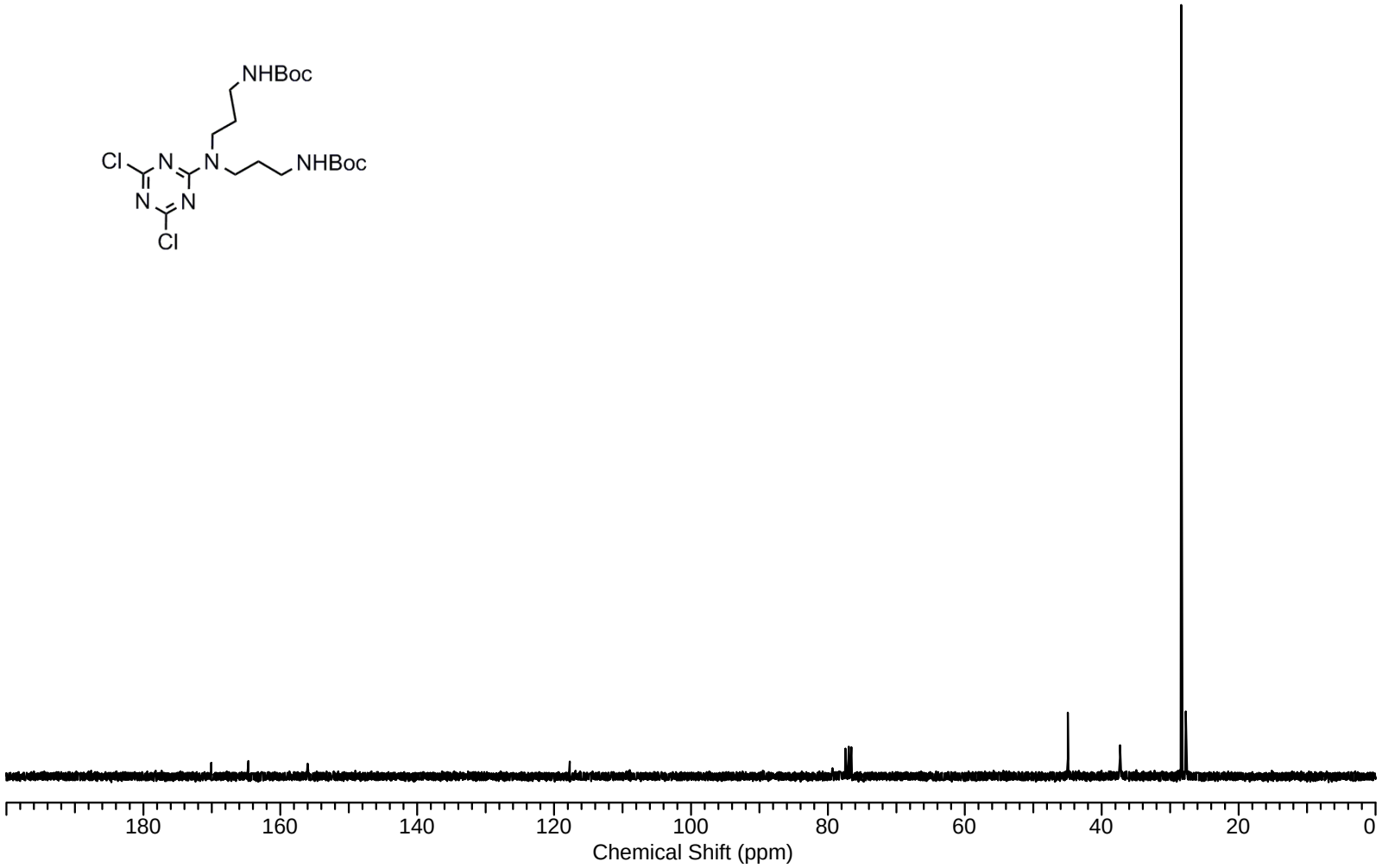

Mass spectrum (ESI) of **3.1**.

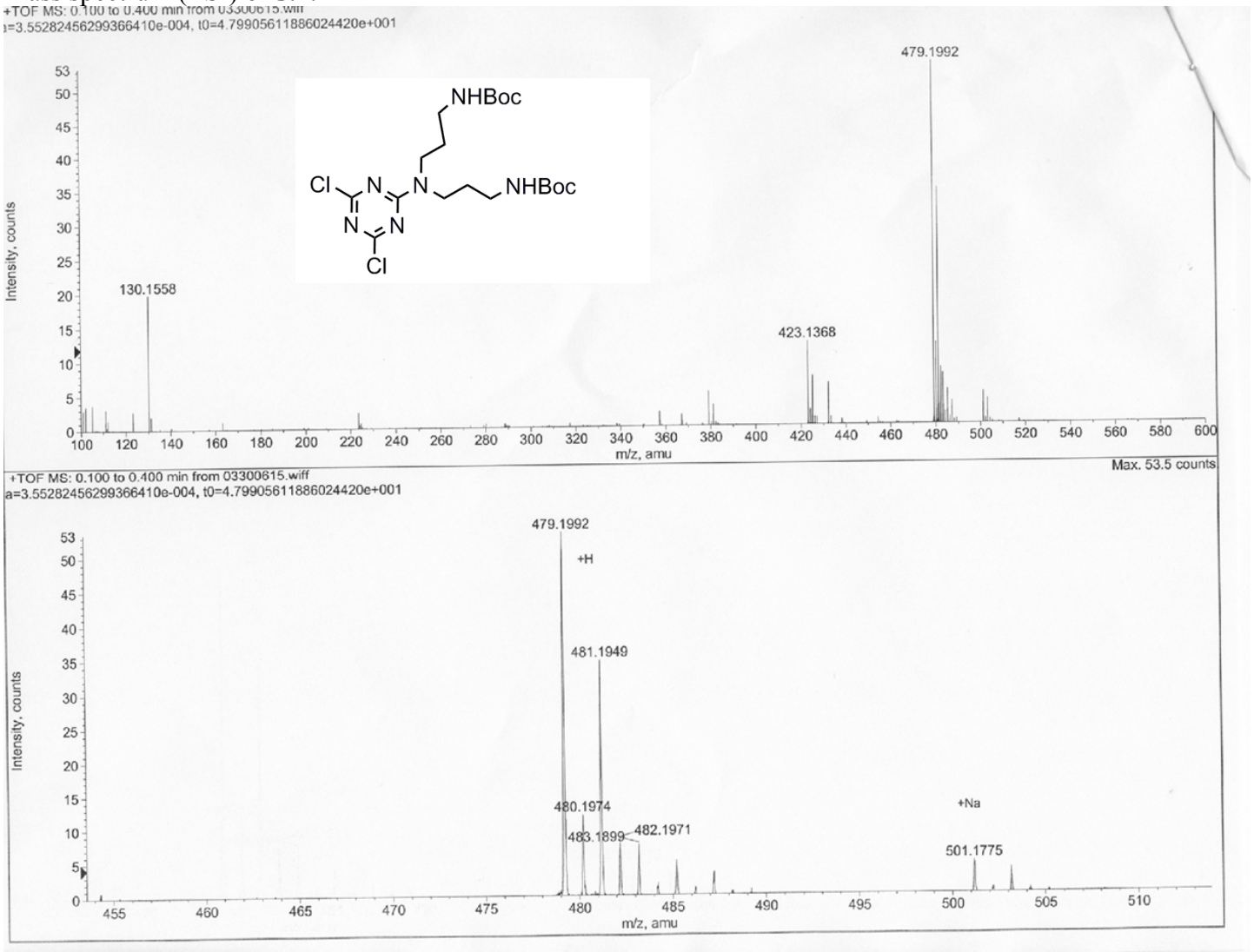

^{1}H NMR spectrum of **G1-Cl** in $CDCl_3$.

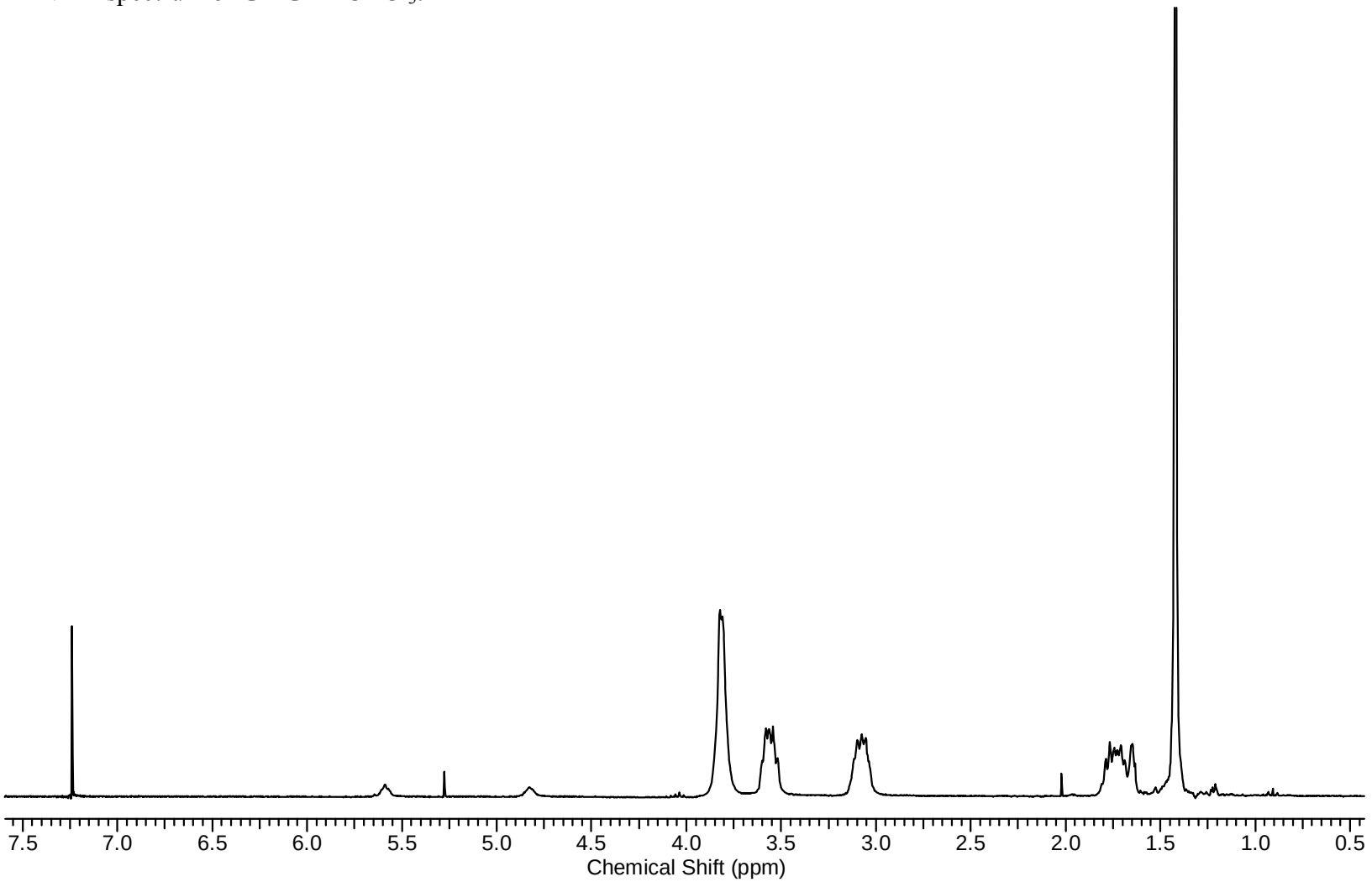

^{13}C NMR spectrum of **G1-Cl** in $CDCl_3$.

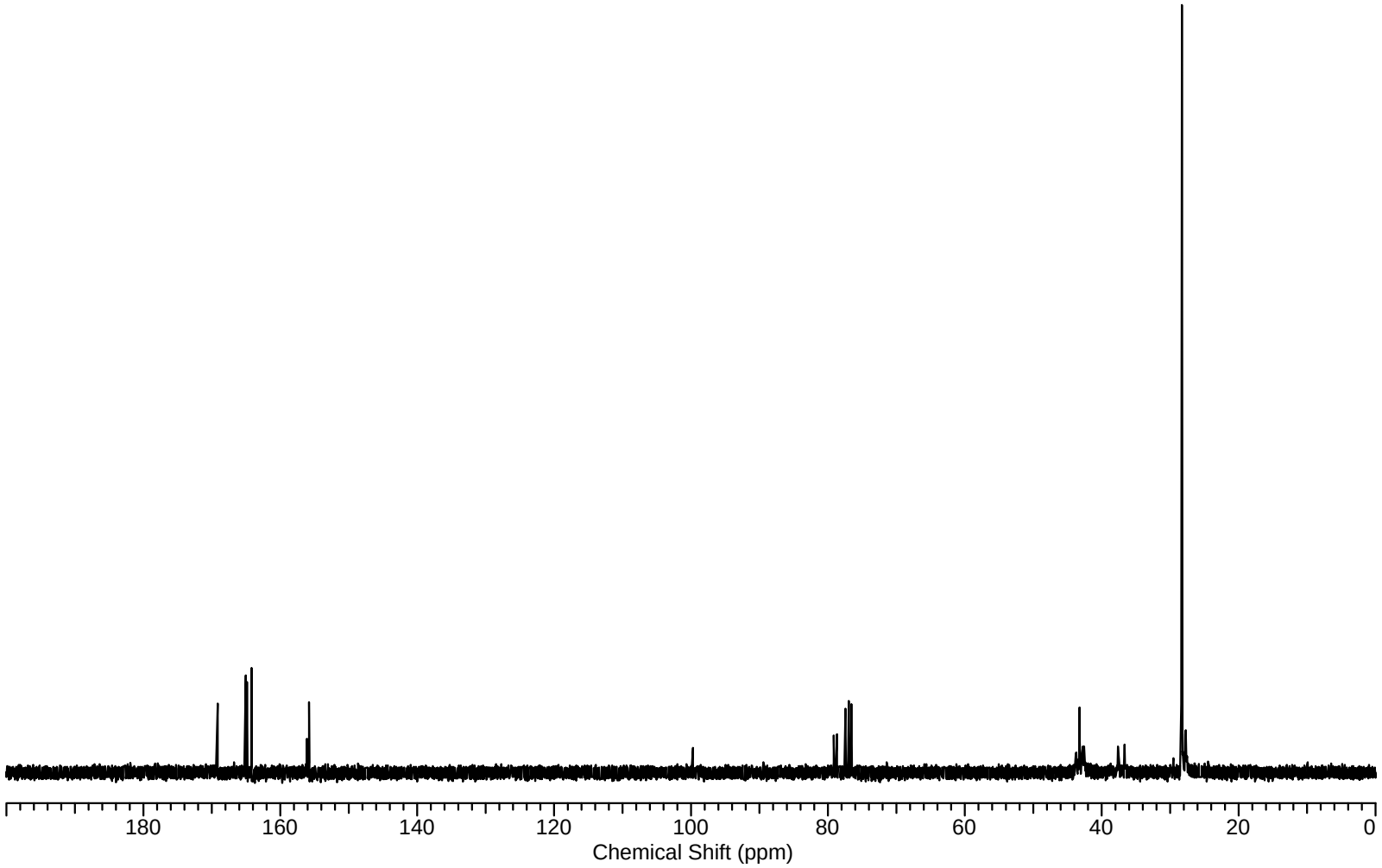

Mass spectrum (MALDI-TOF)of **G1-Cl**.

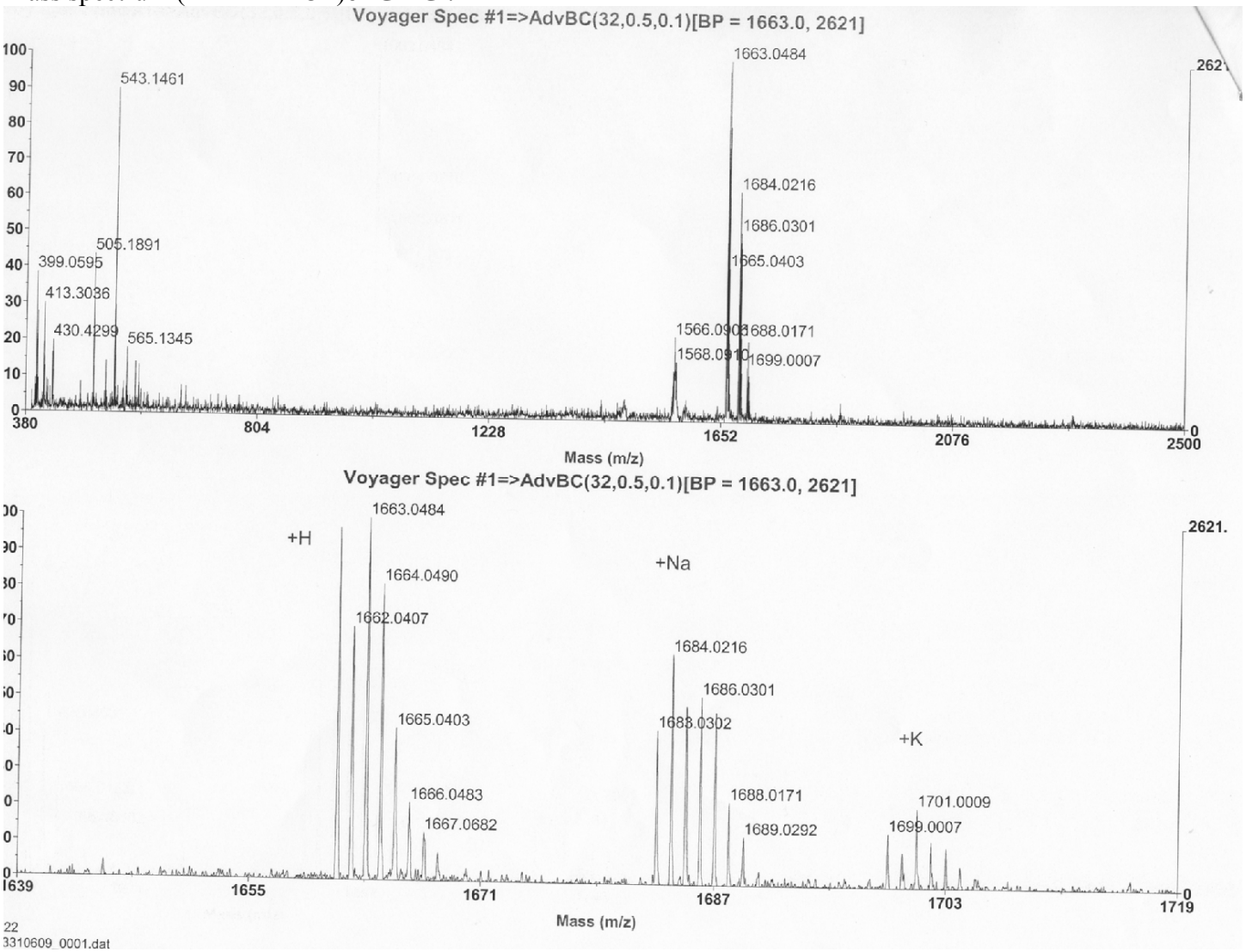

^{1}H NMR spectrum of **G1-pip** in $CDCl_3$.

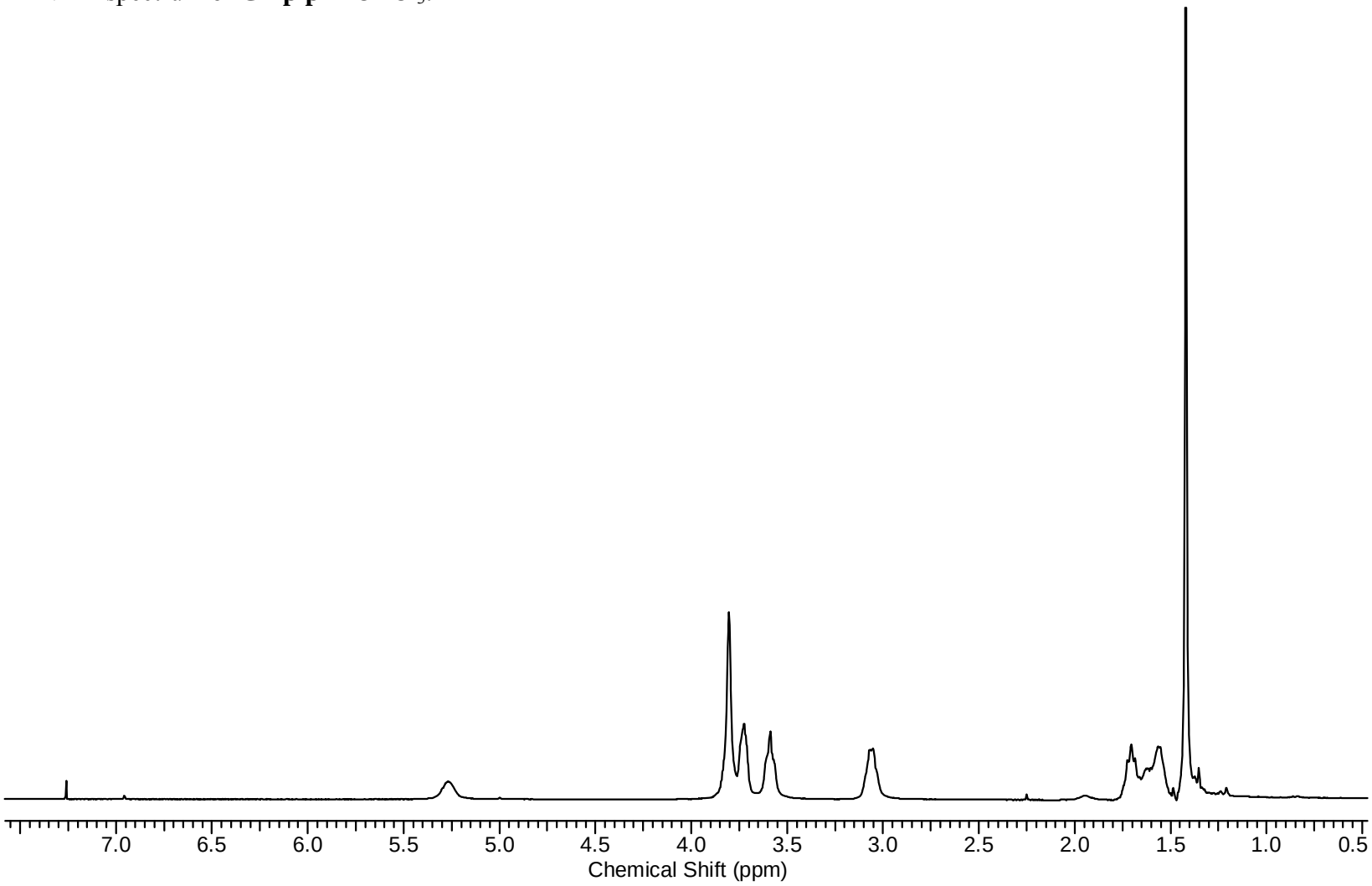

^{13}C NMR spectrum of **G1-pip** in $CDCl_3$.

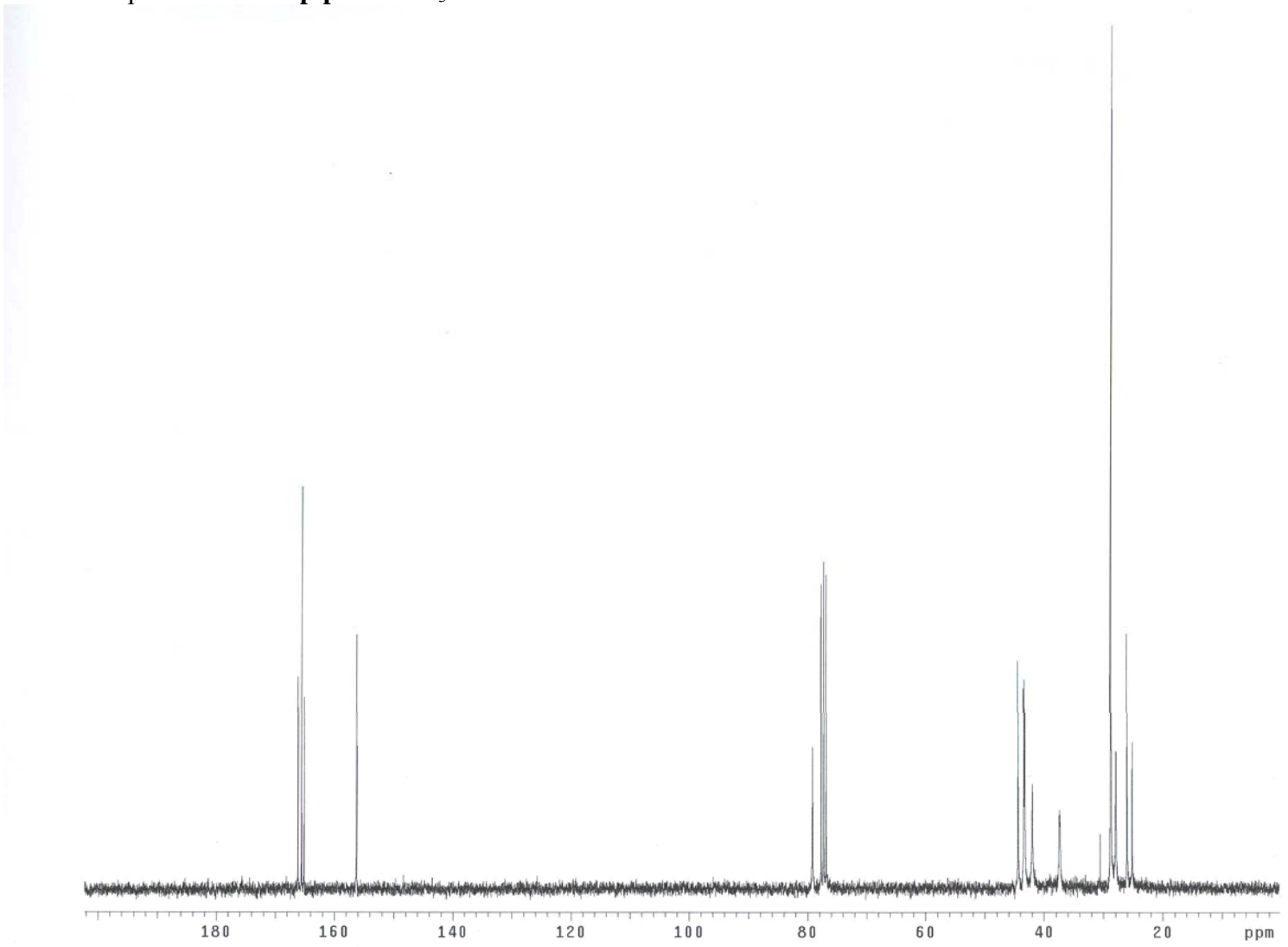

Mass spectrum (MALDI-TOF)of **G1-pip**.

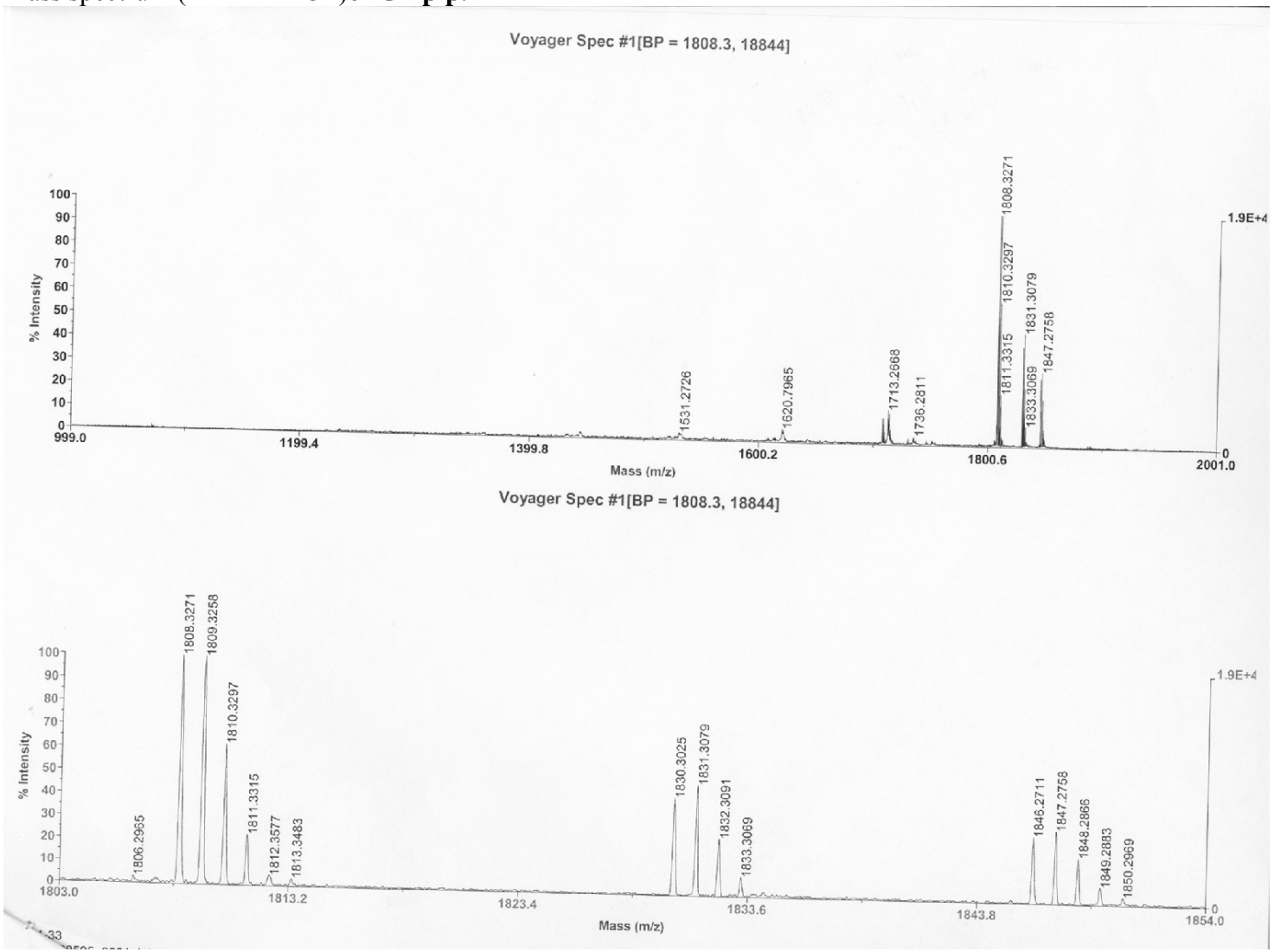

^{1}H NMR spectrum of **G1-NH$_2$** in $CDCl_3$.

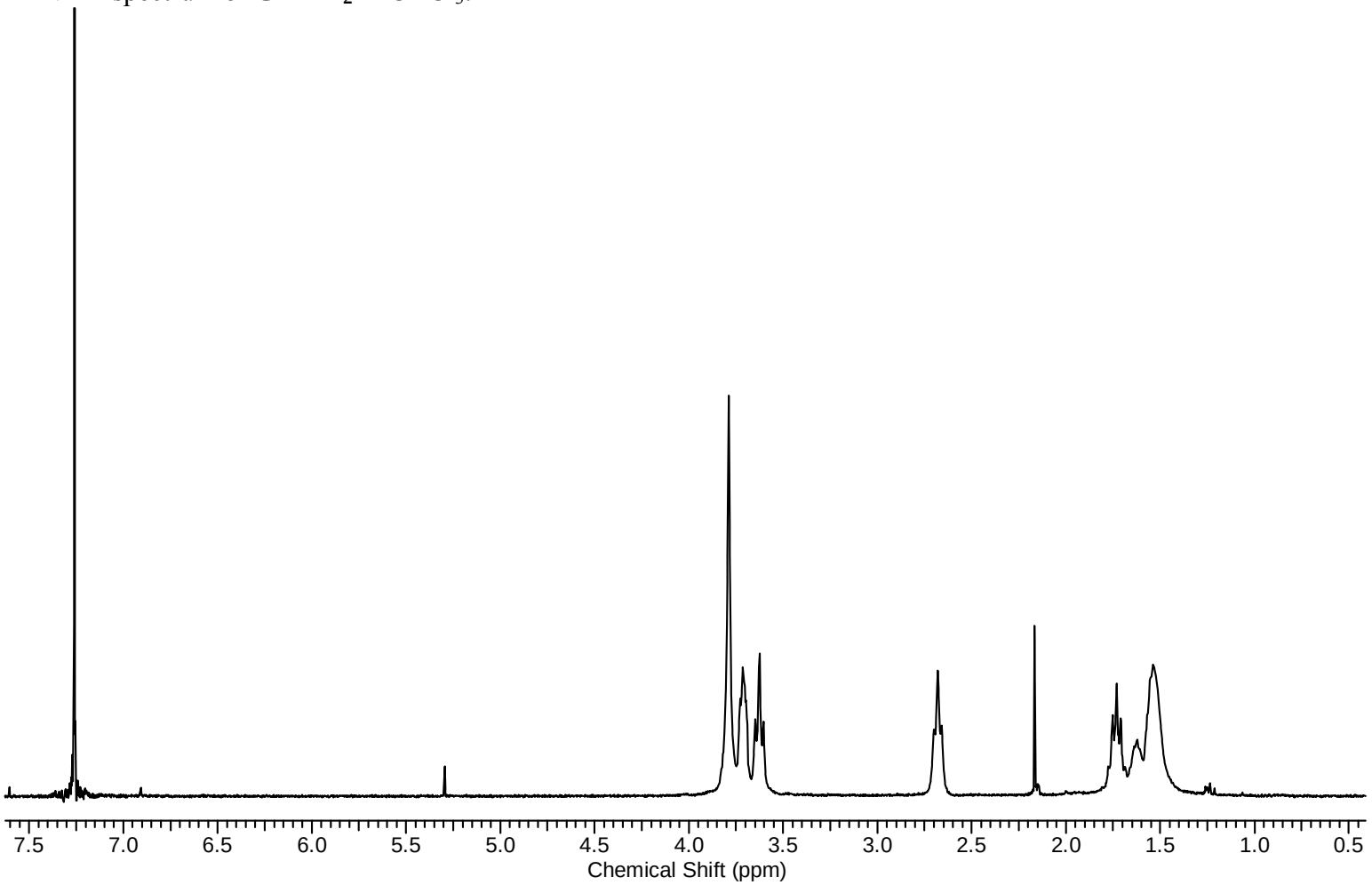

^{13}C NMR spectrum of **G1-NH_2** in $CDCl_3$.

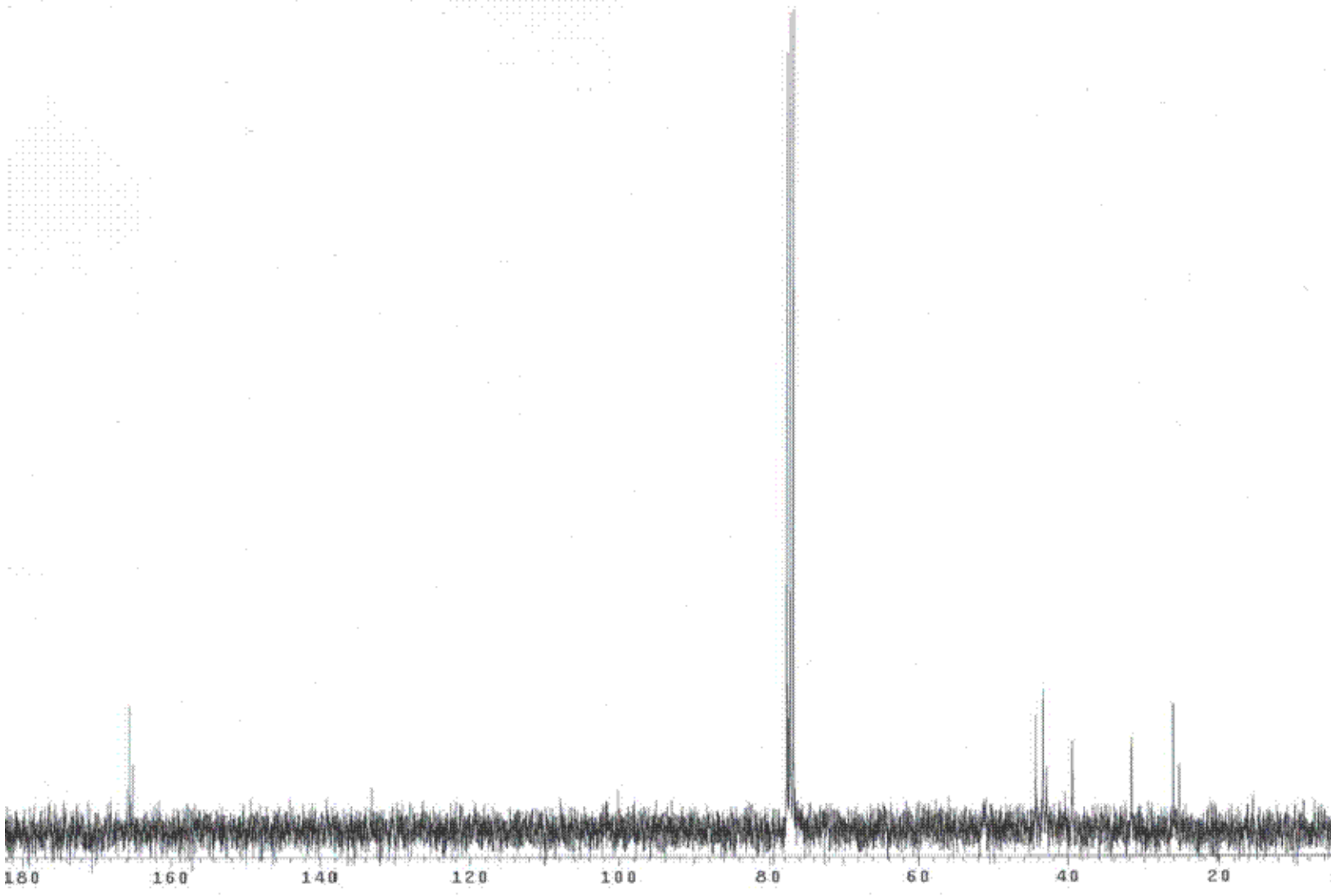

Mass spectrum (MALDI-TOF) of **G1-NH_2**.

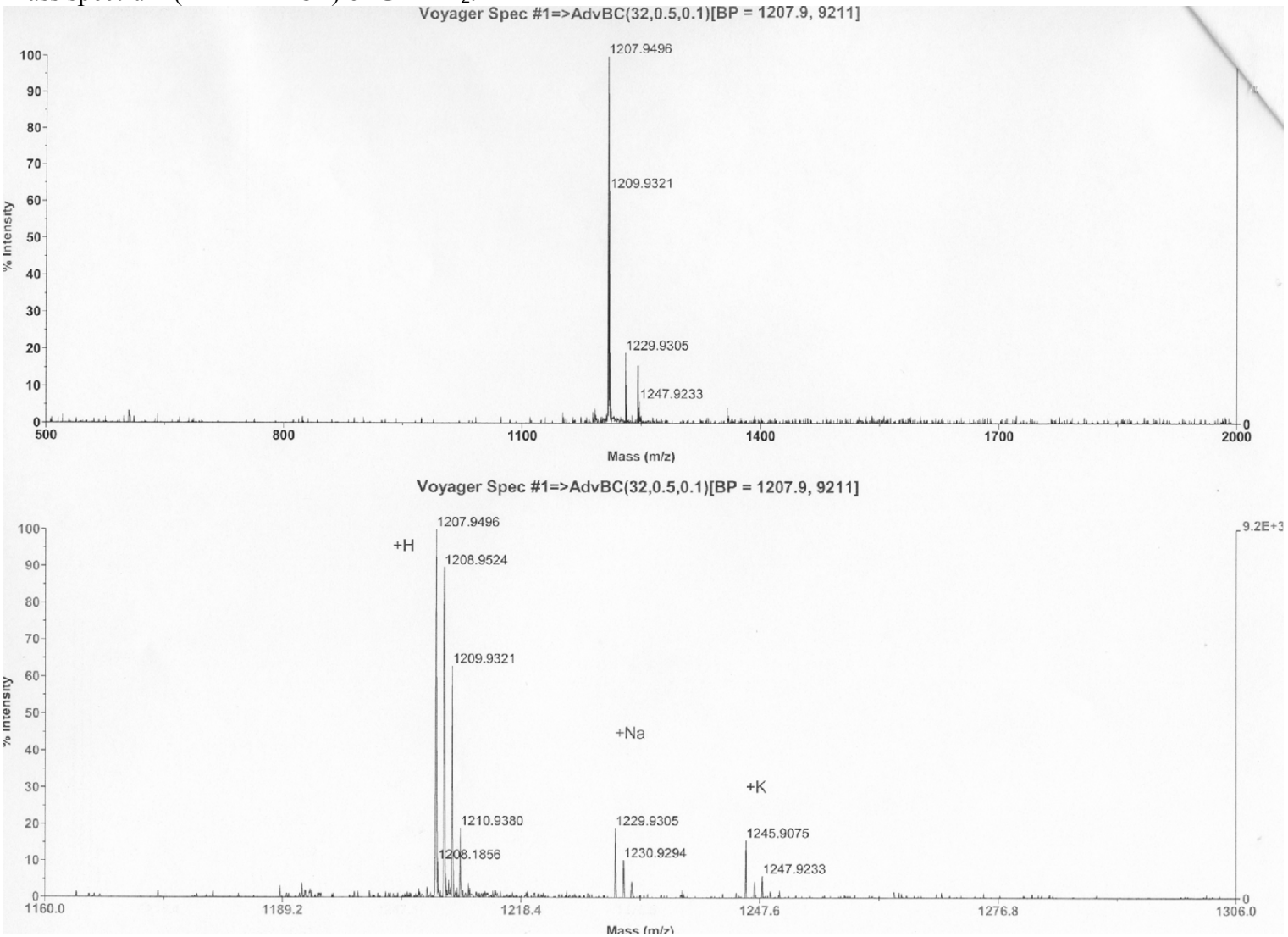

^{1}H NMR spectrum of **G2-Cl** in $CDCl_3$.

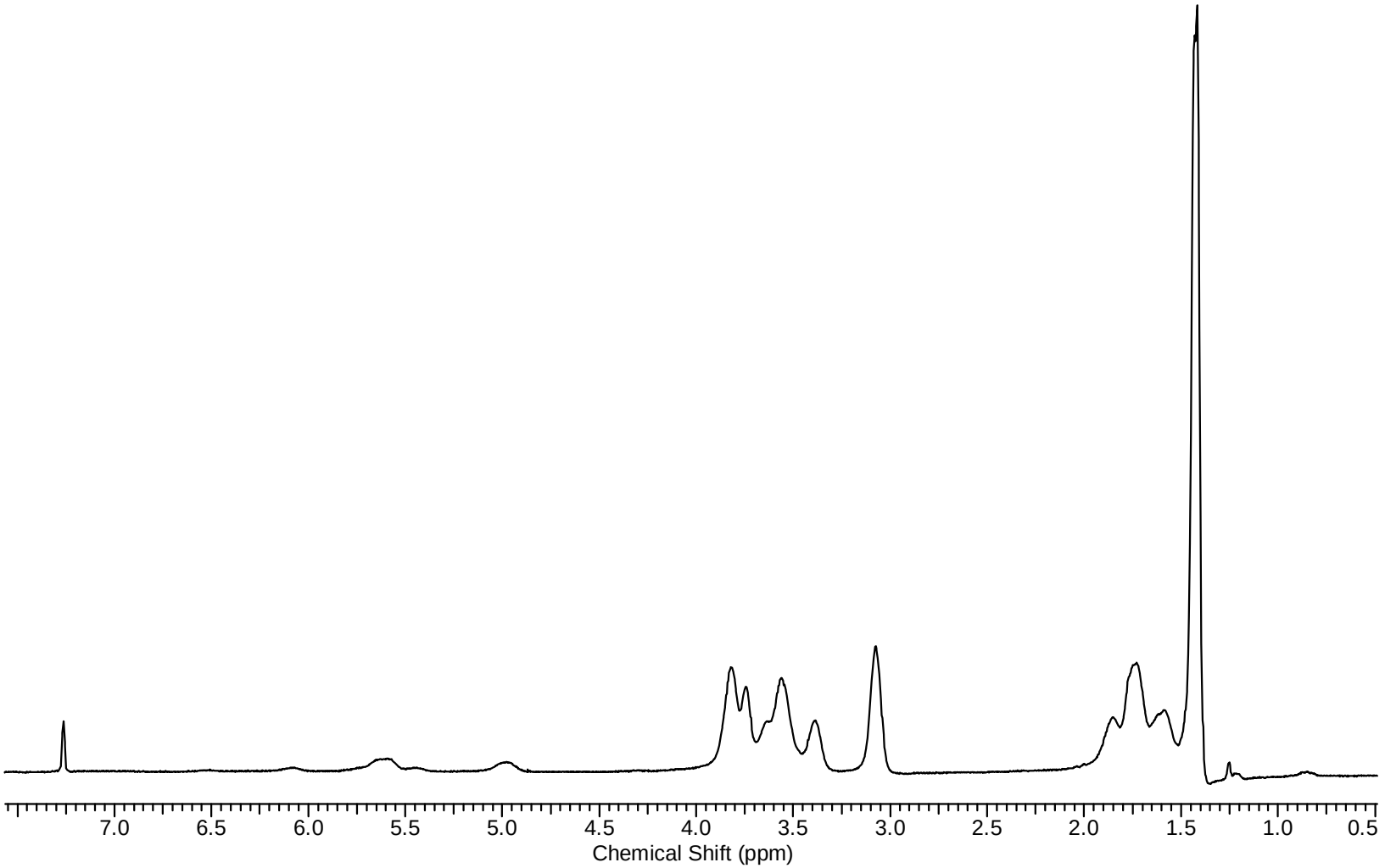

^{13}C NMR spectrum of **G2-Cl** in $CDCl_3$.

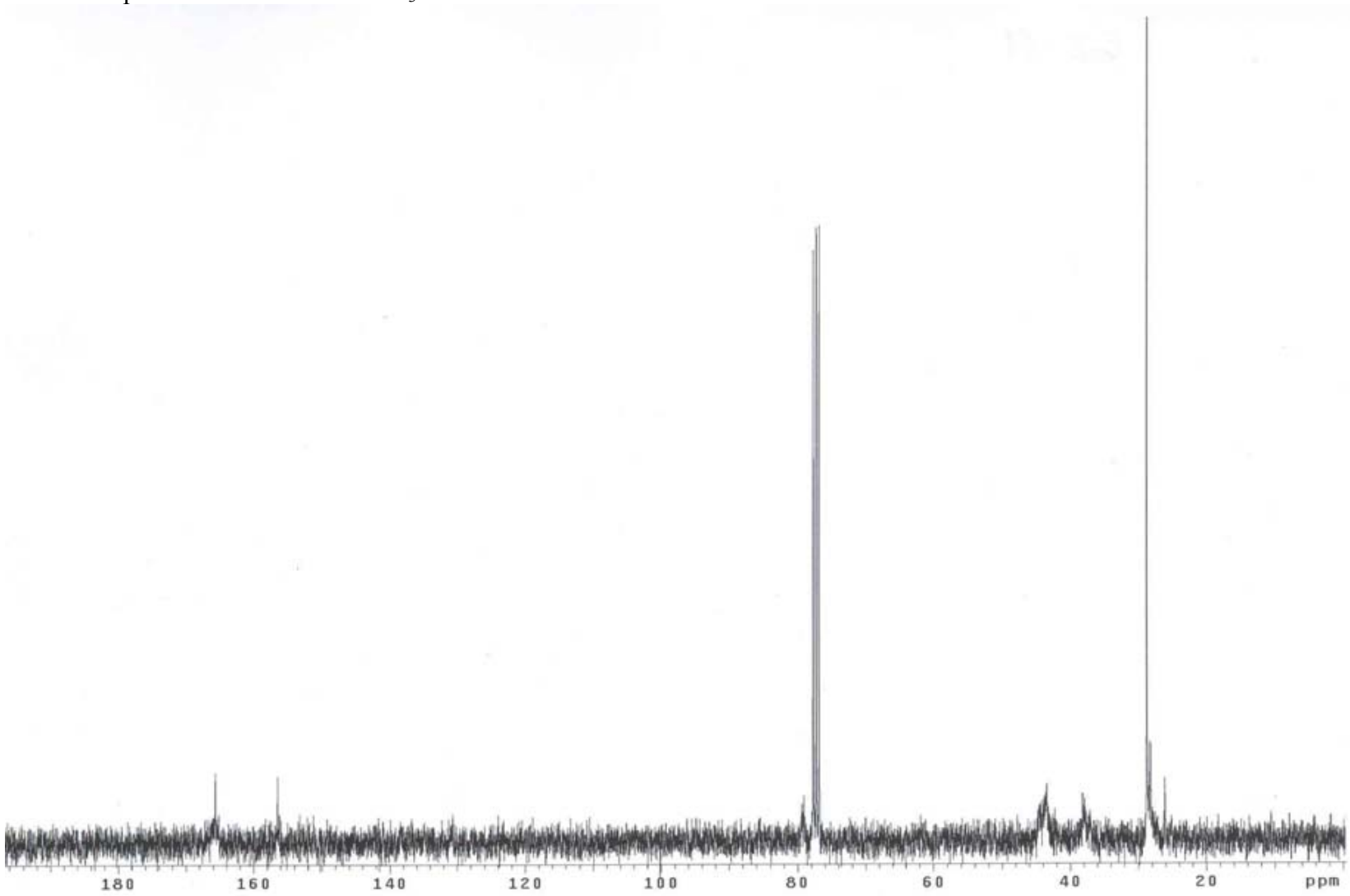

Mass spectrum (MALDI-TOF) of **G2-Cl**.

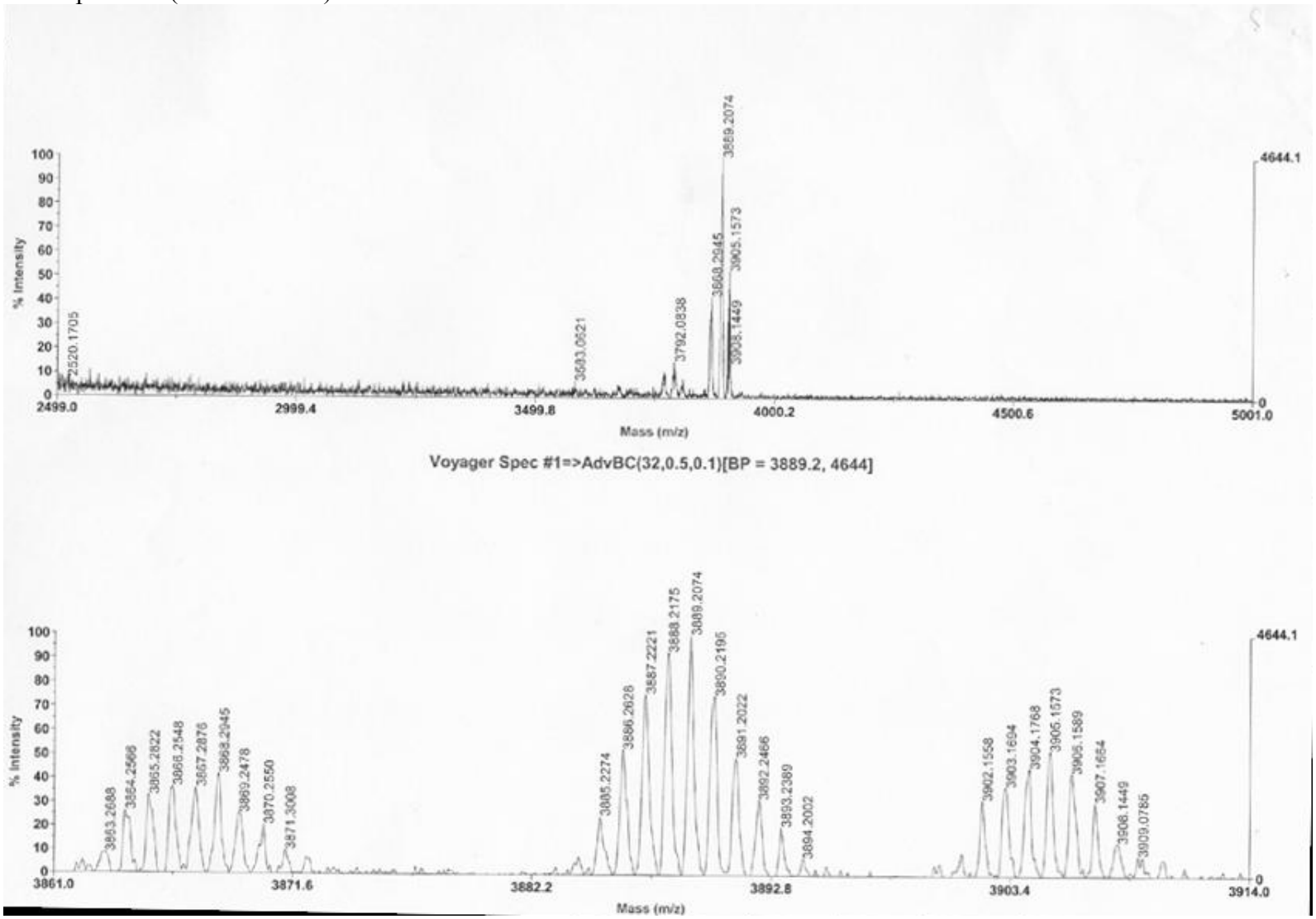

^{1}H NMR spectrum of **G2-pip** in $CDCl_3$.

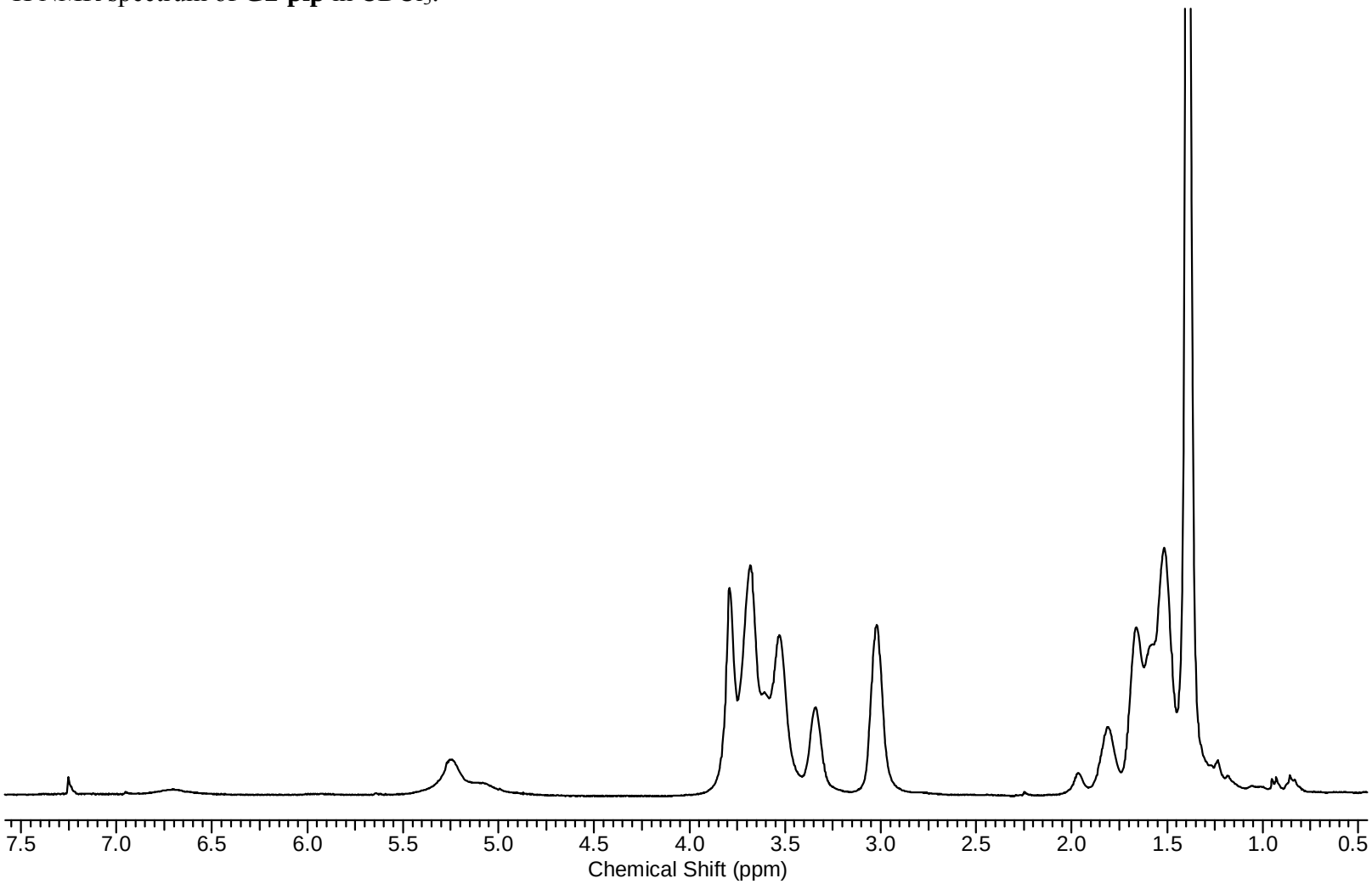

^{13}C NMR spectrum of **G2-pip** in $CDCl_3$.

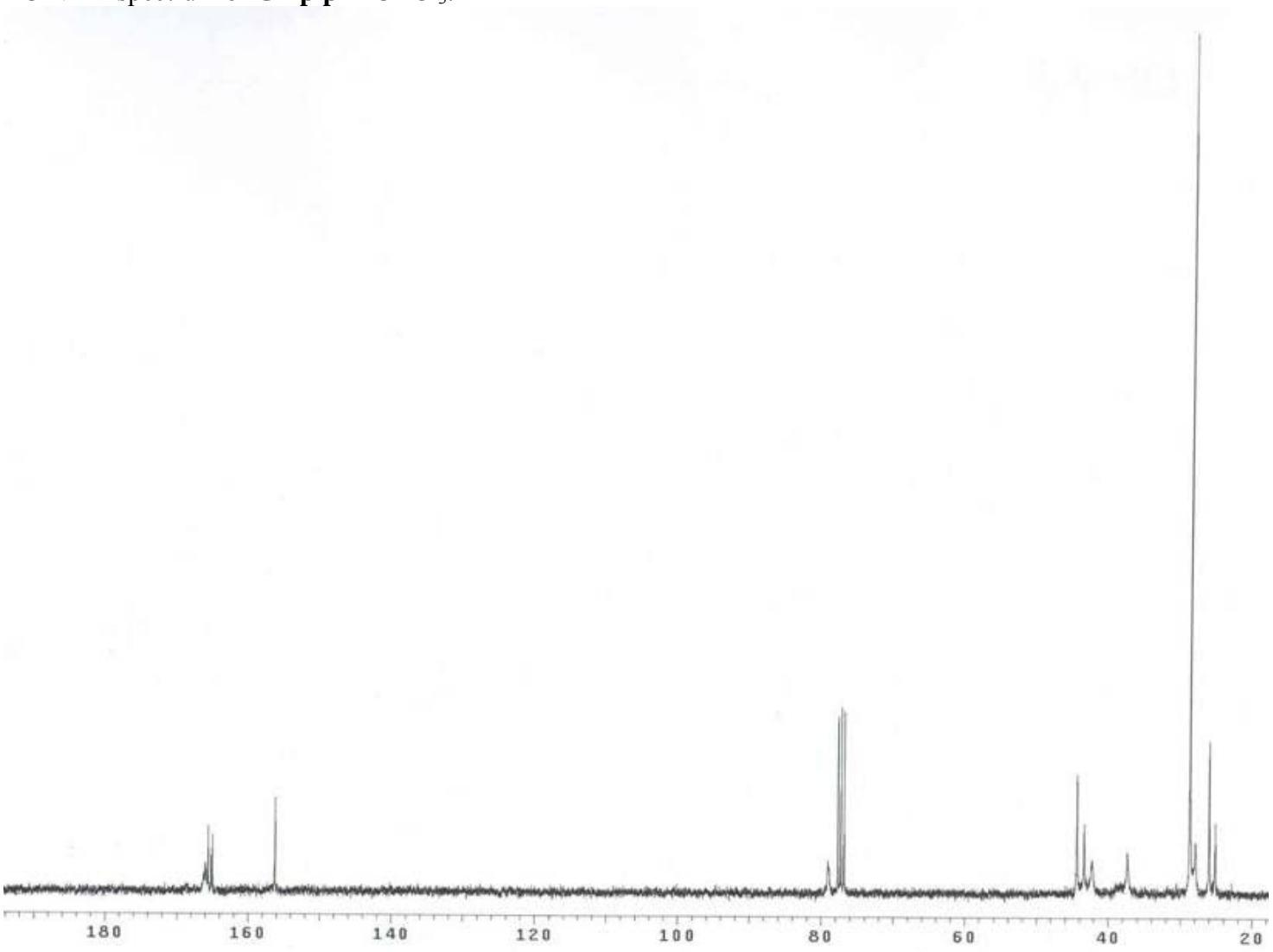

Mass spectrum (MALDI-TOF) of **G2-pip**.

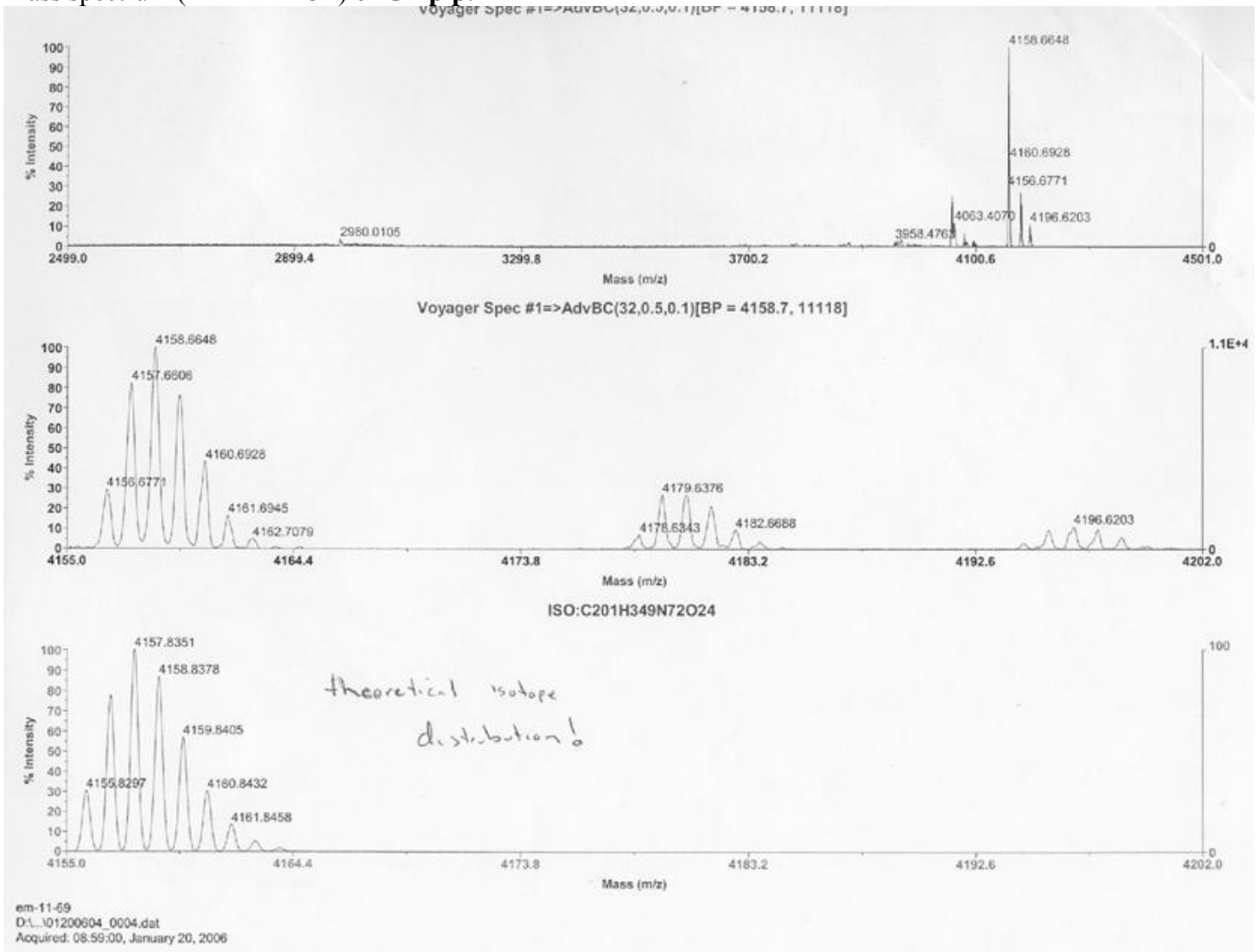

^{1}H NMR spectrum of **G2-NH$_2$** in $CDCl_3$.

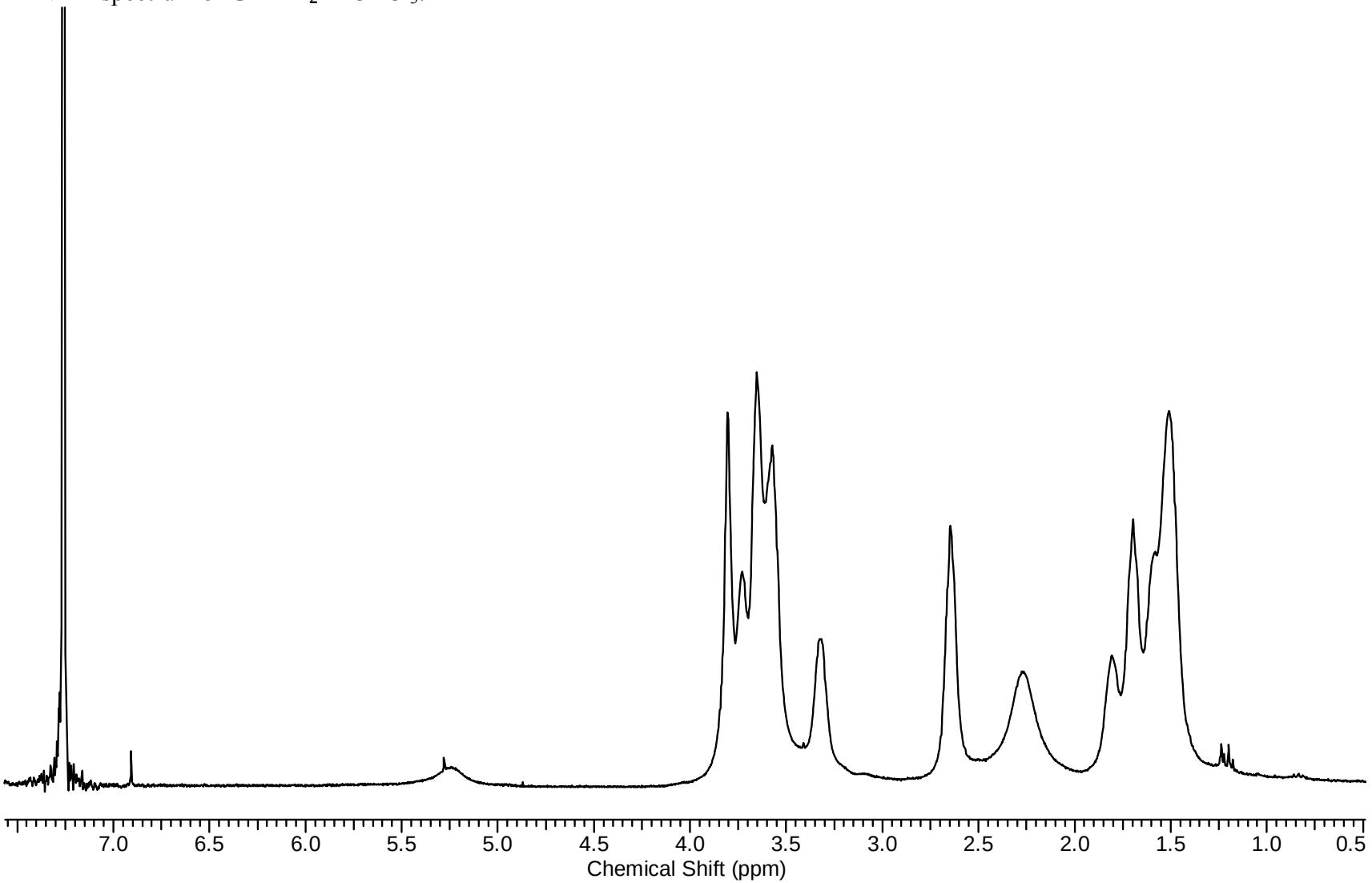

^{13}C NMR spectrum of **G2-NH_2** in $CDCl_3$.

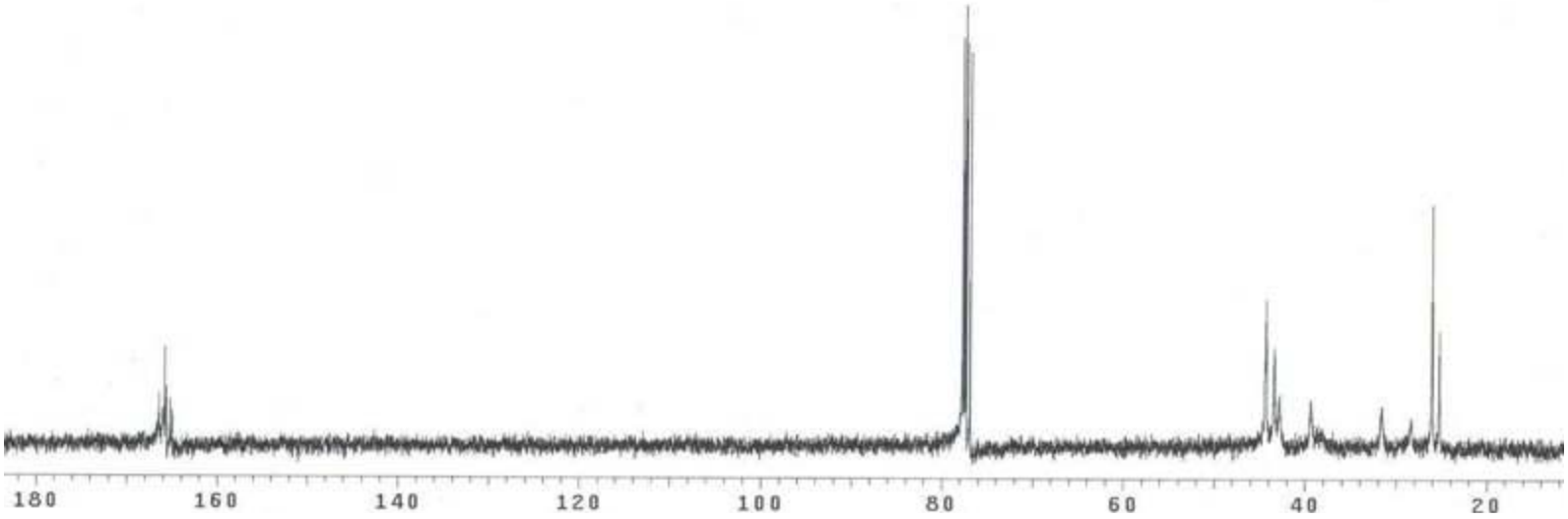

Mass spectrum (MALDI-TOF) of **G2-NH$_2$**.

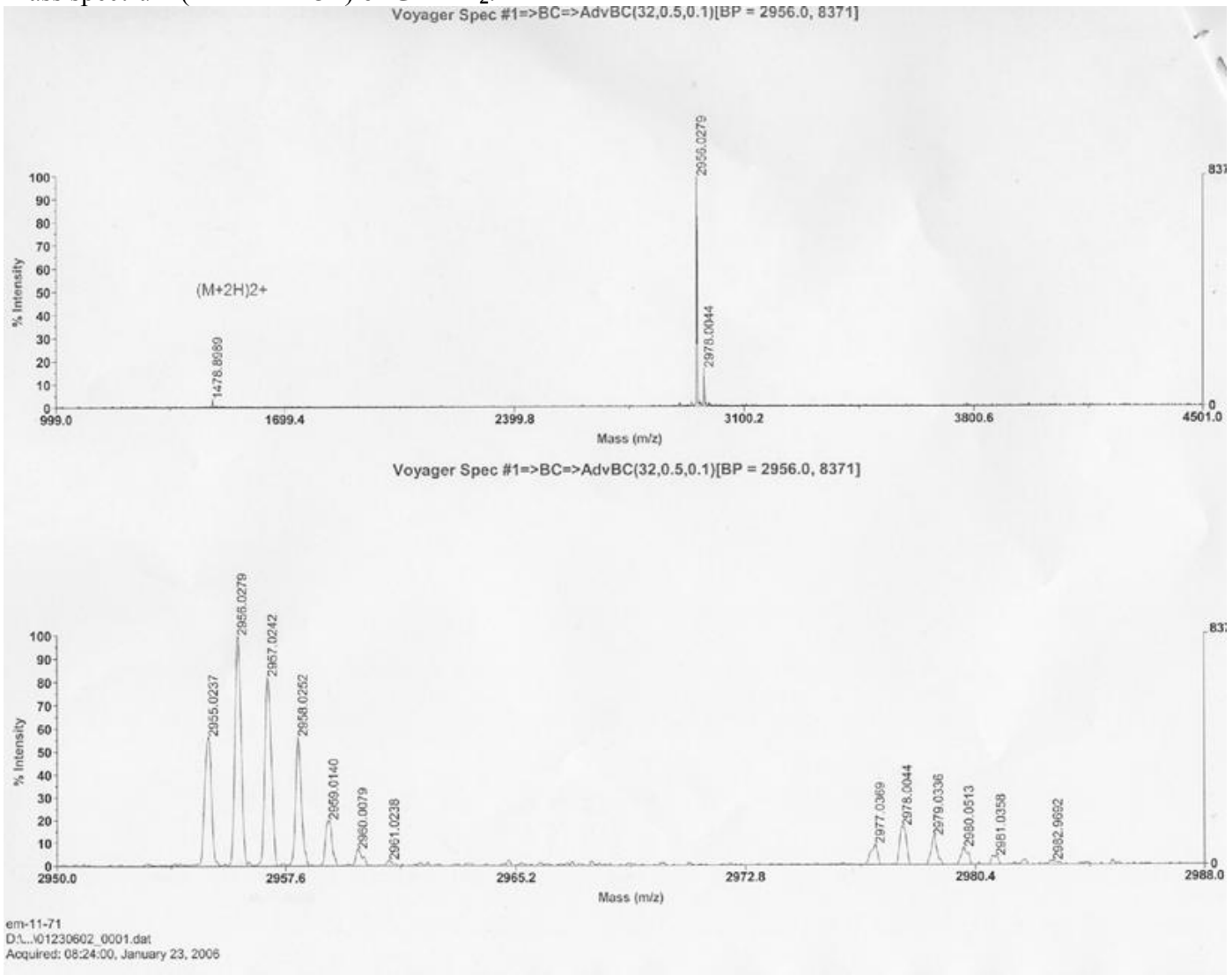

^{1}H NMR spectrum of **G3-Cl** in $CDCl_3$.

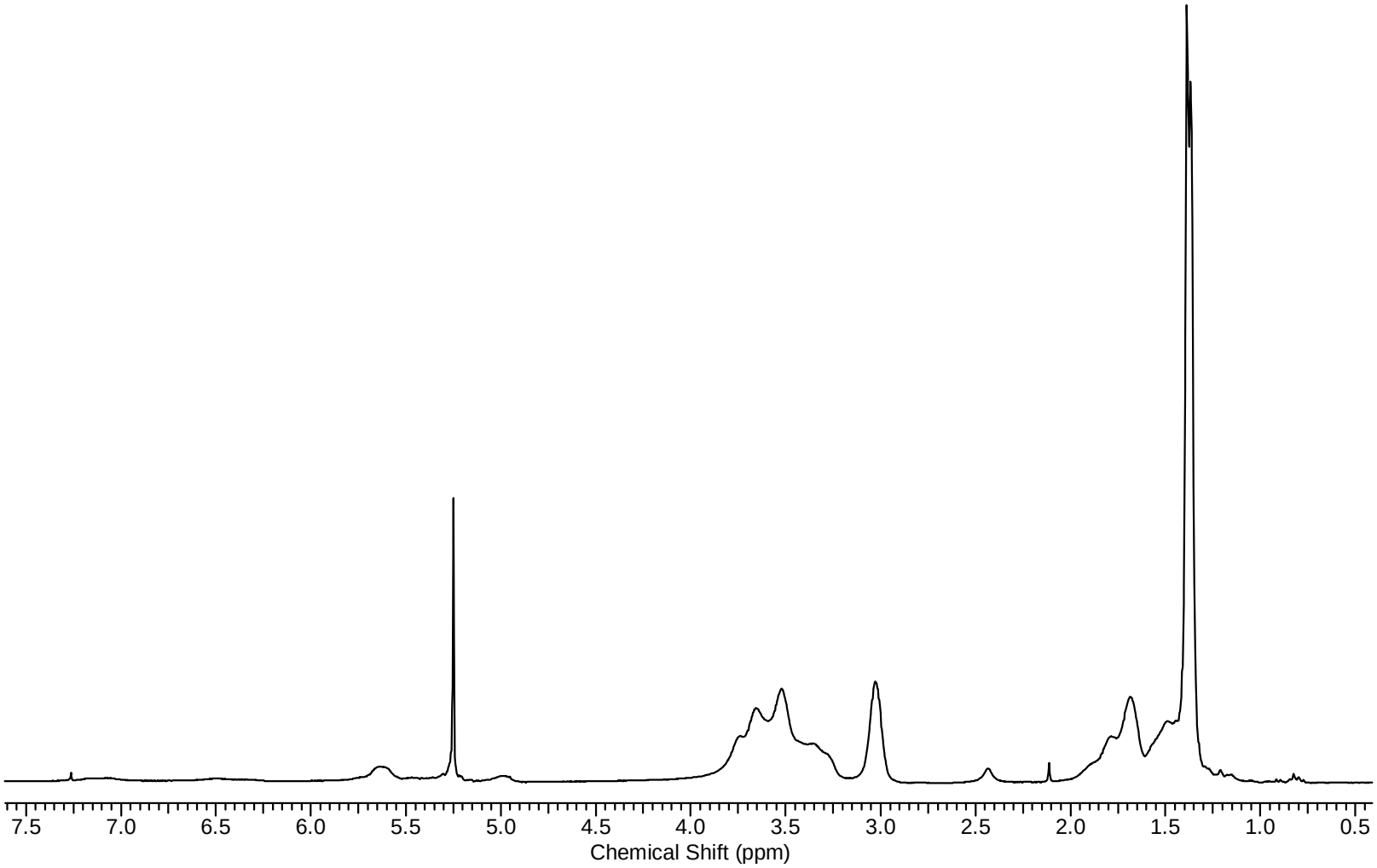

^{13}C NMR spectrum of **G3-Cl** in $CDCl_3$.

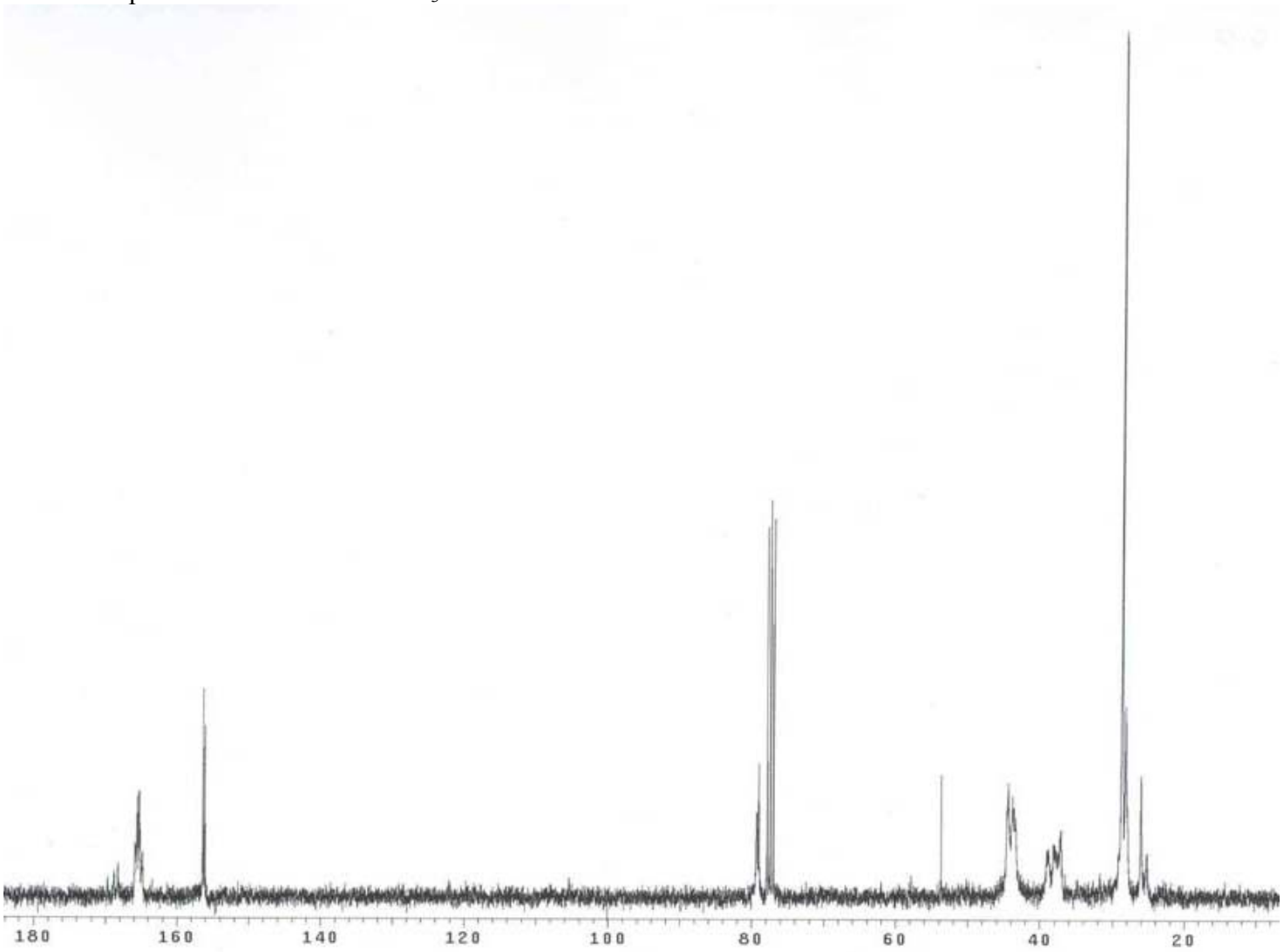

Mass spectrum (MALDI-TOF) of **G3-Cl.**

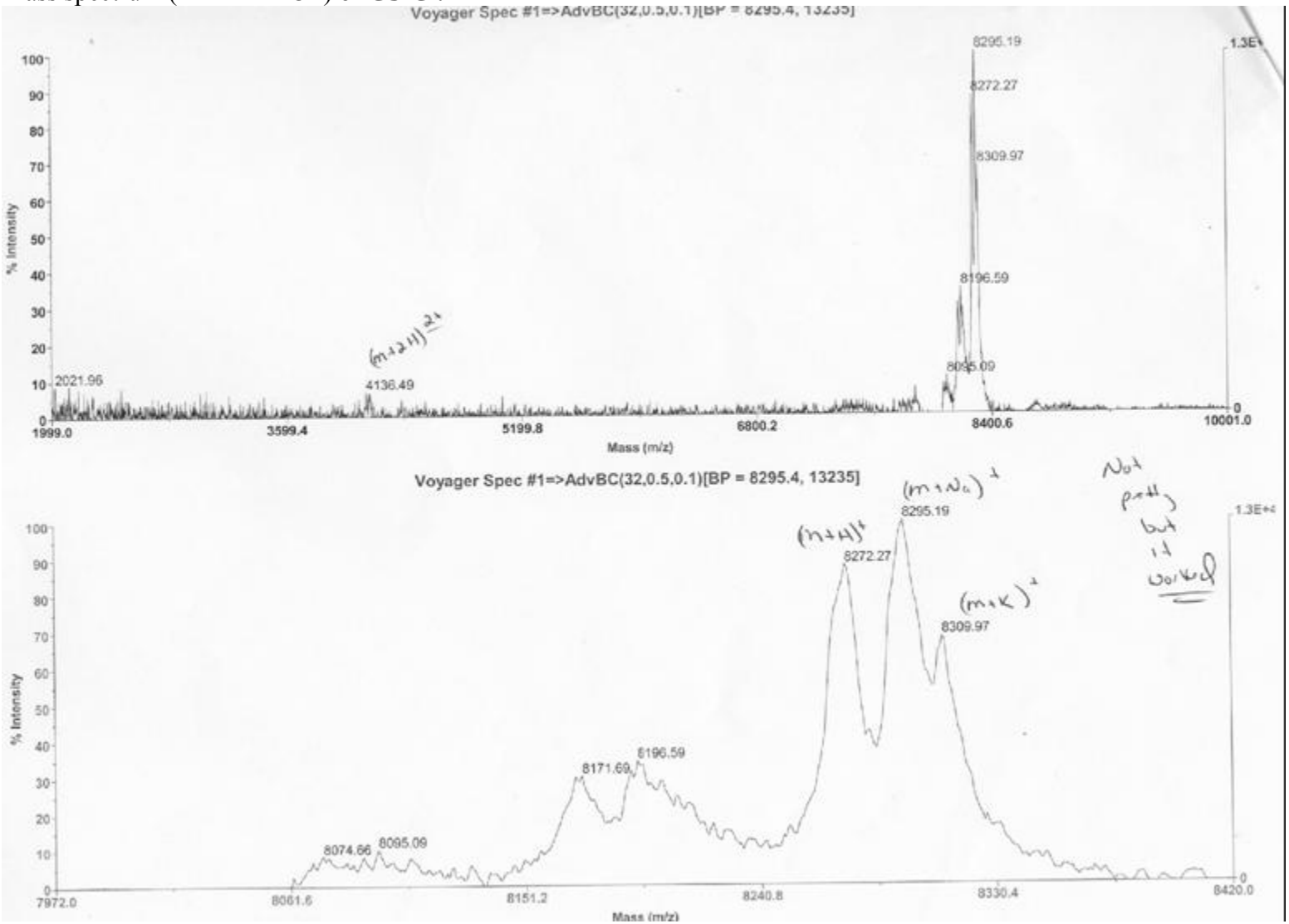

^{1}H NMR spectrum of **G3-pip** in $CDCl_3$.

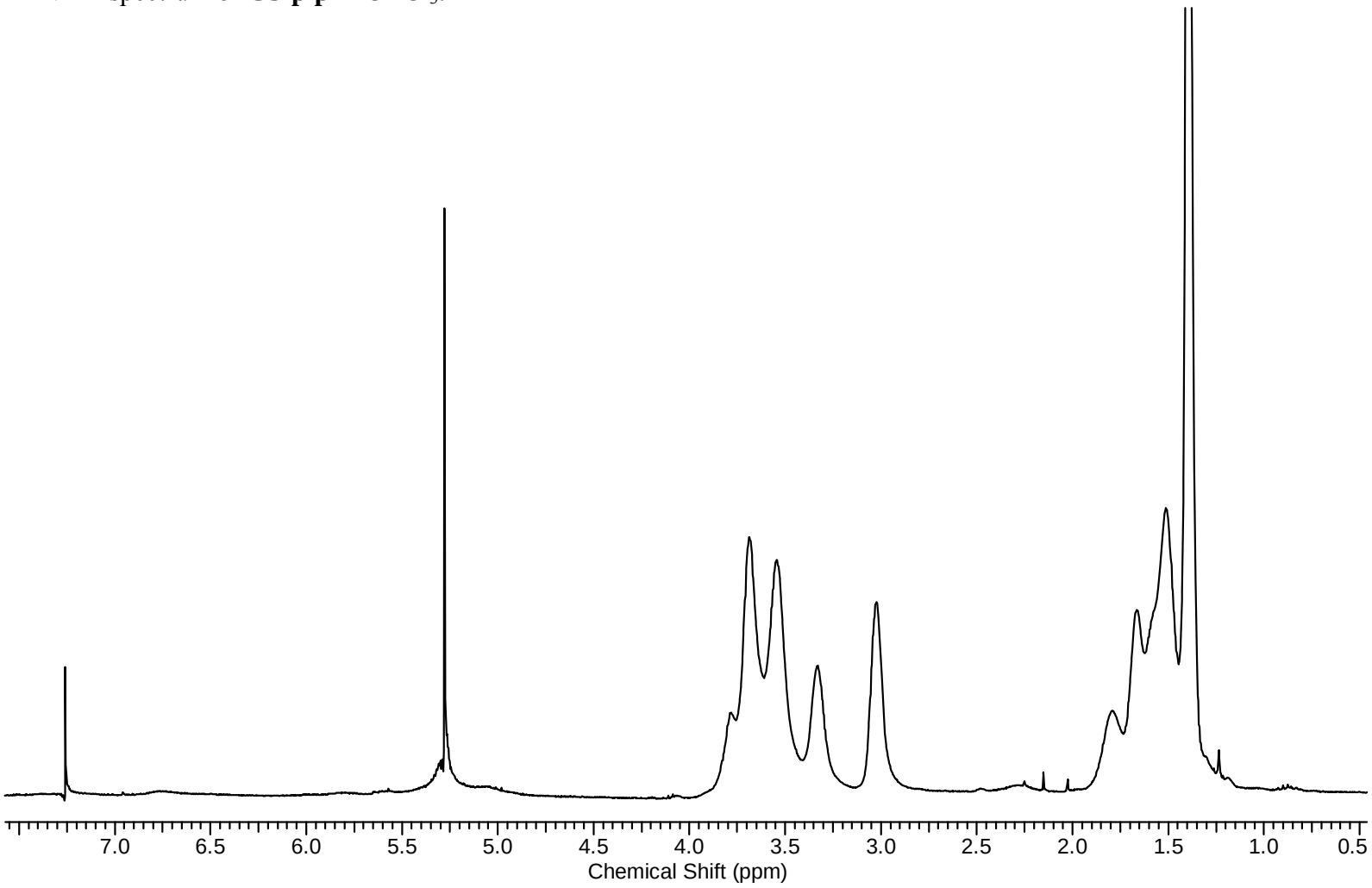

^{13}C NMR spectrum of **G3-pip** in $CDCl_3$.

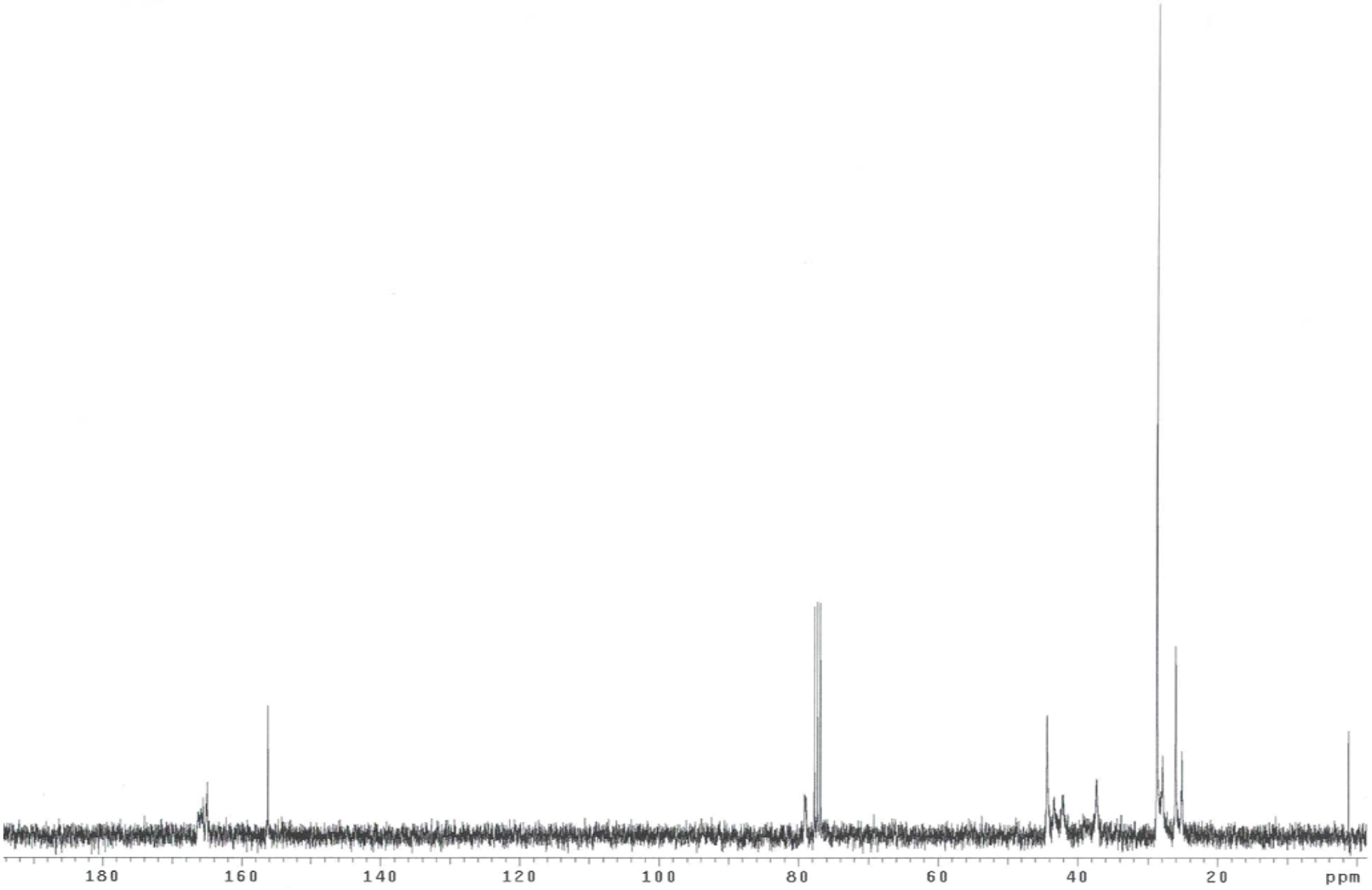

Mass spectrum (MALDI-TOF) of **G3-pip**.

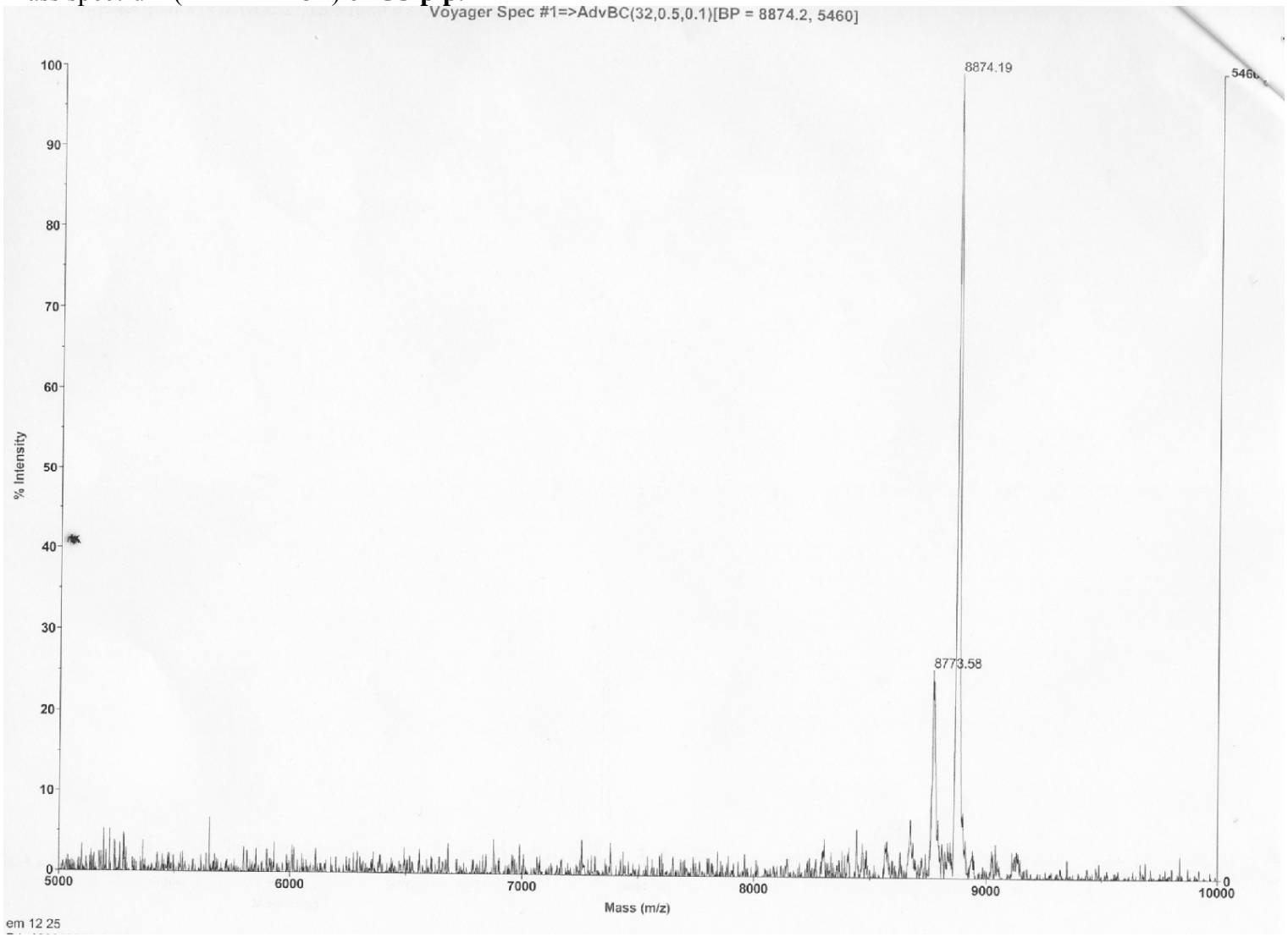

^{1}H NMR spectrum of **G3-NH$_2$** in $CDCl_3$.

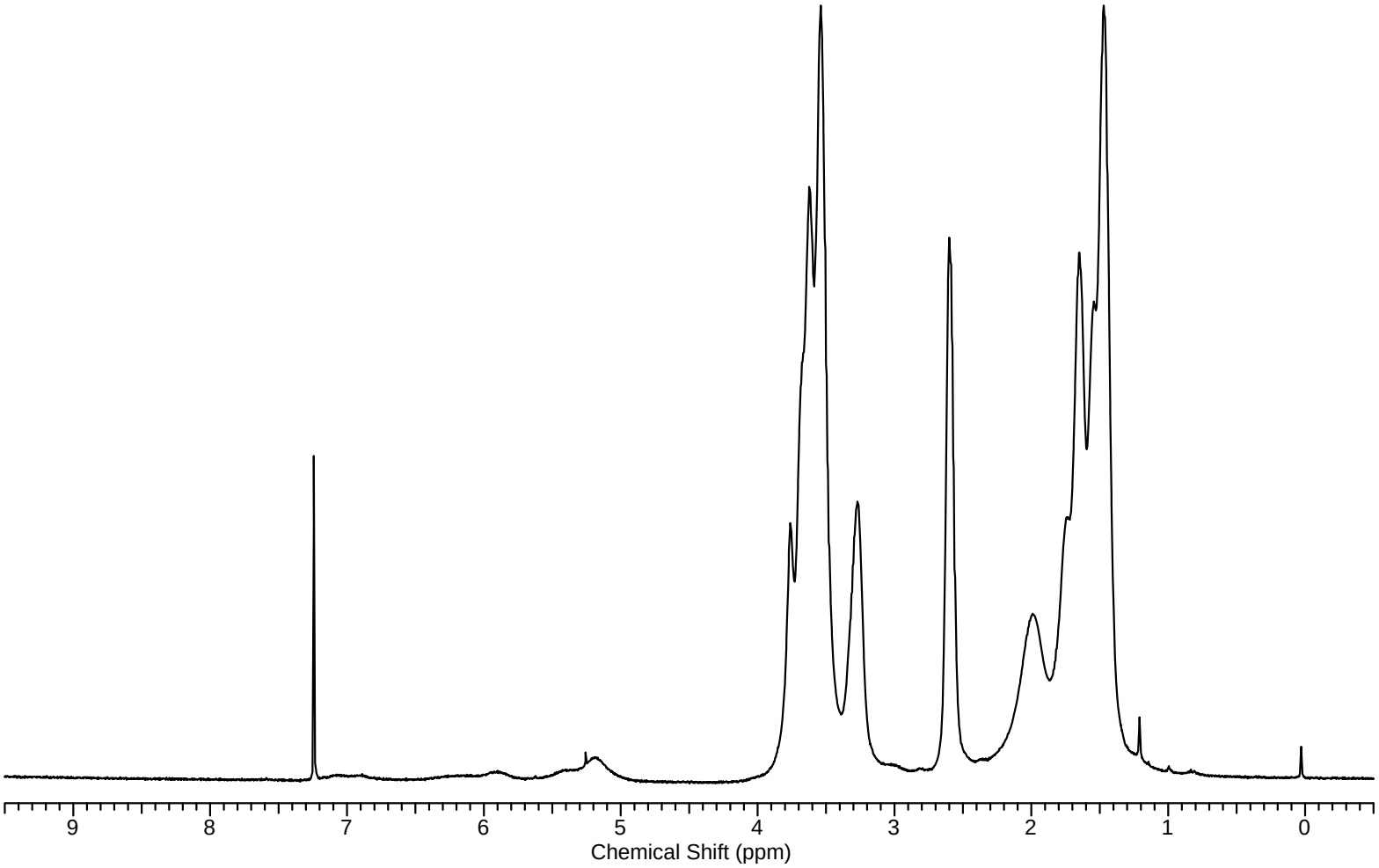

^{13}C NMR spectrum of **G3-NH_2** in $CDCl_3$.

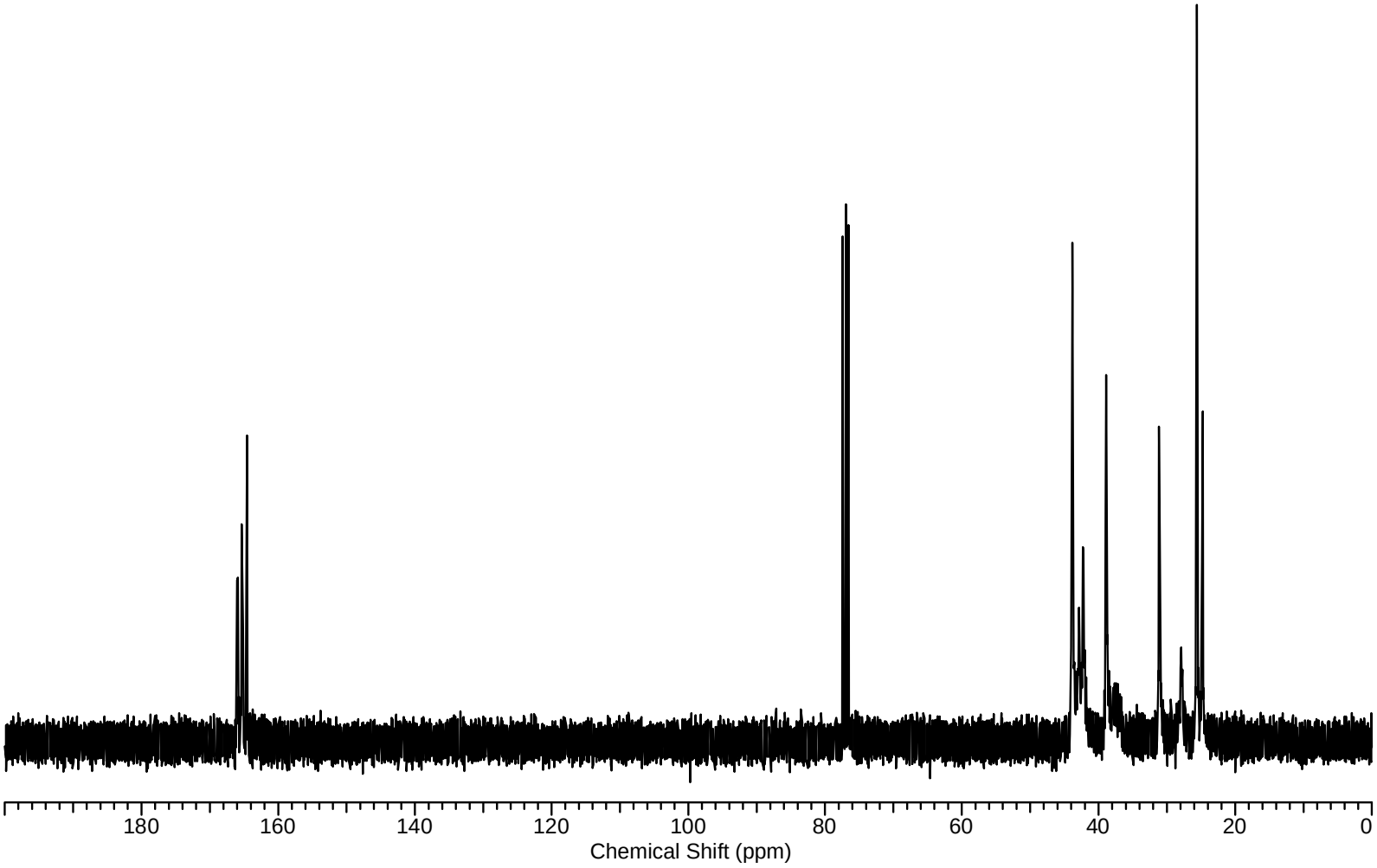

Mass spectrum (MALDI-TOF) of **G3-NH_2**.

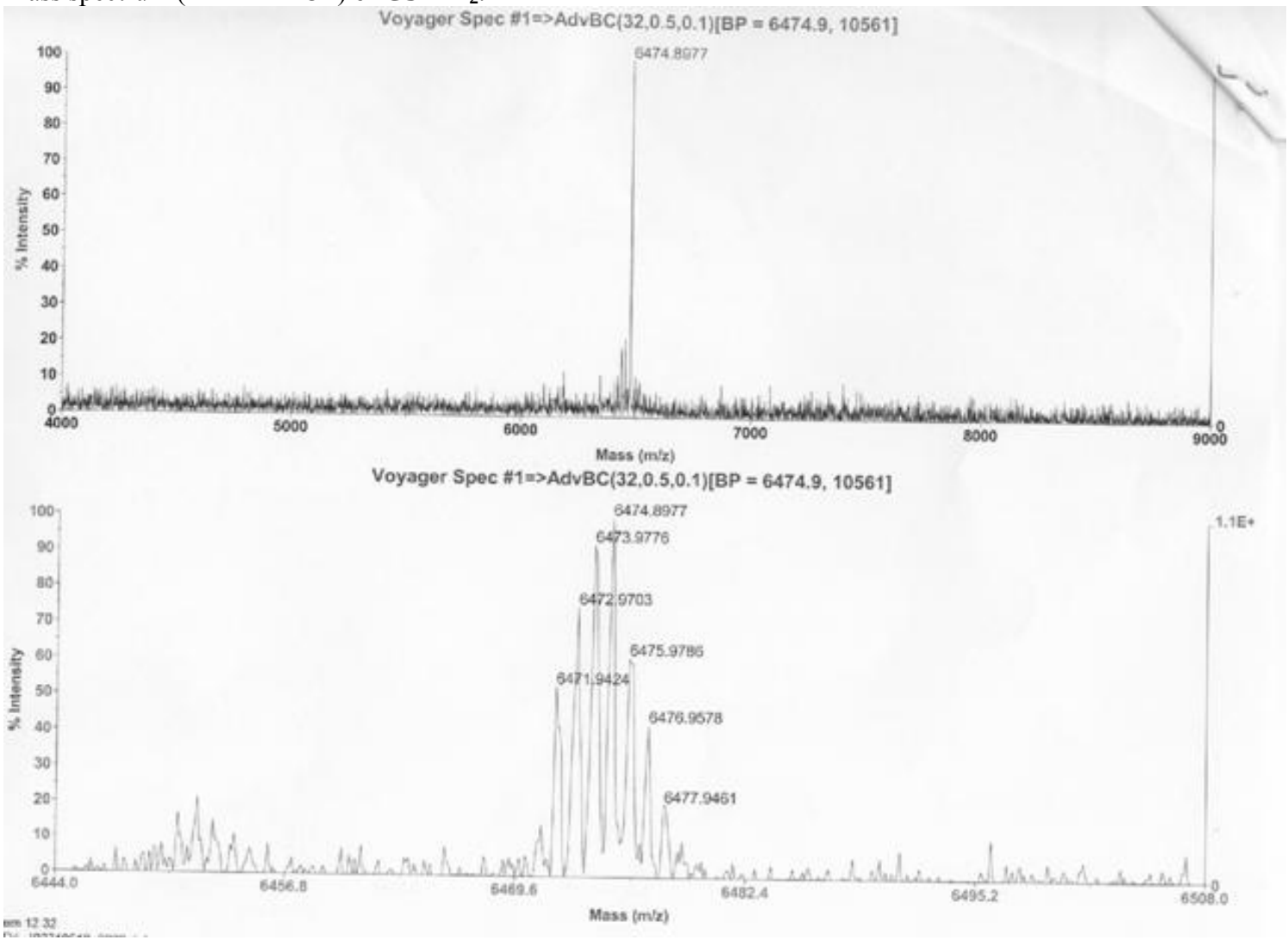

^{1}H NMR spectrum of **G4-Cl** in $CDCl_3$.

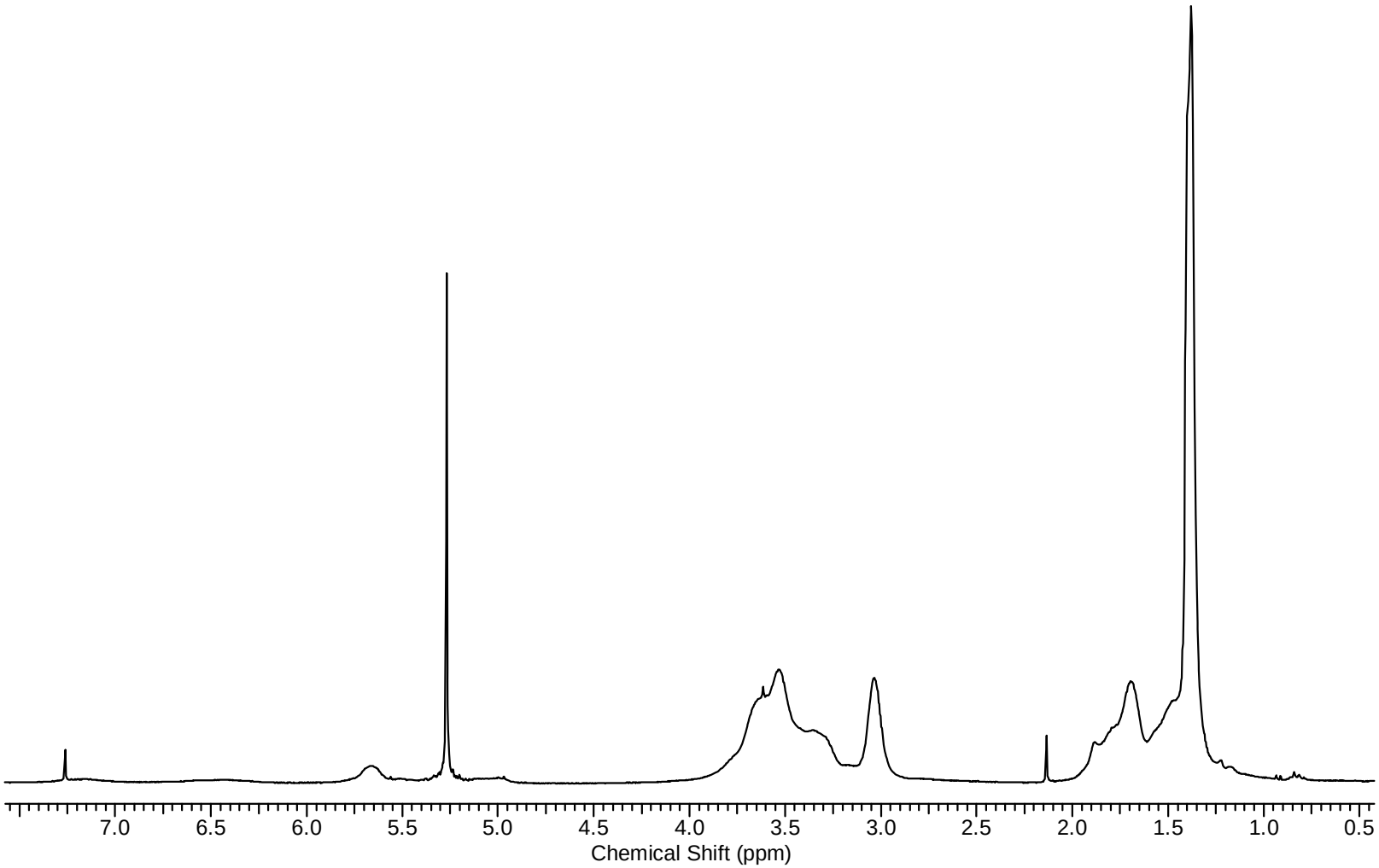

^{13}C NMR spectrum of **G4-Cl** in $CDCl_3$.

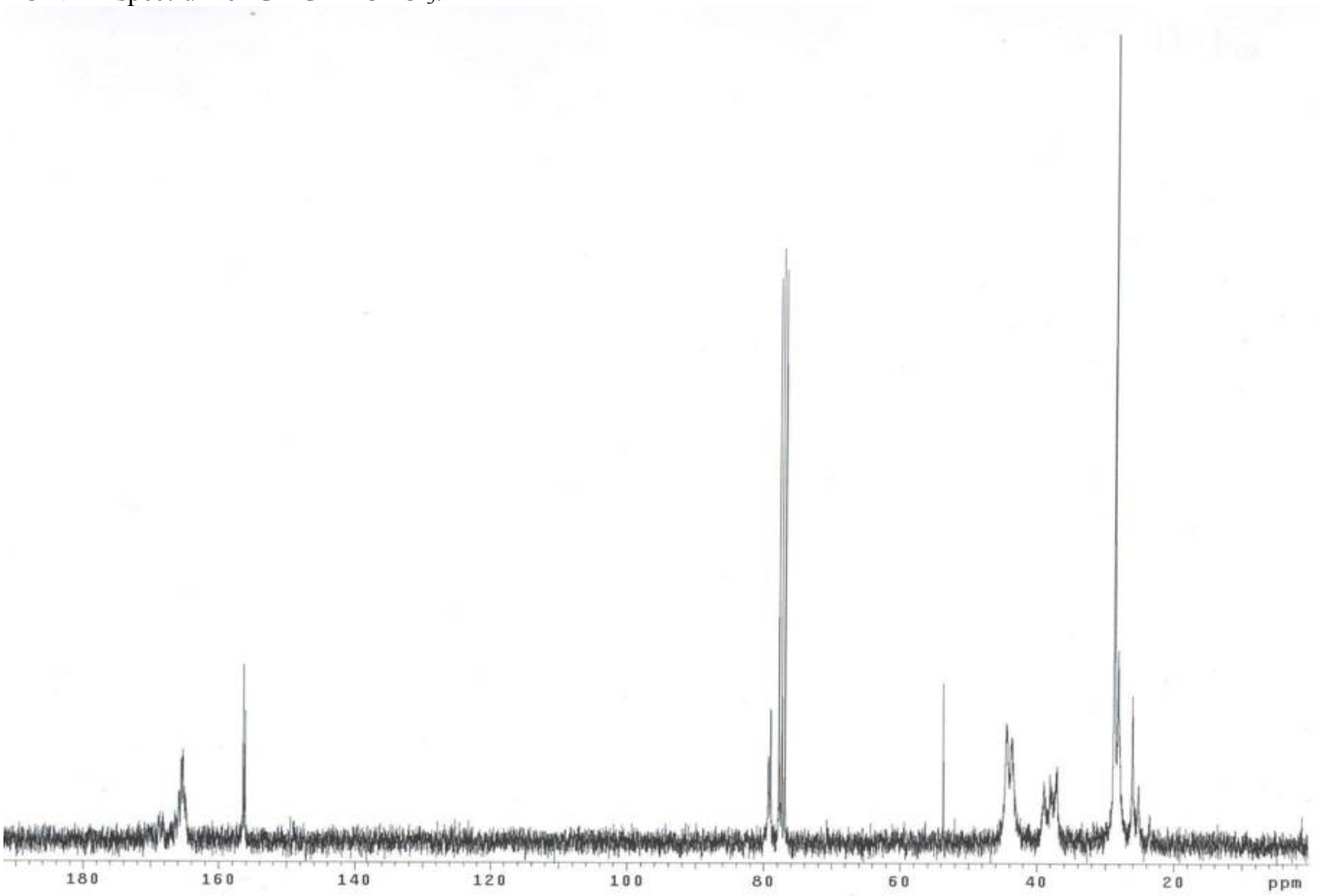

Mass spectrum (MALDI-TOF) of **G4-Cl**.

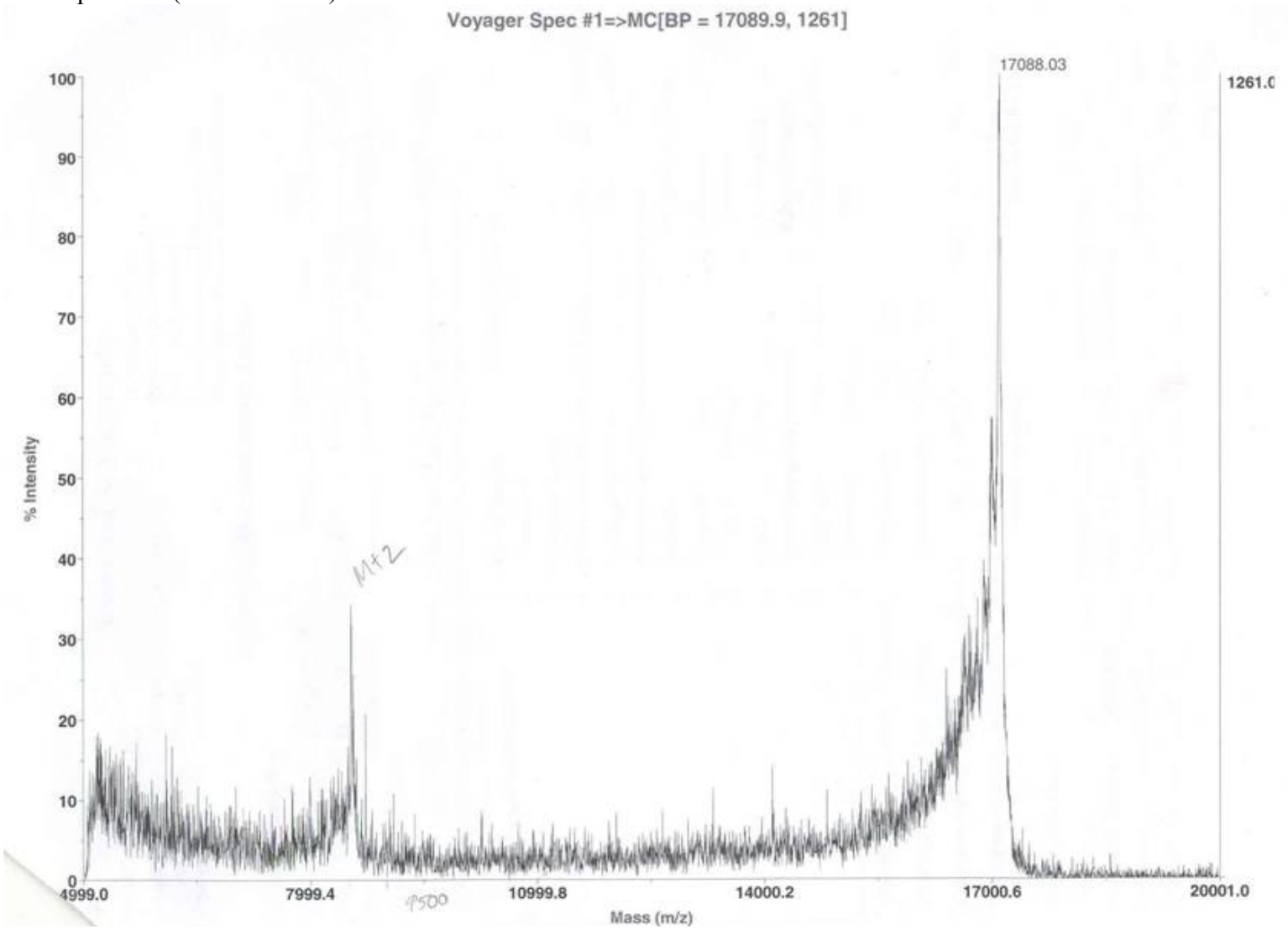

^{1}H NMR spectrum of **G4-pip** in $CDCl_3$.

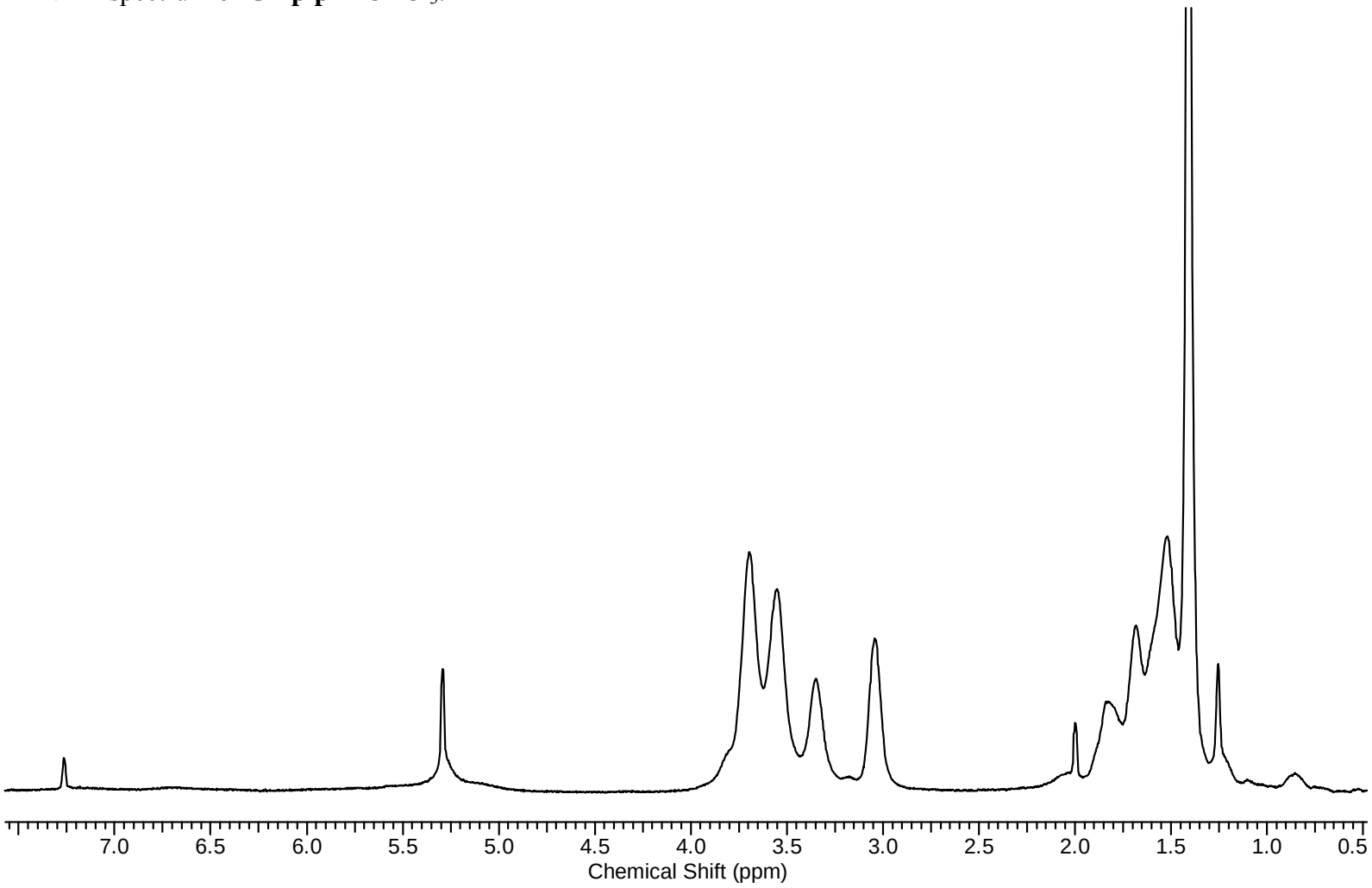

^{13}C NMR spectrum of **G4-pip** in $CDCl_3$.

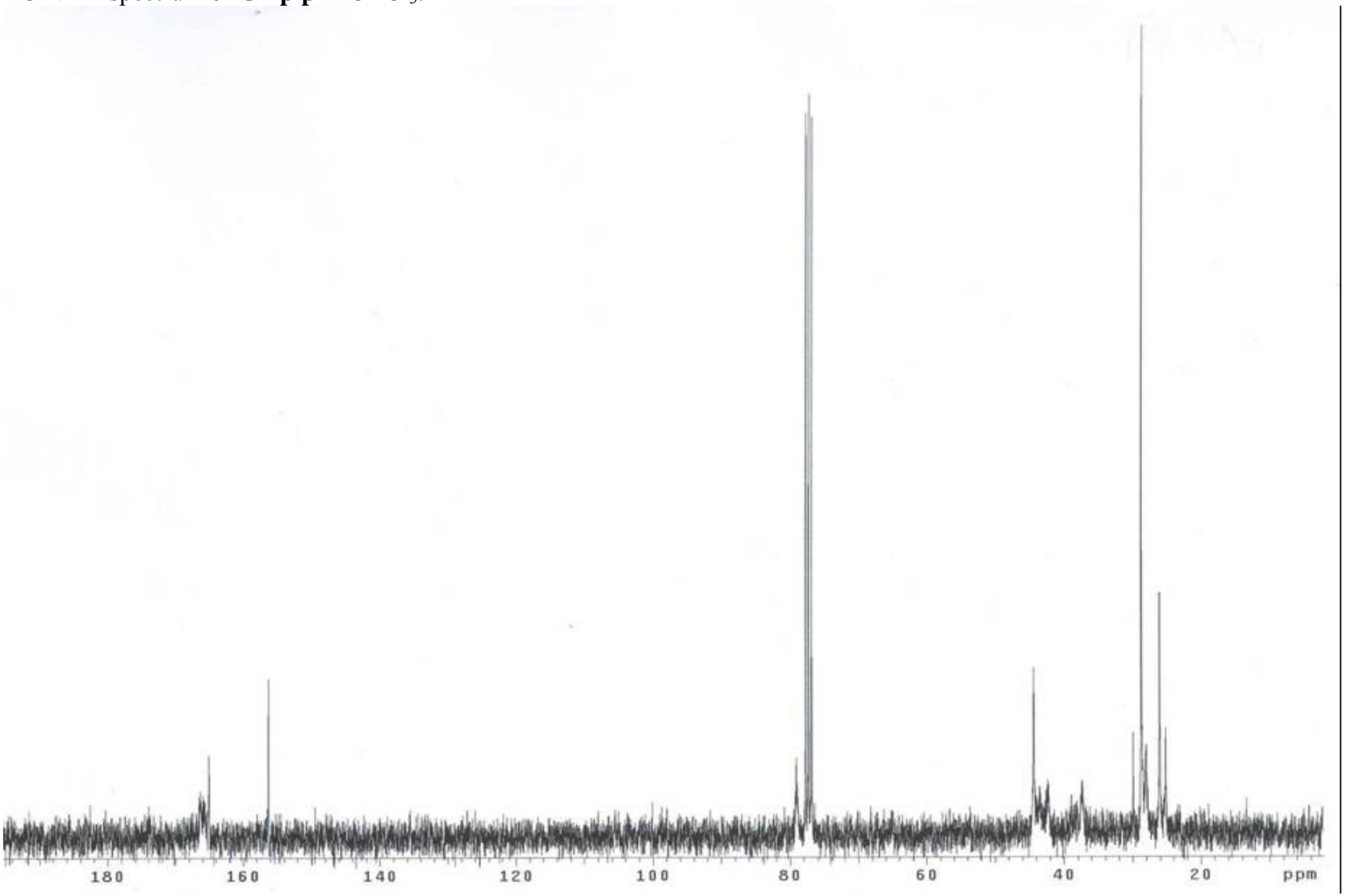

Mass spectrum (MALDI-TOF) of **G4-pip**.

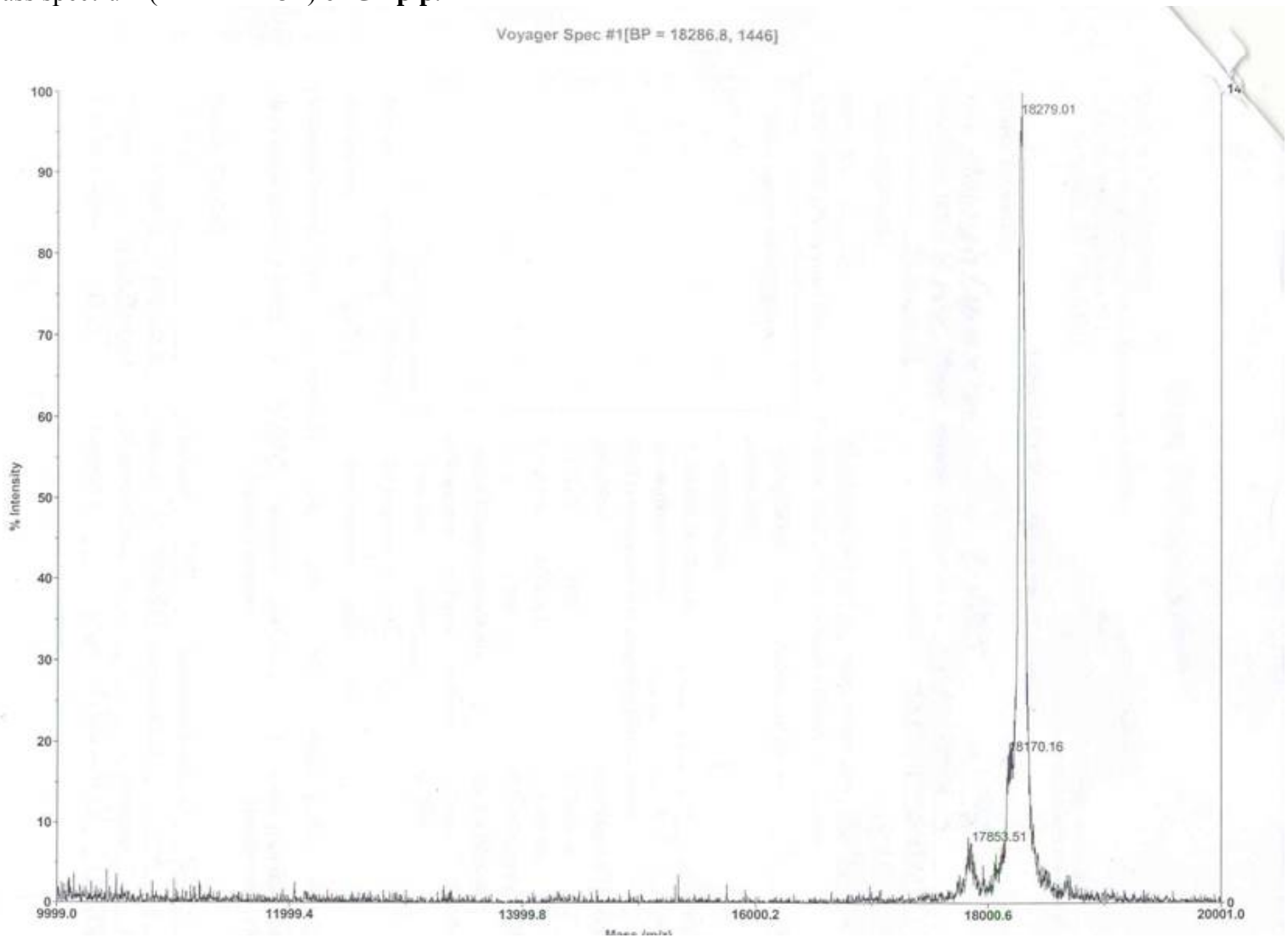

^{1}H NMR spectrum of **G4-NH$_2$** in CD_3OD.

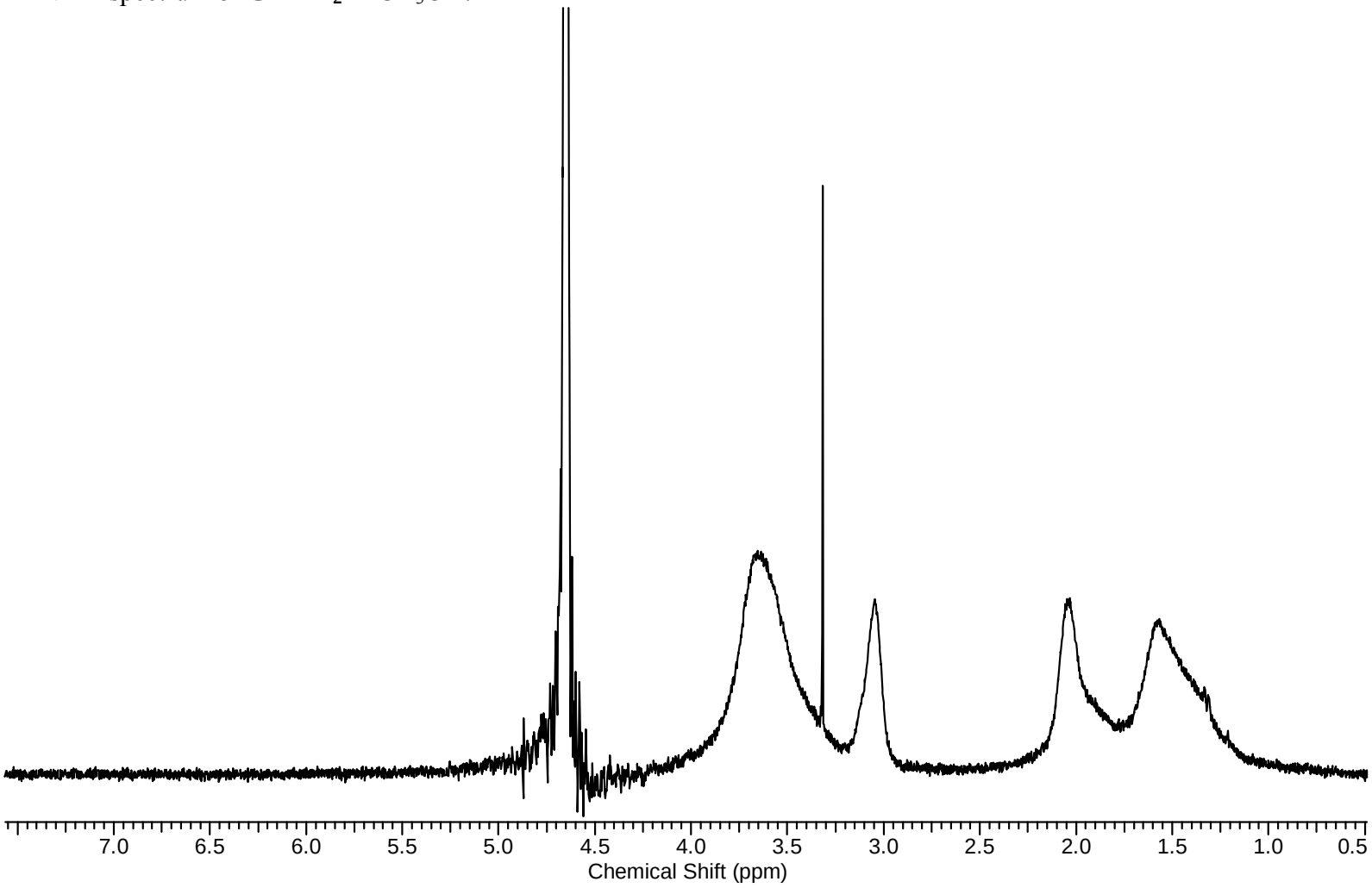

Mass spectrum (MALDI-TOF) of **G4-NH_2**.

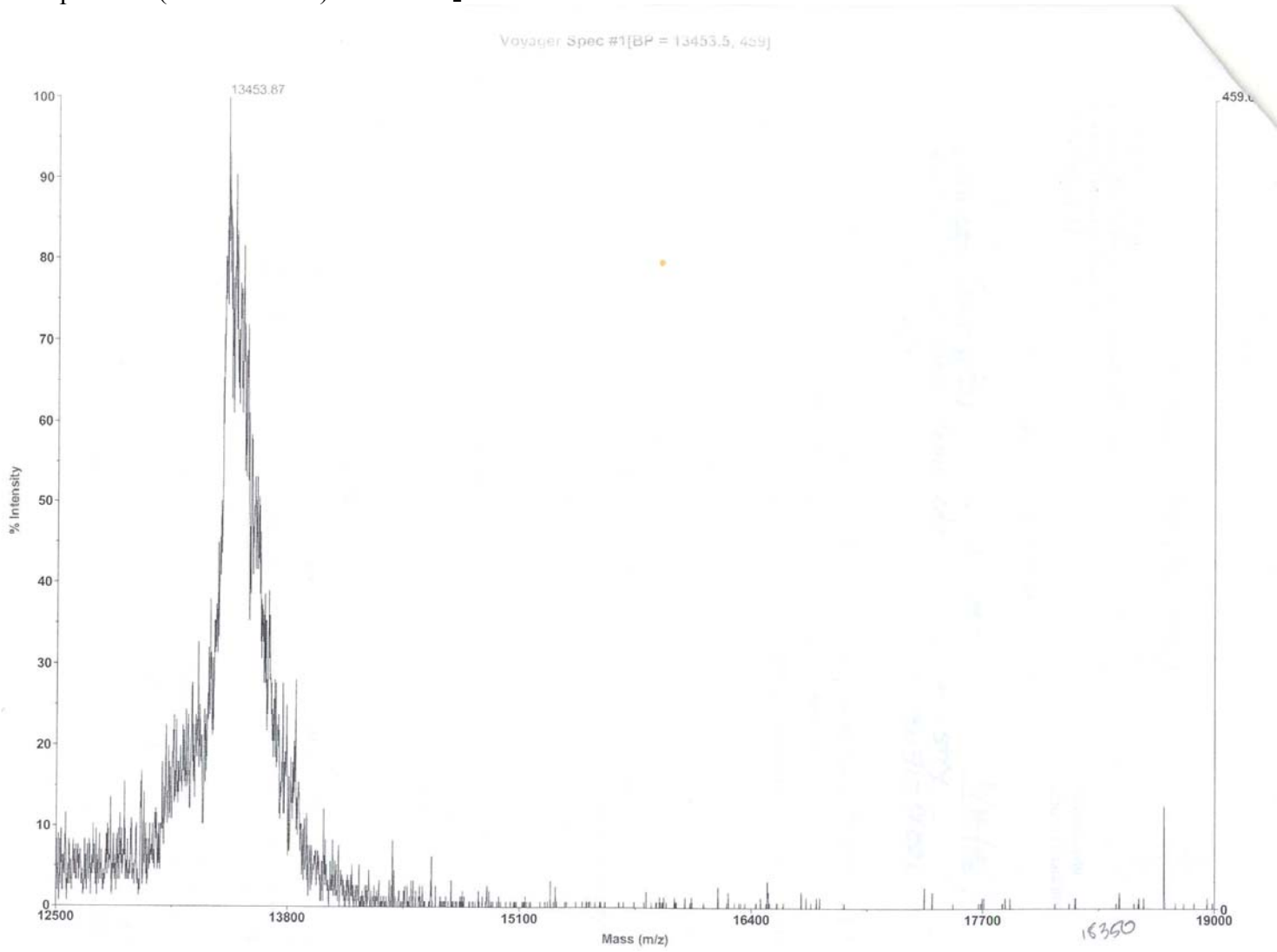

^{1}H NMR spectrum of **G5-Cl** in $CDCl_3$.

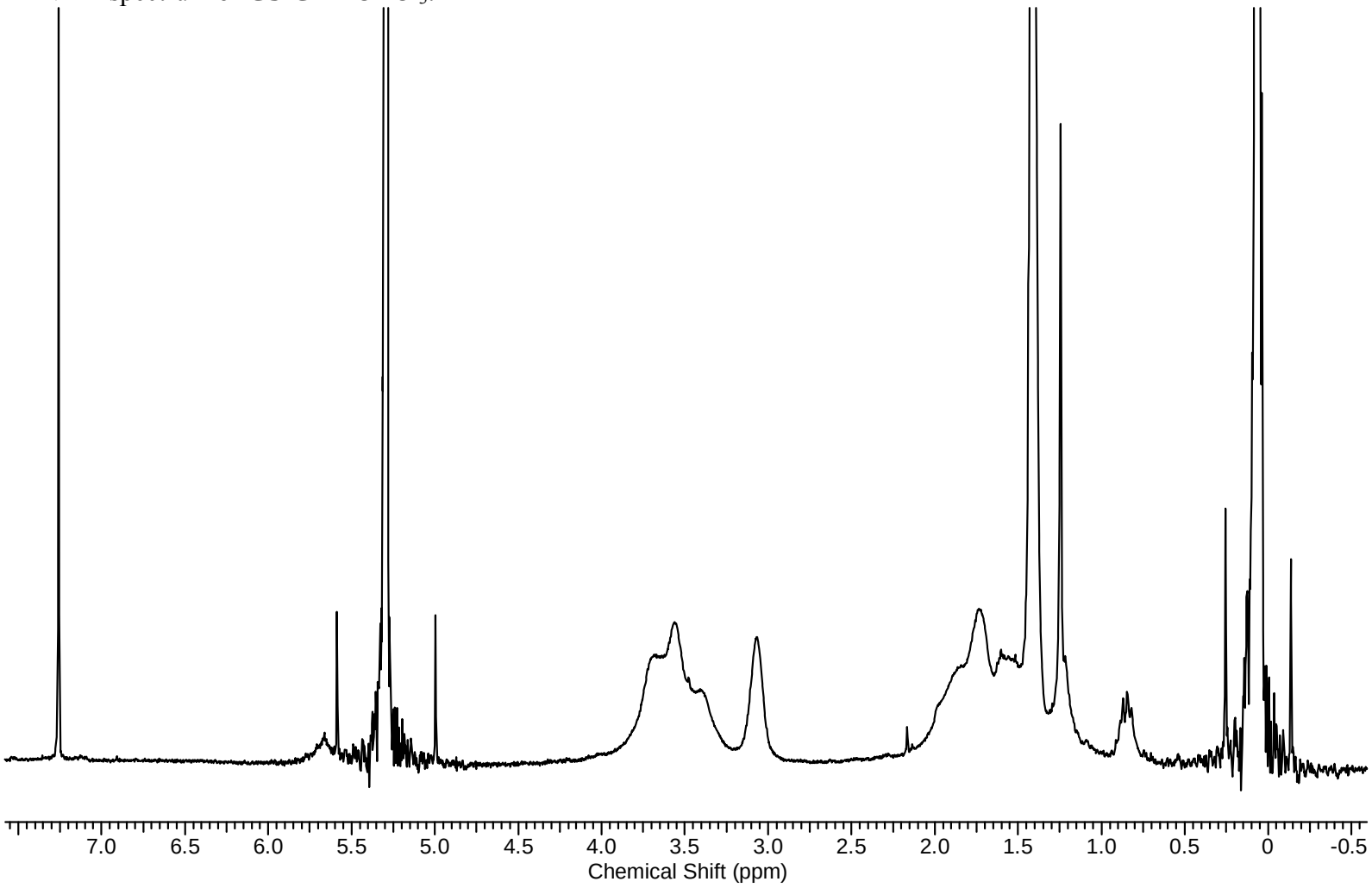

^{13}C NMR spectrum of **G5-Cl** in $CDCl_3$.

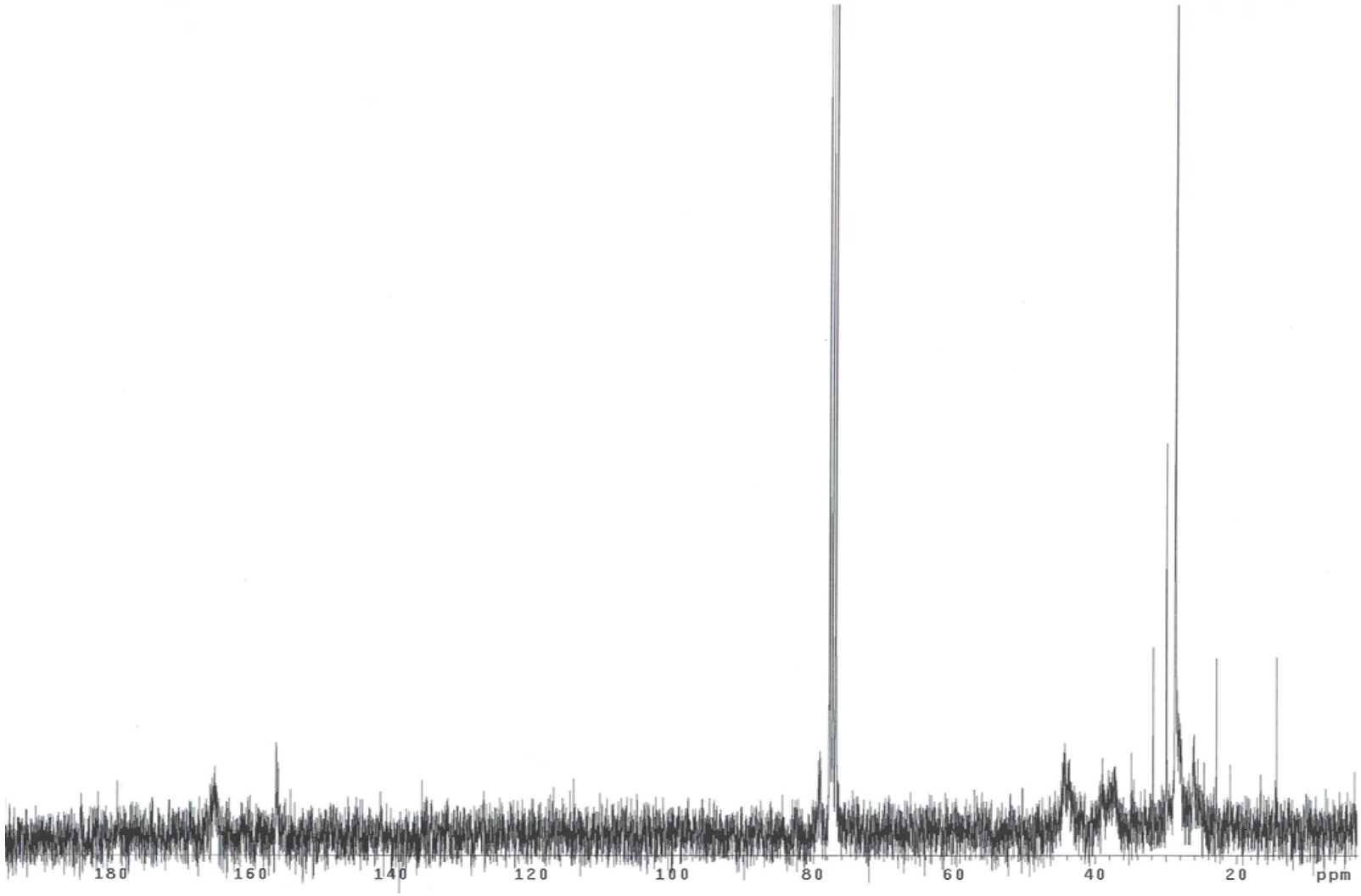

Mass spectrum (MALDI-TOF) of **G5-Cl.**

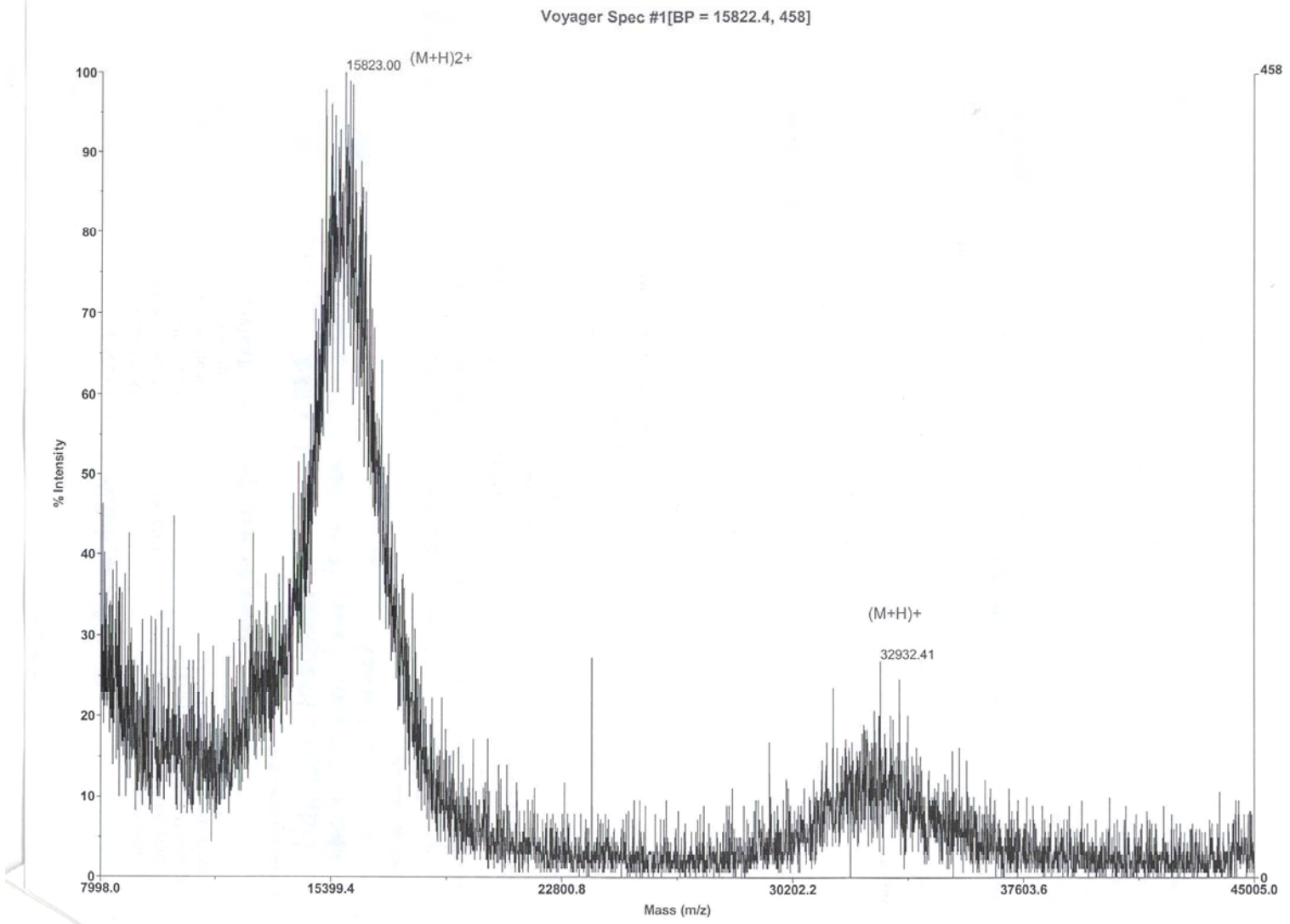

^{1}H NMR spectrum of **G5-pip** in $CDCl_3$.

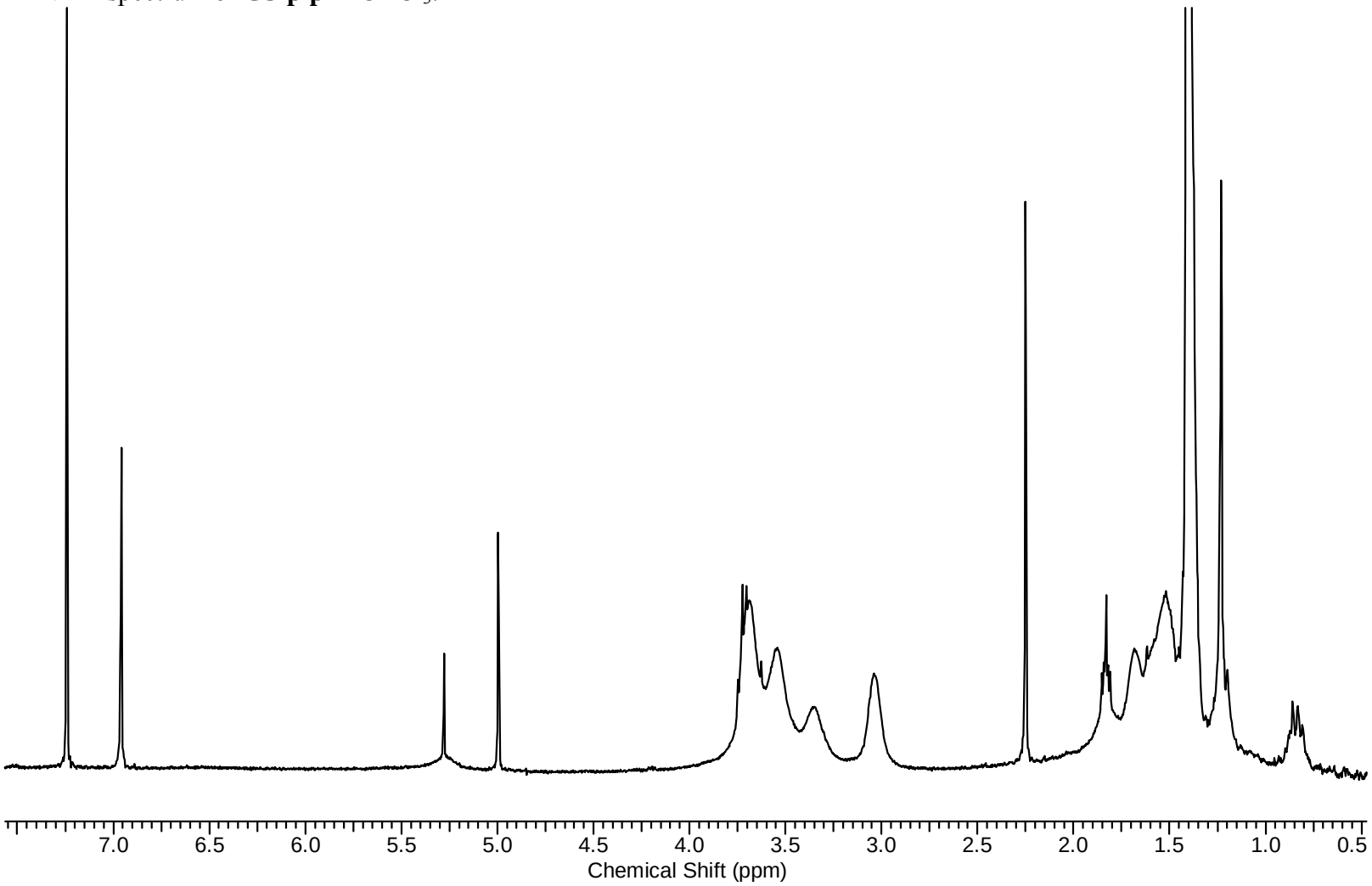

Mass spectrum (MALDI-TOF) of **G5-pip**.

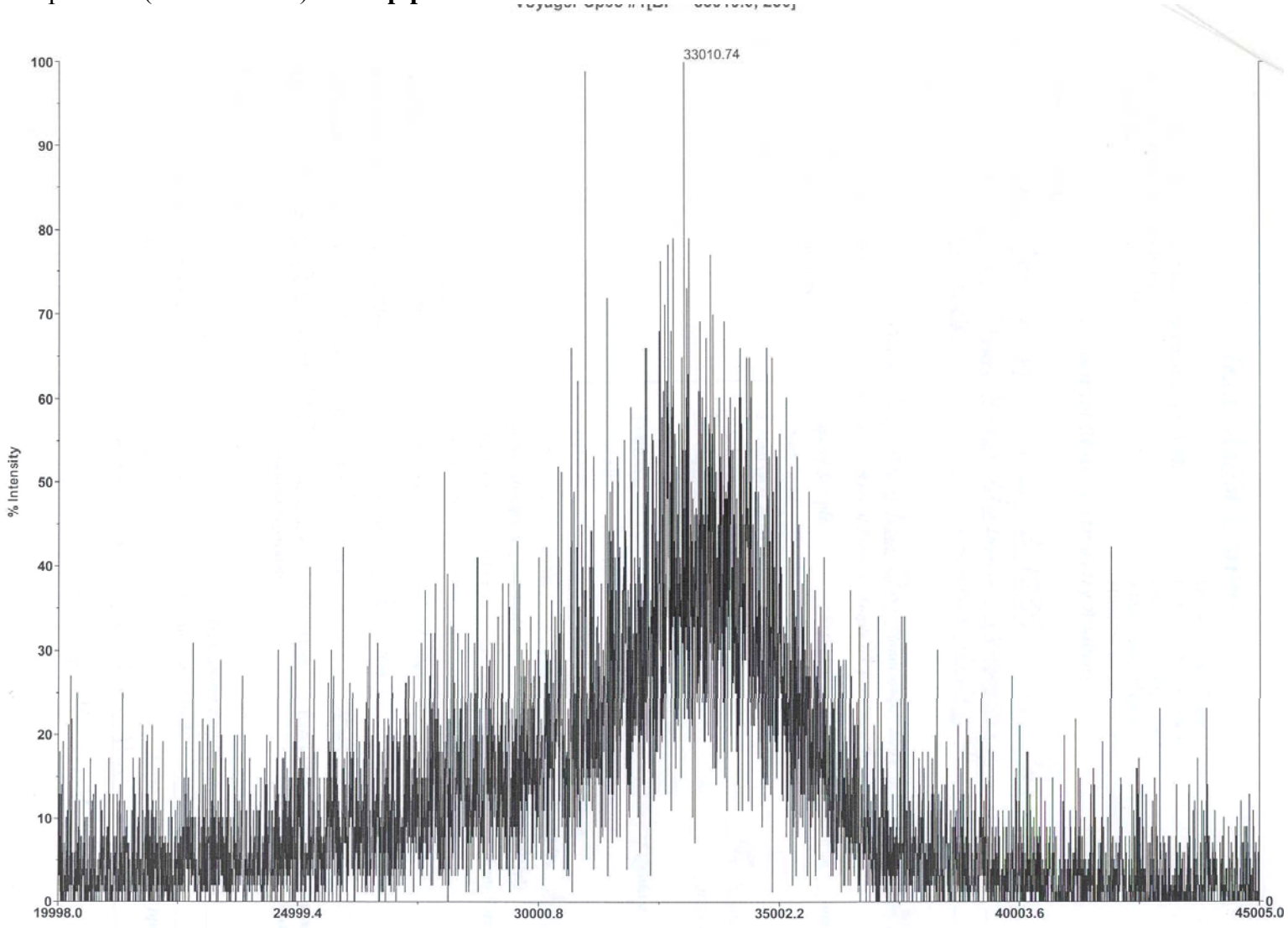

^{1}H NMR spectrum of **G5-NH$_2$** in CD_3OD.

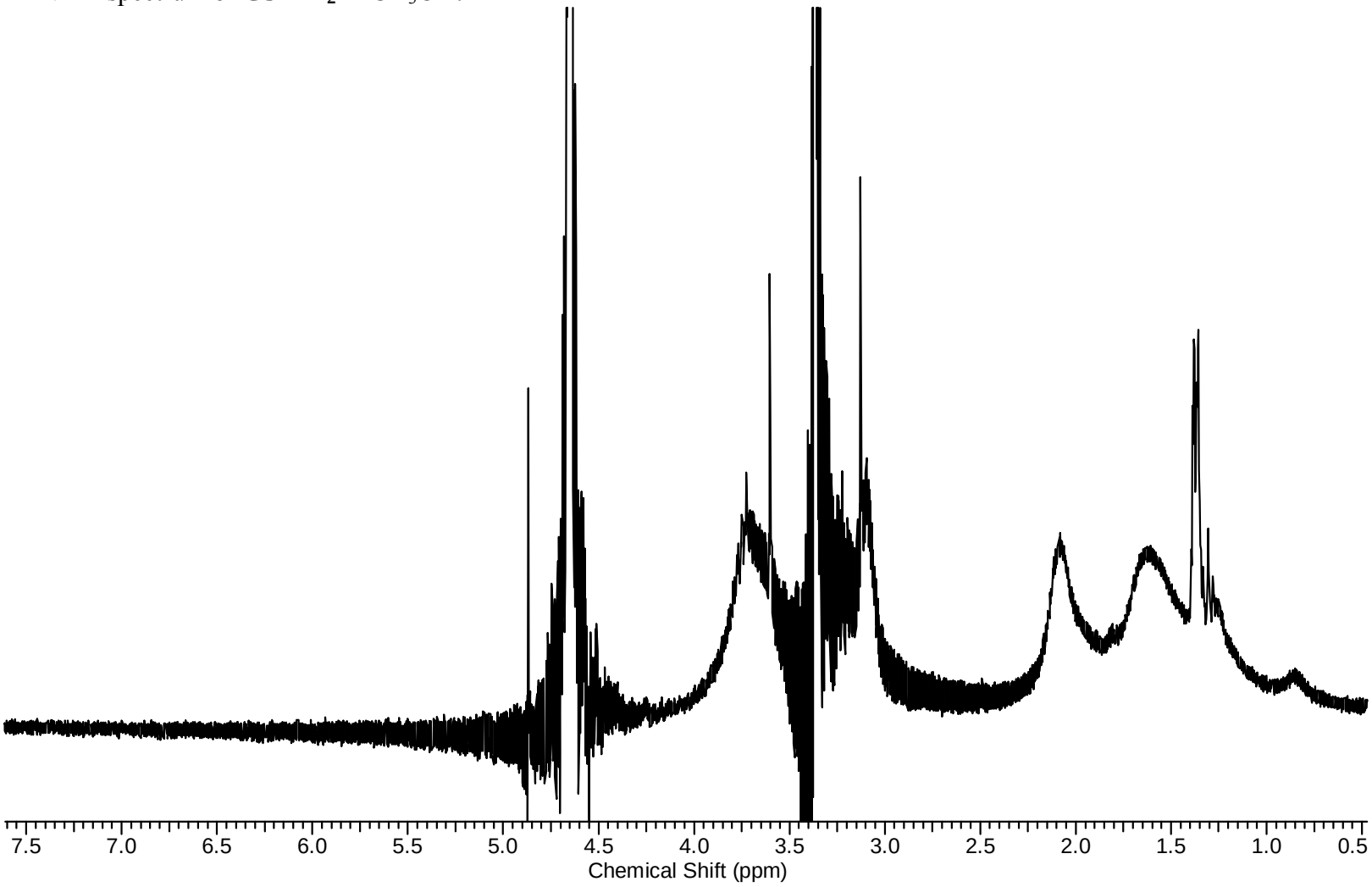

APPENDIX C

^{1}H NMR, ^{13}C NMR, AND MASS SPECTRA FOR COMPOUNDS DESCRIBED IN CHAPTER IV

^{1}H NMR spectrum of **4.1** in $CDCl_3$.

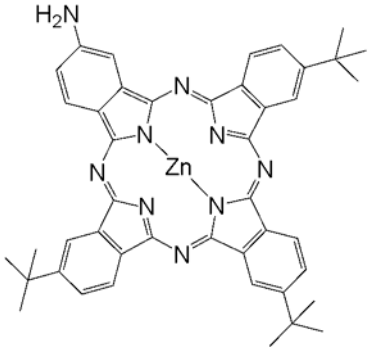

^{13}C NMR spectrum of **4.1** in $CDCl_3$.

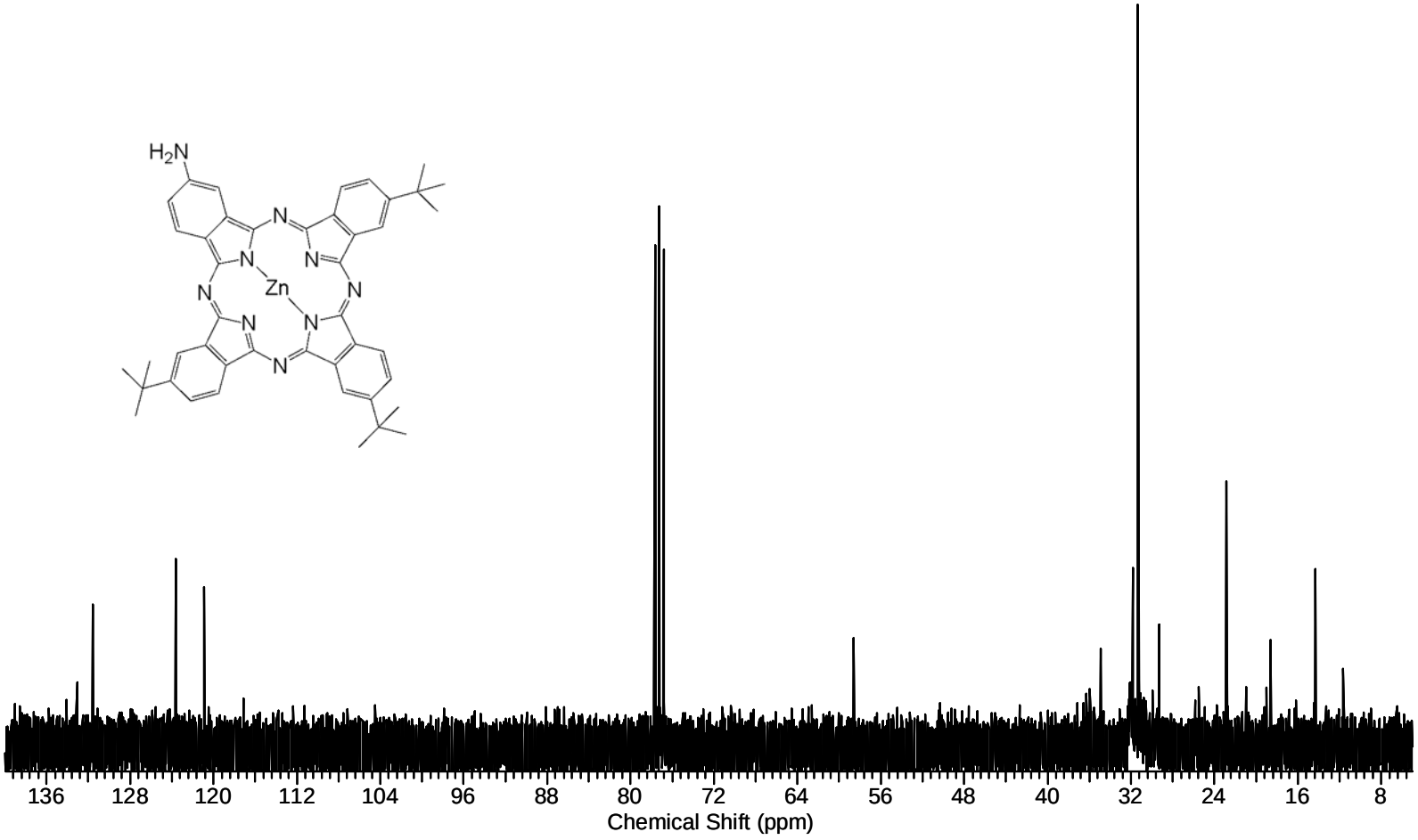

Mass spectrum (MALDI-TOF) of **4.1.**

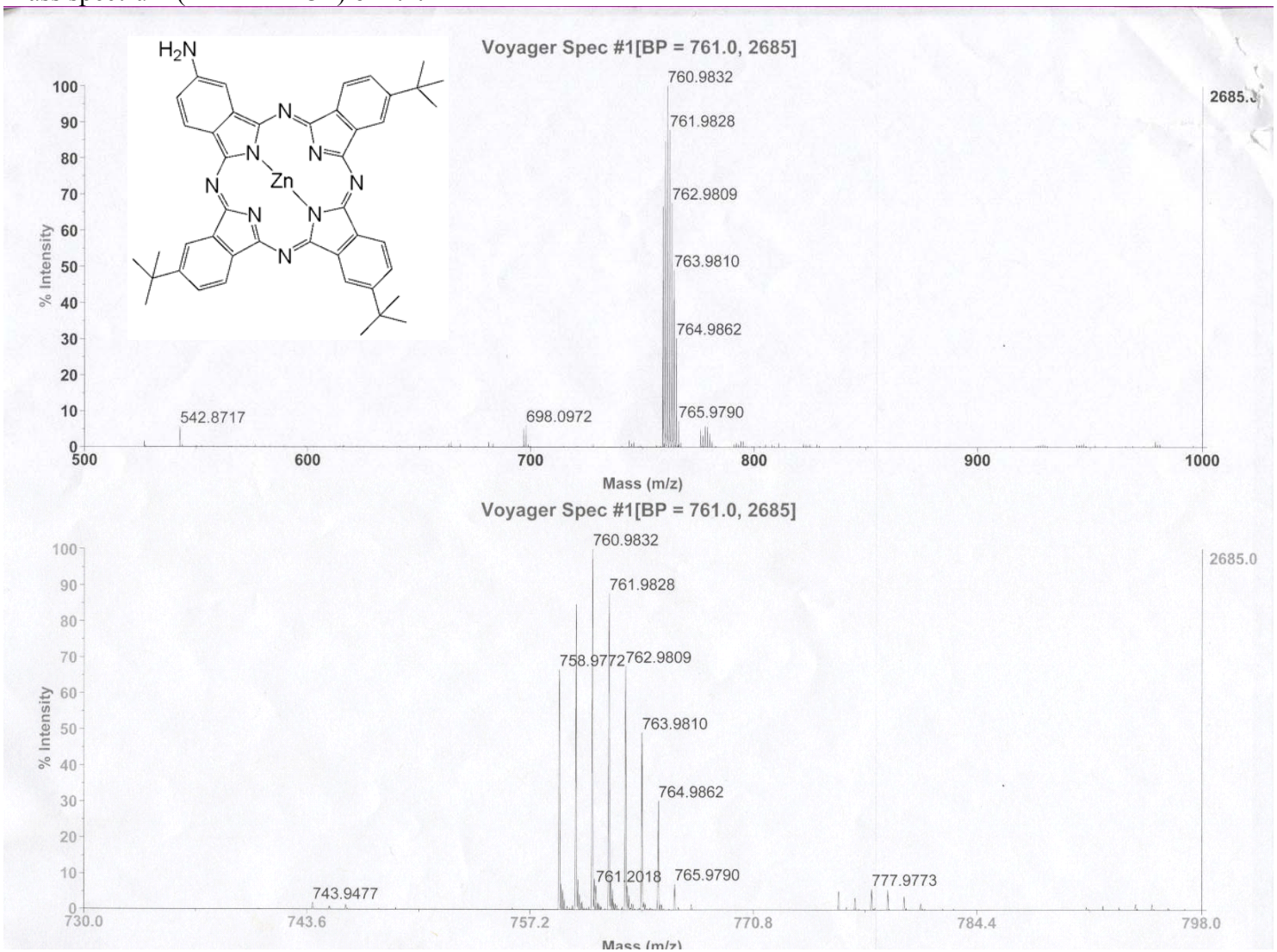

^{1}H NMR spectrum of **4.2** in $CDCl_3$.

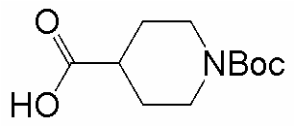

^{13}C NMR spectrum of **4.2** in $CDCl_3$.

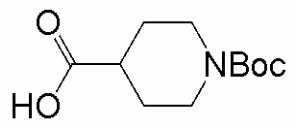

Mass spectrum (ESI) of **4.2.**

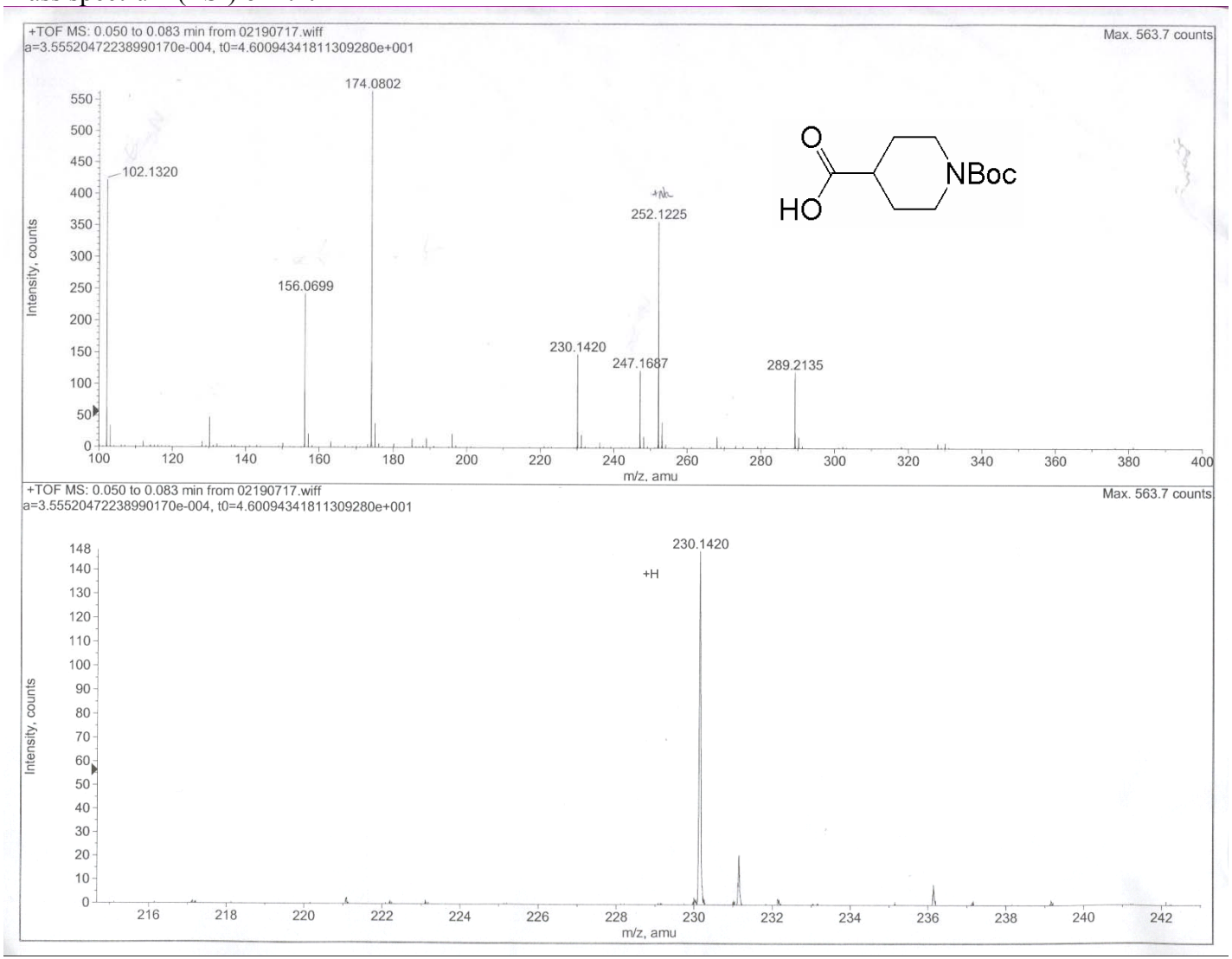

^{1}H NMR spectrum of **4.3** in $CDCl_3$.

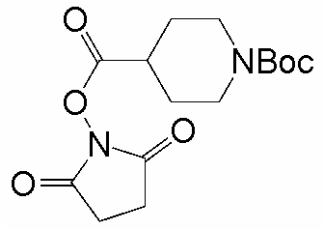

^{13}C NMR spectrum of **4.3** in $CDCl_3$.

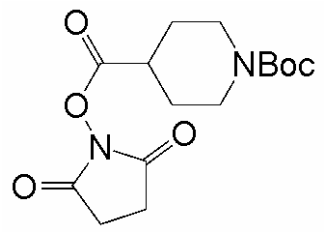

Mass spectrum (ESI) of **4.3**.

Mass spectrum (MALDI-TOF) of **4.4**.

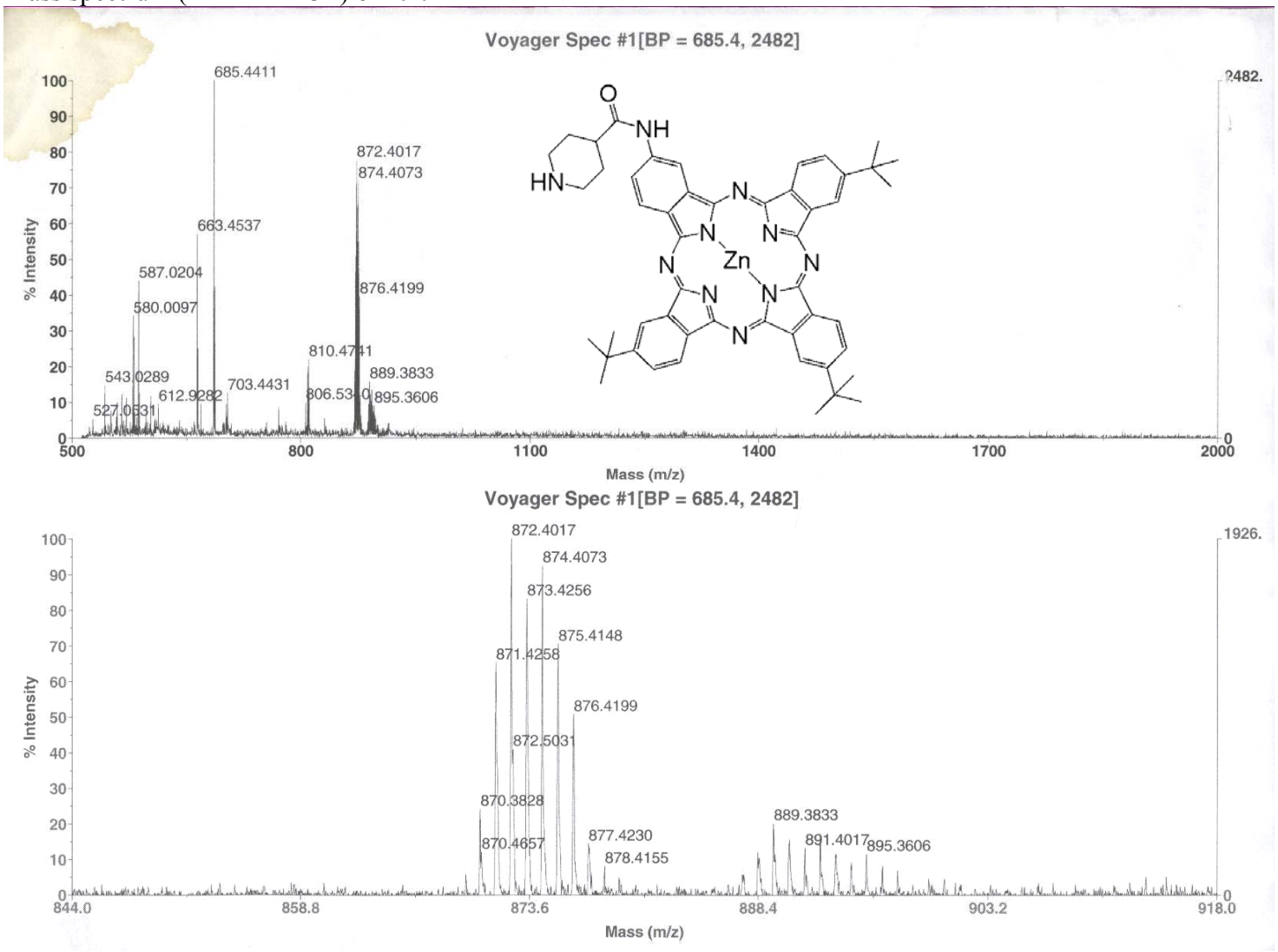

^{1}H NMR spectrum of **4.5** in $CDCl_3$.

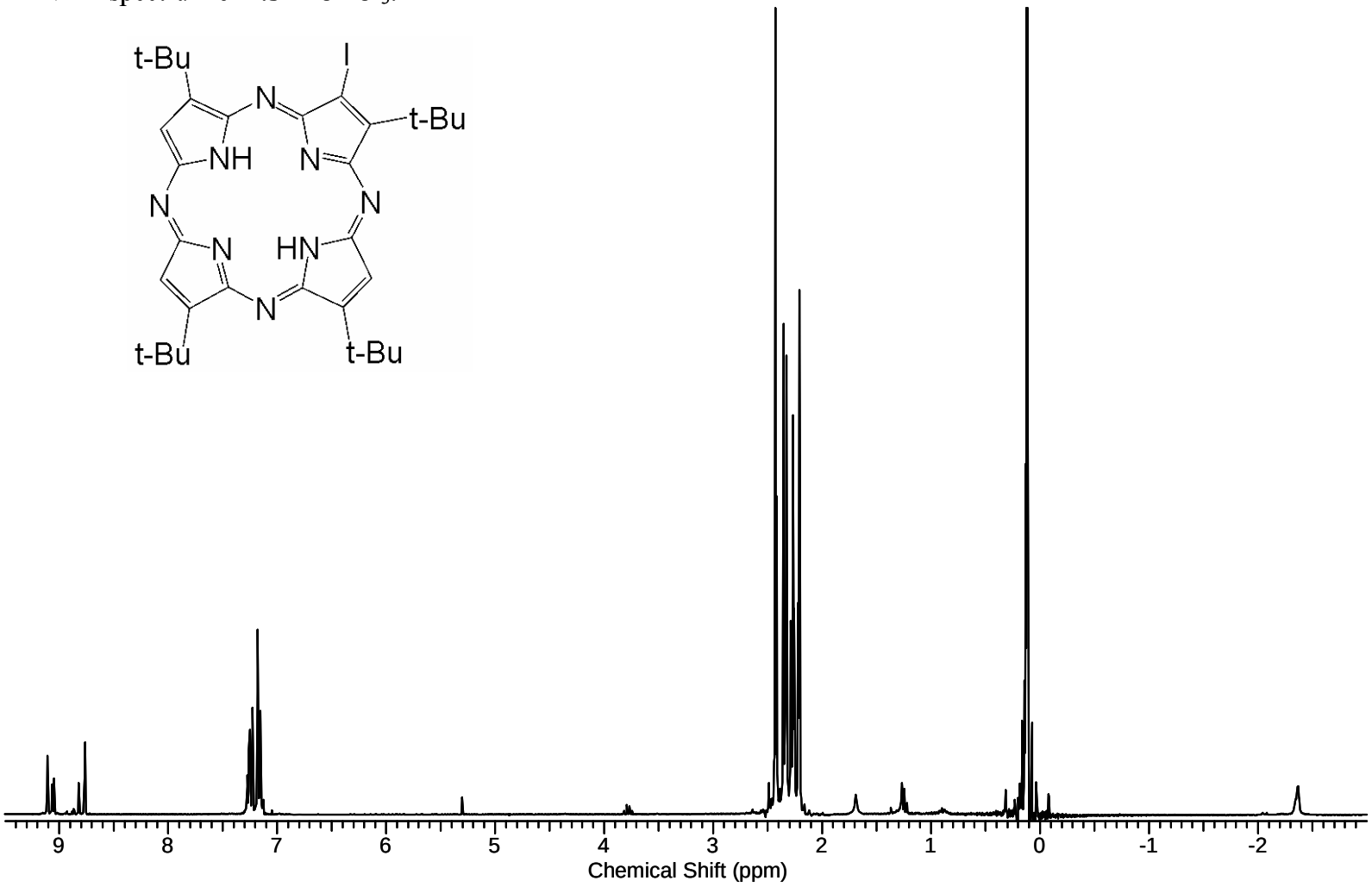

^{13}C NMR spectrum of **4.5** in $CDCl_3$.

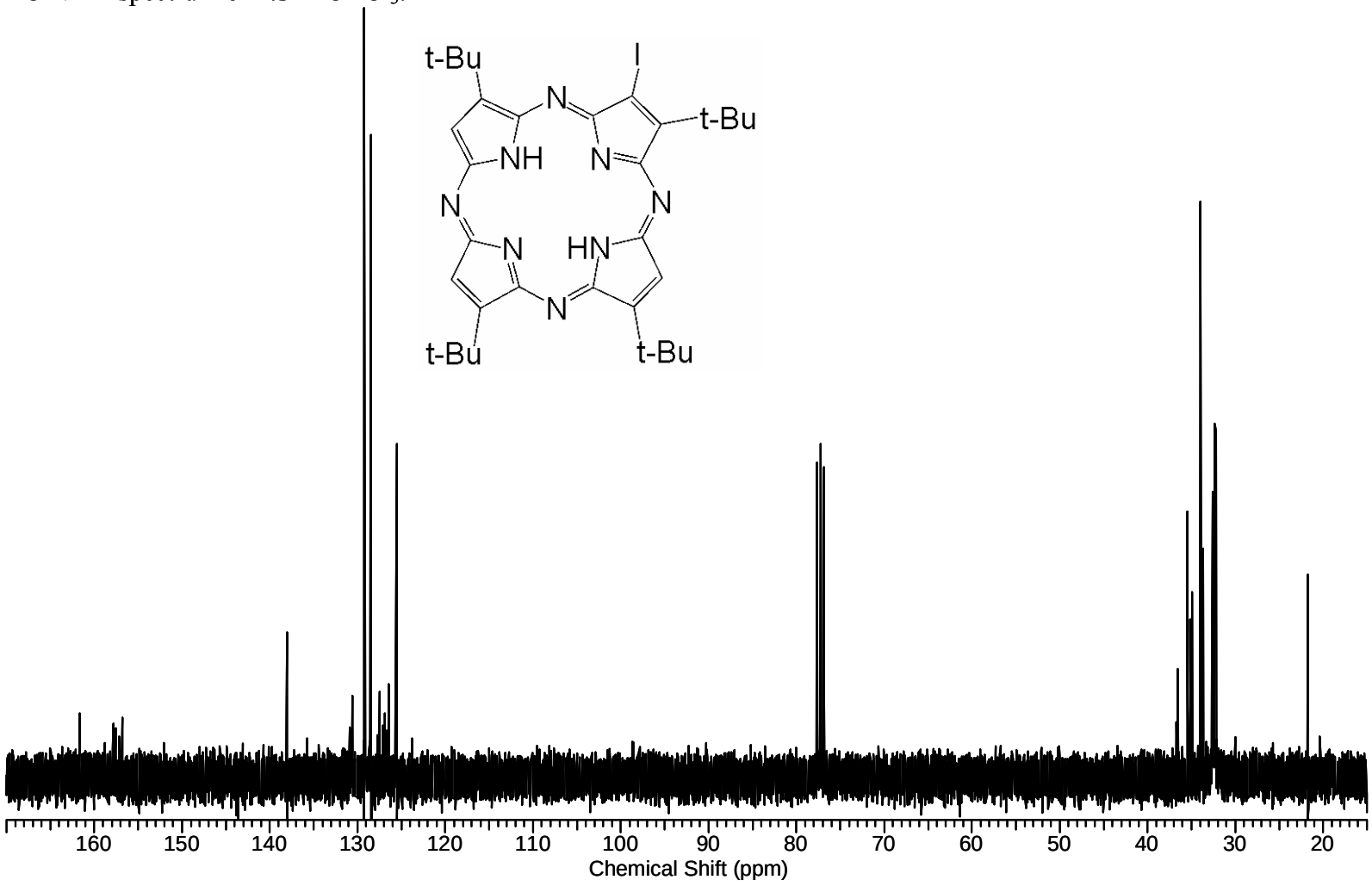

Mass spectrum (MALDI-TOF) of **4.5**.

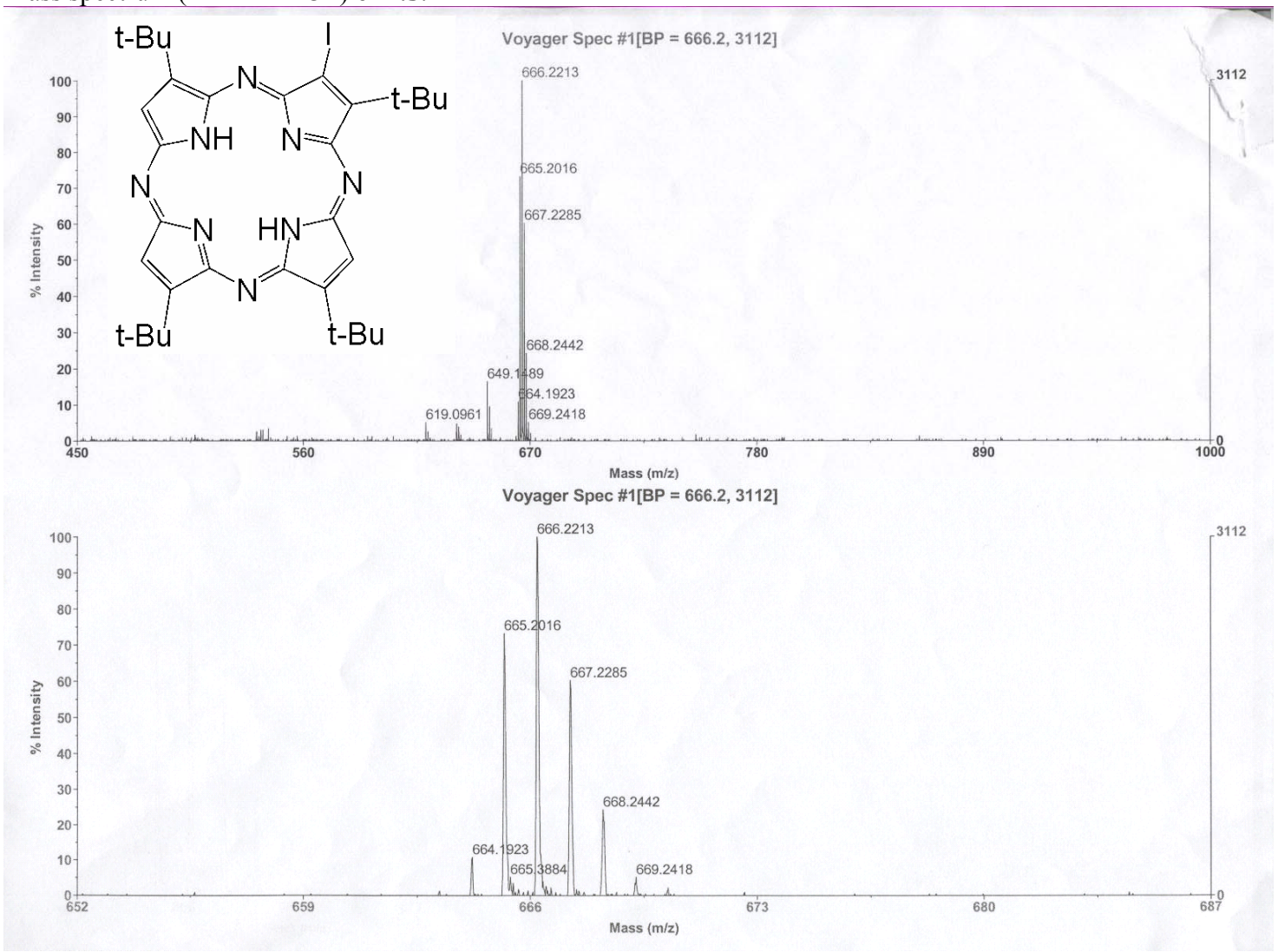

^{1}H NMR spectrum of **4.6** in $CDCl_3$.

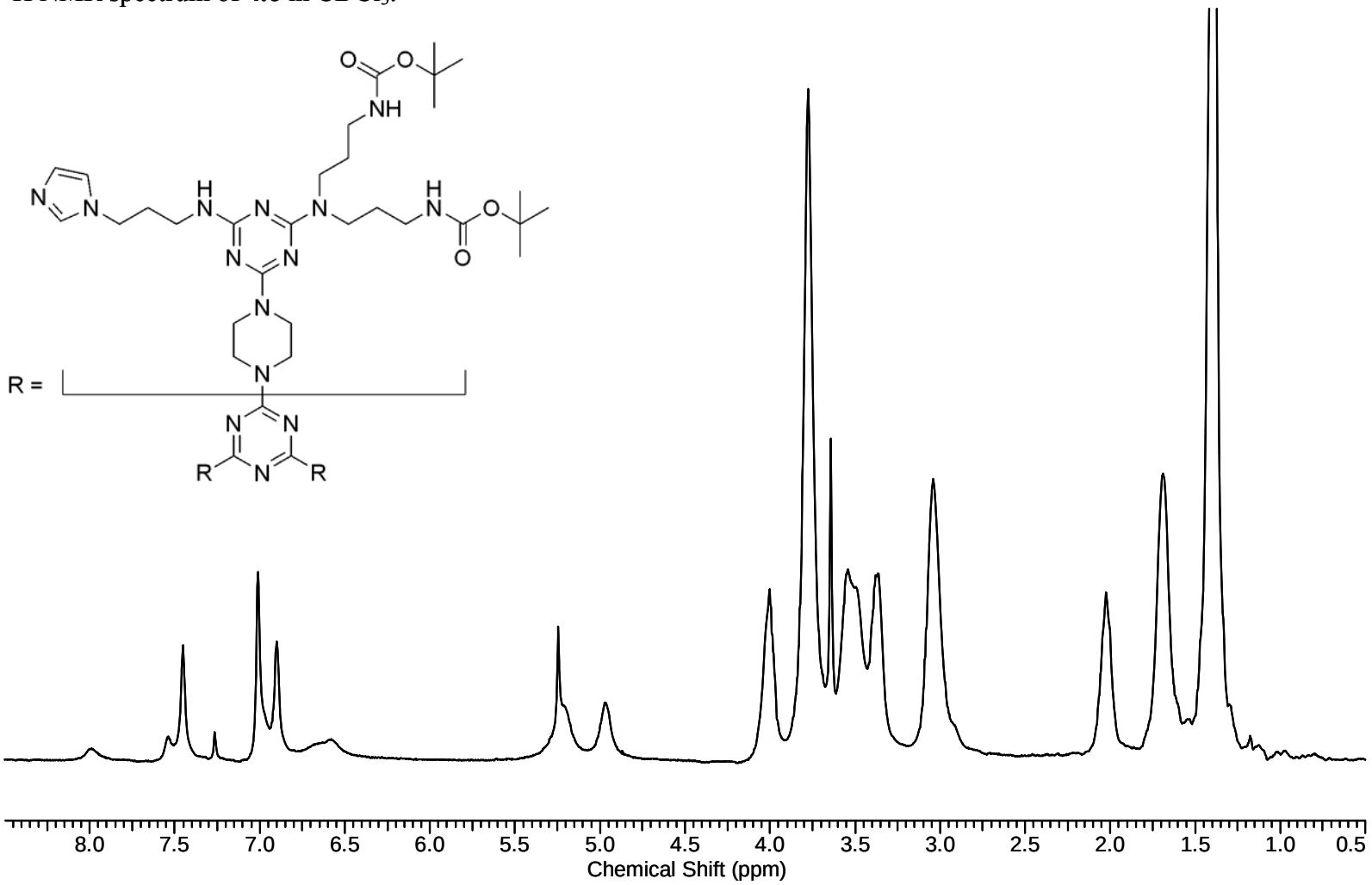

^{13}C NMR spectrum of **4.6** in $CDCl_3$.

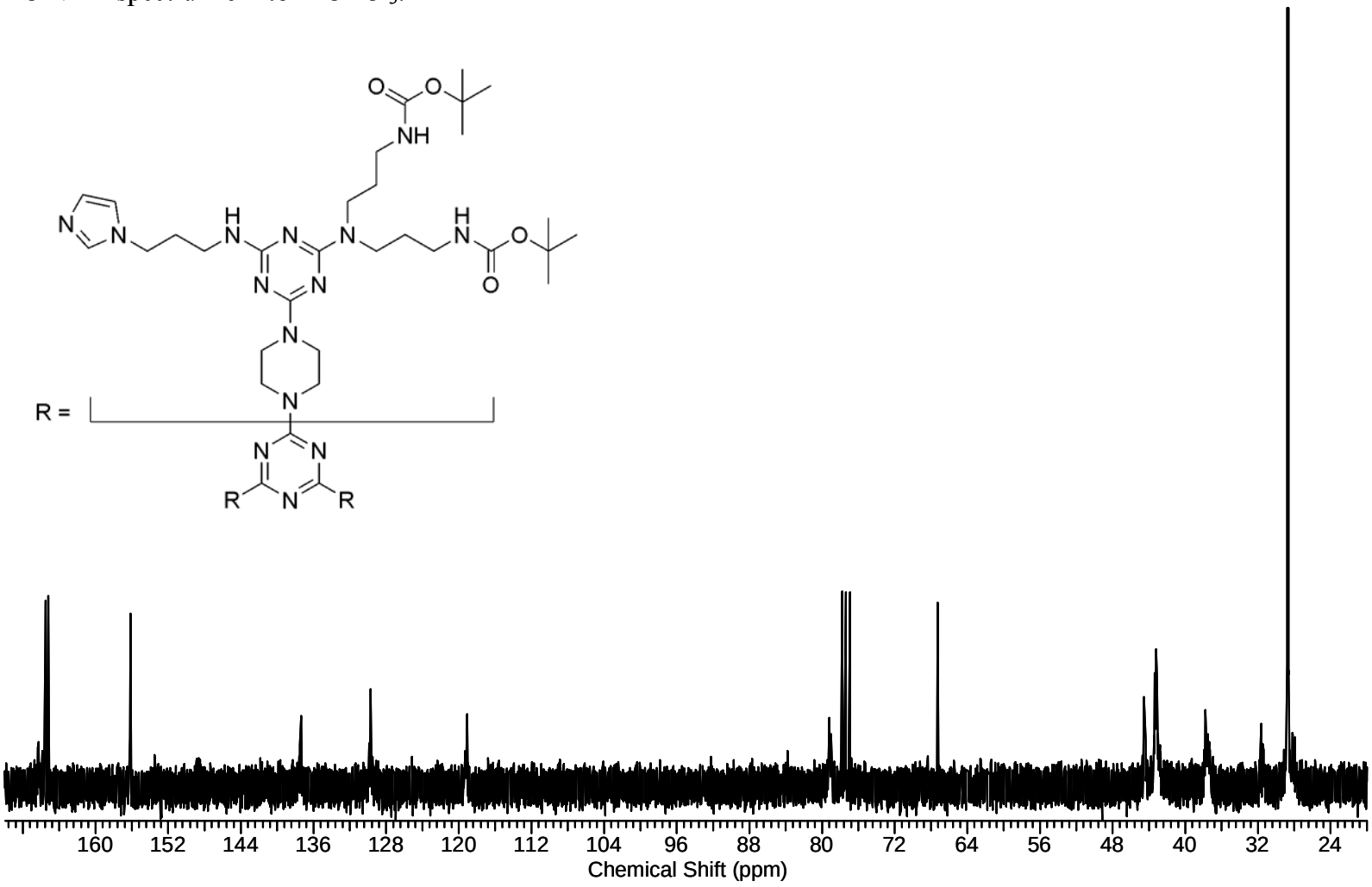

Mass spectrum (MALDI-TOF) of **4.6**.

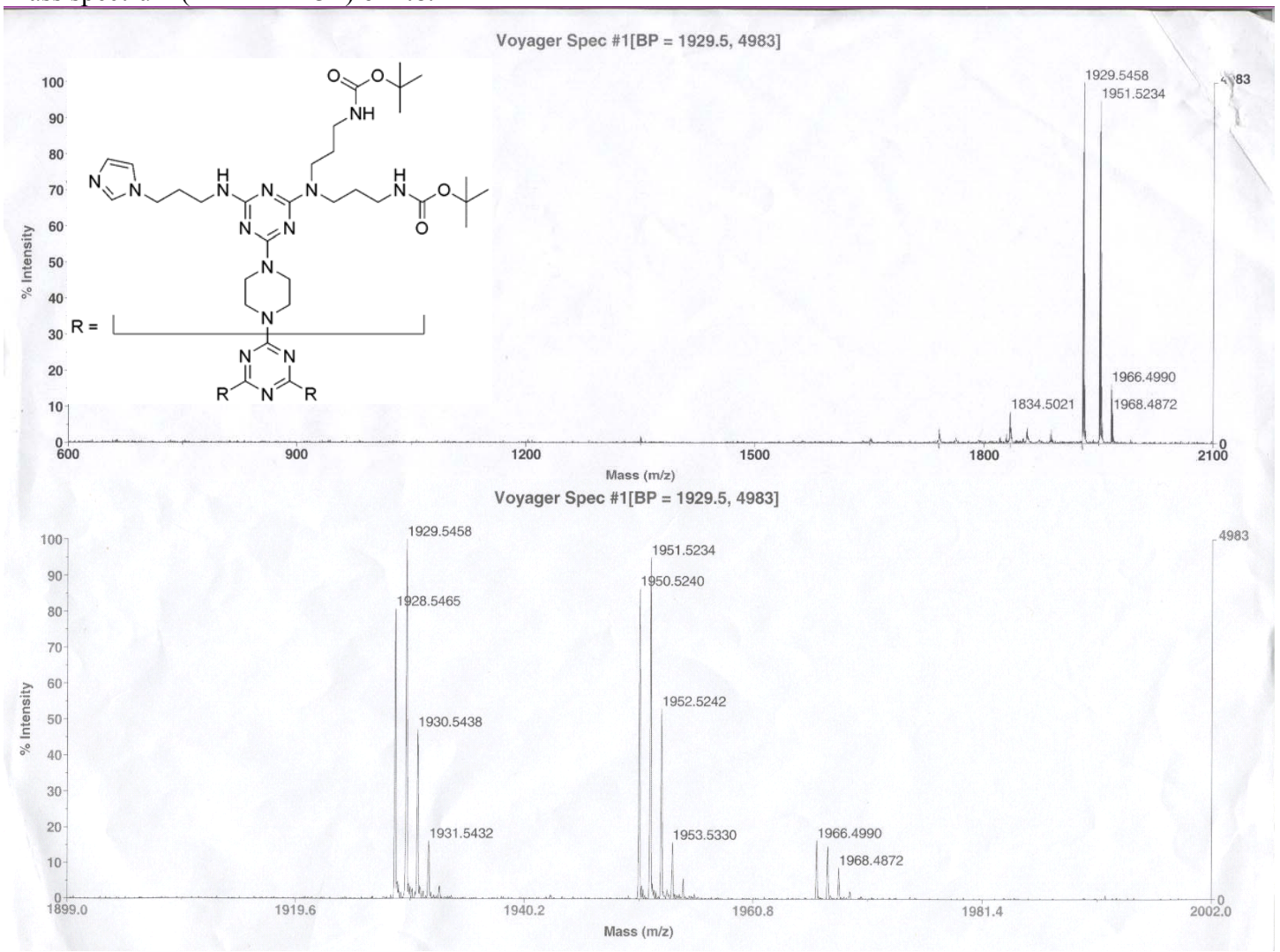

^{1}H NMR spectrum of **4.7** in CD_3OD.

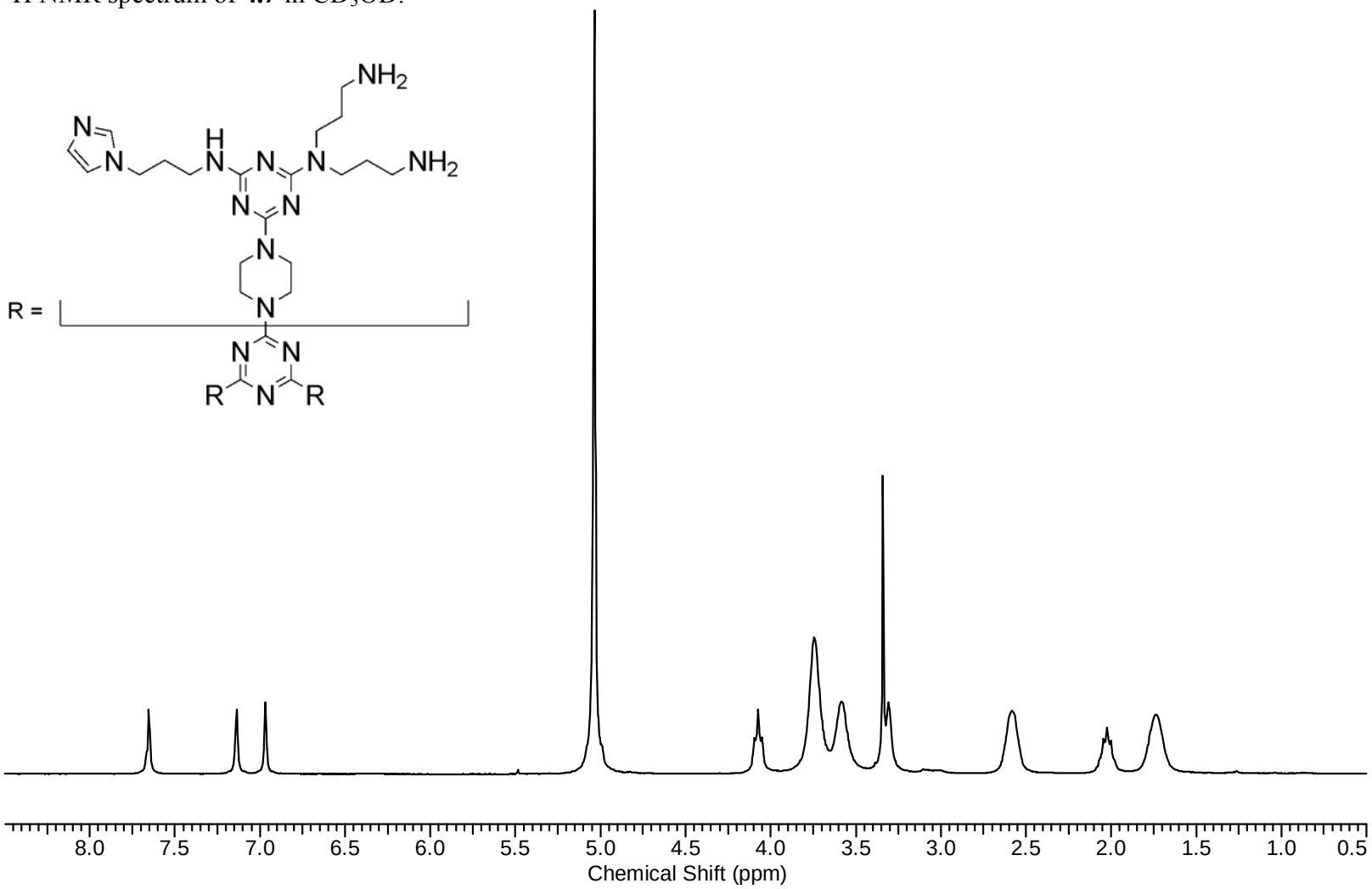

^{1}H NMR spectrum of **4.8** in $CDCl_3$.

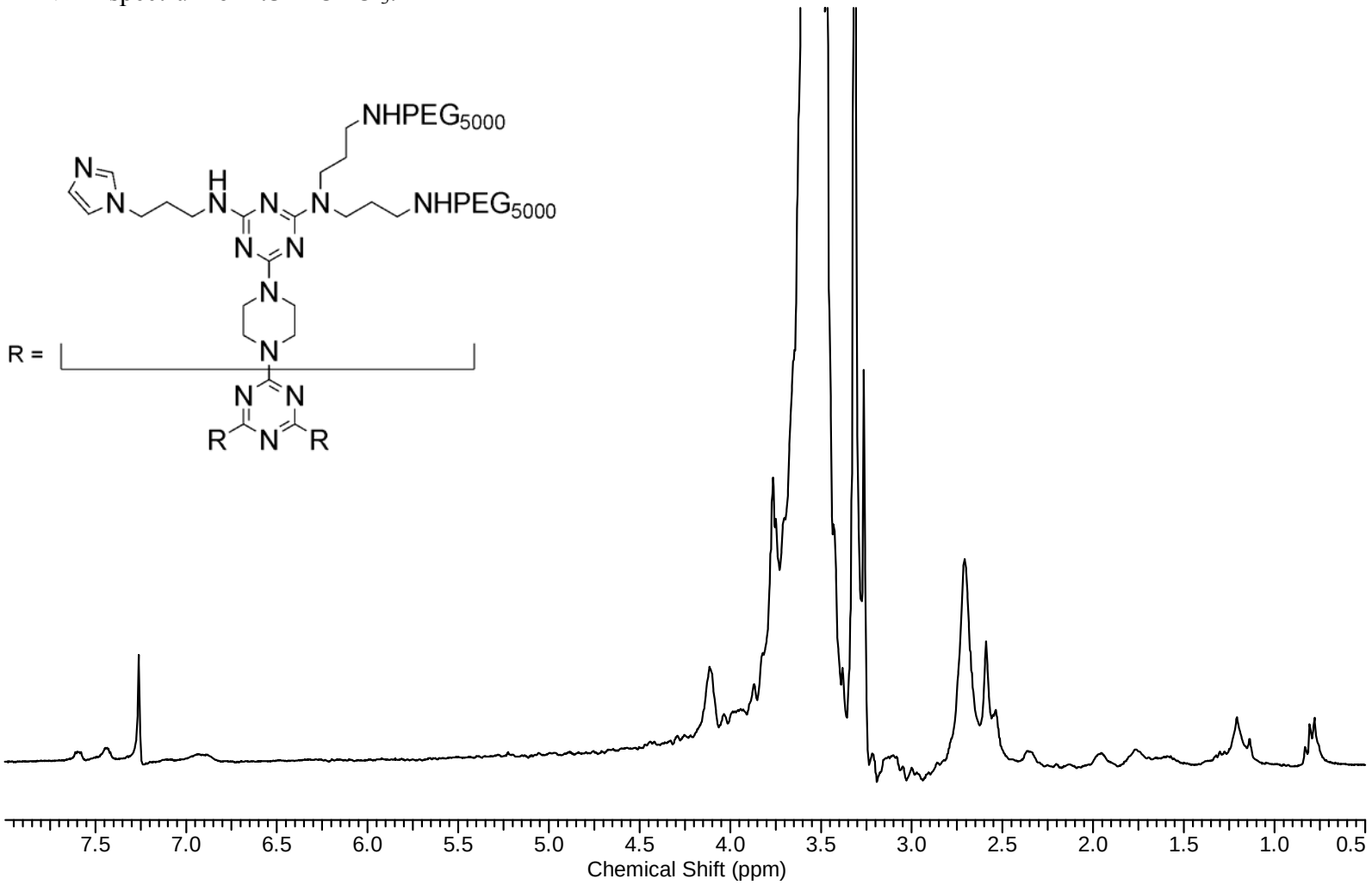

VITA

Name:	Hannah Louise Crampton (Heilveil)
Address:	3220 13th Street Bay City, TX 77414
Email Address:	heilveil@hotmail.com
Education:	B.S., Chemistry, Trinity University, 2004 Ph.D., Chemistry, Texas A&M University, 2008